

# **MODELLING OF LIQUID-LIQUID DISPERSIONS IN BATCH STIRRED VESSELS**

**By**

**Zaki M. O. EL HASSAN (M.Sc., DIC)**

A thesis submitted for the degree of Doctor of Philosophy  
in the Faculty of Engineering of the University of London

Department of Chemical Engineering & Chemical Technology  
Imperial College of Science, Technology & Medicine  
London SW7

1990

*To Manal*

## ABSTRACT

Drop size distributions and dispersed phase fractions were measured at different locations in two geometrically similar batch mixing vessels of standard configuration fitted with flat blade turbines. Experiments were conducted at various stirring speeds and dispersed phase fractions for a dispersion of n-heptane in water.

It was found that dispersions were not homogeneous and, from the shape of the distributions, that there were local variations of turbulence modes.

Although the tank average Sauter mean diameter ( $a_{32}$ ) varied with stirring speed ( $N$ ) as  $a_{32} \propto N^{-1.2}$ , thus suggesting that turbulence was isotropic, the scale-up rule was equal tip speed.

It was then proposed that the dependence of the tank average Sauter mean diameter with stirring speed was due to a combination of isotropic and non-isotropic modes that mimic isotropic behaviour.

In order to study the effect of different turbulence modes on the drop size distribution and Sauter mean diameter, a Monte Carlo simulation algorithm that incorporates different forms of breakage and coalescence functions was developed. The algorithm proved to be very efficient in the evaluation of drop interaction functions and achieved a significant reduction in computational load in comparison to other Monte Carlo algorithms reported in the literature.

Results showed that an  $a_{32} \propto N^{-1.2}$  dependence and an equal tip speed scale-up rule could be obtained with a combination of turbulence modes acting simultaneously at different tank locations.

## ACKNOWLEDGMENTS

I wish to express my sincere thanks to Dr. E. S. Perez de Ortiz for her patient and consistent guidance, assistance and encouragement throughout the course of this work.

My thanks to various members of the Department, especially Mrs. M. A. Tatsis, Mr. R. King and his colleagues at the Workshop, Mr. K. Gurney, Mr. P. Amrit and his colleagues at the Postgraduate Lab. Services, Mr. M. Dix, Mr. L. Moulder, Dr. N. Baghaei-Yazdi, Mrs. E. Corbett, Ms. A. Knox, Mr. C. Haddow, Mr. I. W. Drummond and Mr. R. Wood for his consistent help with both hardware and software.

This acknowledgment would't be complete without mentioning few of my friends and colleagues who provided the much needed support and encouragement, especially Mr. B. Chauhdary, Dr. C. Savastano, Dr. S. Mansour, Mr. A. S. Loata, Mr. A. M. Ibrahim, Mr. A. M. Bakheit, Mr. H. A. el-Fadil, Mrs. N. Karrar, Dr. C. V. M. Murthy, Dr. M. T. Saeed, Dr. I. Urua, Dr. K. O'Connor, Mr. I. Nanda, Dr. Seye, Ms. S. Srinivasan and Dr. L. A. Ajawin for introducing me to Imperail College.

Financial support in the form of a Study Grant from the University of Khartoum, Sudan, is gratefully acknowledged.

I would like to express my gratitude to my family especially my uncle Izz-el-din for their persistent support.

# TABLE OF CONTENTS

ABSTRACT .....	3
ACKNOWLEDGMENT .....	4
TABLE OF CONTENTS .....	5
TABLE OF TABLES .....	11
TABLE OF FIGURES .....	12
CHAPTER I: INTRODUCTION .....	15
CHAPTER II: LITERATURE REVIEW .....	17
2.1 Dispersions .....	17
2.2 Turbulence .....	17
2.3 Power Consumption and Power Number .....	21
2.4 Specific Power Input $\epsilon$ .....	22
2.5 Minimum Stirrer Speed for Dispersion .....	23
2.6 Scale-Up of Liquid-Liquid Dispersions .....	24
2.6.1 Theoretical scale-up criteria .....	25
2.6.1.1 Kinematic Similarity .....	25
2.6.1.2 Dynamic Similarity .....	25
2.6.1.3 Thermal and Chemical Similarity .....	25
2.6.2 Empirical Scale-Up Criteria .....	26
2.7 Modelling of Stirred Tank Reactors (STR) .....	27
2.8 Dispersion Simulation .....	28
2.9 Breakage and Coalescence of Drops .....	29
2.9.1 Breakage of Drops .....	29
2.9.1.1 Maximum Drop Size .....	30
2.9.1.2 Minimum Drop Size .....	33
2.9.1.3 Sauter Mean Diameter ( $a_{32}$ ) and Drop Size Distribution .....	34
2.9.1.4 Transient Drop Sizes .....	36
2.9.1.5 Drop Breakage Rate .....	36
2.9.1.5.1 Breakage Frequency .....	37



3.6.2 Hold-up Measurements .....	58
<b>CHAPTER IV: EXPERIMENTAL RESULTS AND</b>	
<b>DISCUSSION .....</b>	<b>67</b>
4.1 Hold-up results .....	67
4.1.1 Unsteady state behaviour of $\phi^*$ .....	68
4.1.2 Spatial variations of the local hold-up values .....	69
4.1.2.1 Variations with the distance from the tank central axis	
.....	69
4.1.2.2 Variations within the vertical distance from the	
impeller .....	70
4.1.3 Effect of impeller speed on local Hold-up .....	70
4.1.4 Tank Hold-up ( $\phi_0$ ) effect: .....	71
4.1.5 Effect of the vessel scale on $\phi^*$ .....	71
4.1.6 Mass balance over the whole vessel: .....	72
4.1.7 Conclusions .....	72
4.2 Drop sizing results .....	73
4.2.1 Local values of Sauter mean diameter .....	74
4.2.1.1 Horizontal variation .....	74
4.2.1.2 Vertical variations .....	75
4.2.1.3 Effect of variation of stirring speed .....	75
4.2.2 Local drop size distributions .....	77
4.2.2.1 Horizontal variations .....	77
4.2.2.2 Vertical variations .....	78
4.2.2.3 Effect of the variation of stirring speed .....	78
4.2.2.4 Effect of variation of the hold-up .....	78
4.2.3 Average Sauter mean diameter and Drop size distribution	79
4.2.4 Effect of Vessel scale .....	79
4.2.5 Conclusions .....	80

<b>CHAPTER V: DISPERSION MODELLING AND SIMULATION .....</b>	<b>115</b>
5.1 Modelling and description of flow and dispersion in agitated vessels .....	115
5.1.1 Flow in stirred tanks .....	115
5.1.2 Modelling of dispersion behaviour inside the tanks .....	116
5.1.2.1 Drop breakage .....	118
5.1.2.1.1 Breakage Frequency $g(a)$ .....	119
5.1.2.2 Drop coalescence .....	120
5.1.2.2.1 Collision frequency .....	121
5.1.2.2.2 Collision efficiency .....	121
5.2 Simulation of liquid-liquid dispersions .....	124
5.2.1 Definitions .....	124
5.2.2 System Definition .....	124
5.2.3 Monte Carlo Simulation Technique .....	125
5.2.4 Coalescence Frequency Approximation .....	125
5.2.5 Coalescence Frequencies Evaluation .....	127
5.2.6 Simulation Time Management .....	128
5.2.7 Daughter Droplets .....	130
5.2.7.1 Number of daughter droplets .....	130
5.2.7.2 Daughter droplets distribution .....	130
5.2.8 Simulation Algorithm .....	130
<b>CHAPTER VI: SIMULATION MODEL BEHAVIOUR AND RESULTS .....</b>	<b>145</b>
6.1 General description of the simulation model behaviour .....	146
6.1.1 Evaluation of constants in the breakage and coalescence functions .....	146
6.1.2 Computational load in the evaluation of population coalescence frequencies .....	148
6.1.3 Effect of the interval size on the coalescence frequencies ...	148
6.1.4 Comparison between the two algorithms .....	149
6.1.4.1 Sauter and average mean diameters .....	149
6.1.4.2 Breakage and Coalescence frequencies .....	150

6.1.4.3 Computational Load .....	150
6.1.4.4 Drop Size distribution .....	150
6.1.5 General observations on Simulation model behaviour .....	151
6.1.5.1 Transient Sauter and average mean diameters .....	151
6.1.5.2 Transient drop size distributions .....	151
6.1.5.3 Transient breakage and coalescence frequencies .....	152
6.1.5.4 Effect of variation of stirring speed .....	152
6.1.5.4.1 Sauter mean diameter .....	152
6.1.5.4.2 Drop Size Distribution .....	153
6.1.5.4.3 Effect of the variation of hold-up .....	153
6.1.5.4.3.1 Sauter mean diameter .....	153
6.1.5.4.3.2 Drop size distributions .....	153
6.1.6 Comparison between isotropic and non-isotropic model behaviour .....	153
6.1.6.1 Sauter and arithmetic mean diameters .....	154
6.1.6.2 Drop size distribution .....	154
6.2 Comparison between the simulated and experimental results .....	155
<b>CHAPTER VII: CONCLUSIONS AND RECOMMENDATIONS .....</b>	<b>174</b>
<b>APPENDIX I: Physical properties of the systems .....</b>	<b>177</b>
<b>APPENDIX II: Kolmogoroff's length scale calculations .....</b>	<b>178</b>
<b>APPENDIX III: Hold-up measurements results .....</b>	<b>180</b>
APPENDIX III-1: Tank diameter = .22 m ; $\phi_o = .1$ .....	181
APPENDIX III-2: Tank diameter = .22 m ; $\phi_o = .2$ .....	187
APPENDIX III-3: Tank diameter = .22 m ; $\phi_o = .3$ .....	193
APPENDIX III-4: Tank diameter = .22 m ; $\phi_o = .4$ .....	199
APPENDIX III-5: Tank diameter = .44 m ; $\phi_o = .2$ .....	205
<b>APPENDIX IV: Drop size measurements results .....</b>	<b>210</b>
APPENDIX IV-1: Tank diameter = .22 m ; $\phi_o = .1$ .....	211
APPENDIX IV-2: Tank diameter = .22 m ; $\phi_o = .3$ .....	225

APPENDIX IV-3: Tank diameter = .44 m ; $\phi_o = .1$ .....	226
APPENDIX V: Monte Carlo Simulation Program .....	240
APPENDIX V-1: Simulation program nomenclature .....	241
APPENDIX V-2: Simulation Program .....	243
APPENDIX V-3: Simulation Sample output .....	251
APPENDIX VI: Experimental Data of Okufi(1984) .....	257
NOMENCLATURE .....	258
BIBLIOGRAPHY .....	261

## TABLE OF TABLES

<b>Table 2.1</b>	: Correlation for Sauter mean diameter .....	48
<b>Table 3.1</b>	: Tanks Dimensions .....	59
<b>Table 4.1</b>	: Stirring speed and $\phi_o$ for hold-up measurements .....	82
<b>Table 4.2</b>	: Positions for unsteady state hold-up measurement .....	82
<b>Table 4.3</b>	: Local hold-up $\phi^*$ values for 700 rpm and $\phi_o = .2$ .....	83
<b>Table 4.4</b>	: Mass balance over the whole tank .....	84
<b>Table 4.5</b>	: Stirring speed and $\phi_o$ for drop sizing .....	85
<b>Table 4.6</b>	: Effect of number of realizations on Sauter mean diameter .....	85
<b>Table 4.7</b>	: Local Sauter mean diameters (mm) .....	86
<b>Table 4.8</b>	: Local Sauter mean diameters(mm) and hold-up values $\{\phi^*\}$ .....	86
<b>Table 4.9</b>	: Local values for the slope of Sauter mean diameters vs stirring speed .....	87
<b>Table 4.10</b>	: Percentage difference between the local Sauter mean diameter and $\{\phi^*\}$ values and tank averages .....	87
<b>Table 4.11</b>	: Standard deviation of local drop size distribution around the arithmetic mean diameter .....	88
<b>Table 4.12</b>	: Skewness factor of local drop size distribution around the arithmetic mean diameter .....	88
<b>Table 4.13</b>	: Curtosis factor of local drop size distribution around the arithmetic mean diameter .....	89
<b>Table 4.14</b>	: Average Sauter and arithmetic mean diameters .....	89
<b>Table 4.15</b>	: Percentage difference in local Sauter mean Diameter value for the two tank: equal tip speed scale up criteria .....	90
<b>Table 6.1</b>	: Breakage and coalescence functions' Constants .....	156
<b>Table 6.2</b>	: Computer time for the evaluation of the coalescence frequencies .....	157
<b>Table 6.3</b>	: Comparison between the population coalescence frequencies $f_c$ produced by the two algorithms .....	157

## TABLE OF FIGURES

<b>Figure 3.1</b>	: Standard tank configuration .....	60
<b>Figure 3.2</b>	: General design of mixing vessels .....	61
<b>Figure 3.3</b>	: Impeller details .....	62
<b>Figure 3.4</b>	: Endoscope sleeve details .....	63
<b>Figure 3.5</b>	: Photograph of the endoscope and the sleeve .....	64
<b>Figure 3.6</b>	: Photograph of the experimental set-up .....	65
<b>Figure 3.7</b>	: Endoscope photograph of the dispersion .....	66
<b>Figure 4.1</b>	: Positions for hold-up measurements .....	91
<b>Figure 4.2</b>	: Unsteady hold-up measurements .....	92
<b>Figure 4.3</b>	: Horizontal hold-up variations .....	93
<b>Figure 4.4</b>	: Horizontal planes standard deviation from $\phi_o$ .....	94
<b>Figure 4.5</b>	: Local hold-up values $\phi^*$ for two vertical planes .....	95
<b>Figure 4.6</b>	: Vertical planes standard deviation from $\phi_o$ .....	96
<b>Figure 4.7</b>	: Effect of variation of stirring speed on $\phi^*$ .....	97
<b>Figure 4.8</b>	: Effect of stirring speed variation on the overall tank standard deviation from $\phi_o$ .....	98
<b>Figure 4.9</b>	: Effect of tank total hold-up $\phi_o$ on overall tank standard deviation .....	99
<b>Figure 4.10</b>	: Effect of tank total hold-up $\phi_o$ on local values $\phi^*$ .....	100
<b>Figure 4.11</b>	: Positions for photography .....	101
<b>Figure 4.12</b>	: Effect of number of realizations on drop size distribution	102
<b>Figure 4.13</b>	: Horizontal variations in local Sauter mean diameter values	103
<b>Figure 4.14</b>	: Vertical variations in local Sauter mean diameter values	104
<b>Figure 4.15</b>	: Effect of stirring speed change on local Sauter mean diameter values (Vertically) .....	105
<b>Figure 4.16</b>	: Effect of stirring speed change on local Sauter mean diameter values (Horizontally) .....	106
<b>Figure 4.17</b>	: Variation of Sauter mean diameter with stirring speed .....	107
<b>Figure 4.18</b>	: Drop size distributions : Horizontal comparison .....	108
<b>Figure 4.19</b>	: Drop size distributions : Vertical comparison .....	109

<b>Figure 4.20</b>	: Drop size distributions : Effect of stirring speed (Height = 2 cm ; distance from centre = 9 cm) .....	110
<b>Figure 4.21</b>	: Drop size distributions : Effect of stirring speed (Height = 10 cm ; distance from centre = 7 cm) .....	111
<b>Figure 4.22</b>	: Drop size distributions : Effect of stirring speed (Height = 18 cm ; distance from centre = 9 cm) .....	112
<b>Figure 4.23</b>	: Drop size distributions : Effect of tank scale (Height = $6 D_T/22$ ) .....	113
<b>Figure 4.24</b>	: Drop size distributions : Effect of tank scale (Height = $6 D_T/22$ ) .....	114
<b>Figure 5.1</b>	: Flow inside stirred tanks .....	132
<b>Figure 5.2</b>	: Effect of turbulence mode on Sauter mean diameter dependency on stirring speed .....	133
<b>Figure 5.3</b>	: Drop breakage process .....	134
<b>Figure 5.4</b>	: Generalized plot of equation 5.13 : Breakage frequency vs drop size .....	135
<b>Figure 5.5</b>	: Simulation algorithm : General block diagram .....	136
<b>Figure 5.6</b>	: Simulation algorithm : Initiation .....	137
<b>Figure 5.7</b>	: Simulation algorithm : Simulation pass .....	138
<b>Figure 5.8</b>	: Simulation algorithm : Event selection and execution .....	139
<b>Figure 5.9</b>	: Simulation algorithm : Type of event selection .....	140
<b>Figure 5.10</b>	: Simulation algorithm : Breaking drop selection .....	141
<b>Figure 5.11</b>	: Simulation algorithm : Daughter droplets size selection ...	142
<b>Figure 5.12</b>	: Simulation algorithm : First coalescing drop selection .....	143
<b>Figure 5.13</b>	: Simulation algorithm : Second coalescing drop selection	144
<b>Figure 6.1</b>	: Comparison between the two algorithms : Sauter Mean Diameter(mm) .....	158
<b>Figure 6.2</b>	: Comparison between the two algorithms : Arith. Mean Diameter(mm) .....	159
<b>Figure 6.3</b>	: Comparison between the two algorithms : Transient breakage frequency .....	160
<b>Figure 6.4</b>	: Comparison between the two algorithms : Transient coalescence frequency .....	161
<b>Figure 6.5</b>	: Comparison between the two algorithms : Computer time	162

<b>Figure 6.6</b>	: Comparison between the two algorithms : Drop size distribution (Number of events = 500) .....	163
<b>Figure 6.7</b>	: Comparison between the two algorithms : Drop size distribution (Number of events = 5000) .....	164
<b>Figure 6.8</b>	: Comparison between the two algorithms : Drop size distribution (Number of events = 15000) .....	165
<b>Figure 6.9</b>	: Transient algorithm behaviour : Sauter & Arith. mean diameters .....	166
<b>Figure 6.10</b>	: Transient algorithm behaviour : Drop size distribution evolution .....	167
<b>Figure 6.11</b>	: Transient algorithm behaviour : Breakage and coalescence frequencies .....	168
<b>Figure 6.12</b>	: Effect of stirring speed on Sauter mean diameter .....	169
<b>Figure 6.13</b>	: Effect of tank hold-up on drop size distribution .....	170
<b>Figure 6.14</b>	: Comparison between the isotropic and non-isotropic drop size distributions .....	171
<b>Figure 6.15</b>	: Comparison between the simulated and experimental Sauter mean diameters .....	172
<b>Figure 6.16</b>	: Comparison between the simulated and experimental drop size distributions .....	173

# CHAPTER I

## INTRODUCTION

Liquid-Liquid dispersions are frequently encountered in chemical process industries such as metal extraction, nitration of hydrocarbons, and the separation of emulsions. The stringent economic constraints imposed upon the industry make it necessary to increase the understanding of the dispersion process so that better models could be developed for the design and scale-up of contacting equipment.

When two immiscible liquids are agitated in a batch or flow system, breakage and coalescence commence and the rates at which these processes continue are dependent on :

- (i) the physical and chemical properties of the liquids;
- (ii) the geometry of the mixing equipment;
- (iii) the system hydrodynamics and the operating parameters.

The process of disintegration is caused by the dynamic forces that act on the fluid globules as power is supplied to the system. Large drops tend to break down until a size is reached below which further breakage is unlikely. On the other hand, drop collisions promote drop coalescence leading to increase in drop sizes. These rate processes govern the resultant drop size distribution and mean diameters of the dispersion.

The difficulties associated with the study of the local hydrodynamics of the tank and the complexity of the process itself have so far prevented the development of general models from fundamentals.

Thus design equations for contacting equipment are still mostly based on empirical or semi-empirical correlations based on the experimental behaviour of selected systems. This raises the question of their applicability when designing outside the range of physical properties or operating conditions of the data banks from which these correlations were developed. In addition, the cost of pilot testing associated with empirical design practice adds to the overall economic pressures on the processes.

Scale-up is also a difficult problem to approach theoretically. In order to scale-up process equipment, some similarity requirements are to be satisfied. Complete similarity of model and equipment requires geometric, kinematic, dynamic, thermal and chemical similarity. Since it is impossible to achieve such combination due to incompatible conditions, partial similarity through empirical scale-up criteria is often used. Examples of these are the equal tip speed and equal power dissipation per unit mass criteria. The latter is supported by the Kolmogoroff theory of local isotropic turbulence while the former indicates the presence of non-isotropic turbulence.

However, dispersions studied in this Department have shown the dependency of Sauter mean diameter with stirring speed characteristic of isotropic turbulence but on scale-up they followed the equal tip speed rule.

The purpose of this study was to investigate this apparent inconsistency. This was achieved by studying the dispersion local characteristics in order to examine the assumption of spacial homogeneity used by different workers in the modelling of dispersions and its relevance to equipment size. The parameters measured were local hold-up values, drop size distributions and Sauter mean diameters.

Having found that the dispersions showed local non-isotropic characteristics, the effect of a combination of isotropic and non-isotropic turbulence modes on drop size distribution was studied using a specially developed simulation algorithm that introduced a new method for interaction evaluation.

In the following chapter, the literature relevant to dispersions inside tanks is reviewed. A full description of the experimental equipment used and the results of the experimental measurements are given in chapters III and IV. The simulation algorithm and the simulated results are given in chapters V and VI.

Finally, a summary of the conclusions and recommendations for future work is given in chapter VII.

## CHAPTER II

### LITERATURE REVIEW

In the following sections, the literature relevant to dispersions is reviewed. This includes drop breakage and coalescence as well as the measurement techniques used to evaluate dispersion properties.

#### 2.1 Dispersions

When two immiscible liquids are agitated together, one of them forms drops and becomes dispersed into the other which is then called the continuous phase. The resulting mixture is called a dispersion.

Dispersions can be stabilized by agitation. Coalescence and separation commence as soon as the agitation is stopped.

Three types of dispersions may be defined :

- (i) Complete dispersions in which separate fluid layers disappear.
- (ii) Uniform dispersions, which in addition to being complete, have local values of hold-up the same all over the vessel.
- (iii) In addition to 1&2 a dispersion may be called homogeneous if the local interfacial area and the Sauter mean diameter and drop size distribution are spatially uniform.

The process of dispersion is caused by the shear stresses produced by rotating impellers and cascaded through the fluid stream.

The performance of a mixing system depends on :

- (i) Impeller size, shape, position and speed of rotation.
- (ii) Tank size, shape, and internal fittings (e.g. baffles)
- (iii) Depth of liquid, physical properties and phase ratio.
- (iv) Ratio of impeller to tank diameter.

#### 2.2 Turbulence

*"Turbulent motion is an irregular condition of flow in which the various quantities show a random variation with time and space coordinates so that statistically distinct average values can be discerned (Hinze 1975)"*

Two turbulence criteria are defined :

- (i) Wall turbulence : generated by friction forces at fixed walls i.e. conduits or flow past solid (e.g. impeller blade)
- (ii) Free turbulence : generated by the flow of layers of fluid of different velocities past each other.

In turbulent flow, viscosity tends to convert the kinetic energy into heat, making turbulence dissipative in nature and causing it to become more homogeneous and less dependent on direction.

Homogeneous turbulence refers to the structure being the same in all parts of the flow field. Isotropic turbulence exists when the statistical averages are independent of direction (complete disorder) and no average shear stress or velocity gradient exists. If the statistical features show any preference for direction then the turbulence is called nonisotropic.

In the case of a constant average shear stress the nonisotropic turbulence is called homologous while it is called pseudo-homogeneous if the statistical features show a distinct constant periodicity in time and space.

For stationary and homogeneous turbulence<sup>1</sup> :

$$\overline{\dot{u}} = \overline{\ddot{u}} = \overline{\varepsilon} \quad (\text{ergodic hypothesis}) \quad (2.1)$$

The instantaneous velocity is given by :

$$u = \bar{u} + u' \quad (2.2)$$

where  $u'$  is the velocity fluctuations around the mean  $\bar{u}$ .

The time average velocity is given by :

$$\bar{u} = \bar{u}_x i + \bar{u}_y j + \bar{u}_z k \quad (2.3)$$

---

1 Three methods to average Eulerian velocity exist:

1. Time average for a stationary turbulence :

$$\overline{\dot{u}}(x_o) = \lim_{T \rightarrow \infty} \frac{1}{2T} \int_{-T}^{+T} u(x_o, t) dt$$

2. Space average for a homogeneous turbulence :

$$\overline{\dot{u}}(t_o) = \lim_{x \rightarrow \infty} \frac{1}{2x} \int_{-x}^{+x} u(x, t_o) dx$$

3. Ensemble average of N identical experiments :

$$\overline{\dot{u}}(x_o, t_o) = \frac{\sum_{n=1}^N U_n(x_o, t_o)}{N}$$

where  $\bar{u}_x$ ,  $\bar{u}_y$  and  $\bar{u}_z$  are the time average velocities in the  $x$ -,  $y$ - and  $z$ -direction respectively,  $i$ ,  $j$  and  $k$  being the unit vectors.

Similarly the turbulent velocity fluctuation is given by :

$$u' = u'_x i + u'_y j + u'_z k \quad (2.4)$$

For turbulence to be isotropic :

$$u'_x = u'_y = u'_z \quad (2.5)$$

must be satisfied.

According to Kolmogoroff(1941a, 1941b), if the Reynolds number of the flow is high enough, the small scale components of the turbulent velocity fluctuations are independent of the turbulence generating mechanism and consequently the turbulence is uniquely determined by the power dissipation per unit mass and the kinematic viscosity.

A length scale  $\eta$  and a velocity scale  $v$  were defined by Kolmogoroff as follows :

$$\eta = \left[ \frac{v^3}{\varepsilon} \right]^{1/4} \quad (2.6)$$

$$v = (v\varepsilon)^{1/4} \quad (2.7)$$

For isotropic turbulence to exist the linear scale  $L_e$  of the energy containing eddies must be large compared to the scale of energy dissipating eddies  $\eta$ , or

$$\left[ \frac{vL_e}{v} \right]^{3/4} \gg 1 \quad (2.8)$$

Two different flow regimes were defined according to the eddies size  $r$  (Kolmogoroff 1941). For  $L_e \gg r \gg \eta$  the flow is in the inertial subrange while it is in the universal equilibrium subrange if  $r < \eta$ .

Relating the two types of flow to the drop breakage phenomena it might be concluded that for  $r < \eta$  the breakage is controlled by the viscous forces which become less important as the size of the drop exceeds  $\eta$  and the inertia forces control the process (Shinnar 1961).

Due to the stochastic nature of turbulent flow fields, the problem is tackled from a statistical point of view. The well known energy cascade of turbulence model assumes that the eddies range in size from ones that are comparable to the dimensions of the vessel down to a small size governed by the balance of the viscous forces.

The large eddies are influenced by the boundaries and the turbulence generating device. Transfer of energy occurs to or from the large eddies by the turbulence generating device. These eddies, in turn, transfer their energy to smaller ones and the process continues until the smallest size reached where energy is dissipated by means of viscous dissipation.

If the field is isotropic, then the small eddies become independent of the large ones and equilibrium exists between the different scales.

In general, the large eddies follow the main flow and form what is known as the large scale flow. The small scale flow is considered to be that of the small eddies which is more important in the case of droplets breakage and coalescence since the drops are affected by their surroundings.

Konno *et al*(1981), Van't Reit(1973), Ali *et al*(1981), Schwartzberg and Treybal(1968) and Sprow(1967) pointed out that, the turbulence in agitated vessels is far from being homogeneous and different structures of turbulence exist. There is an agreement that the impeller discharge region show high periodicity of turbulence parameters and it is nonisotropic [Rao and Brodkey(1972), Mujumdar *et al*(1970), Van't Riet *et al*(1976)]. This was also confirmed by the study of energy spectrum in the form of  $k - \epsilon$  relations. Also it became evident that the intensity of turbulence is much higher within the impeller discharge stream as compared with the average in the vessel [Cutter (1966)].

Studies of drop breakage outside the impeller region indicated that genuine isotropic turbulence exists [Ali *et al*(1981) and Konno *et al*(1981)].

An examination of oscillograms of the velocity fluctuations probability density distribution at a point in space may give a clue to distinguish between isotropic and nonisotropic turbulence since the former gives Gaussian distribution while shear flow gives a skewed distribution [Hinze (1975)].

Considering the different velocity components in a stirred tank, it was found that the vertical component decays rapidly as the distance from the impeller increases while the radial one remains approximately constant over a horizontal cross-section and decreases with the increase of the vertical distance [Schwartzberg and Treybal (1968)].

## 2.3 Power Consumption and Power Number

Usually, the power consumption is related to the impeller rotational speed ( $N$ ) and the impeller diameter through the power number. Studies dated as long as 1880 by Unwin gave the power as :

$$\frac{P}{V} \propto N^3 D^2 \quad \text{for fully turbulent system} \quad (2.9)$$

or

$$N_p = \frac{P}{\rho N^3 D^5}; \quad H = D_T \quad (2.10)$$

where  $N_p$  is the power number which is a function of Reynolds number ( $N_{Re}$ ) and tank geometry as well as impeller type.

Rushton(1950) reported a value of 6.3 for  $N_p$  for  $.22 \leq D_T \leq 2.44m$  while Bates *et al*(1963) obtained 5.0 and attributed this to a lower friction in the torque measuring technique they used. They also found that  $N_p$  is a weak but complex function of impeller to tank diameter ratio and height of impeller above the tank base.

Nienow and Miles(1971) concluded that  $N_p$  increases with  $D$ ,  $D/D_T$  and  $C/D_T$  where  $C$  is the impeller clearance from the bottom of the tank.

Investigations by Van't Reit *et al*(1971), Greaves and Loh(1984) and Bujalski *et al*(1987) reported the change of values of  $N_p$  with scale and impeller disc thickness to impeller diameter ratio even for fully turbulent systems. This contradicts the early work of Rushton(1950) and the repeatedly reported results of  $N_p$  being constant for fully turbulent tanks.

The suggested relation is :

$$N_p = 2.5 \left[ \frac{x_1}{D} \right]^{-2} \left[ \frac{D_T}{T_o} \right]^{.065} \quad (2.11)$$

where  $x_1$  is the impeller disc thickness and  $T_o$  is a reference tank size of 1m (Bujalski *et al* 1987).

Bujalski and coworkers (1987) attributed this dependency to the fact that both skin friction over the impeller and form drag contribute to the forces on the agitators and they commented on the relation of the power number to scale-up and the erroneous results that may be obtained when  $N_p$  is considered to as a constant.

## 2.4 Specific Power Input $\epsilon$

For sufficiently high values of Reynolds number, the power input per unit volume for a standard tank configuration is given by :

$$\epsilon \propto N^3 D^2 \quad (2.12)$$

In a locally isotropic field,  $\epsilon$  may be given theoretically by (Nishikawa *et al* 1976):

$$\epsilon = 30\nu \left[ \frac{u_1'^2}{\lambda_f^2} \right] = 15\nu \left[ \frac{u_2'^2}{\lambda_g^2} \right] \quad (2.13)$$

where  $\nu$  is the viscosity,  $u_1'^2$ ,  $u_2'^2$  are the root mean square values of  $u_i$ ,  $\lambda_f$  is the longitudinal micro scale and  $\lambda_g$  is the lateral microscale and they are related through:

$$\lambda_f = \sqrt{2}\lambda_g \quad (2.14)$$

For systems that deviate from isotropic behaviour, an expression based on the theory of axisymmetric turbulence is used (Batchelor 1953) :

$$\epsilon = \frac{\alpha}{\alpha + \beta} \left[ 30\nu \frac{u_1'^2}{\lambda_f^2} \right] + \frac{\beta}{\alpha + \beta} \left[ 15\nu \frac{u_2'^2}{\lambda_g^2} \right] \quad (2.15)$$

Nishikawa *et al*(1976) studied the energy spectra in three geometrically similar vessels. They noticed that with scale-up, the energy spectra were shifted to the lower wave number side.

Investigating the different turbulence structures in a tank, Okamoto *et al*(1981) postulated two expressions for  $\epsilon$  as follow :

$$\epsilon_i = C_1 \left[ \frac{P}{\rho\nu} \right] \left[ \frac{b}{D_T} \right]^{-1.38} \exp \left[ -2.46 \frac{D}{T} \right] \quad (2.16)$$

for the impeller region, and

$$\epsilon_c = C_2 \left[ \frac{P}{\rho\nu} \right] \left[ \frac{b}{D_T} \right]^{.32} \left[ \frac{D}{D_T} \right]^{.78} \quad (2.17)$$

for the circulation region, where  $b$  is the turbine blade width and  $D_T$  is the tank diameter.

McManamey(1979) obtained better results for the Sauter mean diameter when it was correlated through the specific power input in the impeller region rather than the average power input per unit volume for the whole vessel.

Experimental measurements of the local power dissipation gave  $\epsilon_i$  up to 100 times the average value of  $\epsilon$  (Cutter 1966).

## 2.5 Minimum Stirrer Speed for Dispersion

As mentioned before, there is a minimum level of turbulence below which separate layers of fluid exist. To eliminate segregation a minimum stirrer speed has to be reached. Different workers suggested different correlations for  $N_{\min}$ . Nagata (1950) obtained a correlation for un-baffled tank system with four blades agitator as :

$$N_{\min} = 6D^{-2/3} \left[ \frac{\mu_c}{\rho_c} \right]^{1/9} \left[ \frac{\Delta\rho}{\rho_c} \right]^{26} \quad (2.18)$$

Van Heuven and Beek(1971) obtained :

$$N_{\min} = \frac{3.28g^{.38}\Delta\rho^{.38}\mu_c^{.08}\sigma^{.08}(1+2.5\phi)^{-9}}{D^{.77}\rho_m^{.54}} ; \quad \frac{D}{D_T} = \frac{1}{3} \quad (2.19)$$

Skelland and Seksaria(1978) obtained :

$$N_{\min} = C_o D^{\alpha_o} \mu_c^{1/9} \mu_d^{-1/9} \sigma^3 \Delta\rho^{.25} \quad (2.20)$$

where  $C_o$  and  $\alpha_o$  are functions of the impeller type and location.

In a recent publication, Skelland and Ramsay(1987) proposed the following correlation:

$$\frac{N_{\min}^2 \rho_m D}{g \Delta\rho} = C^2 \left[ \frac{D_T}{D} \right]^{2\alpha} \phi^{.106} \left[ \frac{\mu_m^2 \sigma}{D^5 \rho_m g^2 \Delta\rho^2} \right]^{.084} \quad (2.21)$$

where

$$\mu_m = \frac{\mu_c}{1 - \phi} \left[ 1 + 1.5 \frac{\mu_d \phi}{\mu_d + \mu_c} \right] \quad (2.22)$$

and

$$\rho_m = \rho_d \phi_d + \rho_c (1 - \phi_d) \quad (2.23)$$

are the mean viscosity and density of the dispersion respectively.

Skelland and Moeti(1989) used the previous expression to predict  $N_{\min}$  in the presence of surface contamination. They concluded that the differences between the predictions and measurements could be accounted for by the experimental error, a result, as they pointed out, contradicted the droplet phenomena where more elaborate allowance for contamination effect was required.

Usually  $N_{\min}$  is smaller than the speed required for a uniform dispersion. Skelland and Lee(1978) found that for a standard tank configuration fitted with a turbine impeller,  $N'$  is 8% higher than  $N_{\min}$  and proposed the correlations :

$$\frac{D^{1/2}N_{\min}}{g^{1/2}} = C_1 \left[ \frac{D_T}{D} \right]^{a_1} \left[ \frac{\mu_c}{\mu_d} \right]^{1/9} \left[ \frac{\Delta\rho}{\rho_c} \right]^{.25} \left[ \frac{\sigma}{D^2\rho_c g} \right]^3 \quad (2.24)$$

$$N_{\min} = C_o D^{\alpha_o} \left[ \frac{\mu_c}{\mu_d} \right]^{1/9} \sigma^3 \Delta\rho^{.25} \quad (2.25)$$

and

$$N' = N_{\min}(1 + x) \quad (x = .08 \text{ for standard configuration}) \quad (2.26)$$

where  $N'$  is defined as the speed at which the mixing index reaches 98%.

Van Heuven and Beek(1971) studied the effect of the dispersed phase fraction and obtained :

$$\frac{N_{\min} \rho^{1/2} D^{2/3}}{g^{1/2} \Delta\rho^{1/2} a_{32}^{1/6}} = 10 [N_{Re_{imp}}]^{-1} (1. + 2.5\phi) \quad (2.27)$$

Godfrey *et al*(1984) proposed a correlation between a minimum Reynolds number and a modified Suratman number which they used to correlate the published data.

## 2.6 Scale-Up of Liquid-Liquid Dispersions

It is necessary to define the design problem carefully and specify the objectives to be achieved by the process. This arises from the fact that, in mixing operations, it is possible to scale the process, the power data or the process results. An example is the situation where a rate process is affected only by the interfacial area and not the hydrodynamics (e.g. a very slow interfacial reaction). The objectives will be to maintain a constant specific area within the different tanks.

Normally in agitation and mixing processes, the process results are to be scaled as the case of liquid-liquid extraction. The overall rate of extraction or the extractor performance depends on both, the interfacial area and the mass transfer from the bulk to the interface which are functions of the hydrodynamics.

The latter example shows the need to scale both the process and its results. So an optimization problem arises if the different requirements for scale-up are not

compatible.

Both theoretical and empirical scale-up criteria have been proposed. In all of them geometrical similarity was assumed.

## **2.6.1 Theoretical scale-up criteria**

### **2.6.1.1 Kinematic Similarity**

For a system to be kinematically similar, in addition to geometrical similarity, the ratios of the velocities between the corresponding points in the tanks must be the same, or in other words, corresponding particles should trace out geometrically similar paths in the corresponding intervals of time.

### **2.6.1.2 Dynamic Similarity**

In addition to being geometrically similar, the ratios of all corresponding forces that accelerate or retard the motion have to be equal. That means the ratio of the forces that cause breakage or those tending to separate the coalescing particles are the same in both the model and the equipment at the corresponding points at the same intervals of time.

To apply these scale-up criteria, the following conditions must be satisfied :

1. The regime must be a relatively pure one, i.e. the resultant force within a regime has to be mainly due to viscous, surface or gravitational force and not a combination of them.
2. The flow structure should remain the same with the change in the vessel size.

### **2.6.1.3 Thermal and Chemical Similarity**

Geometrically similar systems are thermally or chemically similar when the corresponding temperatures, concentrations, temperature gradients and/or concentration gradients have the same ratios and the systems, if moving, are kinematically similar.

## 2.6.2 Empirical Scale-Up Criteria

In reality, it is not possible to use the above mentioned criteria for scale-up of agitated vessels due to the complexity and involvement of the tank hydrodynamics which renders it difficult to satisfy all the requirements of scale-up criteria within the vessel when the size changes.

To overcome this problem, the principle of partial similarity was applied for equipment design through the use of empirical criteria. These include :

- |   |                      |
|---|----------------------|
| a- Constant power input per unit volume $\epsilon$    | $\equiv N^3 D^2 = C$ |
| b- Constant tip speed                                 | $\equiv ND = C$      |
| c- Constant Reynolds Number $N_{Re}$                  | $\equiv ND^2 = C$    |
| d- Constant Froude Number $N_{Fr}$                    | $\equiv N^2 D = C$   |
| e- Constant Weber Number $N_{We}$                     | $\equiv N^2 D^3 = C$ |
| f- Constant Volumetric flow per velocity head $Q_v/H$ | $\equiv D/N = C$     |
| g- Constant number of total revolutions               | $\equiv ND^2 = C$    |

When scaling up using partial similarity, depending on the objectives of the process, one of the empirical scale-up criteria may be employed.

Some times the scale-up rule is not similar to any of the forms discussed above. Examples are the results of a polymerization process (Rushton 1977) :

$$N \frac{D^{4.1}}{D_T^3} = C \quad (2.28)$$

$$N \frac{D^{3.7}}{D_T^3} = .45 \quad (2.29)$$

and Nishikawa *et al*(1987) who showed that  $(N^3 D_T^2 D_T) (4P_o/\pi)$  was more appropriate for scaling the system Water-Honeybee wax and McLaughlin *et al*(1985) who proposed a correlation for  $a_{32}$  that included both the specific power input and the tip speed.

Another peculiar example is the scale-up of the minimum stirrer speed for dispersion, where most of the results lie between equal tip speed and equal power input per unit volume, the latter being the upper limit. This lead Skelland to conclude that, the equal power input per unit volume always give values for  $N$  higher than  $N_{min}$  so it is safe to assume equal power input scale-up criterion to insure complete dispersion [ Nagata(1950), Skelland & Seksaria(1978), Skelland & Ramsay(1987), Godfrey *et al*(1984) and Van Heuven & Beek (1971)]

## 2.7 Modelling of Stirred Tank Reactors (STR)

Design of liquid-liquid extractors or mixing equipments rely heavily on laboratory or pilot scale tests. Most of the design depends on experience and trial and error rather than well established theoretical basis. This may be attributed to the complexity and involvement of mixing systems hydrodynamics. The interactions between mass transfer, heat transfer, reaction kinetics and flow structure make it a difficult task to model and design extraction equipments.

The presence of turbulence, which affects the different rate processes, complicates the understanding of the process, since a complete analysis requires the solution of Navier-Stoke equations. Such a solution is not available for a real unsimplified problem. The existence of totally different turbulence regions inside the tank requires a rigorous treatment that recognizes the basic differences as well as establishing the necessary boundary conditions where the regions meet.

Two approaches exist for modelling such systems. The first ones are the non-interacting models which ignore the micromixing problems and use averages for the system properties like the surface area. They include the effective interfacial area models and drop size and residence time distribution models.

The Second category are the interacting models which incorporate microscale processes as well as macroscale ones. They provide a vehicle for treating drop breakage and coalescence and account for their effect on the overall process.

The importance of micromixing has been illustrated by Curl(1963) and Valentas *et-al*(1966). They showed that for chemically reacting systems, any reaction of order other than one is sensitive to micromixing.

The earlier models which can be classified as interacting models are the Population Balance Equation models (PBE's) which have the general form :

$$\frac{\partial M(x;t)}{\partial t} + \nabla(v_e M) + \nabla(v_i M) - B + D = 0 \quad (2.30)$$

The first term represents the rate of change of the dispersion state, the second, the spacial change, the third, the changes resulting from the interface transfer processes such as heat and mass transfer while the last two terms describe the changes due to disappearance and creation of drops i.e. breakage and coalescence.

The PBE's originated in the treatment of microbial growth. The first time the framework of PBE's appeared in chemical engineering literature was by Hulburt and

Katz(1964). Randolph and Larson(1971) discussed the application of PBE's in crystallization. Ramkrishna and coworkers(1976, 1977, 1978, 1981) studied the PBE's in connection with small populations in which random fluctuations would be important. They also discussed the general features of population balances with regard to their applicability in chemical engineering problems[Ramkrishna and coworkers (1973, 1974, 1976, 1981)]. Valentas and coworkers(1966a, b), Jeon and Lee(1986), Sovova(1981), Shah *et al*(1977), Chatzi and Lee(1987) and Laso *et al* (1987, 1988) used the PBE's to simulate liquid-liquid dispersions but at the expense of accuracy as simplifications were introduced.

Normally, when the different rate expressions are incorporated in PBE's, mixed integrodifferential equations result which render PBE's of limited use except for simplified cases.

The difficulties associated with PBE's when the rate processes were tackled, necessitate the search for other methods that can be used to analyse realistic situations. The development of digital computers made it possible to overcome most of PBE's limitations whenever a reliable model for the process was available through simulation which may be considered as an artificial realization of a real system.

## 2.8 Dispersion Simulation

Two different types of systems are to be simulated :

- (i) Deterministic systems which may be simulated by solving the sets of deterministic differential and algebraic equations that govern their behaviour e.g. mass transfer across a fixed interface like kinetic studies in Lewis cell or homogeneous reactions in single phase reactors.
- (ii) Stochastic systems which involve random motion of particles or lumps of fluid that necessitates the statistical treatment and they are best solved by the population balance equations or stochastic simulation methods or Monte Carlo simulation techniques.

As the problems involved in designing mixing equipment are of random nature, the discussion will be limited to the second type of the systems mentioned above.

On digital computers, random numbers that satisfy the calculated probability distributions are generated and used in conjunction with the appropriate models to predict the state of the system at time  $t + \Delta t$  knowing the system status at time  $t$ . This

requires the selection of a set of properties  $\vec{x}$  which in addition to time may define the status or state of both the population and the individual entities.

Two types of variations in the system state may be observed: the deterministic changes which are governed by ordinary algebraic and differential equations and cause variations in the particle state while preserving its identity. The other type is the abrupt changes that cause the loss of a particle identity through death or birth. Breakage and coalescence of drops where entities are destroyed and new ones produced are typical examples of the latter type of changes.

Application of the Monte Carlo simulation techniques requires *a priori* knowledge of the processes at the microscale level which, in case of dispersion splitting and coagulation, are the mechanisms of breakage and coalescence. An adequate algorithm that is free from flaws and redundancy makes it possible to handle mass transfer, heat transfer as well as complex chemical reactions for a real system.

The use of Monte Carlo techniques in chemical engineering was pioneered by Spielman and Levenspiel(1965) then followed by Zeitlin and Tavlarides(1972), Shah *et al*(1977), Gupta *et al*(1976), Ramkrishna and coworkers (1976a, 1976b, 1977a, 1977b), Bapat and Tavlarides(1983), Hsia and Tavlarides(1983), Okufi(1984). All research refer to liquid-liquid and solid-liquid dispersions.

Recently, other applications have been published in the literature such as prediction of the properties of fluids and study of turbulence parameters in complex flow fields(Swaminathan *et al*(1986).

## 2.9 Breakage and Coalescence of Drops

### 2.9.1 Breakage of Drops

In a stagnant or turbulent field, different forces act on the drops. They are :

- (i) buoyancy and gravitational forces
- (ii) inertial forces
- (ii) viscous shear forces
- (iv) interfacial tension forces

These forces act simultaneously on a drop causing deformation and ultimately fragmentation.

Deformation depends on the type of flow as well as the above mentioned forces. Two types of flow exist in stirred tanks, plane hyperbolic and Coutte type.

When the external forces of magnitude  $\tau$  per unit area act on a drop, it undergoes deformation which sets up internal flow which in turn causes viscous stresses as well as dynamic pressure. Interfacial tension gives rise to surface forces that tend to counteract the deformation.

The drop size as well as the physical properties and flow conditions play a prominent role in determining the stability of the entity.

Hinze(1955) studied the breakage of drops in both air and liquid streams and correlated the different parameters through Weber Number ( $N_{We}$ ) which is given by  $\rho u^2 a / \sigma$  where  $\rho$  is the density of the drop,  $u$  is the velocity difference across the drop diameter,  $a$  is the drop diameter and  $\sigma$  is the surface tension. He concluded that there is a maximum value for Weber number,  $(N_{We})_c$ , above which the drop tends to split. This critical value depends to a great extent on the viscosity ratio  $\mu_d / \mu_c$ . Dispersion becomes difficult as  $\mu_d / \mu_c$  deviates from unity until lower and upper bounds beyond which no breakage can occur. These bounds were found by Karam and Bellinger(1968) to be  $.005 \leq \mu_d / \mu_c \leq 4$ .

As  $N_{We}$  becomes much bigger than  $(N_{We})_c$ , the breakage mechanism becomes complicated [Hinze(1955)].

Ali *et al*(1981), Chang *et al*(1981) and Konno *et al* (1981) reported two mechanisms for breakage in stirred tanks, namely, ligament stretching and turbulent fragmentation.

In the next sections breakage and coalescence are discussed in detail and the relevant models are reported.

### 2.9.1.1 Maximum Drop Size

Taylor(1932) pioneered the study of drop breakage in a two dimensional simple extensional flow. He proposed the expression:

$$a_{\max} = \frac{2\sigma(\mu_d + \mu_c)}{\alpha\mu_c\left(\frac{19}{4}\mu_d + 4\mu_c\right)} \quad (2.31)$$

No reference was made for the value to be used for the parameter  $\alpha$  but Shinnar(1961) suggested the use of the root mean square value of the strain rate  $\partial u_1/\partial x_2$ .

From consideration of the forces affecting drops in a turbulent flow field assuming local isotropy, Kolmogoroff proposed

$$N_{We_c} = k \rho_c \varepsilon^{2/3} \frac{a^{5/3}}{\sigma} = \text{constant} \quad (2.32)$$

and

$$a_{\max} = k \left[ \frac{\sigma}{\rho_c} \right]^{3/5} \varepsilon^{-2/3} \quad a \gg \eta \quad (2.33)$$

Shinnar (1961) substituted  $\varepsilon$  by  $\bar{\varepsilon} \Leftrightarrow N^3 D^2$  and obtained :

$$a_{\max} = k \left[ \frac{\sigma}{\rho_c} \right]^{3/5} N^{-6/5} D^{-4/5} \quad (2.34)$$

For a  $\ll \eta$ , the viscous forces dominate and may no longer be neglected. The corresponding expressions for  $(N_{We})_c$  and  $a_{\max}$  are

$$(N_{We})_c = \mu_c \left[ \frac{\delta v}{\delta a} \right] \left[ \frac{a}{\sigma} \right] = f \left( \frac{\mu_d}{\mu_c} \right) \quad (2.35)$$

$$a_{\max} = k \left[ \frac{\sigma v_c^{1/2}}{\mu_c} \right] \varepsilon^{1/2} f \left( \frac{\mu_d}{\mu_c} \right) \quad (2.36a)$$

$$= k' \sigma v_c^{1/2} \mu_c^{-1} N^{-3/2} D^{-1} f \left( \frac{\mu_d}{\mu_c} \right) \quad (2.36b)$$

Rearranging Equation 2.34, we obtain

$$a_{\max} \left[ \frac{\rho_c^{3/5} N^{6/5} D^{4/5}}{\sigma^{3/5}} \right] = c \quad (2.37)$$

Van Heuven (1969) reported  $c$  to be  $12 \times 10^{-2}$  while Van Heuven and Beek(1971) reported a value of  $9.4 \times 10^{-2}$ . Sprow(1967) and Chen and Middleman(1967) reported  $c$  as  $10.2 \times 10^{-2}$ .

This diversity of values may be attributed to the differences in the properties of the systems investigated and the fact that all authors considered the systems to be locally isotropic and neglected the viscous forces effect.

It worth mentioning that the correlations are specific to systems with low hold-up values or  $\phi_o \rightarrow 0$ . To include the effect of the hold-up, a function of the form

$$\frac{a_{32}(\phi)}{a_{32}(0)} = (1 + c'\phi) \quad (2.38)$$

was proposed. Vermeulen *et al*(1955) reported a value of 3.3 for  $c'$  while Van Heuven and Beek(1971) reported a value of 2.5. Other values may be found in **Table 2.1** Van Heuven and Beek(1971) discussed the effect of  $\phi_o$  and deduced that not only enhanced coalescence rate but influence of the drops on the small scale flow is mainly responsible for the increase in drop size with  $\phi_o$ .

Doulah (1975) used the Kolmogorof theory of local isotropy to prove that the maximum value for  $c'$  is 3.

The discussion so far has been confined to locally isotropic systems. If non-isotropy is considered, then it is of primary importance to determine the mechanism of breakage and to evaluate the dependency of velocity fluctuations across the drop diameter on the system parameters.

Two mechanisms or forms of dependency may be specified :

- (i) Velocity fluctuations are functions of the main flow i.e. the small scale flow is not statistically independent of the turbulence generating mechanism.

Assuming that  $\overline{u(a)^2} \propto (ND)^2$  i.e. it is proportional to the large scale flow which is in turn proportional to the impeller rotational speed, the following expression may be deduced for  $a_{\max}$  :

$$\frac{\rho_c N^2 D^2 a_{\max}}{\sigma} = \text{constant} \quad ; \quad a_{\max} \propto N^{-2} \quad (2.39)$$

- (ii) Velocity fluctuations are functions of the spatial distribution of the average velocities of the flow which results in :

$$\frac{\rho_c N^2 a_{\max}^3}{\sigma} = \text{constant} \quad ; \quad a_{\max} \propto N^{-2/3} \quad (2.40)$$

for the inertia subrange.

Results obtained by Sprow(1967) contradict the assumption of negligible viscous forces for  $a \gg \eta$ . His results were best fit for Equation 2.36b although his drop sizes were well above the Kolmogoroff microscale of turbulence  $\eta$ .

Konno *et al*(1977) proposed a function  $\psi(N_{Re})$  to account for the viscous forces or :

$$\rho_c \frac{\overline{u^2(a_{max})} a_{max}}{\sigma} \psi(N_{Re}) = constant \quad (2.41)$$

where

$$N_{Re} = \overline{u^2(a_{max})}^{1/2} a_{max} / \nu_c \quad (2.42)$$

and  $\nu_c$  is the kinematic viscosity.

No correlation for  $\psi(N_{Re})$  was reported in the literature so far and Konno *et al*(1977) mentioned that the form is unknown.

In actual fact, their work was an extension of early work by Hinze(1955) and Arai *et al*(1977) who introduced a viscosity number  $N_{vi}$  to account for the viscous effects. Calabrese and coworkers (1986a, b, c) studied the relative effect of both the viscosity and surface tension.

### 2.9.1.2 Minimum Drop Size

In agitated vessels, turbulence and the physical and chemical properties control the rate of coalescence. Local velocity fluctuations increase the rate of collision giving rise to a higher coalescence probability.

When two drops collide, a continuous film separate them and according to Shinnar(1961) an adhesion force tends to keep them together while the turbulent eddies act to separate them. There exists a minimum size  $a_{min}$  below which the effect of the turbulent eddies becomes insignificant and the drops tend to coalesce. At  $a_{min}$ , the adhesion energy balance the kinetic energy of the drops. Shinnar(1961) calculated  $E_a$  the adhesion energy as :

$$E_a = \int_{h_o}^{\infty} F(h) dh = \pi \int_{h_o}^{\infty} \int_h^{\infty} \frac{a_1 a_2}{a_1 + a_2} f(h) dh dh' \quad (2.43)$$

$$= 2 \frac{a_1 a_2}{a_1 + a_2} A(h_o) \quad (2.44)$$

where  $A(h_o)$  is defined by :

$$A(h_o) = \frac{1}{2} \pi \int_{h_o}^{\infty} \int_h^{\infty} f(h) dh dh' \quad (2.45)$$

is the energy necessary to separate two drops initially their centres at the minimum separation distance  $h_0$  to a distance  $h$ .

For two drops of the same size, Equation 2.44 reduces to :

$$E_a = A(h_0)a \quad (2.46)$$

The kinetic energy of two drops of size  $a$  in movement relative to each other is

$$E_k = \overline{\rho u^2(a)} a^3 \quad (2.47)$$

equating the two energies, it is possible to obtain :

$$\frac{\overline{\rho u^2(a)} a^2}{A(h_0)} = \text{constant} \quad (2.47)$$

In a locally isotropic flow field, the turbulent velocity fluctuations are given by :

$$\overline{u(a)^2} \propto (\epsilon a)^{2/3} \quad (2.48)$$

Equating  $a$  to  $a_{\min}$  and substituting in Equation 2.48 for  $u^2(a)$  we obtain :

$$a_{\min} = c \rho_c^{-3/8} \epsilon^{-1/4} A(h_0)^{3/8} = c' \rho_c^{-3/8} N^{-3/4} D^{-1/2} \quad ; \quad \text{for } a \gg \eta \quad (2.49)$$

If the size  $a$  is less than  $\eta$ , then the viscous shear forces dominate the forces affecting the drop. Sprow(1967) gave the following express in this case :

$$\frac{\mu_c \nabla u' a^2}{F} = \text{constant} \quad (2.50)$$

where  $\nabla u'$  is the local velocity gradient and  $F$  is the adhesion force. Substituting for  $\nabla u'$  by  $\nabla u' = k \epsilon^{1/2} \nu_c^{-1/2}$  he obtained :

$$a_{\min} = k F^{1/2} \mu_c^{-1/2} \nu_c^{1/4} \epsilon^{-1/4} \quad (2.51)$$

### 2.9.1.3 Sauter Mean Diameter ( $a_{32}$ ) and Drop Size Distribution

Most investigators reported a linear relationship between  $a_{32}$  and  $a_{\max}$  in the form :

$$\frac{a_{32}}{a_{\max}} = C \quad (2.52)$$

where the value of  $C$  ranges from .5 (Van Heuven and Beek (1971)) to .65 (Sprow 1967).

A large number of correlations for  $a_{32}$  was given in the literature, perhaps as many as the number of workers in the field. They agreed on the general form :

$$\frac{a_{32}}{D_I} = C_1 f(\phi) N_{we}^{C_2} \quad (2.53)$$

where  $f(\phi)$  accounts for the effect of the dispersed phase fraction and  $C_1$  and  $C_2$  are constants for a specific system.

The most frequently used exponent for  $N_{we}$  is -0.6 which is in accordance with the theory of local isotropy of Kolmogoroff and  $f(\phi)$  is normally given by  $(1 + C_3\phi)$ . A summary of the different correlations used is given in **Table 2.1**

McLaughlin *et al*(1985) gave a different form for  $a_{32}$  :

$$\text{Specific area} = \frac{6\phi}{a_{32}} = 0.186\phi^\alpha \sigma^\beta \mu_d^\gamma \rho_c^\delta \rho_d^{.71} \left(\frac{P}{V}\right)^\zeta \left(\frac{\pi ND}{100}\right)^\theta \quad (2.54)$$

where

$$\alpha = 1.54 + .12 \ln(\phi) + .15 \ln(\mu_d)$$

$$\beta = 5.77 - 1.04 \ln(\sigma)$$

$$\gamma = .74 - .03 \ln(\mu_d)$$

$$\delta = 78.6 - 22.5 \ln(\sigma) - 6.93 \ln(\mu_d)$$

$$\zeta = .68 + .08 \ln(\phi) - 0.1 \ln\left(\frac{P}{V}\right)$$

$$\theta = 1.35 + .12 \ln(\mu_d) - .73 \ln\left(\frac{\pi ND}{100}\right)$$

Drop size distributions are functions of both the physicochemical and hydrodynamic properties of the system. The frequently encountered distributions are the normal and log-normal distributions.

For normal distribution, the following equation holds :

$$Y(a) = \frac{1}{s\sqrt{2\pi}} \exp\left[-\frac{(a - a_{10})^2}{2s^2}\right] \quad (2.55)$$

and for log-normal

$$Y(a) = \frac{1}{\log s \sqrt{2\pi}} \exp\left[-\frac{(\log a - \log a_{10})^2}{2(\log s)^2}\right] \quad (2.56)$$

where  $\bar{a}$  is the mean and  $s$  is the standard deviation.

Other distributions were found in the literature but were limited to specific systems (Chen and Middleman 1967, Gal-Or and Hoelscher 1966).

### 2.9.1.4 Transient Drop Sizes

Attempts were made to correlate the transient drop sizes by Hong and Lee (1985). They related the transient Sauter mean diameter  $a_{32}^*$  to  $a_{32}$  and other system parameters as follows :

$$\frac{a_{32}^* - a_{32}}{a_{32}} = \alpha(Nt)^{-\beta} \quad (2.57a)$$

$$= 29.7 \left[ \frac{D}{D_T} \right]^{-2.015} F^{.5508} (Nt)^{-.7} \quad (2.57b)$$

where F is  $N_{w0}/N_{Re}$  and  $a_{32}^*$  is the transient Sauter mean diameter.

$$Nt_{\min} = 1995.3 \left[ \frac{D}{D_T} \right]^{-2.37} F^{.97} \left[ \frac{\mu_d}{\mu_c} \right] N_{Fr}^{-.66} \quad (2.58)$$

or

$$t = t_{m,c} \quad \text{for} \quad \frac{a_{32}^* - a_{32}}{a_{32}} = C \quad (2.59)$$

### 2.9.1.5 Drop Breakage Rate

From the previous discussion, it may be noticed that most of the work done was concentrated on the forces affecting droplets and on the maximum stable diameter [(Taylor(1932a, 1932b, 1934), Hinze(1955), Shinnar(1961) , Khakhar and Ottino(1986), Cox(1969), Harper and Moore(1968), Mikami *et al*(1975), Rallison and coworkers(1978, 1981a, b, 1984), Hinch and coworkers(1980, 1980) and Sprow(1967)].

Although all these information help to characterize the steady state of the system, it is of no help in the solution of the PBE's or for carrying out the Monte Carlo simulation. This is due to the fact that both methods follow the dispersion evolution through time, hence they require rate expressions for the different processes simulated.

The basic expressions describing breakage rate are :

$$r(a')da = g(a')MA(a')da'$$

$$r(a, a')dada' = g(a')v(a')\beta(a, a')MA(a')dada' \quad (2.60)$$

where  $r(a')da$  is the number of drops with diameter  $a \rightarrow a+da$  breaking per unit time per unit volume;  $M(a, a')da$  is the number of daughter drops of diameter between  $a'$  and  $a'+da'$  produced by the breakage of drops of size  $a \rightarrow a+da$ ,  $M$  is the total number of drops of all sizes present in the system per unit volume,  $A(a')da'$  is the fraction of drops with diameters  $a' \rightarrow a'+da'$ ,  $g(a')$  is the fraction of drops of diameter  $a'$  breaking per unit time per unit volume or breakage frequency and  $v(a')$  is the number of daughter drops produced by the breakage of a drop of diameter  $a'$ .

### 2.9.1.5.1 Breakage Frequency

Valentas and Amundson(1966), Ramkrishna(1974) and Narsimhan *et al*(1979) used a power law for the breakage frequency of the form

$$g(a) = ka^n \quad ; \quad n = 0, 1, 2, 3, \dots \quad (2.61)$$

where zero corresponds to breakage in the colloidal subrange.

Ramkrishna(1974), Narsimhan *et al*(1979) and Shiloh(1973) concluded that this model fits well the data they tested.

Extension of this models to systems other than those studied by the authors is doubtful because they do not account for system properties.

Curl and coworkers(1969, 1971) assumed an analogy between drop breakage and molecular decomposition and obtained :

$$g(a) = k\varepsilon^{1/3} a^{-2/3} \exp\left[-k \frac{\sigma}{\rho_c \varepsilon^{2/3} a^{5/3}}\right] \quad (2.62)$$

$$g(a) = kND^{2/3} a^{-2/3} \exp\left[-k \frac{\sigma}{\rho_c N^2 D^{4/3} a^{5/3}}\right] \quad (2.62b)$$

Coulaloglou and Tavlarides(1977) derived an expression based on the dispersion hydrodynamics which differs from Curl's in the use of the dispersed phase density - rather than the continuous one.

$$g(a) = k\varepsilon^{1/3} a^{-2/3} \exp\left[-k \frac{\sigma}{\rho_d \varepsilon^{2/3} a^{5/3}}\right] \quad (2.63)$$

Delichatsios and Probstein(1976) derived an expression based on the argument that the drop breaks whenever the turbulent velocity fluctuations difference across the diameter exceeds the critical velocity for breakage.

$$g(a) = k \frac{\sqrt{\overline{u^2}}}{a} \left[ \exp\left[-\frac{u_b^2}{2\overline{u^2}}\right] - \exp\left[-\frac{u_c^2}{2\overline{u^2}}\right] \right] \quad (2.64)$$

where

$$u_c = 3\overline{u^2}^{1/2}$$

$$\overline{u^2} = 1.88(\epsilon a)^{2/3}$$

$$u_b = \left( \frac{\sigma}{\rho a} \right)^{1/2}$$

Konno *et al*(1981) derived another expression for  $g(a)$  for the non-isotropic turbulence field with  $u^2(a) \propto (ND)^2$  and found that the solution of the equation for  $g(a)$  was:

$$g(a) = k \operatorname{erfc}(\eta) \quad (2.65)$$

where

$$\eta = k \left[ \frac{\sigma^{3/2}}{N^3 D^3 \rho_c^{3/2} a^{3/2}} \right]^{1/3} \quad (2.66)$$

A careful examination of their equations pointed out that the correct solution was not equation 2.66 but

$$g(a) = k N^3 D^2 \exp\left[-k \frac{\sigma}{\rho_c a N^2 D^2}\right] \quad (2.67)$$

For isotropic turbulence the same authors obtained :

$$g(a) = k \left[ \frac{N^3 D^2}{a^2} \right]^{1/3} \int_{\zeta}^{\infty} 3 \sqrt{\frac{6}{\pi}} x^2 \exp\left[-\frac{3x^2}{2}\right] dx \quad (2.68)$$

where

$$\zeta = k \frac{\sigma^{1/2}}{\rho_c^{1/2} N^{2/3} a^{5/6}} \quad (2.69)$$

Stamatoudis(1977) used Curl and Ross model with the kinetic energy replaced by the shear energy in order to derive expressions for both laminar and transitional flow regimes. The shear energy  $E_s$  is given by :

$$E_s \propto \mu_c G^2 a^3 t_{br} \quad (2.70)$$

where  $G$  is the shear stress given by :

$$G \propto \left[ \frac{P}{\mu_c} \right]^{1/2} N D^{3/2} \quad (2.71)$$

for laminar flow, and

$$G_{eff} \propto \left( \frac{P}{\mu_c} \right) \propto \left[ \rho_c^{m+1} \frac{N^{m+1}}{\mu_c^{m+1}} \right]^{1/2} D^{(2m+5)/2} \quad (2.72)$$

for the transitional region, in which case  $G_{eff}$  is an effective shear stress that accounts for the fact that both laminar and turbulent flow exist.

The index  $m$  increases with  $(N_{Re})_T$  from -1 at  $(N_{Re})_T = 15$  to a maximum of .16 at  $(N_{Re})_T = 1300$  and then decreases to zero.

The corresponding frequency expressions are :

$$g(a) = k \exp \left[ -k \frac{\sigma}{\mu_c a N D T^2} \right] \quad (2.73)$$

for laminar region, and

$$g(a) = k \exp \left[ -k \frac{\sigma}{\mu^{-m} \rho_c^{m+1} a N^{m+2} D^{2m+3} T^2} \right] \quad (2.74)$$

for transitional region.

The expressions derived by Colaloglou and Tavlarides(1977) were based on the actual fluid dynamics. They are more realistic compared to the rest despite the fact that they were derived for an ideal system with vanishing dispersed phase fraction. A similar approach is followed in this work for the dispersion modelling.

## 2.9.2 Droplets coalescence

Due to the presence of turbulent velocity fluctuations, drops in a turbulent flow regime collide with each other. A thin continuous film separate the colliding drops. The film thickness decreases with time as long as the drops remain intact and the forces sustaining the drops prevail. This drainage process continues until a critical thickness is reached where the film rupture occurs and the drops coalesce. So an important factor in coalescence is the time the drops stay in contact. If this time is less than the time required for film drainage, the drops separate again and no coalescence takes place. This gave rise to the concept of efficiency of collision.

The general expression for coalescence rate is

$$F(a, a') da da' = Z(a, a') da da' \lambda(a, a') \quad (2.75)$$

$$Z(a, a') da da' = h(a, a') MA(a) MA(a') da da' \quad (2.76)$$

where  $F(a, a') da da'$  is the rate of coalescence per unit volume,  $\lambda(a, a')$  is the collision

efficiency of collision of drops  $a$ ,  $a'$  and  $h(a, a')$  is the collision frequency between drops  $a$ ,  $a'$  and  $MA(a)$ ,  $MA(a')$  are the number of drops per unit volume of diameters  $a \rightarrow a+da$  and  $a' \rightarrow a'+da'$  respectively.

### 2.9.2.1 Collision Frequency $h(a, a')$

Most of the work in the literature expressed the collision frequency as a function of the impeller speed, impeller diameter, tank diameter, hold-up and the system physical properties.

From consideration of the system hydrodynamics and analogy with the kinetic theory of gases, several models for the collision frequency and efficiency were derived.

For a uniform shear flow, Smoluchowski(1917) derived the expression

$$h(a, a') = \frac{4}{3} \left[ \frac{a}{2} + \frac{a'}{2} \right]^3 G \quad (2.77)$$

where  $G$  is the velocity gradient in direction perpendicular to the direction of particle movement.

Camp and Stein(1943) extended the equation for turbulent flow by substituting  $G$  by  $(\epsilon/\nu)^{1/2}$  the turbulent velocity gradient.

Saffman and Turner(1956) obtained

$$h(a, a') = \frac{8\pi}{15} \left[ \frac{a}{2} + \frac{a'}{2} \right] \left[ \frac{\epsilon}{\nu} \right]^{1/2} \quad (2.78)$$

for drops smaller than  $\eta$ , the microscale of turbulence and with  $\rho_d/\rho_c \approx 1$ .

For drops larger than  $\eta$ , the effect of the impact of the eddies on them is to cause random movement. From analogy with the kinetic theory of gases Rietema(1964), assuming two identical drops, obtained :

$$h(a, a) = k a^2 \overline{u(r)} NA(a) \quad (2.79)$$

where  $u(r)$  is the turbulent velocity fluctuations at the average distance between the drops.

Kuboi *et al*(1972) obtained a similar expression :

$$h(a, a) = k a^2 \overline{u^2(a)}^{1/2} NA(a) \quad (2.80)$$

where  $\overline{u^2(a)}$  is given by  $2.0 (\epsilon a)^{2/3}$

Abrahamson(1975) obtained :

$$Z(a, a') = 5NA(a)NA(a') (a + a')^2 (\overline{u^2(a)} + \overline{u^2(a')})^{1/2} \quad (2.81)$$

Coulaloglou and Tavlarides(1976) obtained the following expression from analogy with the kinetic theory of gases :

$$h(a, a') = \frac{\pi}{2} (a^2 + a'^2) [\overline{u^2(a)} + \overline{u^2(a')}]^{1/2} \quad (2.82)$$

Delachatsios and Probstein also using the kinetic theory of gases obtained :

$$h(a, a') = k(a + a')^2 \left[ u^2 \left( \frac{a}{2} + \frac{a'}{2} \right) \right]^{1/2} \quad (2.83)$$

All expressions for collision frequency were derived from the analogy with the kinetic theory of gases. The assumption of an ideal behaviour at a vanishing dispersed phase fraction is rather doubtful and a better understanding of the interaction between the approaching drops within a fluid medium is yet to be developed.

### 2.9.2.2 Collision Efficiency

As mentioned before, not all collisions result in coalescence. Collisions become efficient only when the time the drops stay intact is larger the time required for the drainage of the continuous phase film separating the drops.

Valentas *et al*(1966) used a constant for the collision efficiency if the drop size is less than  $a_{\max}$ . Otherwise, it was a function of  $a$  and  $a_{\max}$  :

$$\lambda(a, a) = k \quad a < a_{\max} \quad (2.84)$$

$$\lambda(a, a) = k' \exp[-k(a - a_{\max})^2] \quad a \geq a_{\max} \quad (2.85)$$

Other workers tried to relate the contact time  $\bar{t}$ , which was assumed to be randomly distributed, to the coalescence time  $\bar{\tau}$  which was considered to be deterministic.

The general expression used was :

$$\lambda(a, a') = \exp\left(-\frac{\bar{\tau}}{\bar{t}}\right) \quad (2.86)$$

where both  $\bar{\tau}$  and  $\bar{t}$  are averages.

From the kinetic theory of gases, Coulaloglou and Tavlarides(1977) obtained :

$$\lambda(a, a') = \exp\left[-k \frac{\mu_c \rho_c \varepsilon}{\sigma^2 (1 + \phi)^3} \left( \frac{aa'}{a + a'} \right)^4\right] \quad (2.87)$$

while Ross and Curl obtained :

$$\lambda(a, a') = \exp\left[-kf(h_o, h_c) \frac{\mu_c \rho E}{\sigma^2} \left(\frac{aa'}{a+a'}\right)^4\right] \quad (2.88)$$

both equations being for deformable drops.

In actual fact, the two expressions are identical since  $f(h_o, h_c)$  is constant and  $(1 + \phi)$  is a term to account for the turbulence damping due to the presence of the dispersed phase.

For rigid drops, Coualoglou obtained :

$$\lambda(a, a') \propto \exp\left[-k \frac{v_c}{\epsilon^{1/3}} (a+a')^{4/3}\right] ; \quad a+a' \gg \eta \quad (2.89)$$

and

$$\lambda(a, a') \propto \exp\left[-k \frac{v_c^{3/2}}{\epsilon^{1/2}} (a+a')^2\right] ; \quad a+a' < \eta \quad (2.90)$$

Sovova(1981) on the other hand replaced the mechanism of film drainage by the effect of collision impact in accordance with Howarth(1964) :

$$\lambda'(a, a') = \exp\left[-\frac{k\sigma}{\rho_d N^2 D^{4/3}} \frac{(a^2+a'^2)(a^3+a'^3)}{a^3 a'^3 (a^{2/3}+a'^{2/3})}\right] \quad (2.91)$$

If the two mechanisms coexist then :

$$\lambda_{eff}(a, a') = \lambda(a, a') + \lambda'(a, a') - \lambda(a, a')\lambda'(a, a') \quad (2.92)$$

Recently, Das *et al*(1987) criticized the assumption that  $\bar{t}$  and  $\bar{\tau}$  are independent and  $\bar{\tau}$  is not random. They pointed to the fact that  $\bar{\tau}$  is governed by the turbulent forces fluctuations which lead to doubts about the validity of the assumption.

They treated the film drainage as an stochastic process and derived an expression for the film drainage :

$$\frac{dh}{dt} = -\frac{2hF(t)}{3\pi\mu_c} \left[\frac{1}{a} + \frac{1}{a'}\right] \quad (2.93)$$

where  $F(t)$  is a rapidly fluctuating white-noise process given by :

$$F(t) = \bar{F} - \delta T_f^{1/2} \zeta(t) \quad (2.94)$$

where  $F(t)$  is the instantaneous force on the drop pair,  $\bar{F}$  the mean force,  $\delta$  is the standard deviation of the force fluctuation,  $T_f$  is a time scale associated with force fluctuation and  $\zeta(t)$  is a Gaussian white noise.

Experimental measurements of coalescence frequencies, showed an increase with the dispersed phase fraction, stirrer speed and turbulence level, while a decrease with the increase of electrolyte concentration and density difference.

## **2.10 Measurements in Liquid-Liquid Dispersions**

Different techniques exist for the evaluation of dispersion parameters. The techniques may be divided into two main categories :

- (i) methods for the determination of drop size distribution
- (ii) methods for the measurement of the Sauter mean diameter

### **2.10.1 Methods for the determination of drop size distribution D.S.D.**

#### **2.10.1.1 Photography**

##### **2.10.1.1.1 Direct photography through a window or vessel wall**

Only suitable for very low dispersed phase fraction because of the drops interference with the light path. It requires large area of glass, or a transparent material imposing severe restrictions on the equipment construction.[Saito *et al*(1980), Bouyatiotis and Thornton(1967), Chen and Middleman(1967)]

##### **2.10.1.1.2 Photography using *in situ* probes**

More suitable for high hold-up fractions and large vessels. It normally consists of a microphotographic probe assembly inserted inside the vessel with a suitable design to minimise the disturbances to the flow.[Coulaloglou (1977), Brown & Pitt (1972), Calderbank (1958), Mlynek and Resnick(1972), Giles *et al*(1971)]

##### **2.10.1.1.3 Photography using fibre optics probes**

Two optical fibre rods with their ends facing each other with a proper clearance are inserted in a suitable assembly inside the vessel. One of the branches is used to project the light while the other, which is connected to the camera, is used as an image conduit.[Kirou *et al*(1988), Park and Blair(1975)]

Despite being the most reliable means for drop sizing, photography is tedious and time consuming due to analysis requirements. Drops overlapping and poor boundary definition prevent the effective use of automatic image analysers.

### **2.10.1.2 Sample Withdrawal Methods**

Different methods exist but they can be divided into three categories according to the method used for drop sizing.

#### **2.10.1.2.1 Photography**

The sample is drawn with a relatively large diameter tube and the dispersion is photographed while passing through it.[Godfrey *et al*(1987 )]

#### **2.10.1.2.2 Laser or Light refraction methods**

For this purpose, a small bore tube (~.05 -.2 mm dia.) is usually used. As the drops pass through the tube, they become cylindrical slugs. As the laser or light beam passes it suffers some refraction. The emerging beam is collected using a photodiode and the duration of the change in the current generated is an indication of slug length and the intensity is a measure of the intensity.[Verhoff(1969), Curl and coworker(1969), Janjua(1982), Okufi(1984), Kirou *et al*(1986, 1988)]

#### **2.10.1.2.3 Drop Stabilization**

A surfactant is added as the drops were withdrawn to prevent coalescence. The sample is then analysed by photography, microscopy or image analysers.[Tanaka (1985), Mlynek and Resnick(1972)]

Sample withdrawal methods suffer from two main drawbacks

- (i) Disturbance of the flow field
- (ii) The difficulty of maintaining iso-kinetic conditions for sample withdrawal.

As a consequence, most of the results reported so far indicated large values for the Sauter mean diameter compared to the results obtained by photography for the same systems.

### 2.10.1.3 Laser Doppler Anemometry

Crossing two laser beams at an angle  $\alpha$ , results in the creation of fringes of alternating dark and light areas with distinctive frequencies. A proper arrangement to receive and analyse the scattered light can give an unambiguous information about both size and velocity. Generally speaking, the methods may be divided into four main categories :

- (i) Correlation of the drop sizes with the signal visibility or fringe contrast.
- (ii) correlation of the drop size with the overall signal intensity
- (iii) correlation of the drop size with the time difference between signals received from two or more spatially separated detectors
- (iv) correlation of the drop size using a time of flight approach.

For the Laser Doppler Anemometry technique to be effective, the drops have to exhibit a Mie scattering pattern which require small drop sizes (<.15mm)

Recent attempts were made to extend the range of drop sizes and dispersed phase fraction.[Yeoman *et al*(1982), Bachalo & Houser(1985), Semiat & Dukler(1981), Plawsky and Hatton(1986), Lee & Srinivasan(1978), Costes & Couderc(1988), Hanzevack *et al*(1987)]

### 2.10.1.4 Drop Stabilizing Method

The vessel contents or a part of it (using a suitable trap) is stabilized either by encapsulation by a suitable film or rapid freezing. The drops then analysed by suitable means such as microphotography or microscopy[Tanaka(1985)]

### 2.10.1.5 Conductivity

The method depends on the changes in conductivity that takes place when a droplet suspended in strongly conducting liquid passes between two electrodes. The size is correlated to the conductivity and hence a drop size distribution as well as a drop mean diameter are obtained.[Hoffer and Resnick (1975)]

## **2.10.2 Methods for the determination of $a_{32}$**

The following techniques do not provide for the evaluation of drop size distribution but an average value for the Sauter mean diameter.

### **2.10.2.1 Chemical Methods**

The method can be used for systems with known kinetics. Normally a pseudo first order chemical reaction is used. Only the total interfacial area is obtained, not the drop size distribution.[Sharma and Fernandese 1967,

### **2.10.2.2 Light Scattering Techniques**

#### **2.10.2.2.1 Light-Extinction Method**

If a detector is aligned with the source of light which is passing through the dispersion, then the ratio of the intensity of the light received to the one received in the absence of the dispersion is a measure of the average drop size in the dispersion.(Miller *et al*(1963), Calderbank(1958)]

#### **2.10.2.2.2 Two-angle scattering method**

The method make use of the distribution of the scatter intensity rather than the intensity it self. It can give a mean and an indication for the drop size distribution.[Deich *et al*(1971, 1972)]

## **2.10.3 Hold-Up Measurements**

Surprisingly enough, very few investigations were reported in the literature for hold-up values in stirred vessels. The main interest is concentrated on the average hold-up values for continuous systems. Numerous studies were reported for other contactors e.g. reciprocating plate columns or multistage stirred columns. Also only average values are reported but not interstage hold-up profiles.

For stirred tanks, most researchers considered the initial hold up to be numerically

prevailing all over the tank. As a consequence, very few techniques were developed for local hold-up measurements.

The technique so far reported are :

- (i) For continuous operations, the flow is suddenly stopped and the tank contents were allowed to settle before the volumes were measured.
- (ii) Sample withdrawal using capillaries.
- (iii) A recently developed ultrasonic technique. Used only for columns. It correlates the hold up to the time taken by a sound signal to travel through dispersion to that taken through pure phases[Bonnet and Tavlarides(1987), Kirou *et al*(1988)]

Investigators	Correlation	Technique	
Bouyatiotis and Thornton(1967)	$a_{32} = a_{32}^0 + 1.18\phi \left[ \frac{\sigma^2}{\mu_c^2 g} \right] \left[ \frac{\Delta\rho\sigma^2}{\mu_c^2 g} \right]^{-0.62} \left[ \frac{\Delta\rho}{\rho_c} \right]^{0.65}$ $\frac{a_{32}^0 \rho_c^2 g}{\mu_c^2} = 29 \left[ \frac{\epsilon^3 g_c^3}{\rho_c^2 \mu_c g^4} \right]^{-0.32} \left[ \frac{\rho_c \sigma^2}{\mu_c^2 g} \right]^{0.14}$	Photography	6 bladed turbine
Doulah(1975)	$a_{32} = k(1 + 3\phi)\epsilon^{-2.7} \left( \frac{\sigma}{\rho_c} \right)^{3.5}$		Theoretical
Godfrey and Grilc(1984)	$a_{32} = 10^{(-1.118 + 0.74\phi)} \epsilon^{-2.735} \left[ \frac{\sigma g_c}{\rho_c} \right]^{1.734}$ <p>(Coalescing systems)</p>	Photography	6 bladed turbine (square X-section tank)
McManamey (1979)	$a_{32} = k \left( \frac{\sigma}{\rho} \right) P_{M7}^{-2.4}$ $P_{M7} = \frac{4}{\pi} P_c \left( \frac{D}{W} \right) N^3 D^2$ $= \frac{4P}{\pi D^2 W}$		Correlated other workers data

Table 2.1 : Correlations for Sauter mean diameter

Investigators	Correlation	Technique	
Nishikawa et al(1987)	$a_{32} \doteq 105 \bar{\epsilon}^{-\frac{2}{3}} \left( \frac{D_I}{D_T} \right)^{\frac{2}{3}} (1 + 2.5 \phi^{\frac{2}{3}}) \left( \frac{\mu_d}{\mu_c} \right)^{\frac{1}{3}} \left( \frac{\mu_c}{\mu_e} \right)^{\frac{1}{3}} \left( \frac{\sigma}{\rho} \right)^{\frac{2}{3}}$ $a_{32} \doteq 095 N_p^{-\frac{2}{3}} (1 + 2.5 \phi^{\frac{2}{3}}) \left( \frac{\mu_d}{\mu_c} \right)^{\frac{1}{3}} \left( \frac{\mu_c}{\mu_e} \right)^{\frac{1}{3}} N_{We}^{-\frac{2}{3}}$ (Break-up region) $a_{32} \doteq 0371 \bar{\epsilon}^{-\frac{1}{4}} \left( \frac{D_I}{D_T} \right)^{\frac{1}{4}} (1 + 3.5 \phi^{\frac{2}{4}}) \left( \frac{\mu_d}{\mu_c} \right)^{\frac{1}{4}} \left( \frac{\mu_c}{\mu_e} \right)^{\frac{1}{4}} \left( \frac{\sigma}{\rho} \right)^{\frac{3}{4}}$ $a_{32} \doteq 035 N_p^{-\frac{1}{4}} (1 + 3.5 \phi^{\frac{2}{4}}) \left( \frac{\mu_d}{\mu_c} \right)^{\frac{1}{4}} \left( \frac{\mu_c}{\mu_e} \right)^{\frac{1}{4}} N_{We}^{-\frac{3}{4}} D_I^{-\frac{3}{4}}$ (Coalescence region)	Drop stabilization	
Skelland and Lee(1981)	$a_{32}/D = 6.71310^{-4} \phi^{0.188} \left[ \frac{D_I}{D_T} \right]^{-1.034} N_{Re}^{-0.558} N_{Oh}^{-1.075}$ $N_{Oh} = \mu_c / \sqrt{\rho_c D_I \sigma}$	Photography	6 bladed turbine
Weinstein and Treybal(1973)	$a_{32} = 10^{(-2.319 + 0.672 \phi \sqrt{v_c}^{0.0722} \bar{\epsilon}^{-1.96})} \left[ \frac{\sigma g_c}{\rho_c} \right]^{-1.96}$	Light transmittance	6 bladed turbine (unbaffled vessel) Continuous system
Brown and Pitt(1974)	$a_{32} = k \left[ \frac{\sigma}{\rho \bar{\epsilon} t_c} \right]^{0.6}$	Light transmittance	6 blade turbine
	$a_{32}/D = 0.051(1 + 3.14\phi) N_{We}^{-0.6}$	Light transmittance	6 bladed turbine

Table 2.1 (Cont.)

Investigators	Correlation	Technique	
Calabrese and coworkers(1986)	$a_{xz}/D = 0.054 \left( \frac{ru_c N^2 D^3}{\sigma} \right)^{-0.6} \left[ 1 + 4.42 \left( \frac{ru_c}{ru_d} \right)^5 \frac{\mu_d ND}{sgma} \left( \frac{a_{xz}}{D} \right)^{1/3.6} \right]$	Photography	
Calderbank(1958)	$a_{xz}/D = 0.06(1 + 3.75\phi)N_{w_0}^{-0.6}$	Light transmittance	4 bladed paddle,
	$a_{xz}/D = 0.06(1 + 9\phi)N_{w_0}^{-0.6}$	Light transmittance	6 bladed turbine
Chen and Middleman(1967)	$a_{xz}/D = 0.045N_{w_0}^{-0.57}$	Photography	6 bladed turbine
Coulaloglou and Tavlari-des(1976)	$a_{xz}/D = 0.081(1 + 4.47\phi)N_{w_0}^{-0.6}$	Photomicrography	6 bladed turbine
Eckert et al(1985)	$a_{xz} = 6\phi \left( 0.186\phi^\alpha \sigma^\beta \mu_d^\gamma \rho_c^\delta \rho_d^{.71} \left( \frac{P}{V} \right)^\zeta \left( \frac{\pi ND}{100} \right)^\theta \right)$ where $\alpha = 1.54 + .12\ln(\phi) + .15\ln(\mu_d)$ $\beta = 5.77 - 1.04\ln(\sigma)$ $\gamma = 74 - .03\ln(\mu_d)$ $\delta = 78.6 - 22.5\ln(\sigma) - 6.93\ln(\mu_d)$ $\zeta = 68 + .08\ln(\phi) - 0.1\ln\left(\frac{P}{V}\right)$ $\theta = 1.35 + .12\ln(\mu_d) - .73\ln\left(\frac{\pi ND}{100}\right)$	Light transmission	
Fernandes and Sharma(1967)	$a_{xz} = kN^{-1}\phi^{1.0}$	Chemical reaction	6 bladed turbine, paddles and propeller
Godfrey and Grilc(1984)	$a_{xz}/D = 0.058(1 + 3.6\phi)N_{w_0}^{-0.6}$	Photography	6 bladed turbine (square X-section tank)

Table 2.1 (Cont.)

Investigators	Correlation	Technique	
Godfrey et al(1987)	$a_{xz}/D = .084(1 + 0.98\phi^{.45})We^{-.6}\mu_v/\mu_c^{.44}$	Capillary photography	General Mills Impeller
	$a_{xz}/D = .187(1 + 1.18\phi^{.5})We^{-.6}\mu_v/\mu_c^{.37}$	Capillary photography	Square X-section vessel Davy impeller with rectangular spoiler Square X-section vessel
Keey and Glen(1969)	$a_{xz} = 1.26 \frac{D_I^{0.4}}{(D_I N)^{1.2}} \left[ \frac{D_T}{D_I} \right]^{1.2}$	Photography	6 bladed baddle
Kolarik and Pipkin(1982)	$a_{xz} \propto N^x$ .75 < x < 2	Photography	77mm Cylindrical vessel 70 mm cubic vessel
Konno et al(1977)	$\frac{\rho_c u^2 (a_{max}) a_{max}}{\sigma} \beta(N_{Re}) = C$	Photography	6 bladed turbine
Konno et al (1988)	$a_{xz}/D = 0.3N_{We}^{-0.93} \left( 1 + 0.6 \left( \frac{N_{We}^{1.2}}{N_{Re}^*} \right)^{.63} \right)$		
Lee & Soong(1985)	$a_{xz}/D = .05C_s(1 + 2.316\phi)N_{We}^{-.6}N_{Fr}^{.13} \left( \frac{D}{D_T} \right)^{-.75}$	Photography	Studied the effect of surfactants
Mlynek and Resnick(1972)	$a_{xz}/D = 0.058(1 + 5.4\phi)N_{We}^{-0.6}$	Photography	6 bladed turbine
Rodger et al(1956)	$a_{xz} = kN_{We}^{-0.36}(D_I/D_T)^{-.1}$	Light transmittance	6 bladed turbine
Shinnar(1961)	$a_{xz} = k[\sigma D_I]^{-.34}N_{We}^{-.34}$	Photography	Paddle turbine

Table 2.1 (Cont.)

52

Investigators	Correlation	Technique	
Sprow(1967)	$a_{32}/D = 0.0524N_{We}^{-0.57}$	Coulter Counter	6 bladed turbine Modified turbine
	$a_{32}/D = k(\rho_c \mu_c)^{-0.5} \left[ \frac{\rho_c}{\sigma D_I} \right]^{-0.25} N_{We}^{-0.75}$	Coulter Counter	Strongly coalescing system 6 bladed turbine Modified turbine
Tanaka(1985)	$a_{32} \propto N^{-1.1}$	(Impeller region)	Photography
	$a_{32} \propto N^{-0.85}$	(Circulation region)	
Van Heuven and Beek(1971)	$a_{32}/D = 0.047(1 + 2.5\phi)N_{We}^{-0.6}$	Photomicrography	6 bladed turbine
Vermeulen et al(1955)	$a_{32} = kN_{We}^{-0.6}$	Light transmittance	4 bladed paddle
Weinstein and Treybal(1973)	$a_{32} = 10^{(-2.044 + 0.732\phi) V_c^{0.047} E^{-2.84} \left[ \frac{\sigma g_c}{\rho_c} \right]^{2.47}}$	Light transmittance	6 bladed turbine (unbaffled vessel) Batch system

Table 2.1 (Cont.)

## CHAPTER III

### EXPERIMENTAL SET-UP AND PROCEDURE

The aim of the experimental programme was to establish the local characteristics of the dispersion in two geometrically similar tanks of standard configuration and different diameters so that the effect of scale-up could also be investigated. The following experiments were performed :

- i- Determination of the steady state drop size distributions and Sauter mean diameters at different locations in the vessels.
- ii- Local hold-up measurements to establish the pattern of spatial variation
- iii- Transient hold-up values at selected locations

In this chapter, a full description of the apparatus used as well as the experimental procedure is given. Schematic drawings and photographs of the experimental set-up are also shown

#### 3.1 Mixing Apparatus

Two geometrically similar stainless steel tanks of diameters 22cm and 44cm were used. The two tanks were of standard configuration as defined by Rushton et al(1950).

Figure 3.1 shows the standard tank configuration while Figure 3.2 shows the detailed design of the tanks used including the provision for sampling and photography. Table 3.1 gives the dimensions of the two tanks.

The impellers used for both tanks were six-blade turbines of diameter  $D_i$  being  $1/3$  of the tank diameter, centrally located and  $1/3 D_T$  from the bottom.

The impeller blade width is one fifth of the impeller diameter, the impeller blade length is  $1/4$  of the impeller diameter, half of it being mounted on the central disk which has a diameter equal to  $1/4$  of the tank diameter. A schematic diagram of the impeller is given in Figure 3.3.

For the small tank, the motor used is a Parvalux 1/6 hp 5000 rpm dc shunt motor with a digital speed controller operated from the mains. A similar motor of 1/4 hp was used for the 44 cm tank.

For both motors, a mechanism independent of the original motor circuit was used to measure the stirring speed. This was in addition to the motor original one.

A brass disc with 60 notches on the rim was mounted on the stirrer shaft. The rim passes between the two arms of an infra red detector which was connected to another digital counter which displayed the speed reading directly in revolutions per minute. This arrangement measured and controlled the speed within  $\pm 1 \text{ rpm}$ .

Each tank was fitted with 5 ports vertically located midway between the baffles as provisions for photography and hold-up sampling as shown in **Figure 3.2**. At any time, only one port was in use, the rest being sealed by stainless steel discs and ptfе washers.

For safety requirements, the 44cm tank was covered, sealed and fastened to the metal frame carrying it.

### **3.2 Reagents and their Preparation**

The fluids used to produce the dispersion in this study were:

- i- Double distilled water
- ii- n-Heptane (GP grade) provided by BDH

The physical properties of the system are given in Appendix I.

For hold-up studies as well as drop size measurements, the appropriate volumes were measured and left in contact for at least 24h. This was done to ensure that the phases were mutually saturated and no interfacial mass transfer was taking place during the conduct of the experiments

### **3.3 Drop Size Measurement**

Drop size distributions were measured at different locations and the Sauter mean diameters were calculated from the results.

Since it was not the aim of the project to design a new drop sizing technique, an investigation was carried out to choose an adequate technique among the available ones.

The main objective being the study of spatial variations in drop sizes, the direct photography technique was discarded because:

- i- The technique requires very low hold-up values.
- ii- Results obtained were specific to the wall region

Two other techniques were considered:

- i- Continuous capillary sampling.
- ii- *In situ* microphotography using an Endoscope.

The first technique was extensively used by Janjua (1982), Okufi(1984), Curl and et Al (1973) and Tavlarides et Al(1986, 1987, 1989). It was discarded for the following reasons :

- i- The difficulty of maintaining isokinetic conditions at the capillary mouth.
- ii- For the drop sizes under investigation a very fine capillary bore was required to minimise the error in drop volume predictions. This led to very high pressure drops which in turn could result in very high suction rates, a requirement limited by the dynamics of flow inside the capillary. The same conclusion has been reached by Tavlarides et al(1989) where they found that the minimum capillary size they could use was .05mm.

#### **3.3.1 Endoscope photography**

A 90° view endoscope of 30 cm working length was used. The endoscope was covered by a 30 cm long stainless steel sleeve of an inside diameter of 6.53 mm and outside diameter of 7.92 mm. A window, 13 mm in length and 1mm in depth

was cut at one end. A microscopic glass slice was fitted onto the window and secured using a slow setting Araldite adhesive which is an epoxy resin that is inert to the solvents used.

The sleeve was used to prevent the endoscope from coming into direct contact with the liquids that could leak inside. In addition, it improved the quality of the photographs by preventing the organic phase from wetting the endoscope window.

Figure 3.4 shows the design of the endoscope and the sleeve, while Figure 3.5 is a photograph of the assembly

The endoscope eye piece was connected through an adaptor to a Fujica FX2 35mm SLR camera which was fitted with a 21 cm extension tube and bellows attachment. The bellows, being adjustable, increased the flexibility of the system. A Kodak 125 X-Pan black and white film was used.

The light was provided by a Pulse Instruments Argon jet flash unit of a 300 ns duration at a power of 2.5 joules.

The flash head was modified in order to connect a flexible liquid light guide of 1.8m length. The other end of the light guide was fitted with a stainless steel tube the aim of which was to protect the light guide and keep it in position. The tube was secured to the metal frame. A quartz rod was fitted through an adaptor to the light guide tip.

### **3.4 Hold-up Measurements**

Most techniques developed for hold-up measurements give an average value within a contactor stage or inside a vessel rather than local values. An exception was the sample withdrawal method in which the volume withdrawn was assumed to be representative of the fluid at the point of withdrawal.

Stainless steel tubes of .82 mm inside diameter and .39 mm thickness were used to withdraw the sample. They were cut into 20cm and 30cm length and soldered

to the mouth of stainless steel needles using silver soldering. The thickness of the tubes increased their mechanical stiffness and ensured that they stayed in the desired position.

### **3.5 Cleaning Procedure**

The presence of contaminants alter the surface tension drastically thus affecting the drop diameters. A thorough cleaning procedure was followed :

- i- The tank and all the fittings were rinsed using acetone to dissolve any oil or n-heptane residue.
- ii- The tank was filled with a solution of 2% Micro detergent (Provided by International Products Corporation) and left in contact with the solution for a minimum period of 24h.
- iii- Tap water was used to rinse the detergent. 5 rinses were given.
- iv- Tank and fittings were rinsed with a 1% solution of sulphuric acid.
- v- Distilled water was then used to rinse the equipment. The process was repeated for at least 5 times.
- vi- Analar grade acetone was used to rinse the equipment thoroughly. The process was repeated for a minimum of three times
- vii- Distilled water was used again to rinse the apparatus for a minimum of three times.

The same procedure was followed for any piece of equipment that came into contact with the fluid inside the tank.

### **3.6 Experimental Procedures**

#### **3.6.1 Drop Size Measurements**

After the tank was cleaned and dried it was mounted and sealed on the metal frame that holds the motor. All ports were sealed except for the one at the required level where the endoscope was inserted and secured in position. The camera was then connected to the endoscope eyepiece and the light guide was adjusted in position facing the endoscope window. **Figure 3.6** is a photograph

of the assembly the details of which were shown in **Figure 3.2**.

The appropriate volumes of fluid were loaded into the tank. The motor was started and set at the desired speed using the two measurement mechanisms mentioned earlier. The system was then left running for at least one hour before any photographs were taken in order to attain steady state. This time was considered well in excess of the 40 minutes period required to reach steady state at the lowest stirring speed in the 22 cm diameter tank. This result was obtained by measuring the drop size distribution at 5 minutes intervals.

The films were developed for 6 minutes at  $20 \pm 1^\circ\text{C}$  using Kodak D-19 high contrast developer and fixed by a bath of Kodafix. The negatives were then analysed using an ASM (Vids-II) image analyser. The information was then transferred to the college main frame computer for analysis. **Figure 3.7** is a typical dispersion photograph obtained following the outlined procedure.

### **3.6.2 Hold-up Measurements**

When the tank was in position, all ports were sealed and a sampling tube was inserted at the level concerned. The relevant fluid volumes were then loaded. The motor speed was adjusted and one hour was allowed for the dispersion to reach steady state before the first sample was withdrawn. For every measurement at least two samples of not less than 20 ml were taken.

After sampling at one point, the tube position was re-located and the system left to run for another half hour before sampling. The process was repeated until all points at the level under investigation were covered.

The samples, in sealed glass tube, were left to separate and the volumes of the phases were measured using pipettes of .02 ml graduation. The pipettes were cleaned using acetone then dried before re-use.

Tank Diameter (cm)	V <sub>1</sub>	V <sub>2</sub>	V <sub>3</sub>	V <sub>4</sub>	V <sub>5</sub>	D <sub>T</sub>	D <sub>I</sub>	H	C	b	d	a	s	t
22	2.	6.	10.	14.	18.	22.0	7.33	22.0	7.33	2.2	5.5	1.83	0.92	1.47
44	4.	12.	20.	28.	36.	44.0	14.67	44.0	14.67	4.4	11.0	3.67	1.83	2.93

**Table 3.1** *Dimensions for general design drawing of mixing vessels (Figures 3.1, 3.2 and 3.3)*  
*(All dimensions in cm)*

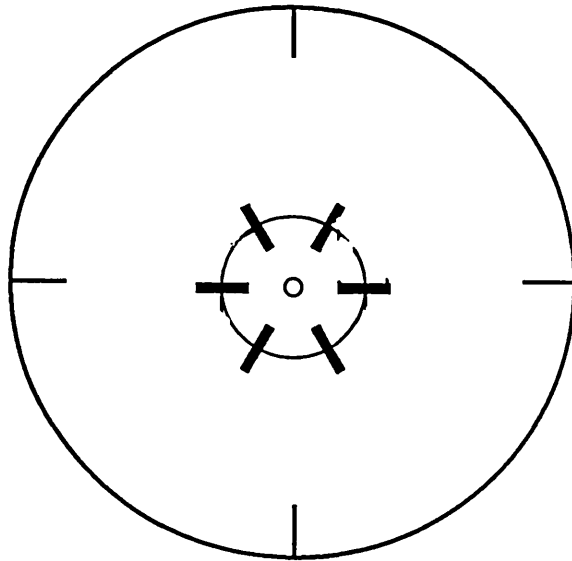
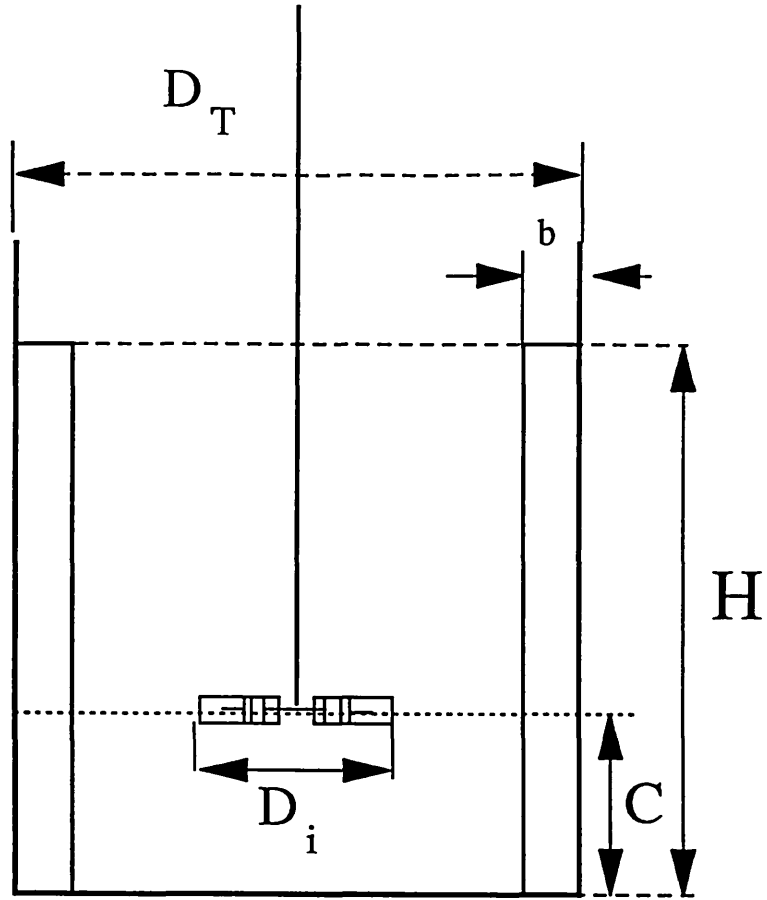
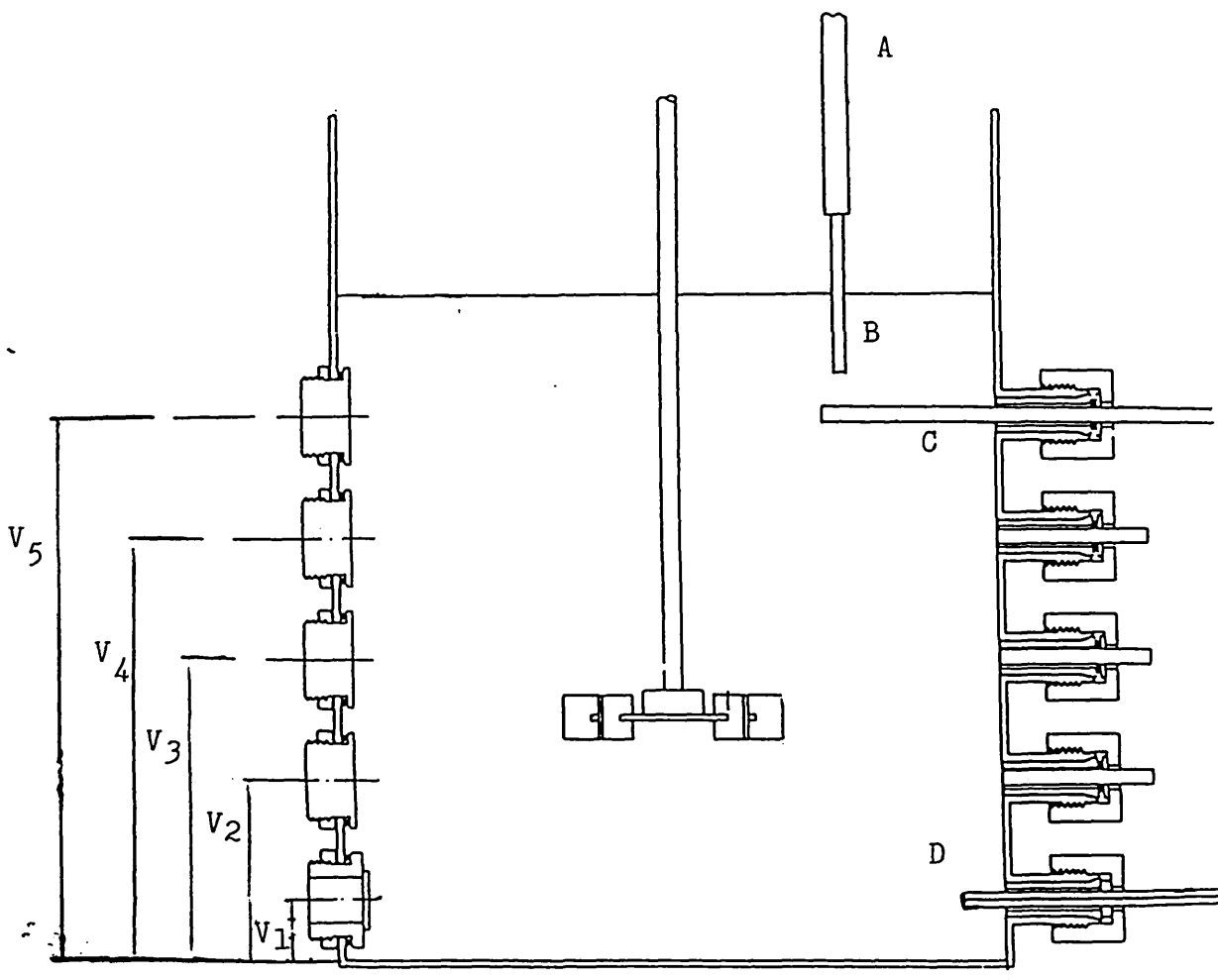


**Figure 3.1 : Standard tank configuration**

(See Table 3.1 and Figure 3.3 for dimensions and impeller details)



- A Light Guide
- B Quartz Rod
- C Endoscope
- D Hold-up Sampling Tube
- V<sub>1</sub>..V<sub>5</sub> See Table 3.1

**Figure 3.2 : General design of mixing vessels**

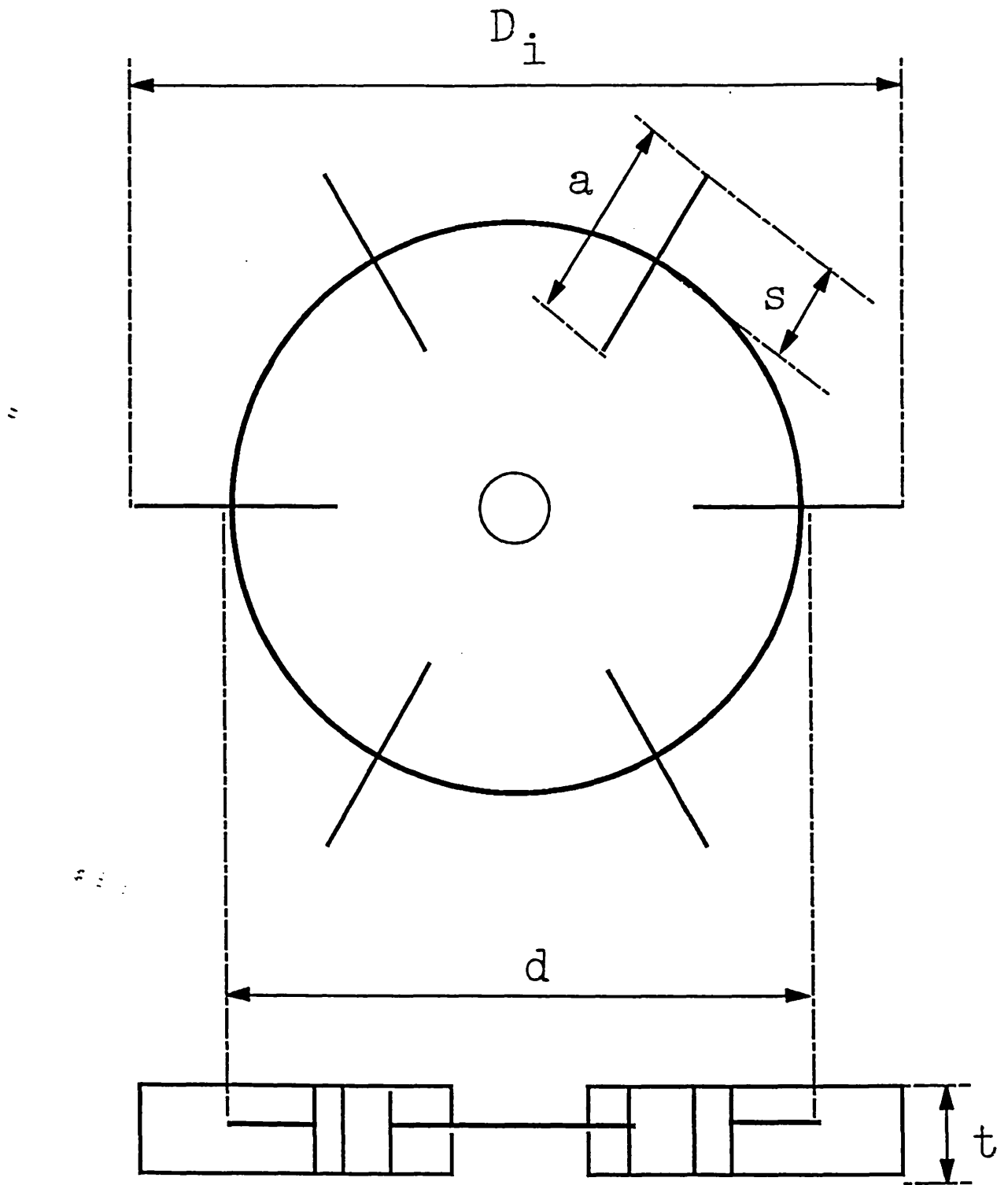


Figure 3.3 : *Impeller details*

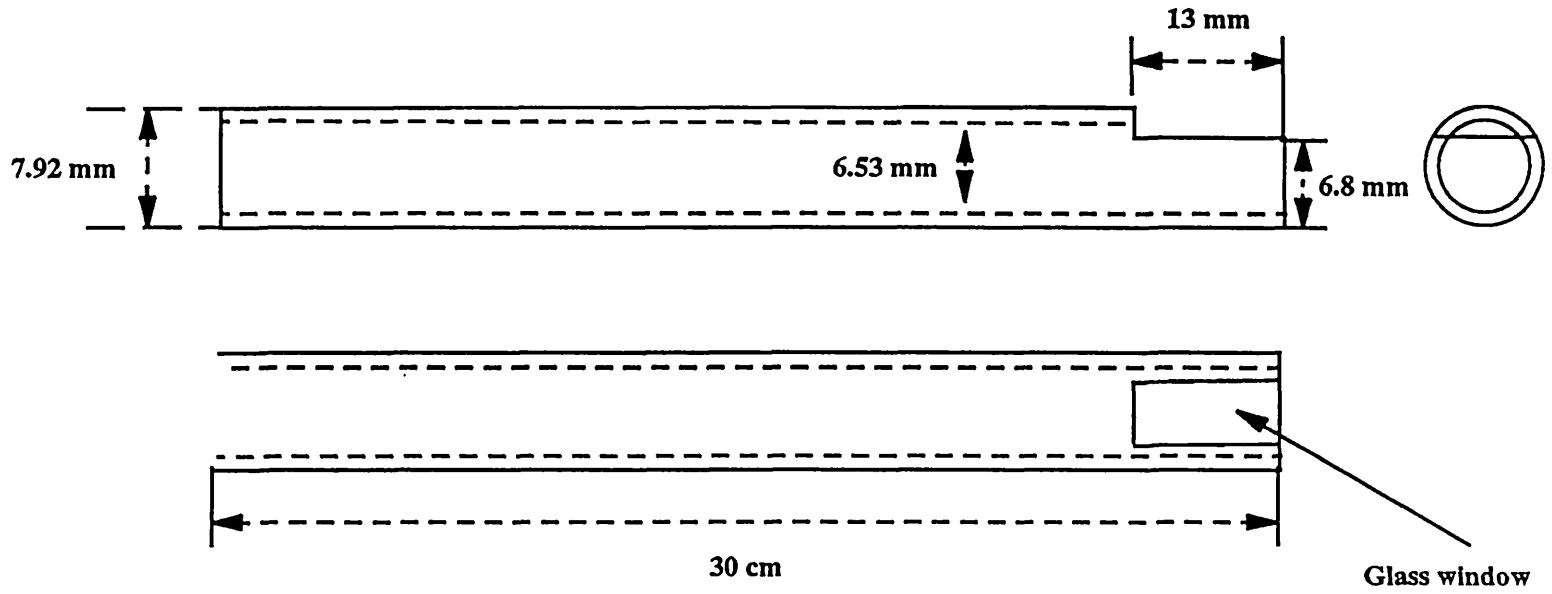
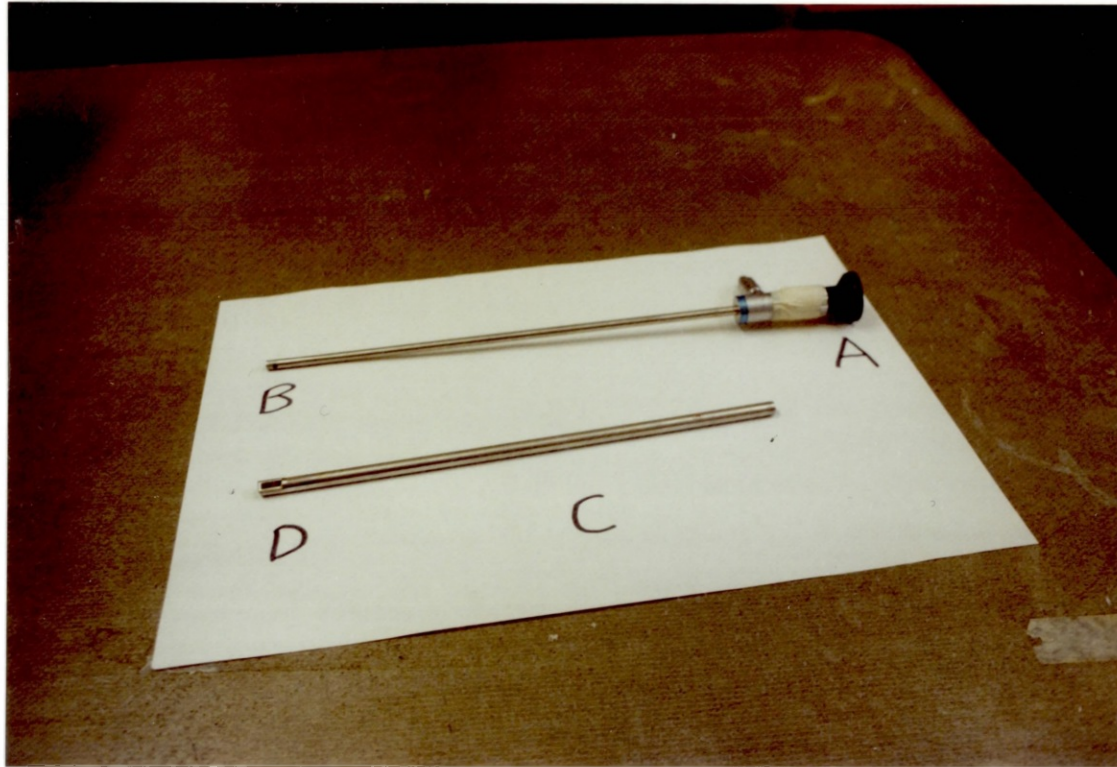


Figure 3.4 : Endoscope sleeve details



A Endoscope Eye Piece  
C Sleeve

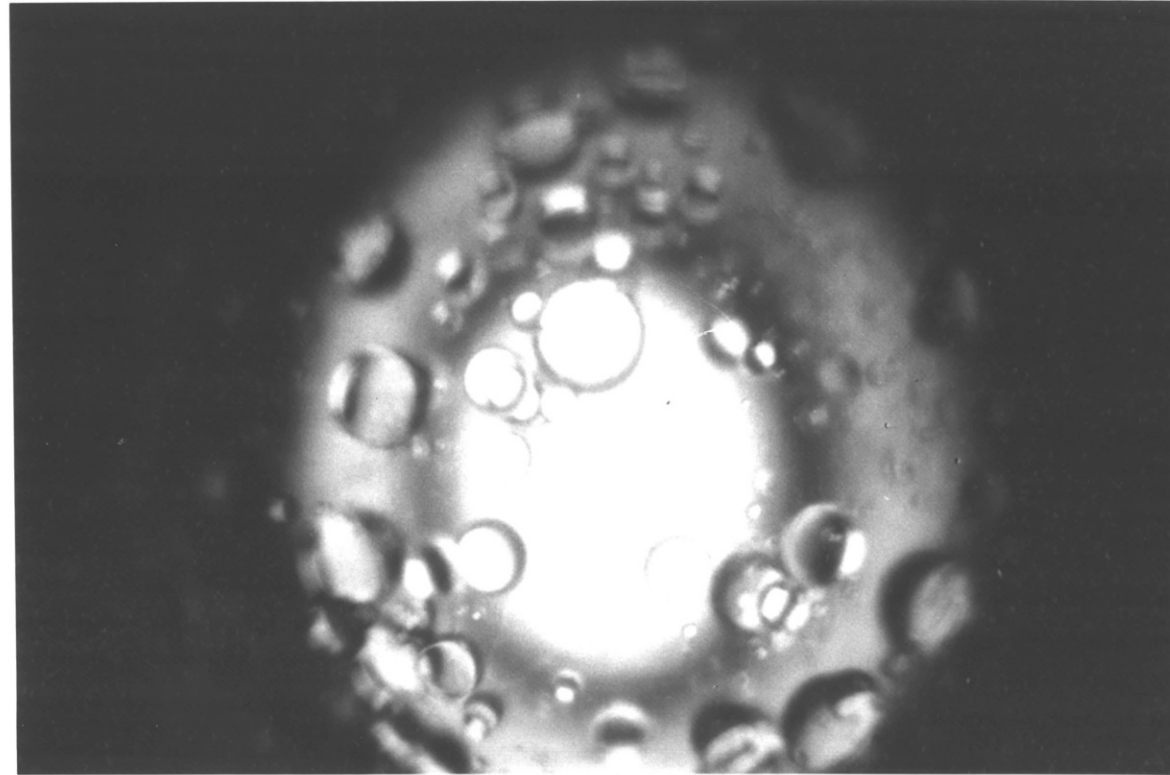
B Endoscope Window  
D Glass Window

**Figure 3.5** : *Photograph of the endoscope and the sleeve*



- |   |                  |   |                      |
|---|------------------|---|----------------------|
| A | Mixing Vessel    | B | Argon Jet Flash Head |
| C | Speed Controller | D | Digital Counter      |
| E | Endoscope        | F | Camera               |
| G | Motor            | H | Light Guide          |

**Figure 3.6** : *Photograph of the experimental set-up*



1mm

**Figure 3.7 :** *Endoscope photograph of the dispersion*

# **CHAPTER IV**

## **EXPERIMENTAL RESULTS AND DISCUSSION**

In this chapter, the experimental results for local hold-up values as well as local drop size distributions and Sauter mean diameters for the two tanks (see chapter III) are reported and discussed.

### **4.1 Hold-up results**

The aim of this study was to investigate the local values of dispersed phase fraction at different positions in the two tanks under varying operating conditions. In the following sections, results for local hold-up are reported and discussed. Most published work on hold-up was done in agitated columns in which single stages were modelled as continuous stirred tanks. The values reported were considered as the average for the stages under investigation assuming homogeneity within individual stages.

As mentioned in chapter II, the only reported work conducted in agitated tanks was done by Weinstein and Treybal (1973) and Thornton and Buoyatiotis (1967) for continuous flow systems. Nothing was reported about batch operations where it was assumed that the turbulence is sufficient to produce uniform dispersions. The measuring technique used in this study is sample withdrawal using stainless steel tubes as described in the previous chapter.

- The following assumptions were made:

- (i) Disturbances to the flow due to the presence of the sampling tube are minimal.
- (ii) The sample withdrawn is a fair representation of the tube tip surroundings, i.e. local homogeneity exists.
- (ii) Sample withdrawal is not selective, i.e. the suction speed does not accelerate one fluid at the expense of the other causing preferential sampling, a hypothesis that could be justified by the fact that the tube used was not a capillary.

The system studied was n-Heptane-Water at various stirring speeds and average hold-up values  $\phi_o$ , which are given in Table 4.1 at the positions shown in Figure 4.1. The phases were separated and measured as described in chapter III.

As a basis for comparison, the following parameters were studied:

- (i) Dimensionless hold-up  $\phi^* = \phi / \phi_o$ , where  $\phi$  is the experimental value of the hold-up at a point.
- (ii) Standard deviation from  $\phi_o$ .

#### 4.1.1 Unsteady state behaviour of $\phi^*$

In order to see if the hold-up values were equilibrium values produced by the operating conditions and system properties, and not random functions of the initial conditions, two sets of experiments were conducted:

- (i) Hold-up values were followed at 2 minute intervals for the first 20 minutes and then at 5 min intervals upto 120 minutes at points (A) and (B) (see Table 4.2 for positions) for 450 and 550 rpm
- (ii) For the same points,  $\phi^*$  was measured 5 and 10 minutes after the start of agitation but starting from different stirring speeds or 0 (the stirring stopped, the contents allowed to settle for 30-40 min, then mixing started again)

For the first set, the values at point (A) took about six minutes to attain steady state but at point (B) no significant change was detected over the same period, as shown in Figure 4.2 for 450rpm and .2 dispersed phase fraction in the 22 cm tank. This may be due to the good mixing achieved near the impeller.

In the second part, the results seemed to be unaffected by the starting point indicating that the hold-up  $\phi^*$  is not a random variable and the rate at which the steady state is achieved is high.

In this work, differences of up to 5% were considered as acceptable experimental errors bearing in mind the limitations of the method used for measurement.

#### 4.1.2 Spatial variations of the local hold-up values

The values calculated from the experimental measurements were found to be highly irregular, exhibiting strong variations depending on the location relative to the impeller, distance from the vessel boundaries, stirring speed, as well as the vessel original hold-up. The effects of these parameters are discussed in the following sections.

##### 4.1.2.1 Variations with the distance from the tank central axis

The general trend observed at up to 600 rpm was a high deviation from  $\phi_0$  near the walls, more uniform values as the bulk of the fluid was approached and a decrease again towards the tank central axis as may be seen in Figure 4.3 where hold-up values are given at four horizontal levels: near the top, impeller region, bottom, and bulk of the fluid in the upper section of the vessel. The variations were above the level set as acceptable experimental errors margin.

In most cases the values near the wall were well below the average values, an observation that may be explained by the presence of the wall boundary layer where turbulence is at its lowest and consequently the lighter phase tends to accumulate at the top.

The effect of the distance from the impeller plane was profound as could be seen in the plots of Figure 4.3. In general, the area adjacent to the agitator displayed more uniformity than the rest of the vessel including the region near the walls.

This is due to the high intensity of turbulence present in this zone which is an order of magnitude higher than the average, as mentioned in the literature review, creating steady flow of both phases unhindered by the gravitational effects.

In the rest of the vessel, results were a clear evidence of gravitational forces playing a dominant role in controlling the local hold-up values.

Near the top fluid surface,  $\phi^*$  was always greater than 1 and it decreased as the depth increased as shown in Figure 4.3.

The effect of both radial distance and height on local hold-up is represented in Figure 4.4 in which the standard deviation from  $\phi_0$  over a given horizontal plane

is plotted against height. It is evident that the most homogeneous hold-up region was the area just above the impeller while the wider spread of values was observed in the bottom region of the tank.

#### **4.1.2.2 Variations within the vertical distance from the impeller**

For vertical planes, gravitational effects were observed at the operating conditions used. An indication that more vigorous agitation would be necessary to prevent the lighter phase from preferentially flowing upwards. **Figure 4.5** shows a typical set of hold-up values obtained at a stirring speed of 500 rpm for two radial distances where a comparison is drawn between the wall region and the fluid bulk. The values of  $\phi^*$  were above unity near the surface, decreased towards the bulk in the upper section, approached unity near the impeller to decrease again as the vessel bottom was approached. Apart from the bottom, the values were close to level averages even at the wall but not necessarily close to  $\phi_o$ .

With the impeller plane as datum, it may be said that values above the impeller tended to move towards unity and deviations were not acute while in the lower section smaller values were experienced. This was in contrast to the expectation that since the lower fluid circuit is shorter compared with the upper one, the dispersion was supposed to be more uniform at the bottom than in the upper part.

In addition to the effect of the gravitational forces, the non-symmetry of the vessel and the presence of large solid surfaces that decelerate the motion contribute to the creation of dead zones at the corners of the baffles and the bottom, thus resulting in lower dispersion efficiency.

**Figure 4.6** is a plot of the standard deviation from the vessel average  $\phi_o$  for different vertical planes vs radial distance. This figure shows the uniformity in the vertical values with the exceptions of the plane near the wall. The most uniform dispersion was obtained half the way between the wall and the impeller.

#### **4.1.3 Effect of impeller speed on local Hold-up**

As mentioned before, the local hold-up was affected by the intensity of turbulence which in turn depended on the stirring speed. The increase in stirring speed reduced the deviations of the local holdup values even at the bottom of the tank

and near the wall.

**Table 4.3** lists the values obtained for  $\phi^*$  at 700 rpm and  $\phi_o = .2$ . The deviations are minimal for the wall and bottom and practically insignificant for the rest of the tank. The standard deviation from the average  $\phi_o$  is small compared to lower speeds.

In order to study the effect of stirring on  $\phi^*$ , measurements were carried out at two points (C) and (D) (see **Table 4.2**) for stirring speeds ranging from 450 rpm to 800 rpm. The results are shown in **Figure 4.7** where it is clear that  $\phi^*$  values approached unity as the speed approached 700 rpm despite the fact that the points displayed high deviations at lower speeds

**Figure 4.8** is a plot of standard deviation over the whole tank vs stirring speed at different hold-up values. Regardless of  $\phi_o$ , the deviation decreased as the speed increased. These results indicated that although there is minimum stirring speed for complete dispersion, the stirring speeds required for homogeneous dispersion are substantially higher.

#### **4.1.4 Tank Hold-up ( $\phi_o$ ) effect:**

As the values of  $\phi_o$  were increased, the values of  $\phi^*$  became more uniform, they approached unity and decreased both tank average deviation and standard deviation. The whole tank standard deviation from  $\phi_o$  decreased when the value of  $\phi_o$  increased as shown in **Figure 4.9** which is a plot of tank standard deviation vs  $\phi_o$  for two stirring speeds. **Figure 4.10** shows local hold-up values for the horizontal level of the height 14 cm at  $\phi_o = .1, .2$  and  $.4$  where the same trend as that exhibited by the tank standard deviation may be observed as a more uniform dispersion was obtained when  $\phi_o$  increased.

#### **4.1.5 Effect of the vessel scale on $\phi^*$**

Experiments were also conducted in a 44 cm tank geometrically similar to the 22cm one at geometrically similar points. Only one hold-up value was studied but at 4 stirring speeds that reflect both equal power input per unit mass and equal tip speed scale-up criteria.

Although the same observations made in the previous sections were found to be true, no clear effect of scale-up may be deduced. The results obtained for the large vessel are listed in Appendix III-5

#### **4.1.6 Mass balance over the whole vessel:**

A mass balance was performed over the whole vessel for the stirring speeds and hold-up studied. The vessel was divided into cells with the assumption that the value measured within the cell is a fair representation of a homogeneous entity. Less weight was given to the wall area due to the high level of turbulence that reduces the thickness of the boundary layer on the walls.

Table 4.4 lists the results obtained at the speeds studied. The deviation from unity prompted the experimentation with 700 rpm for the whole tank as well as the measurement of hold-up values at 1 cm below the fluid surface for all stirring speeds and hold-up values used, the results of which were reported earlier. The table shows that as the 700 rpm is approached the average dimensionless hold-up is essentially 1.

#### **4.1.7 Conclusions**

From the results reported, it may be concluded that the local hold-up values  $\phi^*$  were functions of turbulence intensity and the original vessel hold-up  $\phi_o$ . An increase in any of them resulted in increased spacial homogeneity and decreased deviation from  $\phi_o$ .

The profiles showed regularity within the bulk of the fluid while large deviations were observed at the vessel bottom and near the vessel wall. The effect of gravitational forces was observed at the lower stirring speeds and the dispersed phase fluid tended to accumulate at the top of the vessel.

## 4.2 Drop sizing results

Drop sizes of mutually saturated n-Heptane-Water dispersions were measured in the two tanks in order to study the effect of location, flow structure and vessel scale on the resulting dispersion. The complete description of the equipment and the reagents specification was given in the previous chapter. The locations studied are shown in Figure 4.11 for the 22 and 44 cm diameter tanks. The stirring speeds and hold-up values used are given in Table 4.5.

For each run, between 500 and 750 drops were measured depending on photograph quality. In order to study the effect of the number of realizations on statistical properties, a count was done with the number of drops progressively increasing to 1000. Table 4.6 shows Sauter mean diameters results while Figure 4.12 compares the distributions at 500 and 1000 counts.

It may be safely concluded that no significant gain is achieved by increasing the number above 500 provided that a 5% experimental error is not a lax estimate.

The parameters studied were the Sauter mean diameter which is a measure of the specific interfacial area, and drop size distribution. In the following discussion, the statistical parameters were defined as follows:

$$\text{Arithmetic mean diameter} \quad : \quad a_{10} = \frac{1}{N} \sum_{i=1}^N a_i \quad (4.1)$$

$$\text{Sauter mean diameter} \quad : \quad a_{32} = \frac{\sum_{i=1}^N a_i^3}{\sum_{i=1}^N a_i^2} \quad (4.2)$$

$$\text{Standard deviation} \quad : \quad \frac{1}{N} \sum_{i=1}^N (a_i - a_{10})^2 \quad (4.3)$$

$$\text{Skewness factor} \quad : \quad \frac{1}{N} \sum_{i=1}^N (a_i - a_{10})^3 \quad (4.4)$$

$$\text{Curtosis factor} \quad : \quad \frac{1}{N} \sum_{i=1}^N (a_i - a_{10})^4 \quad (4.5)$$

#### 4.2.1 Local values of Sauter mean diameter

Results showed large variations from one location to another. The trend seemed to be the same regardless of the stirring speed or hold-up. The overall profile for one set of operating conditions as shown in Table 4.7 was typical for all the others.

##### 4.2.1.1 Horizontal variation

Profiles of Sauter mean diameter between the centre of the tank and the wall at two levels are shown in Figure 4.13 in which the lines connecting the points do not indicate any functional relationship. The general trend was a low value near the vessel wall which increased towards the midway between the boundaries and the centre. A slight decrease was noticed as the tank central axis was approached but it was not of the same extent as that in the wall region. In general, the variations were too large to be attributed to experimental errors.

In explaining this behaviour, it is important to refer to the early reported hold-up results which showed a similar trend at the corresponding locations. The same correspondence between Sauter mean diameter and  $\phi^*$  trends was observed at most other investigated levels, irrespective of the stirring speed. This can be seen in Table 4.8 where local values of  $a_{32}$  and  $\phi^*$  are given for the 22cm tank at a dispersed phase fraction of .1 and stirrer speed of 450.

Regarding the lower values of the Sauter mean diameters near the vessel wall, another factor in addition to hold-up should be considered, namely drop breakage by collision with the baffles and the vessel wall near the impeller horizontal plane. According to the literature (Ali *et al*(1981)), breakage in this region results in the production of small satellite drops, thus yielding a lower value of  $a_{32}$  than the one produced by binary breakage.

On the other hand, considering the flow profiles of the vortices issuing from the impeller, the drops dispersed by the impeller and entrained by the fluid will move along the vertical cylindrical plane adjacent to the wall before entering the bulk circulation region in the area between the wall and the centre. This motion pattern may lead to the suggestion that not enough time was available for the drops to coalesce while they were passing through the wall jet region.

As the drops mix with the bulk of the fluid within the circulation region they

coalesce, hence the high values reported for  $a_{32}$  within the bulk of the fluid. The two structures in the upper and lower circulation regions are not exactly the same, a fact that could be attributed to the difference in the dimensions of the two regions due to tank configuration. The lower region provides a shorter path for the fluid and hence better mixing and more uniformity in drop sizes. The tank design did not allow for the examination of the stream directly issuing from the impeller. As a result, no measurements were made in that area.

#### **4.2.1.2 Vertical variations**

The vertical variations were readily identifiable and a distinctive peak within the upper circulation region was observed as shown in **Figure 4.14**. The extent to which  $a_{32}$  varies with vertical position is dependent on the horizontal distance from the impeller axis. The maximum variation in the numerical values for a given vertical plane occurred at the plane 7 cm from the wall as it is evident from the numerical values of **Table 4.7**.

These trends may be attributed to the following factors:

- (i) The lower values reported at the lower most level may be a direct result of low hold-up values.
- (ii) The higher values at the third level may be attributed to the fact that drops short circuiting and not entering the impeller stream have been in the circulation region for the time necessary for coalescence to take place thus establishing a new equilibrium state.
- (iii) The low value at the top may be the reverse of 2 where the stream is just departing the wall region and hence a high proportion of small drops that were produced within the impeller region or by collision with the boundaries are still in existence and did not have the chance to coalesce.

#### **4.2.1.3 Effect of variation of stirring speed**

The general profiles of local values of Sauter mean diameter obtained for two different stirring speeds were found to be similar and the same observations made in the previous sections with respect to horizontal and vertical variations of  $a_{32}$  hold. **Figures 4.15** and **4.16** show the effect of stirring speed change at

two different planes. However, the relationship between the Sauter mean diameter and the stirring speed, as given by  $x$  in the expression  $d_{32} \propto N^x$ , was not the same for all locations as shown in **Table 4.9**. These results rule out the possibility of hold-up variations being solely responsible for the local variations in drop sizes in which case the slope should be constant all over the tank. In addition, as the high speed of 600rpm was approached the hold-up deviations from the tank average were much smaller than those for the Sauter mean diameters as shown in **Table 4.10** thus confirming the conclusions made.

Another possible explanation for the variation of  $x$  is that the process is controlled by coalescence, a valid point if the exponents were between -1.2 and -.75 which is not the case in the experimental findings in which values less than -1.2 were observed.

These results tend to support the postulation that more than one turbulence mode is in effect present and contributing to the final outcome of the dispersion characteristics through their effect on the local values of turbulent velocity fluctuations.

**Figure 4.17** is a graphical representation of the relation between the Sauter mean diameter and the stirring speed for 5 different heights midway between the wall and the central axis.

As a conclusion, it may be said that the Sauter mean diameter decreases as the stirring speed increases but at different rates depending on the location. This would be due to two possible situations :

- 1- at some positions the stirring intensity may not be sufficient to overcome the surface forces which tend to prevent drop breakage. A stage could be reached where the sizes are too small for the inertia forces to play a big role in dispersion and other mechanisms may dominate the process(Shinnar(1961)).
- 2- the contribution of the process of drop breakage due to collision with the wall and/or the impeller which can quickly bring the sizes to small values unaffected by inertia forces.

## 4.2.2 Local drop size distributions

Large variations were observed in the local drop size distributions for both vertical and horizontal positions.

To make a meaningful comparison, the distribution moments were evaluated and their values were compared. They are:

- 1- The 2nd moment, standard deviation, is a measure of the spread of drop size spectrum.
- 2- The 3rd moment, the skewness factor, is a measure of deviation from normal distribution, this being a feature of isotropic turbulence
- 3- The 4th moment, the kurtosis factor, is a measure of flatness of the distribution or another measure for the deviation from normal distribution

In general, the distributions were unimodal with the peak either midway between the tails or shifted to the left. The minimum drop size observed was independent of the operating conditions which is in accordance with previous work (Okufi(1984), Janjua(1982)). A point to be stressed is that the limitations of the measuring technique used here may dictate the smallest size detectable.

Tables 4.11..4.13 lists the values obtained for the standard deviation, skewness factor and the kurtosis factor for the 22cm tank at 450 rpm and .1 dispersed phase fraction. In the following sections results will be discussed in terms of the distribution moments.

### 4.2.2.1 Horizontal variations

The same pattern displayed by the Sauter mean diameter was experienced with the drop size distributions standard deviation, skewness and kurtosis. **Figure 4.18** is a graphical representation of the drop size distributions at 3 horizontal locations for a height of 10 cm from the base for the 22 cm tank. The distribution standard deviation was found to be maximum at the vertical plane 7 cm from the centre except for one point at the lower speed of 450 rpm where the peak for the third level occurred at the point near the wall. An explanation that may be suggested is that the point mentioned is at the tip of the upper circulation region. Large drop sizes due to coalescence within the circulation region were expected as well as intermingling with the wall jet, where small size drops were

entrained by the stream issuing from the impeller and flowing upwards. The standard deviation high values indicate a spread in drop size distribution. Again, the central plane (10 cm height) displayed the maximum spread. For other horizontal levels, the distributions tend to get narrower. Regarding skewness and flatness of the distributions, the middle points exhibited peaks for the factors indicating more skewness to the left and more flatness compared with the rest of the tank. All skewness factors were positive indicating a shift to the left in the distribution peak.

#### **4.2.2.2 Vertical variations**

The distributions tend to become narrow and less skewed as the distance from the tank central horizontal plane increases as shown in **Figure 4.19**. The sampling location (10 cm height, 9 cm from the centre) displayed the minimum value for the skewness factor indicating a near perfect normal distribution, a result that is inconsistent with previous workers experimental findings that showed this area to be of high non-isotropy. The only possible explanation for the results reported here is the existence of perfect mixing in the lower part of the tank that have a predominantly isotropic behaviour and the point is not affected by the lower vortex issuing from the impeller. An explanation not compatible with the values obtained for the slope which were different from -1.2.

#### **4.2.2.3 Effect of the variation of stirring speed**

An increase in stirring speed produced narrower drop size distributions and reduced the skewness of the distribution peak moving the system towards isotropy as shown in **Figures 4.20 4.21 and 4.22**. Also the variations between locations decreased as the stirring speed increased, a fact that may be attributed to the development of better mixing conditions. The general profile for the tank is not different from that described in the previous sections.

#### **4.2.2.4 Effect of variation of the hold-up**

With hold-up increases, distributions tend to spread over a larger size span with the flatness increasing and the skewness decreasing. A result that is not consistent

with the assumption that the systems depart from ideal isotropic behaviour as the hold-up increases. The general shape of the graphs is consistent with the ones obtained for  $\phi_o = .1$  and the same remarks apply.

#### **4.2.3 Average Sauter mean diameter and Drop size distribution**

In order to obtain an average  $a_{32}$  and an average drop size distribution over the whole tank, the vessel was divided into cells of equal volume with the sampling points as their centres, then average drop sizes and drop size distributions were calculated. The only assumption made was that the sample is representative of the surroundings or the cell characteristics. The average values of  $a_{32}$  obtained for two values of stirring speed coincided with the local values measured at the position 7 cm from the centre and 6 cm from the base for both speeds as shown in Table 4.14

The differences in the arithmetic mean diameters, albeit being within the experimental errors boundary, indicate a difference in the drop size distribution. This result is a confirmation that a point average may not be suitable when heat, mass or mass transfer with chemical reaction are superimposed to the model. For these cases a more representative mesh should be considered. Since the position for the average found in this work is in the region below the impeller, it does not tend to support the wide belief that the upper circulation region values may be considered as averages.

#### **4.2.4 Effect of Vessel scale**

Two scale-up criteria were tested, namely :

i- Equal power input per unit mass  
and

ii- Equal tip speed.

Previous studies indicated that the system follows the latter criterion for scale-up (Janjua 1982). The tests were carried out at two geometrically similar positions in three geometrically similar tanks. This work is extended to study the scale effect at different locations to test the hypothesis put forward in chapter IV.

The positions studied and the stirring speeds used are given in **Figure 4.12** and **Table 4.5**. A value of .1 was used for the hold-up.

The results obtained were identical to those observed in the 22 cm tank. The effects of stirring speed and position on the Sauter mean diameter and drop size distribution were replica of the small vessel.

From the results obtained for the two scale-up criteria it may be concluded that the equal tip speed criterion is the one that produces a similar map to that obtained in the small vessel, the differences being within the acceptable experimental error margin. **Table 4.15** lists the differences between the drop sizes obtained in the 22 cm and 44 cm tanks for stirring speeds of 450 and 225 respectively which are the corresponding values for the equal tip speed scale-up criteria. The deviations were within the acceptable differences except for two locations near the wall.

The equal power per unit mass criterion resulted in smaller drop sizes and a map inconsistent with the one obtained in the small tank.

Despite the fact that the similarity is not a one to one correspondence, the differences that exist may be easily attributed to experimental errors. **Figure 4.23** compares the drop size distributions for 450 rpm in the 22 cm tank with that of 225 rpm in the 44 cm tank at a point 14 cm from the centre and 28 cm from the base (i.e. within the upper circulation region) while **Figure 4.24** is a comparison near the impeller.

#### **4.2.5 Conclusions**

The local drop size distributions and Sauter mean diameters showed considerable variations depending on the location. The dependency of the Sauter mean diameter on the stirring speed was not the same for all locations in the vessel which indicated the presence of more than one turbulence mode affecting the drop breakage and coalescence. The impeller region and the lower section of the vessel were characterised by smaller drop sizes and narrower drop size distributions.

Unlike the hold-up, the variations in the Sauter mean diameters did not disappear when the stirring speed was increased.

The equal tip speed criteria was found to be the most appropriate to produce similar characteristics in the two vessels. This showed the importance of choosing

a scale-up criterion that results in an overall similarity in the flow patterns rather than equal average power dissipation per unit mass. The latter does not indicate similarity in local power dissipation levels, a condition to obtain the similarity of dispersion characteristics.

	Tank Diameter (cm)	
	22	44
Stirring speed rpm	450, 500, 550, 600	225, 250, 283, 314
Hold-up $\phi_o$	.1, .2, .3, .4	.2

**Table 4.1** *Stirring speed and  $\phi_o$  for hold-up measurements*

Point	Horizontal Distance cm (From centre)	Height (From base) cm
A	7.0	14.0
B	7.0	6.0
C	10.5	2.0
D	10.5	18.0

**Table 4.2** *Positions for unsteady state hold-up measurement*

Height (cm)	Horizontal Distance from centre (cm)					
	1	3	5	7	9	11
2	0.886	0.942	0.969	0.960	0.981	0.952
6	1.012	0.978	0.963	1.037	1.020	0.890
10	1.000	1.000	0.997	0.993	0.978	0.962
14	0.990	0.981	1.000	0.978	0.993	0.953
18	0.992	0.997	1.003	1.000	1.010	0.966
21	1.030	1.000	1.073	1.108	1.024	0.983

Table 4.3 Local hold-up  $\phi^*$  values for 700 rpm and  $\phi_o = .2$

Tank diameter = 22 cm

$\phi_o$	Stirrer speed (rpm)	Tank Average $\phi^*$
.1	450	.9426
.1	500	.9109
.1	550	.9263
.1	600	.9439
.1	700	.9750
.2	450	.9843
.2	500	.9668
.2	550	.9503
.2	600	.9465
.2	700	.9965
.3	450	.97414
.3	500	.96582
.3	550	.9682
.3	600	.9643
.3	700	.9965
.4	450	.9756
.4	500	.9786
.4	550	.959
.4	600	.9631
.4	700	.9964

**Table 4.4** *Mass balance over the whole tank*

*Tank diameter = 22 cm*

	Tank Diameter (cm)	
	22	44
Stirring speed rpm	450, 500, 550, 600	225, 250, 283, 314
Hold-up $\phi_o$	.1 and .3	.1

**Table 4.5** *Stirring speed and  $\phi_o$  for drop sizing*

No. of drops counted	Sauter mean diameter (mm)	% difference from 1000 drops
200	.365	23.81
300	.3278	11.05
500	.310	5.13
600	.3011	2.08
700	.2898	-1.73
800	.3089	4.72
900	.3039	3.01
1000	.2950	-

**Table 4.5** *Effect of number of realizations on Sauter mean diameter*

*Tank diameter = .22 m ;  $\phi_o = .1$  ; Stirrer speed = 450 rpm  
Height = 10 cm ; Distance from centre = 5 cm*

Height (cm)	Horizontal distance from centre (cm)		
	5	7	9
18		.16899	.2228
14	.21394	.2061	.1761
10	.2950	.3184	.2870
6	.23144	.2414	.1861
2		.1999	.19686

**Table 4.7** *Local Sauter mean diameters (mm)*

*Tank diameter = 22 cm ;  $\phi_o = .1$*

Height (cm)	Horizontal distance from centre (cm)		
	5	7	9
18		.16899 {.944}	.2228 {.977}
14	.21394 {.918}	.2061 {1.00}	.176 {.974}
10	.2950 {.893}	.3184 {.894}	.2870 {.872}
6	.23144 {1.00}	.2414 {.927}	.1861 {1.000}
2		.1999 {.830}	.19686 {.823}

**Table 4.8** *Local Sauter mean diameters (mm) and hold-up values*

*{ $\phi^*$ }*

*Tank diameter = 22 cm ;  $\phi_o = .1$*

Height (cm)	Horizontal distance from centre (cm)		
	5	7	9
18		-.90449	-1.4846
14	-.65103	-.71921	-
10	-1.5385	-1.5369	-1.245
6	-1.5385	-1.1925	-.43327
2		-.14888	-.86482

**Table 4.9** Local values for the slope of Sauter mean diameters vs stirring speed plots for  
 Tank diameter = 22 cm ;  $\phi_o = .1$

Height (cm)	Horizontal distance from centre (cm)		
	5	7	9
18		24.92 {6.87}	14.51 {4.36}
14	1.95 {.966}	3.51 {.835}	
10	8.91 {5.31}	17.57 {4.65}	15.28 {.083}
6	3.51 {7.85}	1.15 {3.72}	5.57 {2.34}
2		24.42 {8.56}	11.78 {11.3}

**Table 4.10** Percentage difference between the local Sauter mean diameter and  $\{\phi^*\}$  values and tank averages  
 Tank diameter = 22 cm ;  $\phi_o = .1$  ;  $N = 600$  rpm

Height (cm)	Horizontal distance from centre (cm)		
	5	7	9
18		.00255	.004673
14	.003454	.003453	.002635
10	.010277	.012355	.019985
6	.004006	.004426	.002630
2		.004073	.000039

**Table 4.11** *Standard deviation of local drop size distribution around the arithmetic mean diameter*  
*Tank diameter = 22 cm ;  $\phi_o = .1$  ;  $N = 450$  rpm*

Height (cm)	Horizontal distance from centre (cm)		
	5	7	9
18		.000093	.000319
14	.0001177	.000147	.000141
10	.000534	.000307	.000639
6	.00007479	.000227	.0000718
2		.000186	.000249

**Table 4.12** *Skewness factor of local drop size distribution around the arithmetic mean diameter*  
*Tank diameter = 22 cm ;  $\phi_o = .1$  ;  $N = 450$  rpm*

Height (cm)	Horizontal distance from centre (cm)		
	5	7	9
18		.000021	.000108
14	.000043	.000043	.000036
10	.000349	.000427	.00034611
6	.000052	.000086	.0000234
2		.000056	.000059

**Table 4.13** *Curtosis factor of local drop size distribution around the arithmetic mean diameter*

*Tank diameter = 22 cm ;  $\phi_o = .1$  ;  $N = 450$  rpm*

Stirrer Speed (rpm)	450	600
Sauter Mean Dia. (Av.) (mm)	.2452	.174
Sauter Mean Dia. (point) (mm)	.2414	.172
Arith. Mean Dia. (Av.) (mm)	.171	.129
Arith Mean Dia. (Av.) (mm)	.19549	.135

**Table 4.14** *Average Sauter and arithmetic mean diameters*

*Tank diameter : 22 cm ;  $\phi_o = .1$*

Height (cm)	Horizontal distance from centre (cm)		
	5 x $D_T/22$	7 x $D_T/22$	9 x $D_T/22$
18 x $D_T/22$		8.1	16.7
14 x $D_T/22$	7.3	7.1	27.9
10 x $D_T/22$	7.2	8.16	7.6
6 x $D_T/22$	7.8	7.8	7.3
2 x $D_T/22$		5.9	7.4

**Table 4.15** *Percentage difference in local Sauter mean Diameter value for the two tank: equal tip speed scale up criteria  $\phi_o = .1$ ;  $N = 450$  rpm*

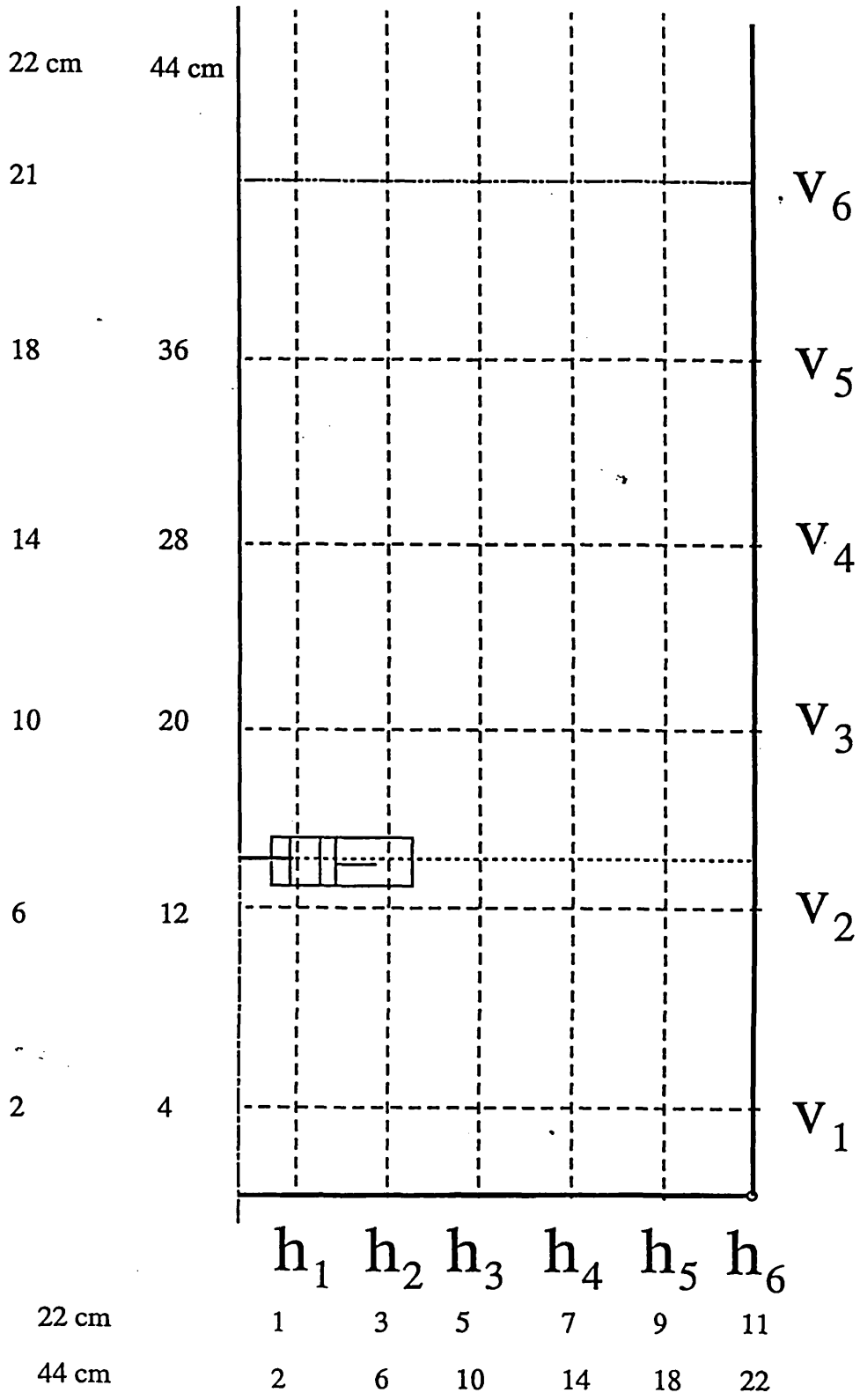


**Figure 4.1 :** *Positions for hold-up measurements*

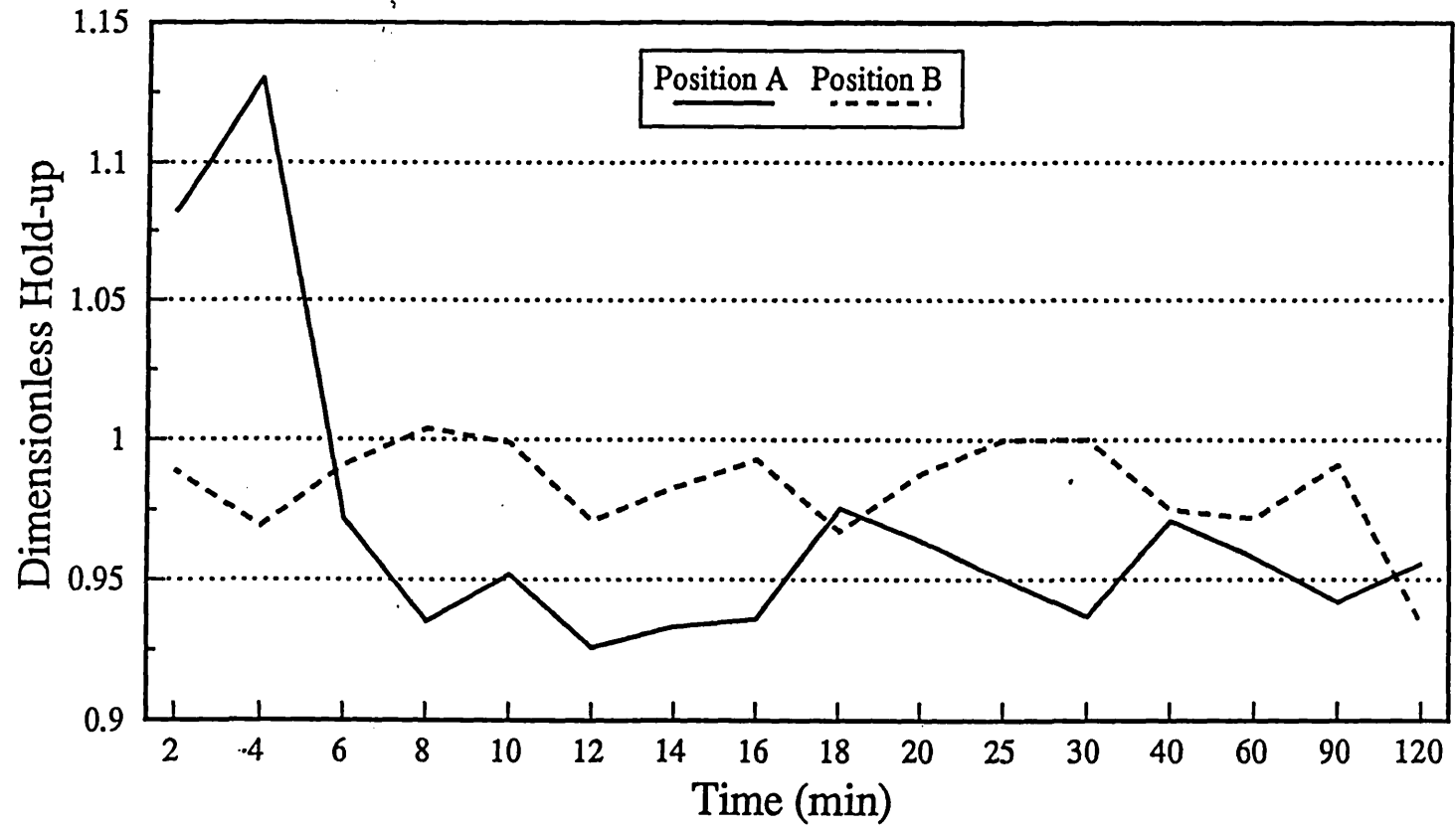


**Figure 4.2 :** *Unsteady hold-up measurements (Positions : A and B (Table 4.2))*

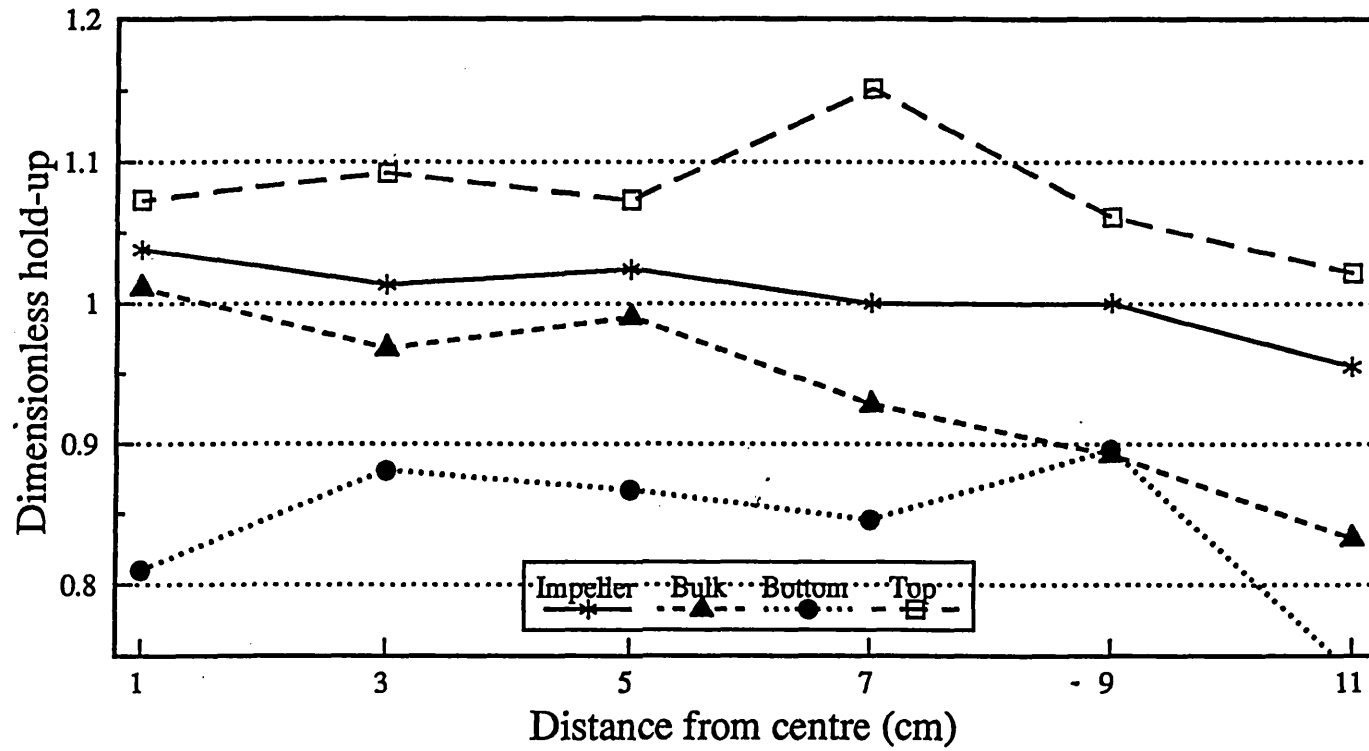


Figure 4.3 : Horizontal hold-up variations  
 $N = 500 \text{ rpm}$  ;  $\phi_o = .2$  ; Tank diameter = 22 cm

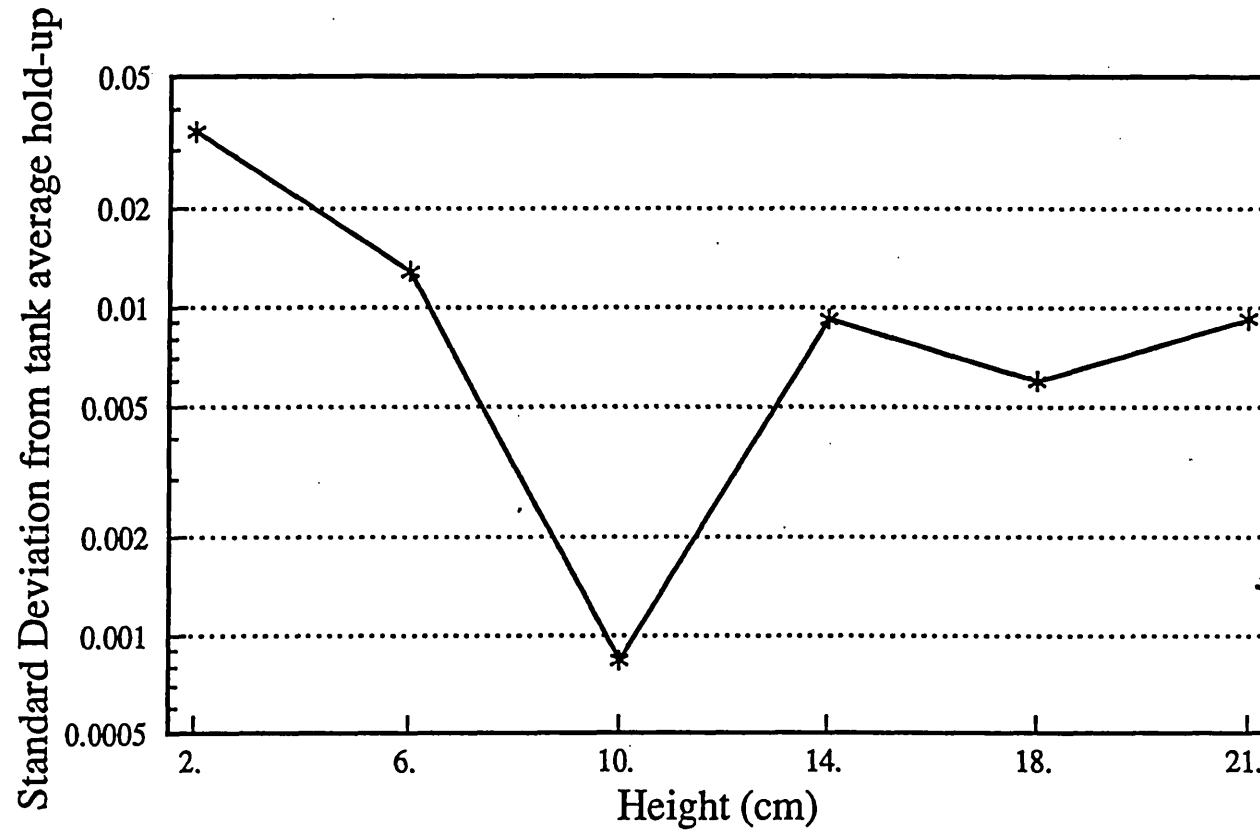


Figure 4.4 : Horizontal planes standard deviation from  $\phi_o$   
 $N = 500 \text{ rpm}$  ;  $\phi_o = .2$  ; Tank diameter = 22 cm

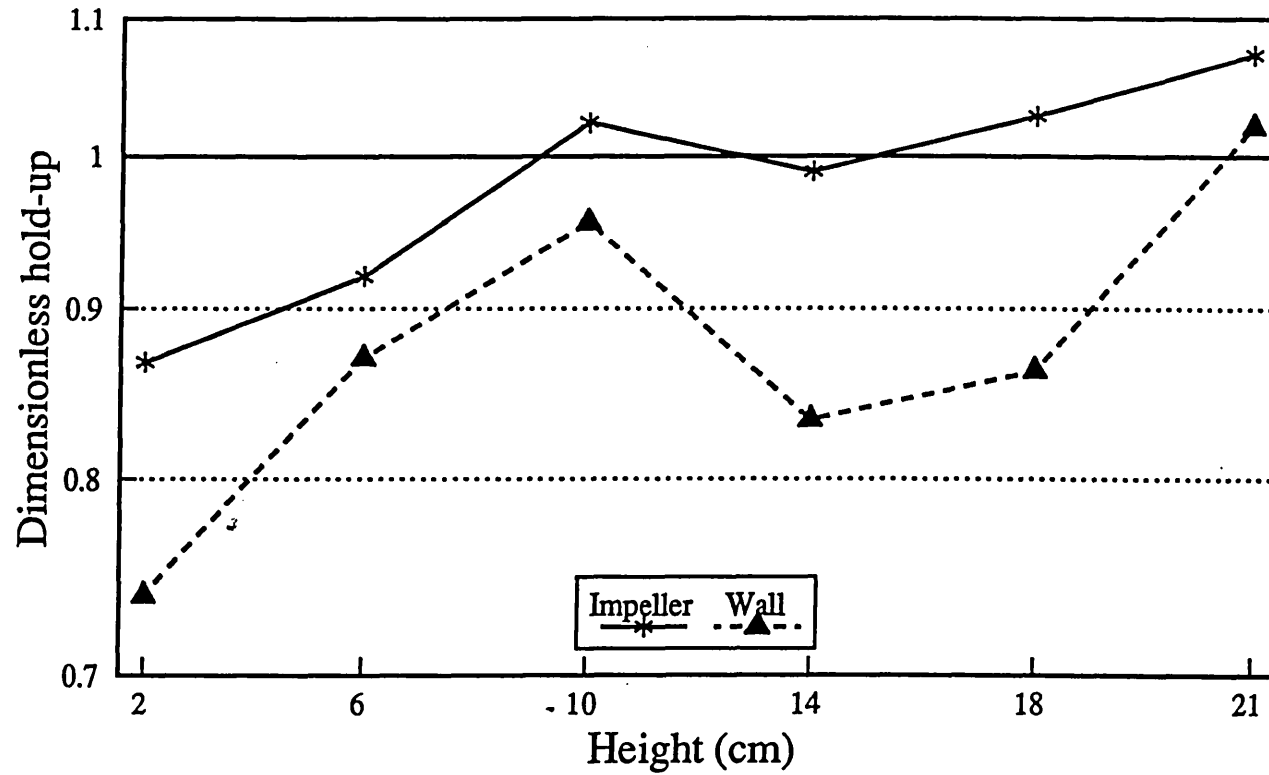
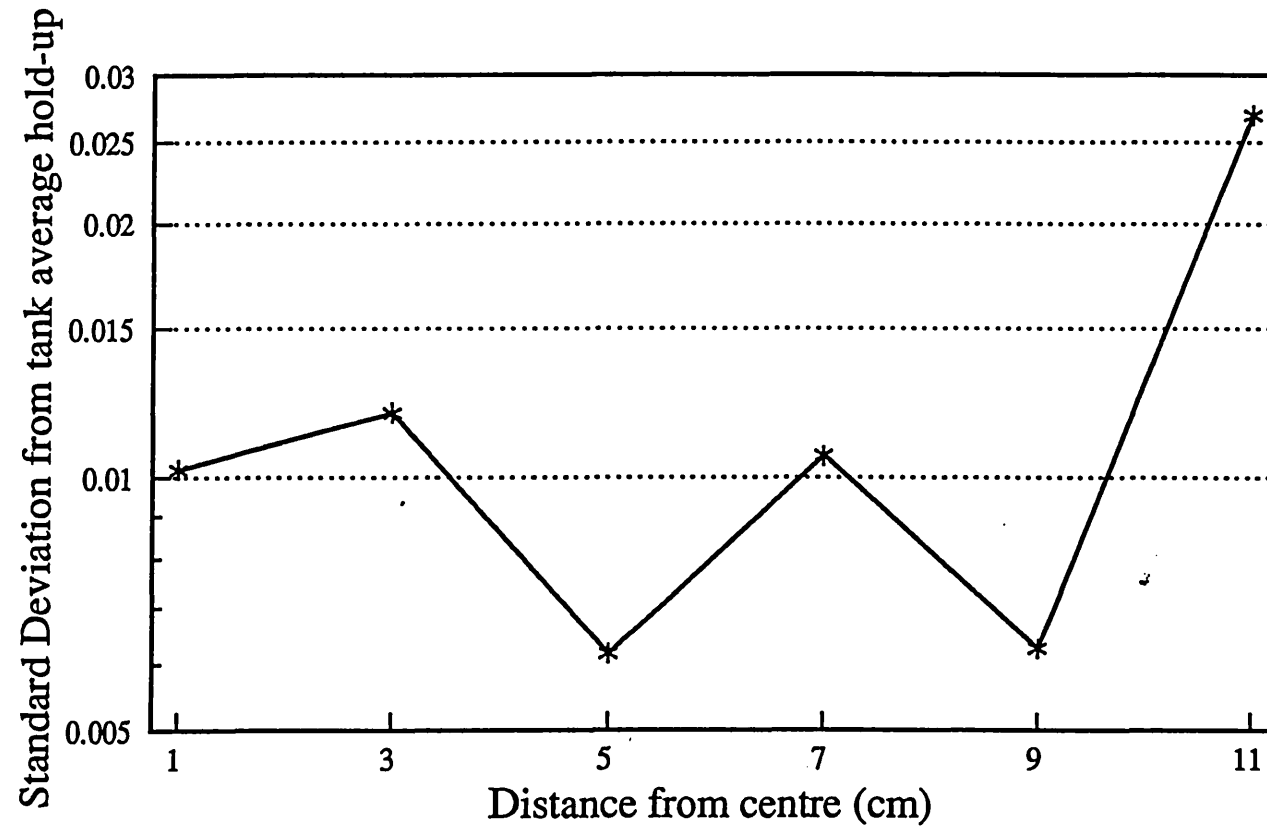


Figure 4.5 : Local hold-up values  $\phi^*$  for two vertical planes  
 $N = 500 \text{ rpm}$  ;  $\phi_o = .2$  ; Tank diameter = 22 cm



**Figure 4.6 :** *Vertical planes standard deviation from  $\varphi_o$*   
 *$N = 500 \text{ rpm}$  ;  $\varphi_o = .2$  ; Tank diameter = 22 cm*

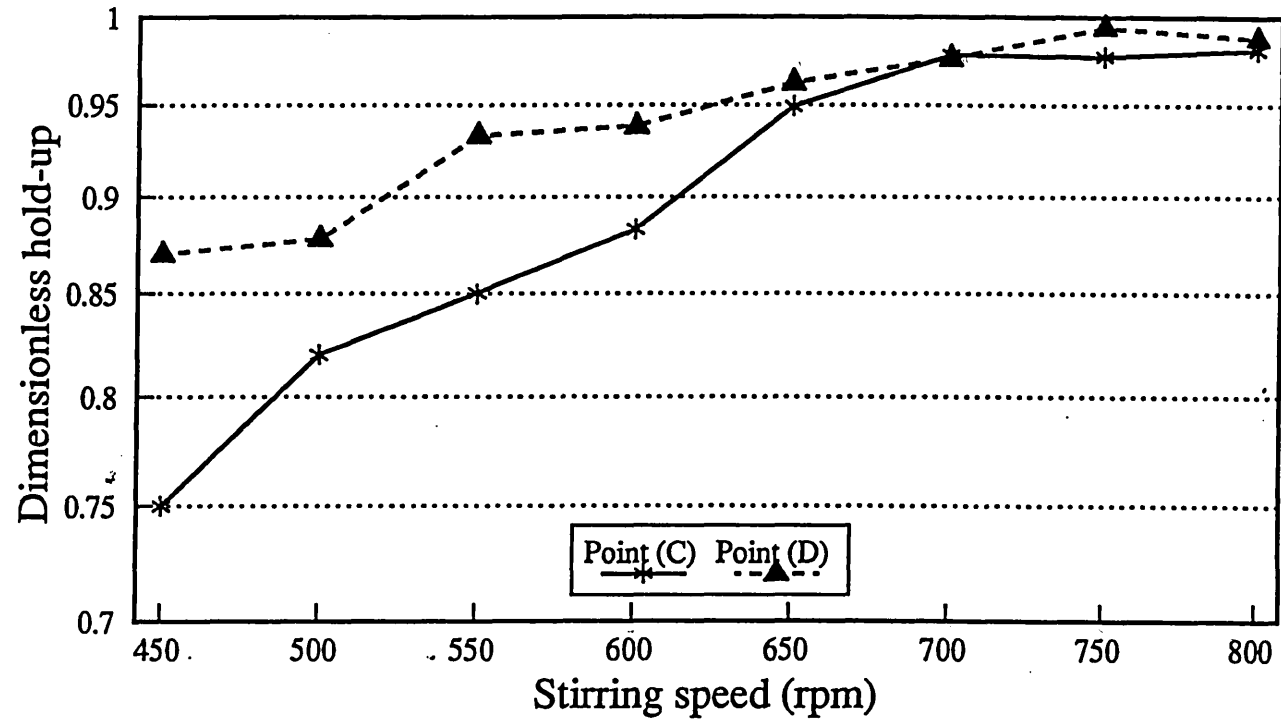
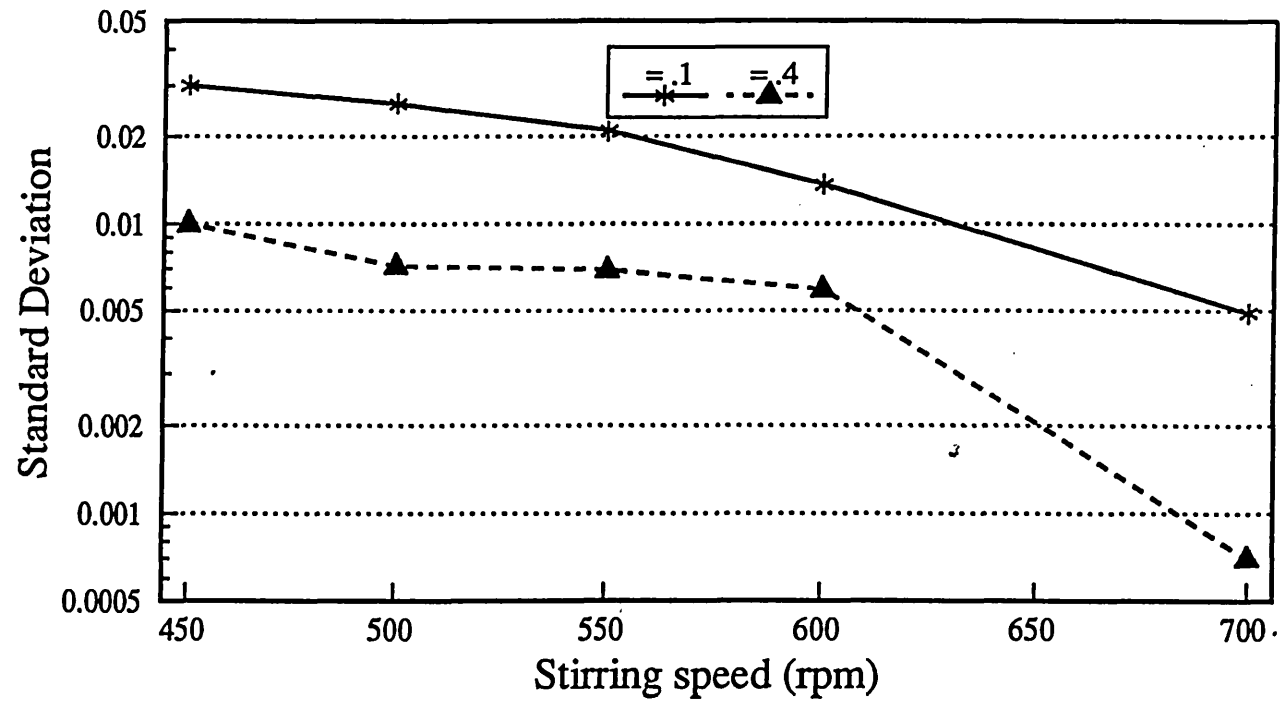
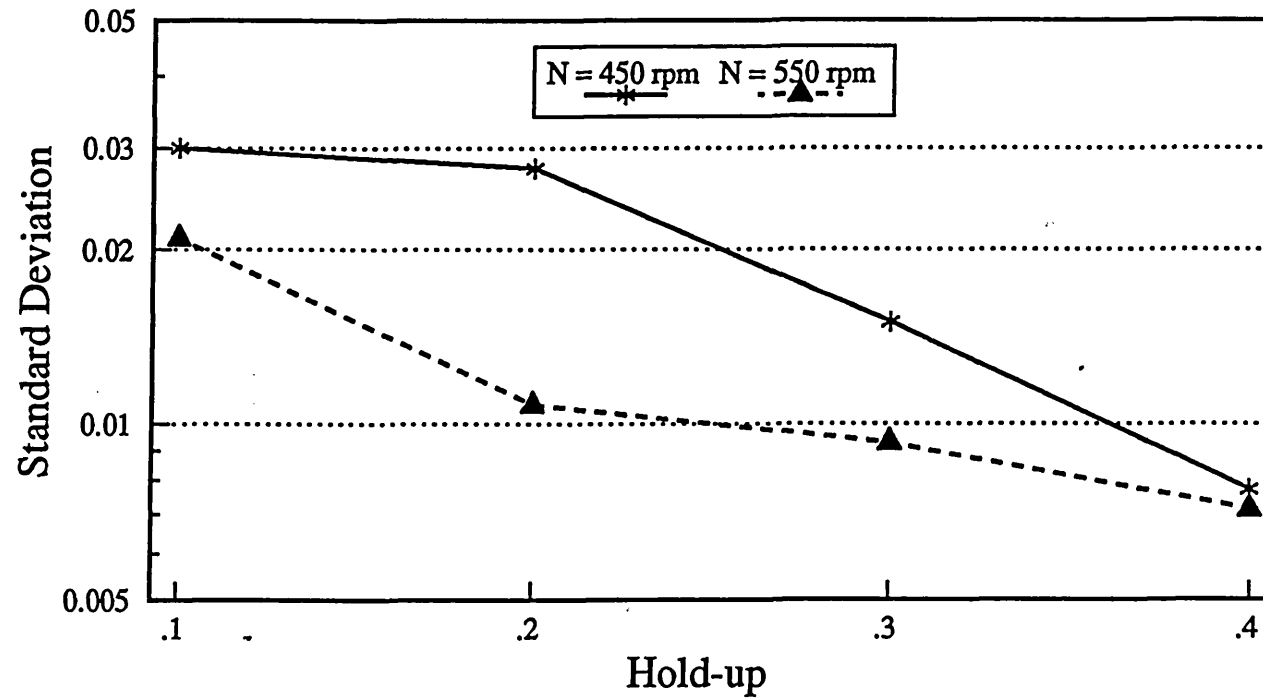


Figure 4.7 : Effect of variation of stirring speed on  $\phi^*$  (see table 4.2 for locations)  
 $\phi_o = .2$  ; Tank diameter = 22 cm



**Figure 4.8 :** *Effect of stirring speed variation on the overall tank standard deviation from  $\phi_0$ . Tank Diameter = 22 cm*



**Figure 4.9 :** *Effect of tank total hold-up  $\phi_o$  on overall tank standard deviation*  
*Tank diameter = 22 cm*

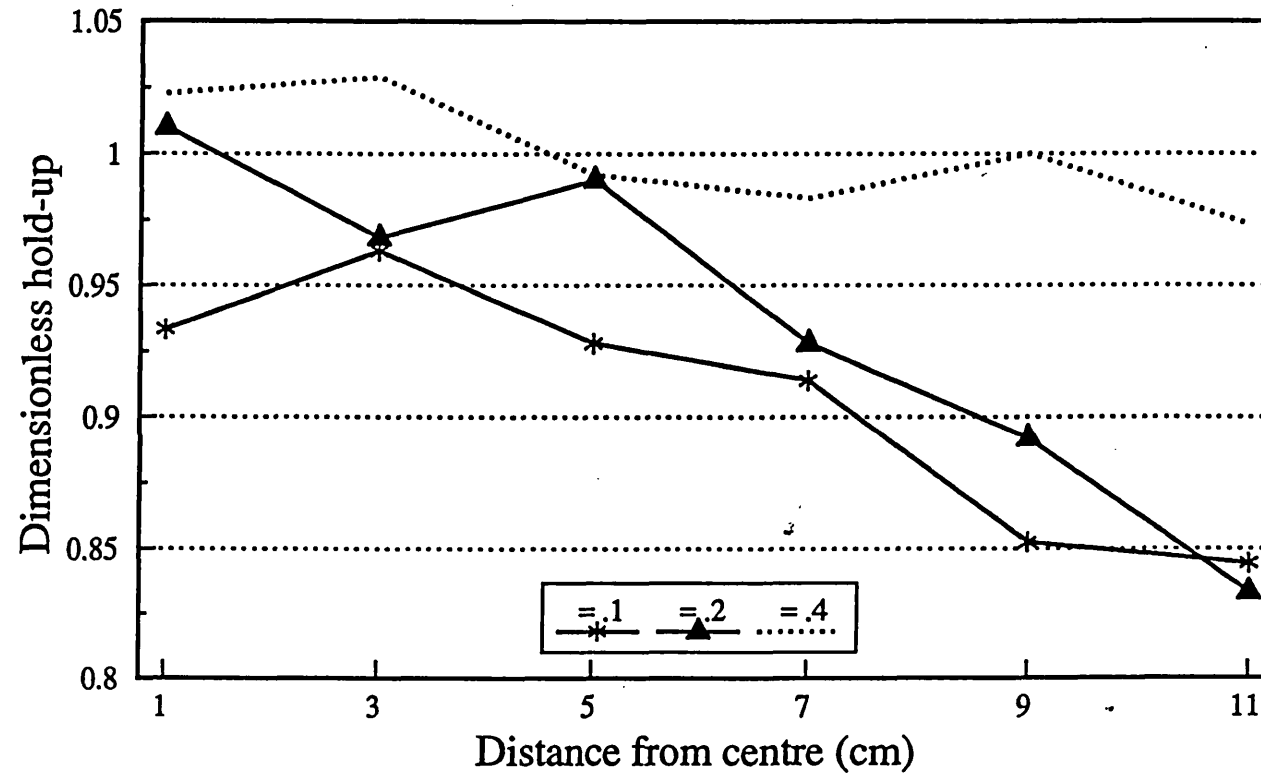


**Figure 4.10 :** *Effect of tank total hold-up  $\phi_0$  on local values  $\phi^*$*   
*Horizontal level : height = 14 cm ; N = 500 rpm*

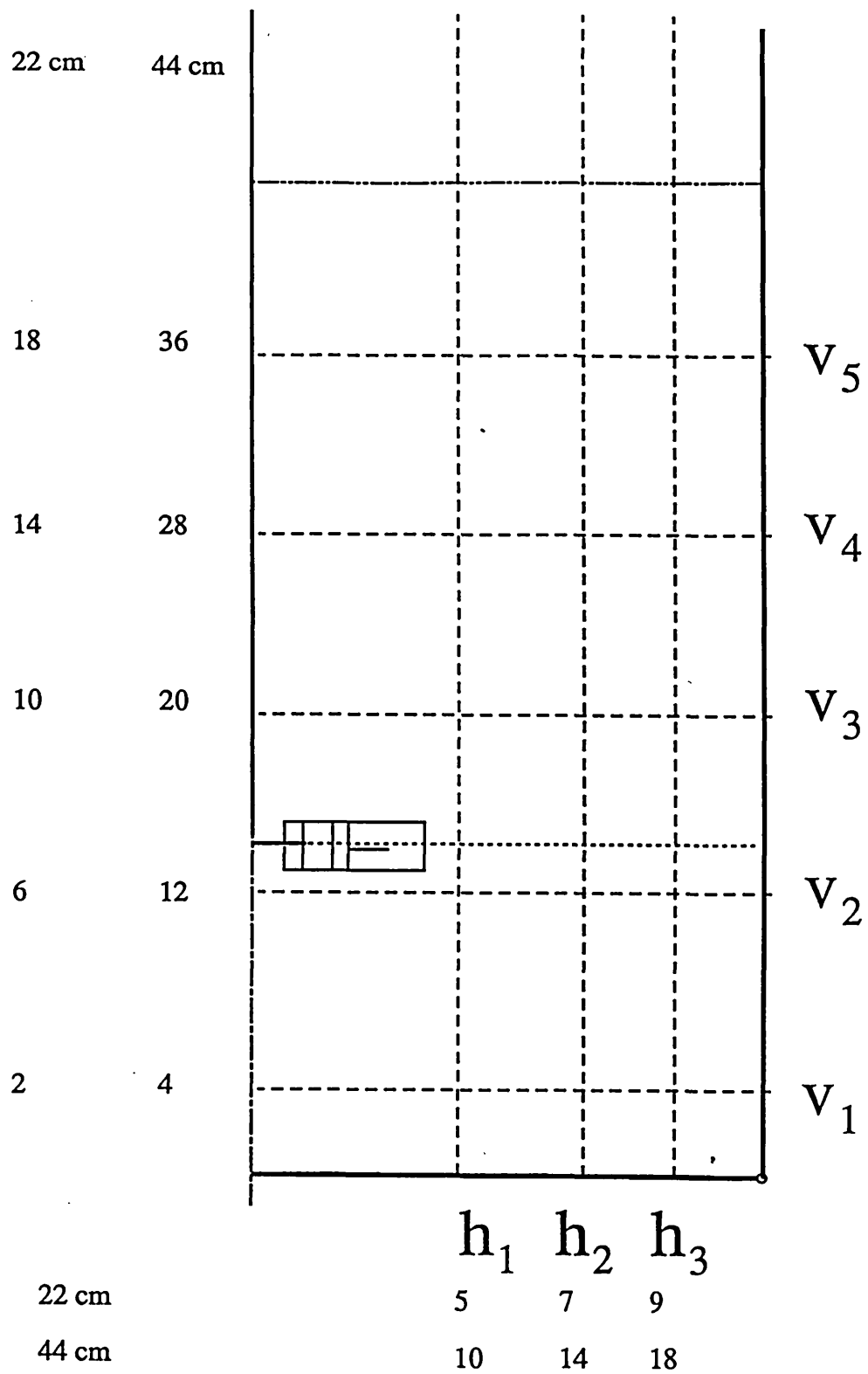


**Figure 4.11 :** *Positions for photography*

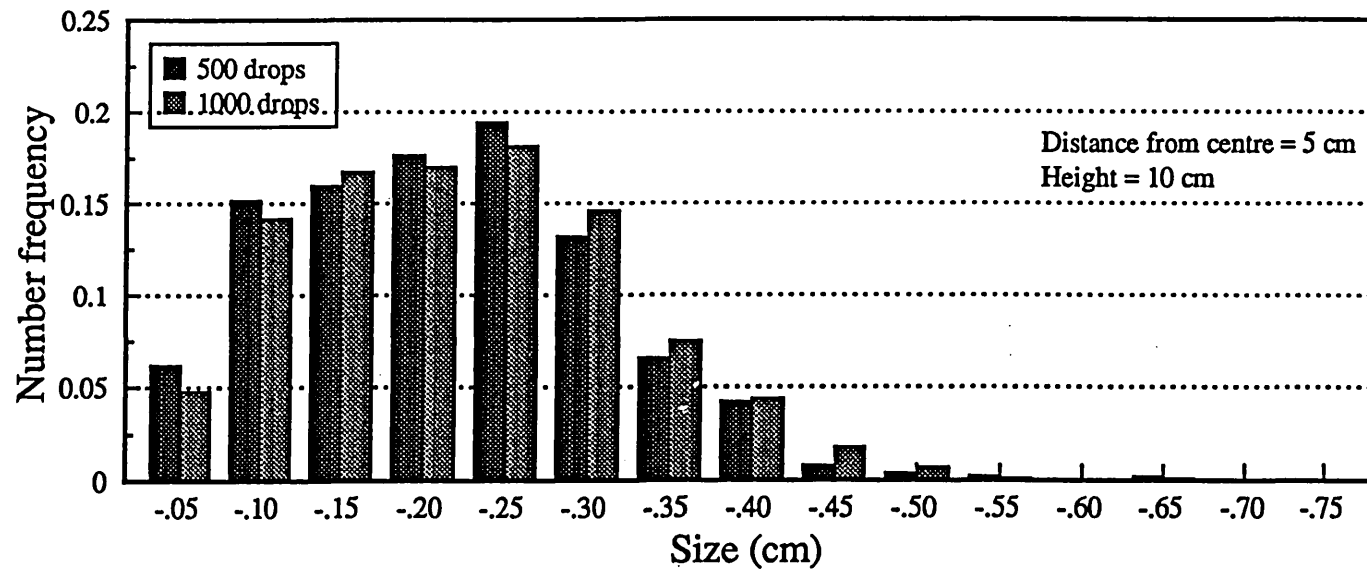


**Figure 4.12 :** *Effect of number of realizations on drop size distribution*  
 $N = 450 \text{ rpm}$  ;  $\varphi_o = .1$  ; Tank diameter = 22 cm

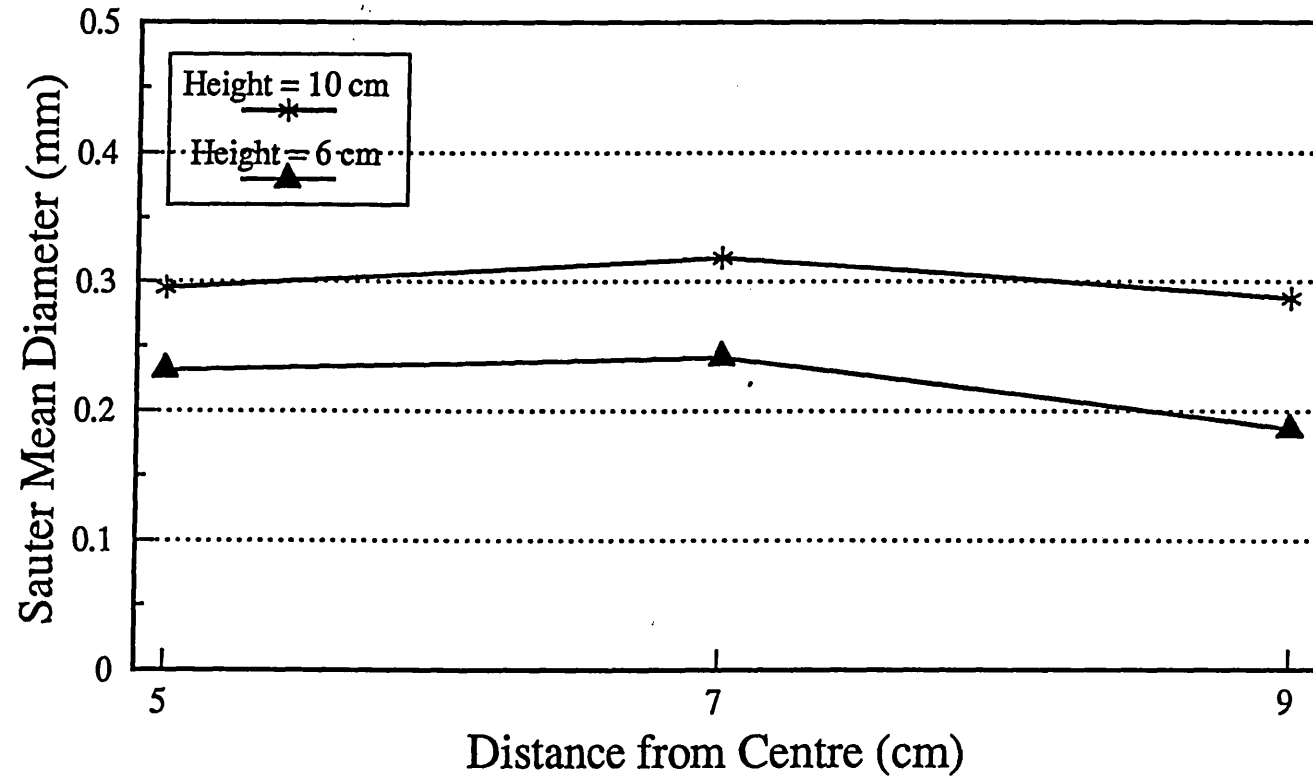
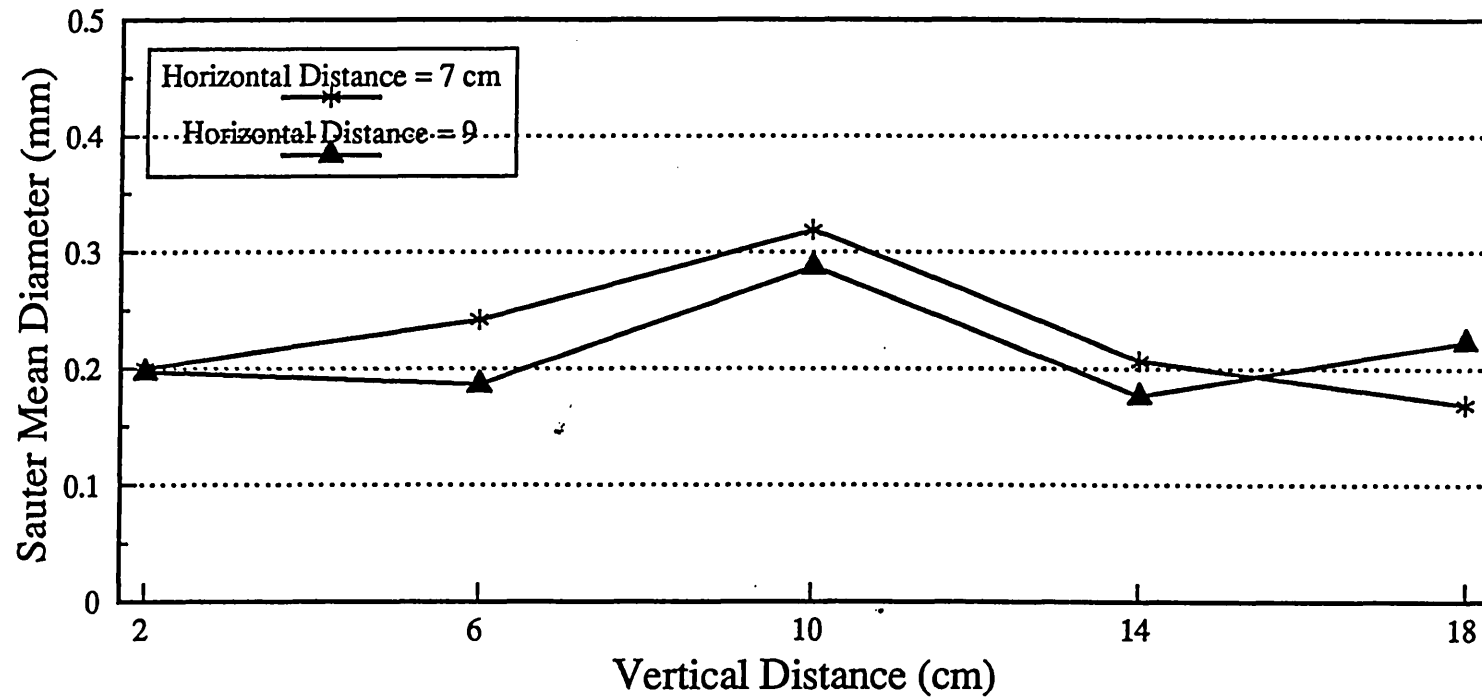
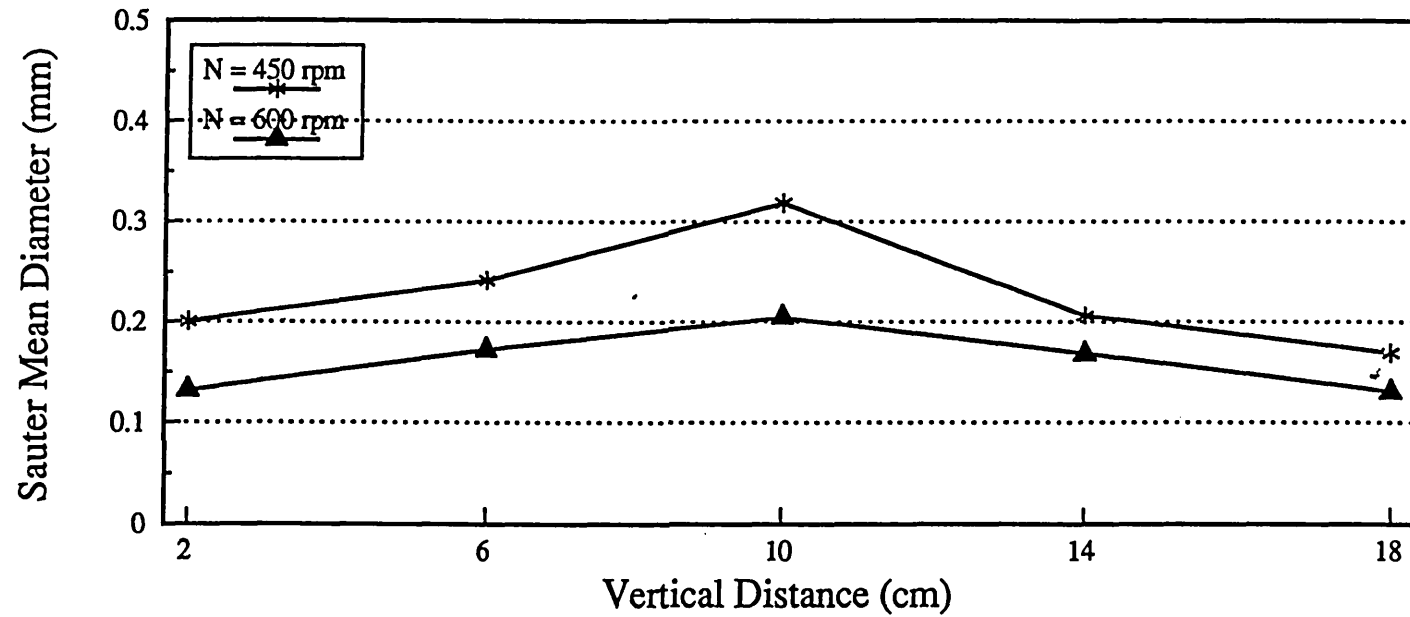


Figure 4.13 : Horizontal variations in local Sauter mean diameter values  
 $N = 450 \text{ rpm}$  ;  $\Phi_o = .1$  ; Tank diameter = 22 cm



**Figure 4.14 :** *Vertical variations in local Sauter mean diameter values*  
 $N = 450 \text{ rpm}$  ;  $\phi_o = .1$  ; Tank diameter = 22 cm



**Figure 4.15 :** *Effect of stirring speed change on local Sauter mean diameter values*  
*Horizontal distance = 7 cm ;  $\phi_o = .1$  ; Tank dia. = 22 cm*

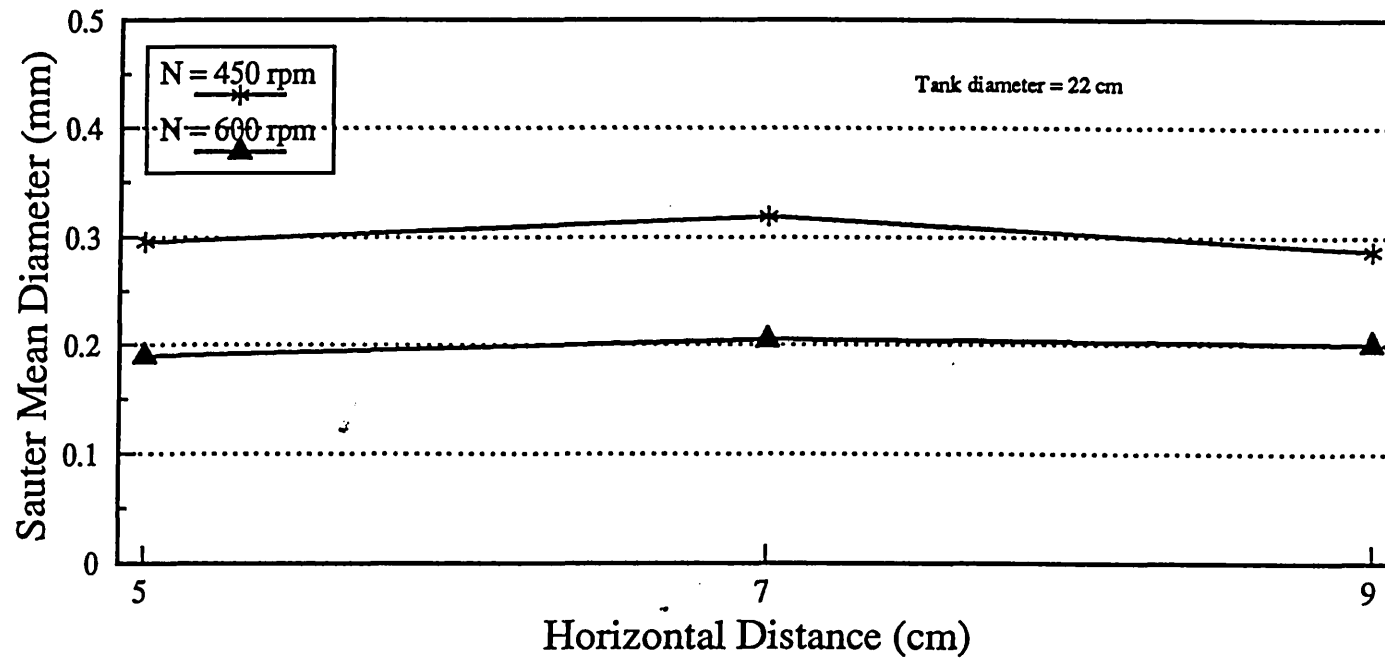
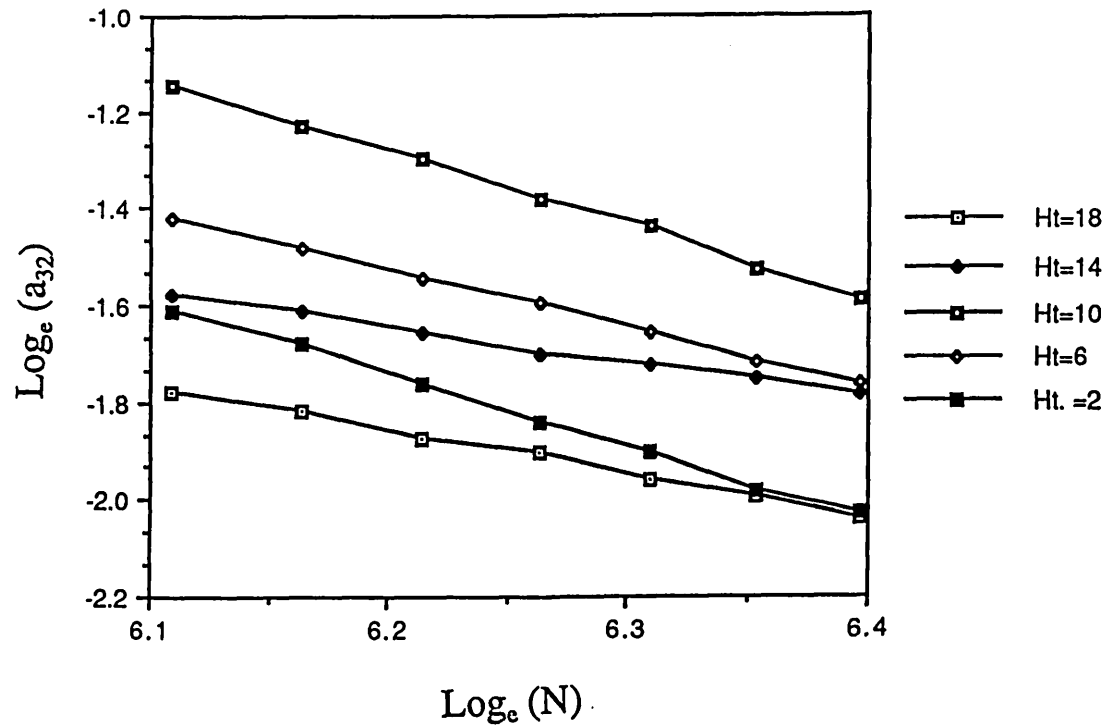
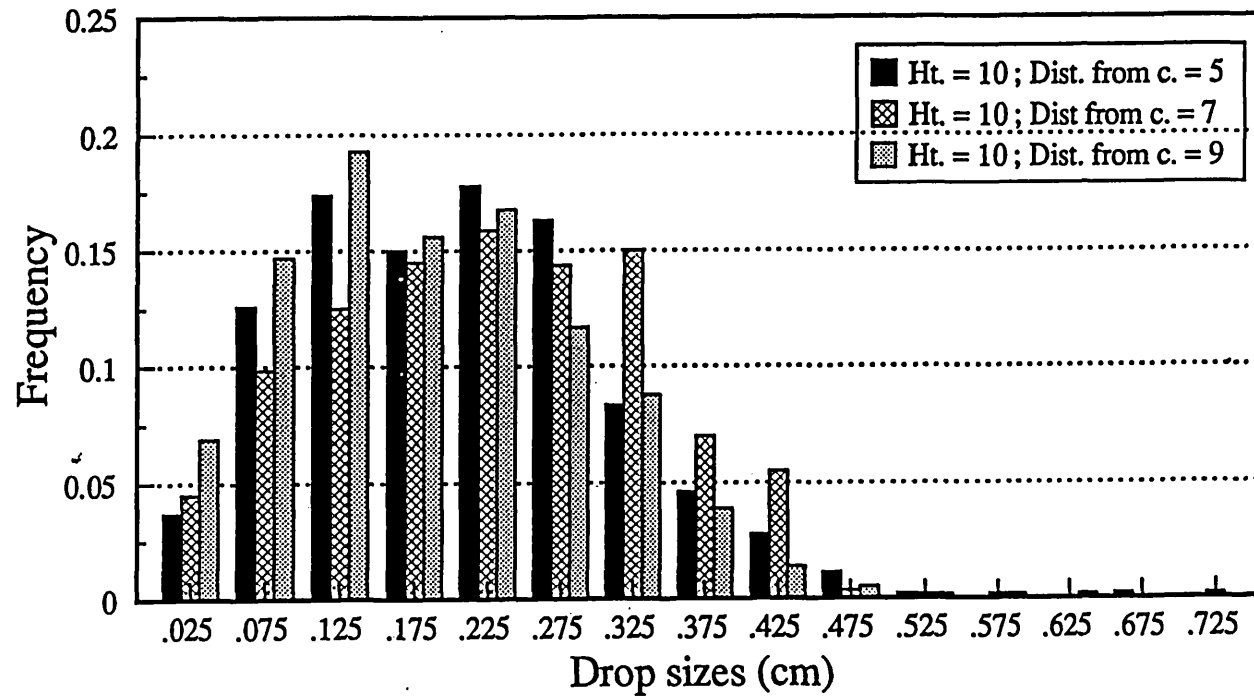


Figure 4.16 : Effect of stirring speed change on local Sauter mean diameter values  
Vertical distance = 10 cm ;  $\phi_o = .1$



(Slopes are given in Table 4.9)

**Figure 4.17 :** *Variation of Sauter mean diameter with stirring speed (Slopes are given in Table 4.9)  
Horizontal distance = 7 cm ;  $\phi_o = .1$*



**Figure 4.18 :** *Drop size distributions : Horizontal comparison*  
 $N = 450 \text{ rpm}$  ;  $\phi_o = .1$  ; Tank dia. = 22 cm

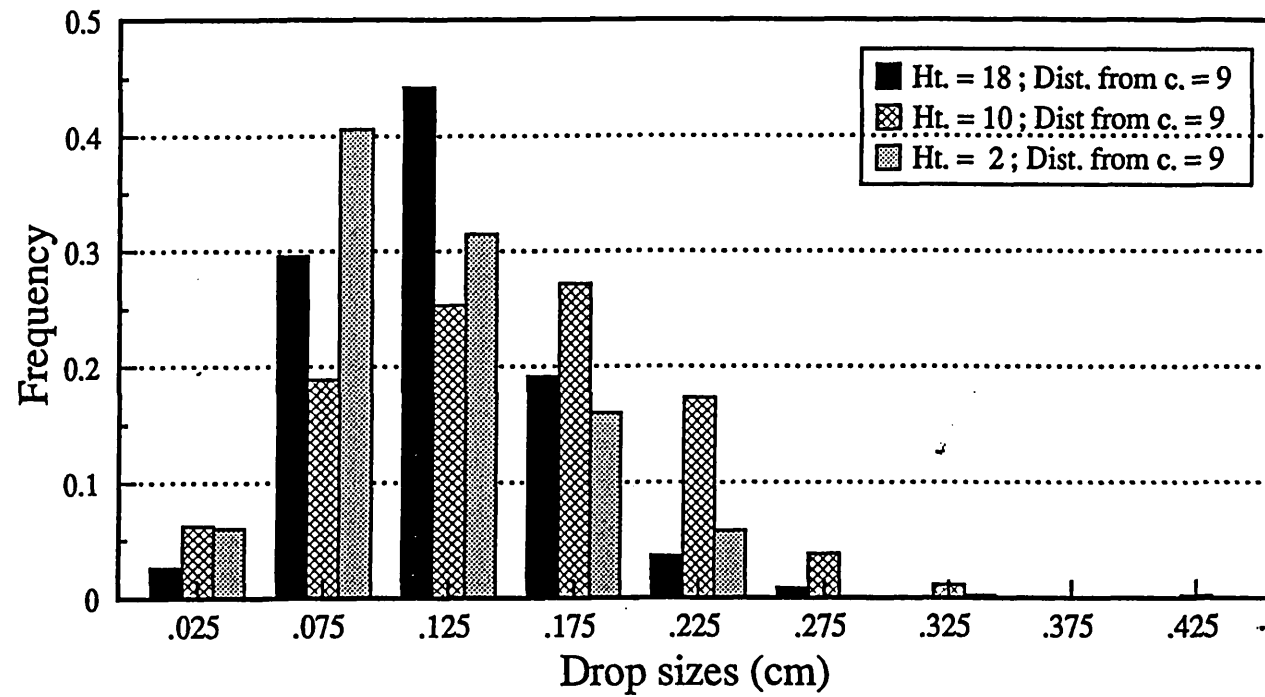


**Figure 4.19 :** *Drop size distributions : Vertical comparison*  
 $N = 600 \text{ rpm}$  ;  $\varphi_o = .1$  ; *Tank dia. = 22 cm*

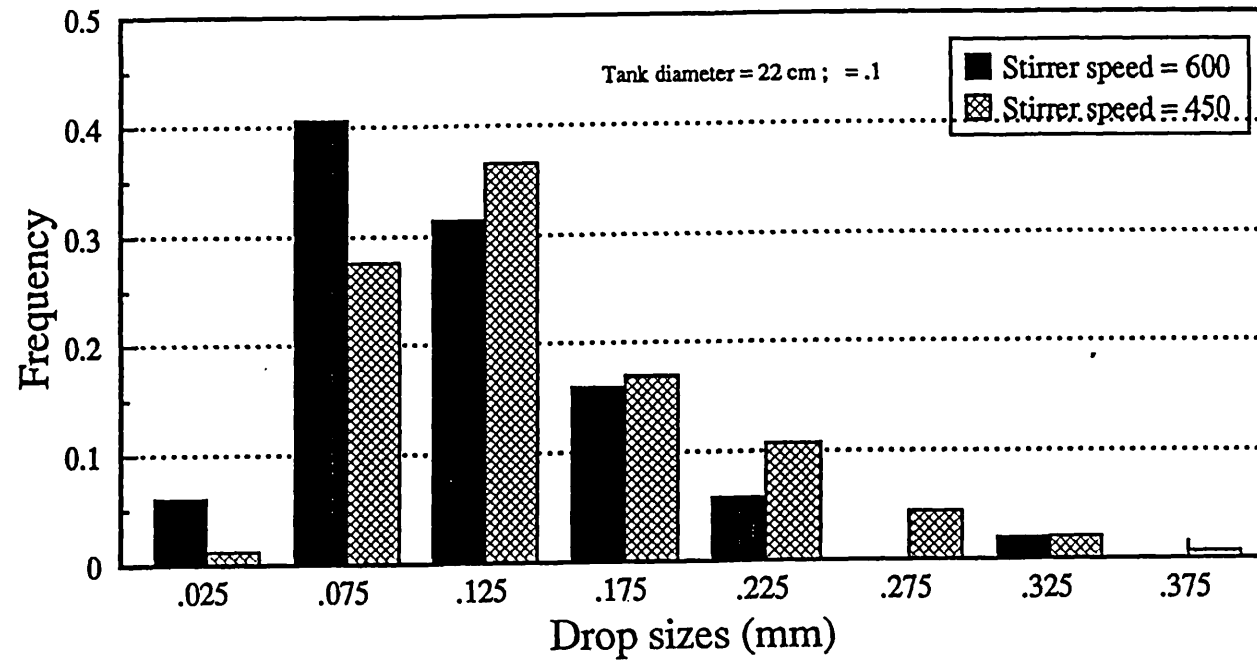


**Figure 4.20 :** *Drop size distributions : Effect of stirring speed*  
*Height = 2 cm ; distance from centre = 9 cm ;  $\phi_o = .1$  ; Tank diameter = 22 cm*

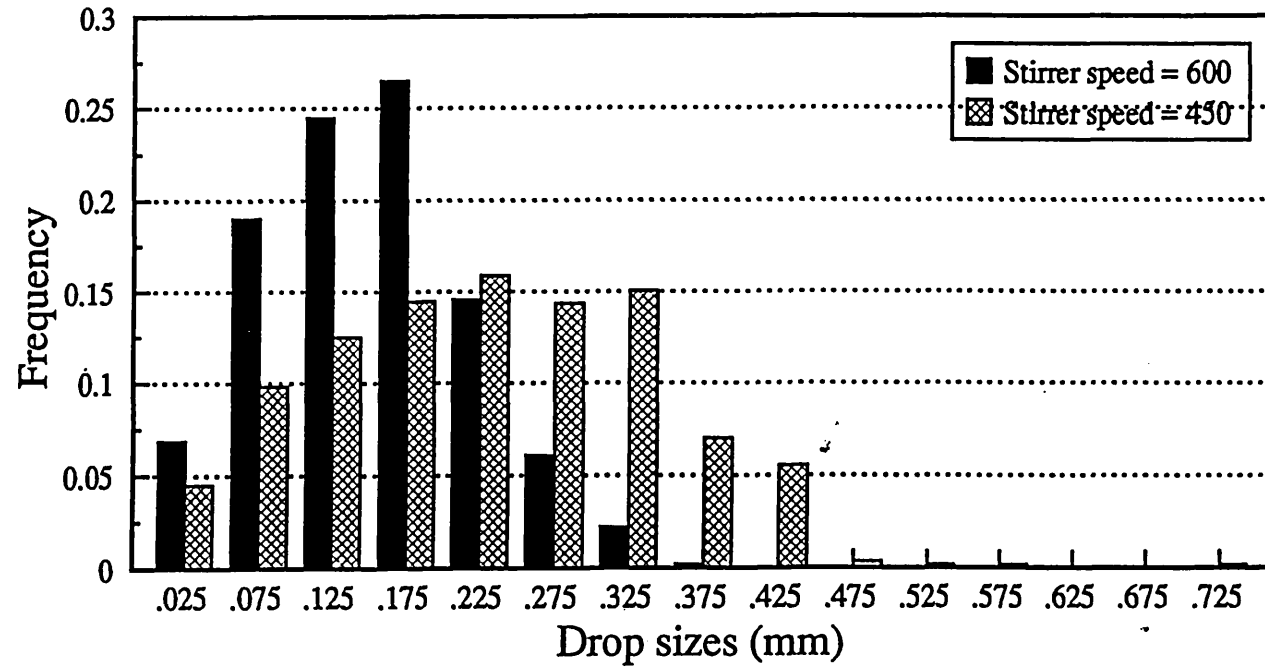


Figure 4.21 : Drop size distributions : Effect of stirring speed  
Height = 10 cm ; distance from centre = 7 cm ;  $\phi_o = .1$  ; Tank diameter = 22 cm

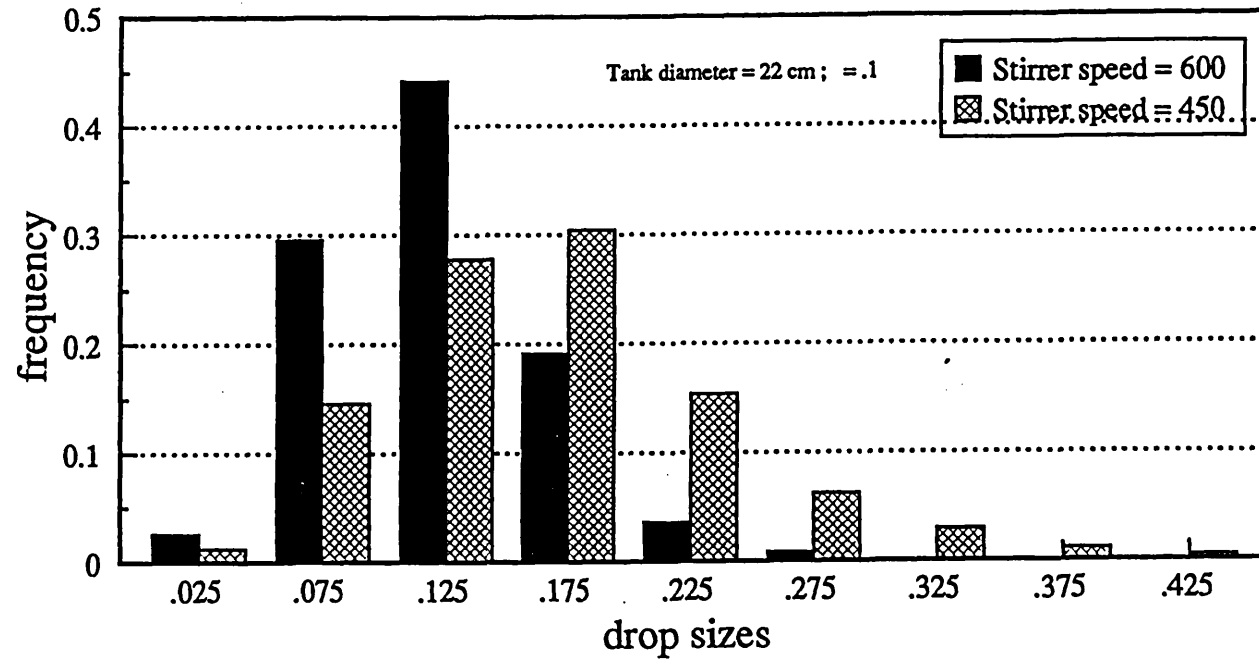


Figure 4.22 : Drop size distributions : Effect of stirring speed  
Height = 18 cm ; distance from centre = 9 cm ;  $\phi_0 = .1$  ; Tank diameter = 22 cm

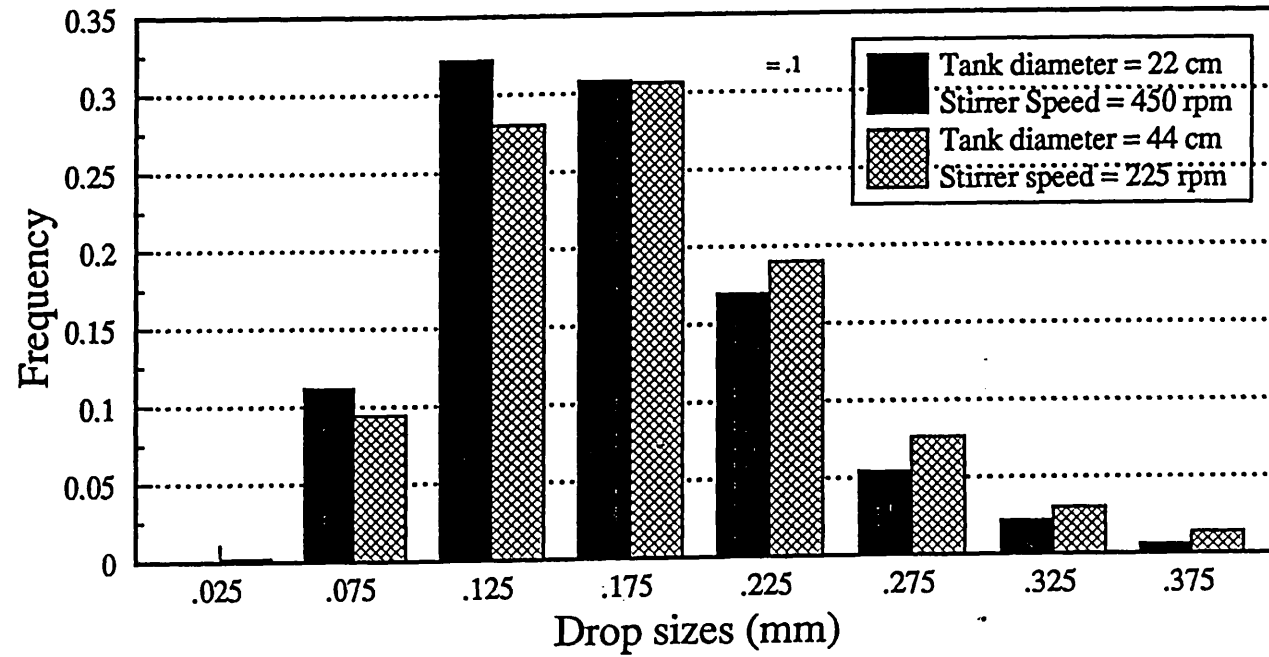


Figure 4.23 : Drop size distributions : Effect of tank scale  
 Height =  $14 D_T/22$  ; Distance from centre =  $7 D_T/22$  ;  $\phi_o = .1$

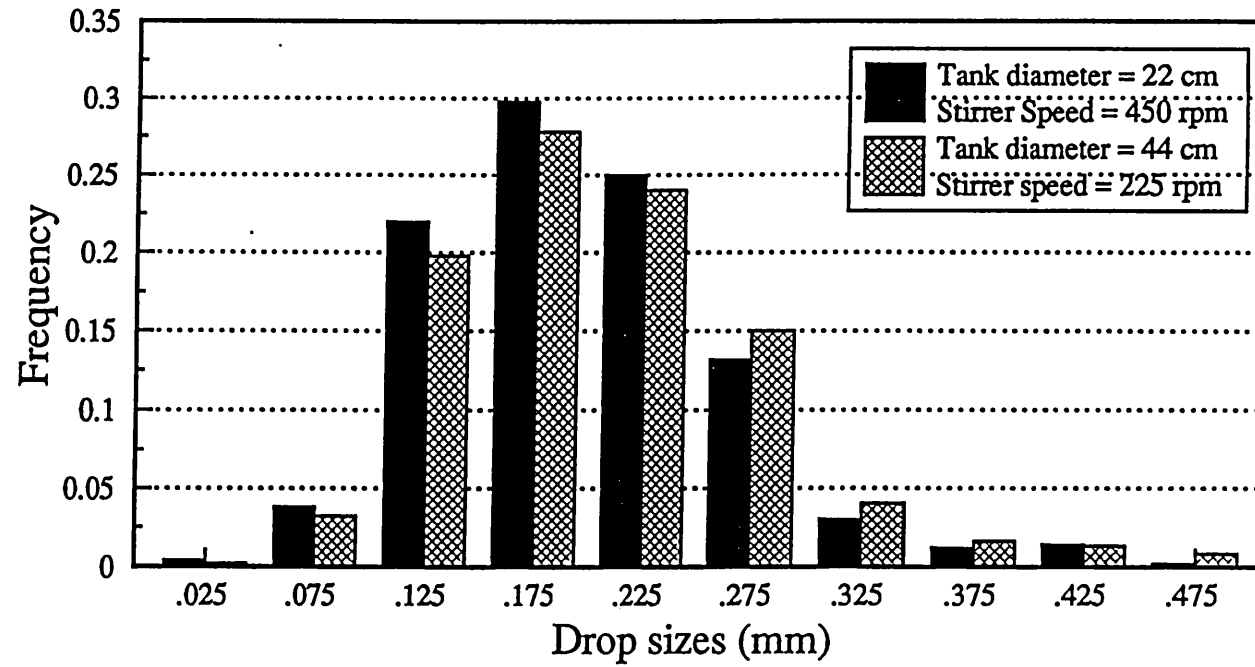


Figure 4.24 : Drop size distributions : Effect of tank scale  
 Height =  $6 D_T/22$  ; Distance from centre =  $7 D_T/22$  ;  $\varphi_o = .1$

# CHAPTER V

## DISPERSION MODELLING AND SIMULATION

The experimental results have shown local variations of the dispersion characteristics. Thus the assumption of a single turbulence mode, e.g. isotropic, affecting drop breakage and coalescence at all tank locations can no longer be accepted. In the following sections the expected local flow conditions and behaviour of drops in the tank are outlined and the simulation model together with the basic expressions necessary for use in the simulation are developed.

### **5.1 Modelling and description of flow and dispersion in agitated vessels**

#### **5.1.1 Flow in stirred tanks**

A qualitative description of the flow inside an agitated tank fitted with a flat blade turbine impeller may be given as follows :

The dispersion from the upper and lower sections of the vessels is sucked through the vertical axis towards the stirrer blades where it merges with vortices originating from the back side of the impeller blades. It then moves towards the tank wall and splits into two streams moving upwards and downwards respectively forming the upper and lower circulation streams as shown in **Figure 5.1**

Initially, after leaving the impeller blades, the vortices form a jet to be broken by the baffles at the wall which also reduce the tangential component of the velocity.

As the fluid elements join the circulating streams, isotropic turbulence tends to develop and energy is dissipated through conventional dissipation mechanisms.

As mentioned in the literature review, it is possible to divide the agitated vessel into two main sections depending on the type and level of turbulence, namely the impeller region and the circulation region.

Experimental investigation of stirred tanks showed a high contrast between the levels of energy dissipation in the impeller and the circulation regions. The former is

characterized by an average value ranging from 30 to 100 times that of the latter as well as a high degree of non-isotropy. In the following sections both regions are described.

#### **a- The Impeller Region**

The impeller region is the volume of the vessel in the vicinity of the impeller which is characterised by a high intensity of turbulence and high fluctuating non-isotropic components of velocity. The flow in this field tends to be towards the vessel wall in the form of two symmetrical vortices separated by the impeller disc.

The volume of the region is a function of :

- (i) Impeller geometry and size
- (ii) Impeller to tank diameter ratio
- (iii) The rotational speed of the impeller
- (iv) The physical properties of the fluid, mainly its viscosity.

#### **b- The Circulation Region**

It constitutes the bulk of the vessel volume and tends to be more homogeneous except for the dead zones that may develop in the corners and behind the baffles in cases of inadequate agitation. The volume of the region is affected by the same factors that govern the impeller discharge zone.

Furthermore, the two regions may be divided into subregions that show distinct properties and have both isotropic and non-isotropic features.

### **5.1.2 Modelling of dispersion behaviour inside the tanks**

In order to account for the effect of the different turbulence modes affecting the drop behaviour and to explain the change of the dependency of Sauter mean diameter on the stirring speed as reported in the previous chapter, three turbulence modes were considered in this work. These are:

1 **Isotropic:** in which the turbulent velocity fluctuations may be expressed as (Kolmogoroff 1941a,b):

$$\overline{u'^2(a)} \propto \bar{\epsilon}^{-2/3} a^{2/3} \quad a \gg \eta \quad (5.1)$$

where  $\bar{\epsilon}$  is given by (Shinnar 1961):

$$\bar{\epsilon} \propto N^3 D_I^2 \quad (5.1a)$$

The corresponding expression for  $a_{max}$  is:

$$\frac{a_{max} \rho_c^{3/5} \bar{\epsilon}^{2/3}}{\sigma^{2/3}} = constant \quad ; \quad a_{max} \propto N^{-6/5} \quad (5.2)$$

2 **Non-isotropic:** two non-isotropic turbulence modes are considered. They are :

2(i) **Non-isotropic (i):** velocity fluctuations are functions of the main flow i.e. the small scale flow is not statistically independent of the turbulence generating mechanism or breakup in the non-isotropic region is controlled by the energy-containing eddies.

Applying Batchelor's turbulence dissipation equation and following Schwartzberg and Treybal(1968) analysis, the turbulent velocity fluctuations may be deduced as follows :

$$\overline{u'^2(a)} \propto \left( \sqrt[3]{u_x'^3(a) + u_y'^3(a) + u_z'^3(a)} \right)^2 \quad (5.3a)$$

The components  $u'_x(a)$ ,  $u'_y(a)$  and  $u'_z(a)$  are in turn proportional to the tip speed (Schwartzberg and Treybal(1968)), i.e.

$$\left( \sqrt[3]{u_x'^3(a) + u_y'^3(a) + u_z'^3(a)} \right) \propto ND \quad (5.3b)$$

Combining equations (5.3a) and (5.3b) :

$$\overline{u'^2(a)} \propto (ND)^2 \quad (5.3c)$$

Substituting for the velocity fluctuations in the expression for the critical Weber number or the maximum drop size proposed by Kolmogoroff(1949) and Hinze(1955), i.e.  $(N_{we})_c = constant$ , the following expression is obtained for  $a_{max}$ :

$$\frac{\rho_c N^2 D^2 a_{max}}{\sigma} = constant \quad ; \quad a_{max} \propto N^{-2} \quad (5.3)$$

2(ii) **Non-isotropic (ii):** Breakup is controlled by the spatial distribution of average velocities of flow. In such a case, the velocity fluctuations across a drop of size  $a$  could be determined by the relative values of the average velocities (Konno *et al*(1983)).

For stirred vessels, the average value of velocity at every point will be proportional to the tip speed(Schwartzberg and Treybal(1968)). Since the drop sizes are small, the velocity fluctuations between two points separated by a distance  $r$  will be proportional to that distance. Therefore, the average velocity fluctuations across a drop of size  $a$  may be expressed as

$$\overline{u^2(a)} \propto (ND)^2 \left(\frac{a}{D}\right)^2 \quad (5.4a)$$

In this case, the maximum drop size may be related to stirring speed through :

$$\frac{\rho_c N^2 a_{max}^3}{\sigma} = constant \quad ; \quad a_{max} \propto N^{-2/3} \quad (5.4)$$

Equation (5.4) applies to the inertia subrange.

Accordingly, a drop moving in a stirred vessel experiences different turbulence effects depending on the turbulent characteristics of the surrounding fluid. In this work, it was assumed that the different turbulence modes are acting on drop population simultaneously with proportions governed by the hydrodynamics of the system and its physical properties. No solid theoretical clues are available so the ratios were fixed by trial and error as described later in chapter VI. Different combinations of turbulence modes result in dependencies of Sauter mean diameter on  $N$  ranging from  $-0.66$  to  $-2.0$ , as shown in **Figure 5.2**.

From the preceding description (section 5.1.1), it is clear a drop has the following possibilities :

- (i) Collision with the impeller blades; shattering may take place.

- (ii) While moving with the vortex issuing from the impeller breakage or coalescence may take place.
- (iii) Collision with the wall or a baffle leading to breakage.
- (iv) Breakage or coalescence within the circulation region.
- (v) A drop may survive the effect of different forces and keep circulating; i.e preserving its identity.

As discussed in the literature review, the complete solution of Navier-Stokes equations, which is needed for describing realistic dispersion behaviour in turbulent fields, is yet to be developed. However (ii), (iv) and (v) involve breakage and coalescence due to turbulent fluid behaviour and could be modelled by stochastic methods utilizing the probability equations governing them.

#### **5.1.2.1 Drop breakage**

Drops moving in a turbulent flow field are subjected to the action of the different forces present. These forces include:

- (i) buoyancy and gravitational forces
- (ii) inertial forces
- (iii) viscous shear forces
- (iv) interfacial tension forces

These forces act simultaneously on the drop causing deformation and breakage but in agitated tanks where the turbulence is normally high and tank Reynolds number is in excess of 10000, the effect of buoyancy and gravitational forces may be ignored in comparison to the other forces.

As mentioned in chapter II, deformation depends on the type of flow and the intensity of the forces and drops break when the inertial and/or viscous shear forces are in excess of the surface forces which tend to restore the original spherical drop shape and preserve its identity.

In the following section the expression for the breakage rate of a drop of diameter  $a$  is derived from the consideration of inertial and interfacial forces, the same approach that followed by Coulaloglou and Tavlarides(1977) but without assuming local isotropy. The viscous forces were ignored because of the fact that the experimental

drop sizes[Okufi (1984), and this work] are well above the Kolmogoroff micro scale of turbulence (see appendix||) beyond which the inertial forces dominate the breakage process and viscous effects become negligible. The number of daughter drops is assumed to be two i.e. binary breakage.

### 5.1.2.1.1 Breakage Frequency $g(a)$

Breakage frequency may be defined as the number of drops breaking per unit time per unit volume for a turbulence mode  $m$  and may be expressed as

$$g_m(a) = \frac{\text{fraction of drops breaking}}{\text{breakage time}} = \frac{1}{t_b} \frac{\Delta M(a)}{M(a)} \quad (5.5)$$

where  $t_b$  is the time sufficient for the forces to cause the deformation that would result in a breakage,  $M$  is the number of drops per unit volume and  $\Delta M(a)$  is the number of drops breaking.

Since drops do not normally break unless their kinetic energy is in excess of their surface one,  $\Delta M(a)/M(a)$  may be considered as the fraction of drops with Weber numbers higher than the critical one or

$$\frac{\Delta M(a)}{M(a)} \propto \exp \left[ -k \frac{\sigma}{\rho_a a u_\phi^2(a)} \right] \quad (5.6)$$

In order to evaluate the breakage time  $t_b$ , an analogy with the relative motion of two lumps of fluid in a turbulent flow field as described by Batchelor(1952) was assumed. The centres of the would be formed drops were assumed to follow the motion pattern of the centres of the fluid lumps. As forces act on the drop, two fluid masses connected by a thread start to shape up. The motion of eddies around the masses tend to separate them further hence decreasing the thickness of the fluid thread connecting them until a critical one is reached where rupture takes place and two new drops form as represented in **Figure 5.3**.

The separation distance  $d(t)$  between the two masses at any time  $t$  during the thread drainage process is proportional to the size of the original drop i.e

$$\text{Separation distance } d(t) \propto \text{drop size } (a) \quad (5.7)$$

or

$$d(t) = k'a \text{ at time } t \quad (5.8)$$

On the other hand, the separation distance between the centres of the masses at any time  $t$  is also proportional to the relative velocity of their centres i.e

$$d^2(t) \propto \overline{u_\phi^2(a)} t^2 \quad (5.9)$$

Rearranging equation 5.9,  $t$  may be expressed as

$$t^2 = \frac{d^2(t)}{k \overline{u_\phi^2(a)}} \quad (5.10)$$

Assuming that the time taken by the eddies to separate the two masses is proportional to the breakage time and substituting for  $d(t)$  from equation 5.8, the following expression for  $t_b$  may be obtained

$$\frac{1}{t_b} = \frac{k}{a} \overline{u_\phi^2(a)}^{1/2} \quad (5.11)$$

Combining equations 5.6 and 5.11 then the breakage frequency  $g(a)$  may be expressed in term of the drop size and physical properties as:

$$g_m(a) = k_{b1m} \frac{\overline{u_\phi^2(a)}^{1/2}}{a} \exp \left[ -k_{b2m} \frac{\sigma}{\rho_a a \overline{u_\phi^2(a)}} \right] \quad (5.12)$$

The effective frequency for the combined turbulence  $g(a)$  modes is defined as:

$$g(a) = \sum_m g_m(a) \quad (5.13)$$

where  $m$  stands for the turbulence mode which could be obtained by substituting the appropriate expressions for  $\overline{u_\phi^2(a)}$  from section 5.1.2.

### 5.1.2.2 Drop coalescence

Due to the presence of turbulent velocity fluctuations, drops in flow field collide giving rise to the probability of coalescence. The collisions takes place because of:

- (i) relative motion of eddies
- (ii) relative motion of the drops within a single eddy

As the turbulent velocity fluctuations cause drops to collide, a thin film of the continuous phase is trapped between the two colliding drops. Depending on the magnitude of forces affecting the drop, eddies cause the two drops to separate or the

continuous film is drained to the critical thickness at which rupture occurs and the two globules merge forming a new drop. As a consequence, coalescence rate is to be expressed by the product of two terms, the collision frequency and collision efficiency

#### 5.1.2.2.1 Collision frequency

Starting from the expressions given in the literature for the collision of molecules in the kinetic theory of gases, an expression for the collision frequency may be derived assuming analogy between the two systems. The expression for molecular gases collision is [Gucker & Seifert(1966), Glasstone(1960)]:

$$Z_{12} = \pi \sigma_{12}^2 \sqrt{c_1^2 + c_2^2} \quad (5.14)$$

where  $c_i$  is the velocity of component  $i$  and  $\sigma_{12}$  is given by:

$$\sigma_{12} = \frac{1}{2}(\sigma_1 + \sigma_2) \quad (5.16)$$

where  $\sigma_i$  is the diameter of component  $i$  molecule.

Replacing  $\sigma_i$  by  $a_i$  the drop diameter and  $c_i^2$  by  $\overline{u_\phi^2(a_i)}$ , the turbulent velocity fluctuation across a distance  $a$ , the collision frequency  $h(a, a')$  may be expressed as

$$h(a, a') \propto k (a + a')^2 (\overline{u_\phi^2(a)} + \overline{u_\phi^2(a')})^{1/2} \quad (5.17)$$

for two drops of sizes  $a$  and  $a'$

#### 5.1.2.2.2 Collision efficiency

Collision efficiency of a collision between two drops of diameters  $a$  and  $a'$   $\lambda(a, a')$  may be expressed, as mentioned in the literature, as the ratio of the average contact time  $\bar{t}$  to the average time needed for the continuous phase film that separate the drops to drain away  $\bar{\tau}$ , or

$$\lambda(a, a') \propto \exp\left[-\frac{\bar{\tau}}{\bar{t}}\right] \quad (5.18)$$

The average draining time for deformable drops was given by Chappellear(1963) as :

$$\bar{\tau} \propto \left(\frac{\mu_c F}{\sigma^2}\right) f(h_o, h_c) \left[\frac{aa'}{(a+a')}\right]^2 \quad (5.19)$$

where  $h_0$  and  $h_c$  are the initial separation distance or the original continuous phase thickness at collision and the critical thickness at which rupture becomes possible respectively and for a given system  $f(h_c, h_0)$  is proportional to a constant,  $F$  is the force compressing the drops which was assumed to be proportional to the mean square velocity difference at either ends of an eddy of diameter  $(a+a')$  and given by

$$F \propto \overline{\rho u_\phi^2(a+a')} \left[ \frac{aa'}{(a+a')} \right]^2 \quad (5.20)$$

The average contact time was assumed to be proportional to the characteristic period of velocity fluctuation of an eddy of size  $(a+a')$  which is according to Levich(1962) is

$$\bar{t} \propto \frac{(a+a')}{[u_\phi^2(a+a')]^{1/2}} \quad (5.21)$$

Rearranging and combining equations 5.18 to 5.21, the collision efficiency may be expressed as

$$\lambda(a, a') \propto \exp \left[ -k \frac{\mu_c \rho_d (\overline{u_\phi^2(a+a')})^{3/2} \left[ \frac{aa'}{a+a'} \right]^4}{\sigma^2} \right] \quad (5.22)$$

Since the coalescence rate  $f_m(a, a')$  is proportional to collision rate times the collision efficiency, it may be expressed as

$$f_m(a, a') = k_{c1m} (a+a')^2 (\overline{u_\phi^2(a)} + \overline{u_\phi^2(a')})^{1/2} \times \exp \left[ -k_{c2m} \frac{\mu_c \rho_d (\overline{u_\phi^2(a+a')})^{3/2} \left[ \frac{aa'}{a+a'} \right]^4}{\sigma^2} \right] \quad (5.23)$$

where  $m$  as before stands for the turbulence mode. The effective frequency as before may be obtained by summation over  $m$  or

$$f(a, a') = \sum_m f_m(a, a') \quad (5.24)$$

Equation 5.23 is the coalescence rate of two drops of diameters  $a$  and  $a'$  in term of drop diameter and fluids physical properties under given turbulence conditions.

It worth mentioning that the collision efficiency for a pair of drops of diameters  $a$  and  $a'$  decreases as the diameters increase which indicate that the probability of a new stable drop being created decreases as the drop sizes increase. This is compatible with the result of the breakage frequency expression that result in high frequencies as the sizes increase or more instability.

For a population of  $M$  drops per unit volume, the breakage frequency for the whole sample is given by

$$f_b = \sum_{i=1}^M g(a_i) \quad (5.25)$$

and for coalescence

$$f_{c,a_i} = \sum_{\substack{j=1 \\ j \neq i}}^M f(a_i, a_j) \quad (5.26)$$

where  $f_{c,a_i}$  is the coalescence frequency of the  $i$ th drop with the rest of the sample,

$$f_c = \frac{1}{2} \sum_{i=1}^M f_{c,a_i} \quad (5.27)$$

$$= \frac{1}{2} \sum_{i=1}^M \sum_{\substack{j=1 \\ j \neq i}}^M f(a_i, a_j) \quad (5.28)$$

where  $f_c$  is the sample coalescence frequency.

The probability of breakage may be defined as

$$P_b = \frac{f_b}{f_b + f_c} \quad (5.29)$$

and the probability of coalescence as

$$P_c = \frac{f_c}{f_b + f_c} \quad (5.30)$$

## 5.2 Simulation of liquid-liquid dispersions

Simulation may be defined as

*"The process of designing a computerized model of a system (or process) and conducting experiments with this model for the purpose either of understanding the behaviour of the system or of evaluating various strategies for the operation of the system" Graybeal and Pooch (1980)*

### 5.2.1 Definitions

In the following discussion the terms used were defined as follows:

Entity	:	drop
Attributes	:	drop diameter, breakage and coalescence frequencies, age and concentration
Event or activity	:	breakage, coalescence or interphase process such as mass transfer, heat transfer or chemical reaction
State of the system	:	a description of all the entities, attributes and activities as they exist at some point in time.
Endogenous events:	:	activities that occur within the system

### 5.2.2 System Definition

Before embarking on the design of a simulation model, a thorough and detailed understanding of the system under consideration is required. Knowledge of the type of the activities involved and the laws governing them as well as the entities concerned is a prerequisite. In short, a system model with its characteristics being representative of those of the real system is to be constructed.

The system under consideration may be defined as a uniform dispersion produced by mixing or agitation of two immiscible and mutually saturated liquids in a batch stirred tank that conforms to the standard tank configuration as defined by Rushton et al(1950). In addition the system may be assumed to be stable with respect to physical properties, i.e. no density, viscosity or surface tension variations are taking place. The flow is turbulent and the drop size ( $a$ ) is greater than the microscale of turbulence.

The activities taking place are drop breakage and coalescence, both endogenous and discrete processes.

The structure of the turbulence inside the vessel is composed of different flow regimes, isotropic and non-isotropic, of unknown distribution.

### **5.2.3 Monte Carlo Simulation Technique**

Due to the random nature of turbulent flows, the events are stochastic processes that may be treated as Markovian with Poisson arrival pattern.

Two main approaches may be used for the solution of the problem under consideration, namely, the Population Balance Equations (PBE) or the Monte Carlo Simulation Techniques as mentioned in chapter II.

The latter method was chosen for the following reasons :

1. It eliminates the need for solving complicated integrodifferential equations (PBE's) that result when transfer processes modelling is added to the simulation.
2. Simulation gives information about fluctuations of mean population characteristics as well as their individual entities around the average values, a feature not always possible with PBE's.
3. It allows for easy implementation of the basic expressions for mass and heat transfer rates without unnecessary simplification that may cause significant differences between experimental and simulation results.

### **5.2.4 Coalescence Frequency Approximation**

Monte Carlo simulations of dispersed systems require considerable computation time. This is due to the nature of the interactions between the different entities specially with respect to coalescence as seen in equation 5.28. A sample of  $M$  drops needs  $M(M-1)/2$  interactions to evaluate the coalescence frequencies of the drops, i.e. the computation load increases almost exponentially as  $M$  increases.

In the attempt to overcome this problem researchers usually resort to unrealistic oversimplification of the interaction functions and/or the simulation algorithms such

as the assumption binary breakage followed by a binary coalescence of two drops of equal sizes(Laso 1987a,b). This in general increases the error or results in discrepancies between the simulation and experiments.

Careful examination of the expressions for breakage and coalescence equations(5.12, 5.23 and 5.28) reveals that the change of the drop coalescence frequency with its size is more or less linear, i.e. the exponential term does not cause sharp increase or decrease in drop overall coalescence frequencies with the population, unlike the case for breakage frequency where the change is gradual until the maximum stable drop size is reached where the function peaks as explained in **Figure 5.4** which is a generalized plot of equation 5.12 or  $g_m(a)$  vs drop sizes.

This stability of the coalescence frequency change is explained by the fact that the coalescence frequency of a drop is a function of the whole size spectrum and not confined to the drop in question , as in breakage.

Making use of this observation, the drop spectrum may be divided into  $NC$  equally spaced intervals for which the sizes were calculated and the coalescence frequencies for all possible interactions,  $NC^2$ , evaluated. An  $NC \times NC$  matrix is created where the frequencies are stored. The matrix may be reduced to an upper or lower matrix since  $f(i,j)=f(j,i)$ , i.e. the matrix is symmetrical.

This procedure results in the linearization of the dependency pattern of the computer time on the sample size, i.e the number of interactions become proportional to the sample size  $M$ , times the Number of intervals  $NC$ .

Thus complexity of the interaction functions is no longer a factor in the actual simulation time. The time required for creation of the  $NC \times NC$  matrix to store the coalescence frequency information is insignificant compared to the simulation time. The accuracy of the calculated coalescence frequencies was found to be in good agreement with the results obtained using the whole drop spectrum as shown later in **Table 6.2** and **Figure 6.4**.

Assuming that  $J$  drops exist per interval, then the overall coalescence frequency of a drop of size  $a_i$  is

$$f_{(c,a_i)} = \sum_{k=1}^{NC} J_k f(a_i, a_k) - f_{(a_i,a_i)} \quad (5.31)$$

and

$$f_c = 0.5 \sum_{i=1}^M f_c(a_i) \quad (5.32)$$

where  $f(a_i, a_k), f(a_i, a_i)$  are given by equation 5.24.

The number of intervals  $NC$  and size increment from one interval to the following one  $\Delta s$  may be chosen according to the accuracy required and rate of change of the coalescence frequency with drop size as discussed later in chapter VI.

### 5.2.5 Coalescence Frequencies Evaluation

The procedure to evaluate the coalescence frequencies may be outlined as follows :

- 1- At the initiation stage, a sample of  $M$  drops, i.e. of the same size as the number of intervals, was created with diameters taking the values

$$a_i = \Delta s(i - 1/2) \quad i = 1, NC \quad (5.33)$$

the diameter of the  $i$ th drop being the value assigned for the  $i$ th interval mid-point or its pivoting point as will be referred to later and  $\Delta s$  is given by

$$\Delta s = \frac{\text{Drop size span}}{NC} \quad (5.34)$$

The different coalescence frequencies between drop pairs were evaluated using equation 5.24 and stored in the coalescence frequencies reference matrix. The number of such distinct pairs was given by  $NC(NC-1)/2$ .

- 2- As all drops frequencies were evaluated at the start of the simulation, the following procedure was followed :

- a- Given the sample size  $M$  and  $j_k$  drops in the interval  $k$ , then a drop in the interval  $int$  may be approximated by a drop of a diameter equal to the

mid-interval value as given by Equation 5.33. For such a drop, the overall coalescence frequency with the whole population is given by :

$$f_c(a_i) \approx (a_i) = \sum_{k=1}^{NC} j_k f_c(a_i, a_k) \quad (5.35)$$

For M intervals the frequency  $f_c(a_{int})$  is evaluated and stored in a temporary array. The number of statements involved is  $NC^2$  ;

b- for each drop in the population, the coalescence frequency was approximated with the value calculated in 2a for the equivalent interval, i.e.

$$f_c(a_i) = f_c \left[ interval \left( \frac{a_i}{\Delta s} + 1 \right) \right] \quad (5.36)$$

The number of statements involved is M.

- 3- After event execution the coalescence frequencies were assigned using the procedure given under 2b.
- 4- In the selection of coalescing drops, the same steps followed in the previous algorithms were repeated.

## 5.2.6 Simulation Time Management

There are two methods of time management : the time driven method (or periodic scan technique) and the event driven method (or Interval of Quiescence (IQ) method). The former simulates the system by choosing between the occurrence or absence of event over a predetermined time increment  $\Delta t$  while the latter advances the system by a random time increment  $t$  calculated from a random number distribution and the system event frequencies. The increment is defined in a way to make it equal to the time necessary to trigger the next event.

In both methods, the abrupt discrete processes, such as breakage and coalescence, were assumed to occur at the end of the time increment allowing the interevent time for continuous smooth variations caused by mass transfer, heat transfer and/or chemical reaction.

Since in the latter method the simulation clock was advanced by the amount of time necessary to trigger the next event, no information was lost and the exact time for

event occurrence can be recorded. This is in contrast to the time driven method where the time increment is predetermined and no account is taken of the exact time for events occurrence.

The IQ method is used in this investigation for the following reasons :

1. It is more effective from the computational point of view.
2. The time increment is random and reflects the state of the system more truly since the actual population attributes were used.
3. It is easy to implement, unlike the time driven method in which special precautions have to be taken in defining the probabilities of events.

The unique interevent time for this discrete process is considered to be the Poisson arrival pattern given by:

$$IQ = -\frac{\ln x}{\sum f_i} \quad (5.37)$$

where  $f_i$  is the frequency of the  $i$ th activity and  $x$  is a uniformly distributed random number.

The Poisson distribution is a discrete distribution which has been widely used to model arrival distributions and other seeming random processes. Its main properties are:

- (i) the probability that an event takes time within small time interval  $\Delta t$  is  $\Lambda \Delta t + O(\Delta t)$  where  $\Lambda$  is the arrival rate and  $O(\Delta t)$  includes all higher terms in  $\Delta t$  such that  $\lim_{\Delta t \rightarrow 0} O(\Delta t)/\Delta t = 0$ .
- (ii) the probability of two or more events in  $\Delta t$  is  $O(\Delta t)$  and hence can be neglected.
- (iii) The number of events on non-overlapping time intervals is statistically independent.

## 5.2.7 Daughter Droplets

### 5.2.7.1 Number of daughter droplets

In the absence of sound conclusions about the number of drops formed by breakage, two droplets were assumed to be formed by the breakage of a parent drop.

### 5.2.7.2 Daughter droplets distribution

In contrast to the assumptions made by some investigators regarding the resultant drop diameters being equal[Laso et al(1987a,b, Curl(1963)], a Beta distribution was adopted of the form

$$\beta(a, a') = 30 \left( \frac{a'}{a} \right)^6 \left( 1 - \frac{a'}{a} \right)^2 \quad (5.38)$$

such that

$$\int_0^1 \beta(a, a') d \left( \frac{a'}{a} \right) = 1 \quad (5.39)$$

a distribution found to be more representative of the experimental results than the assumption of splitting into equal sizes(Peleg & Normand (1986)).

## 5.2.8 Simulation Algorithm

A simplified Monte Carlo algorithm, of which a general flow diagram is given in **Figure 5.5**, was used to simulate the dispersion. The algorithm was initiated (**Figure 5.6**) by reading the data which includes the physical properties, hydrodynamic parameters and tank dimensions. Either a uniformly distributed drop population (typically 400) was created or the sizes read from another file if the run was a continuation of a previous one.

An  $NC \times NC$  coalescence frequency reference matrix was created where the  $i, j$  coalescence interactions were stored. They were to be used later for frequency calculations.

All variables that can be calculated only once were grouped together and evaluated in order to prevent unnecessary redundant operations. The different attributes were calculated and assigned storage.

The simulation run is divided into passes (**Figure 5.7**) that in turn divided into event cycles(**Figure 5.8**). The simulation pass starts by evaluating the system statistics. Every simulation pass consists of event cycles.

The event cycle starts by calculating the IQ, then a random number is projected on the event probability axis to determine the event type as shown in **Figure 5.9**.

To find the drops taking part in the event another random number is projected on the normalized cumulative frequency axis as shown in the **Figures 5.10** through **5.13**.

The Event was executed and the sample frequencies were updated. The change in breakage frequency is only affected by the drops taking part in the events while the coalescence frequency is a function of the whole sample. As a consequence a large increase in the computation time is experienced.

A test for the time elapsed from the start of the pass was carried out. If it was found to be less than the time assigned for the pass another event cycle was executed otherwise the statistical features were calculated and written in the result file.

The pass time is then modified making use of the number of events in the previous pass as well as the sample frequencies. This was done primarily to allow for approximately the same number of events per pass.

A test for steady state(S.S.) was carried out. The S.S. was defined as the Sauter and arithmetic mean diameters being within  $\pm 1\%$  over three consecutive cycles. The procedure was continued until steady state was achieved.

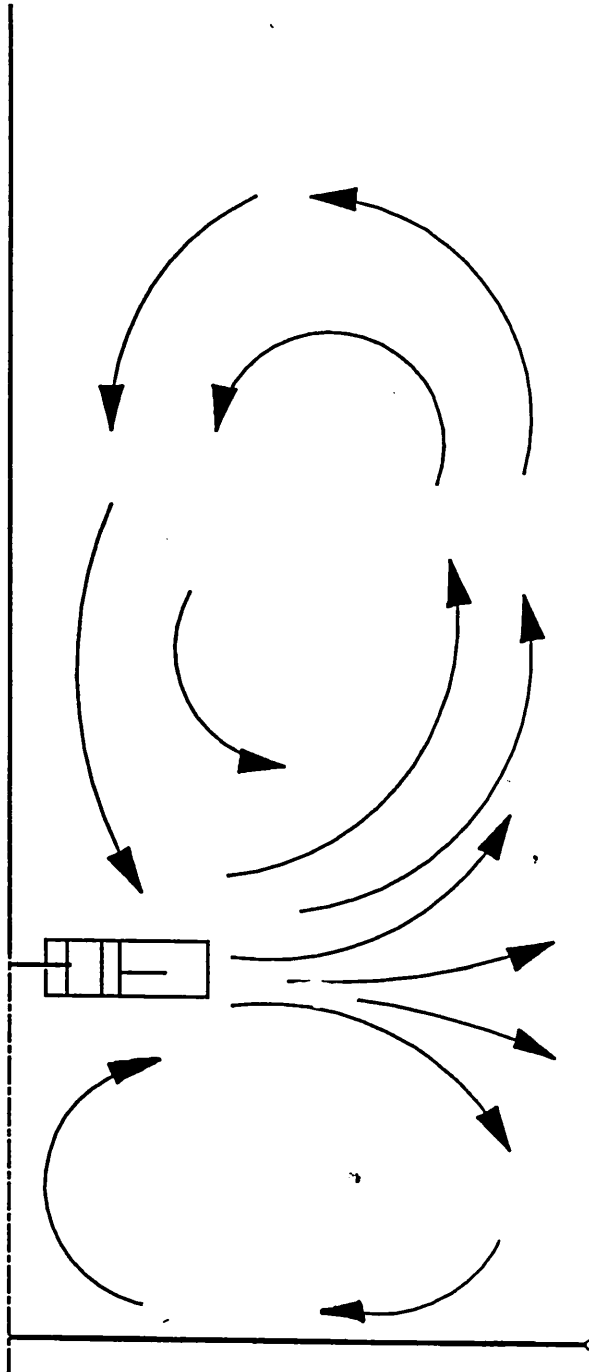


**Figure 5.1 :** *Flow inside stirred tanks*

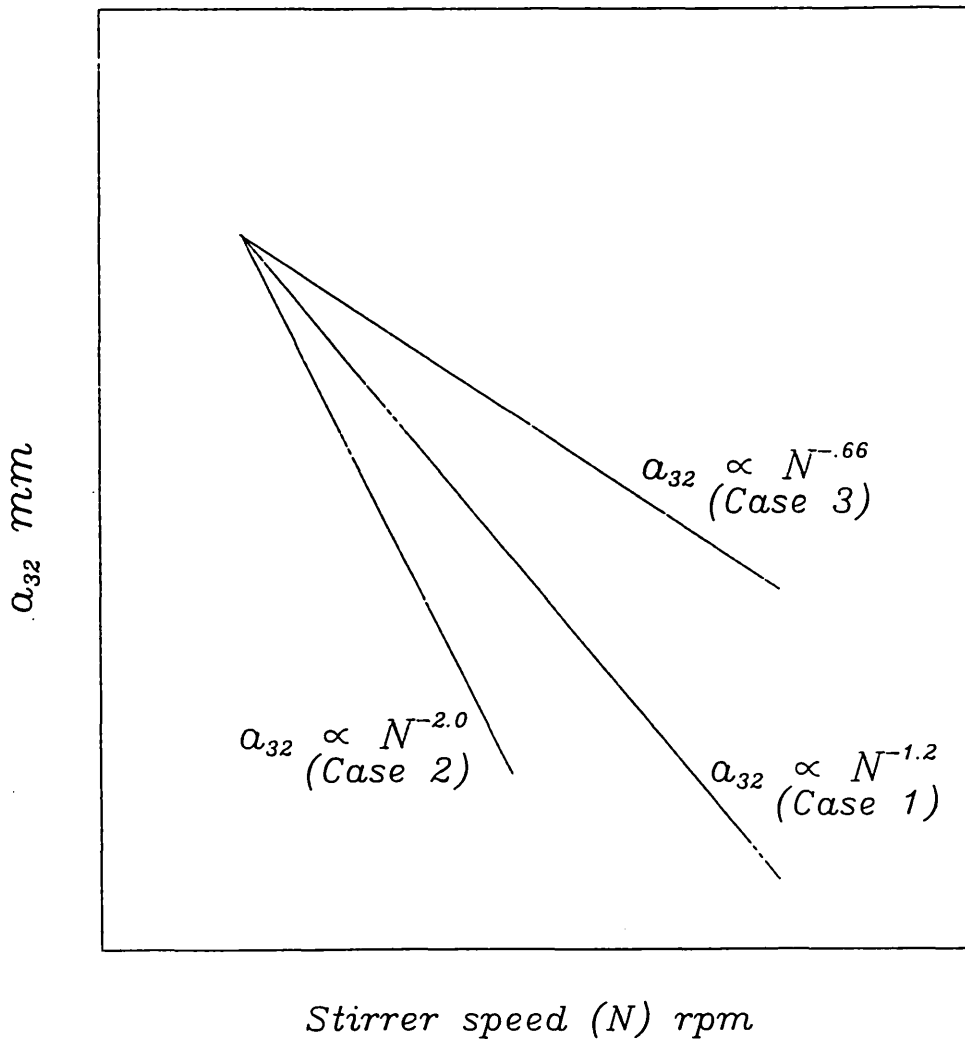


**Figure 5.2 :** *Effect of turbulence mode on Sauter mean diameter dependency on stirring speed*

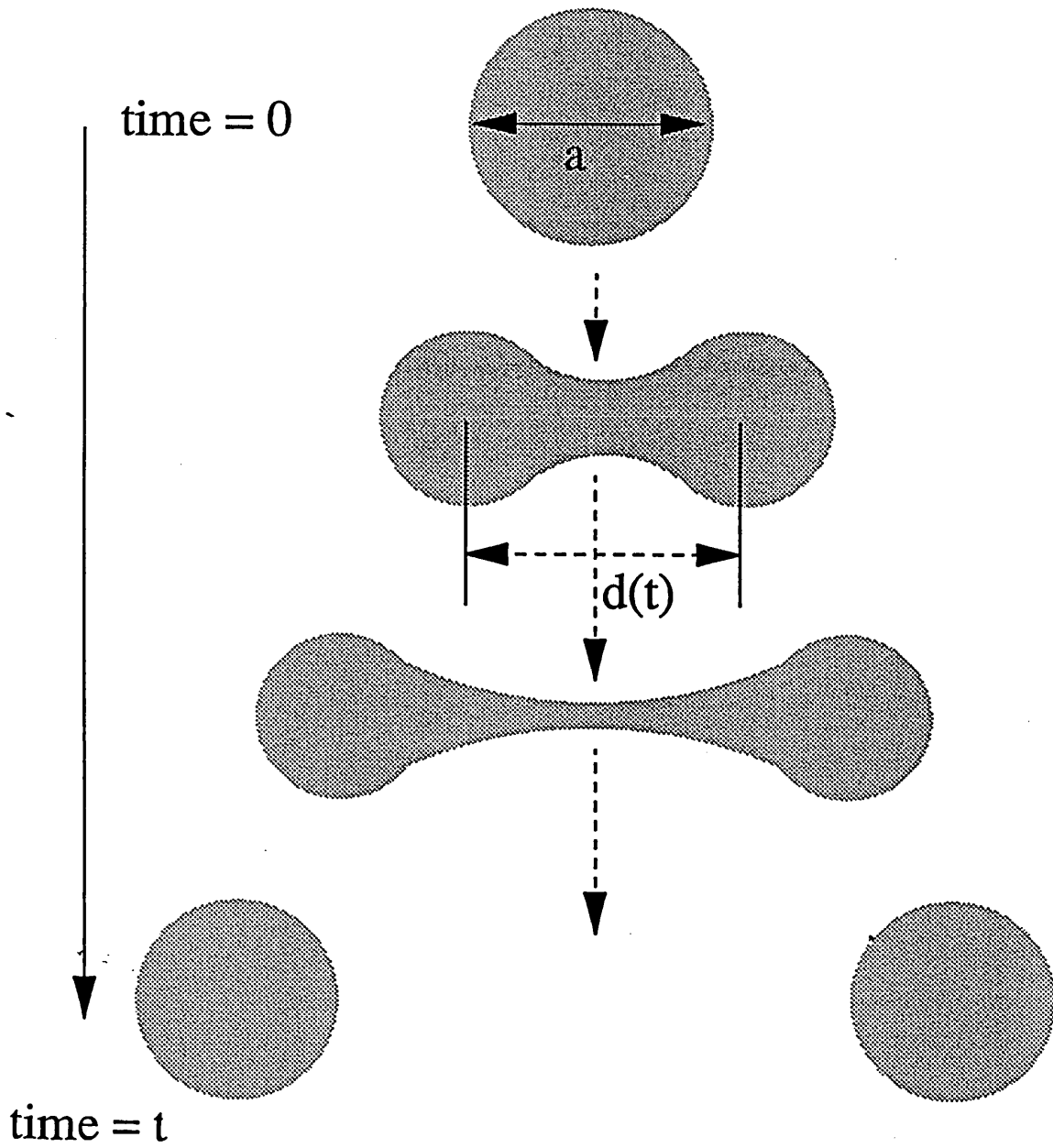


**Figure 5.3 :** *Drop breakage process*

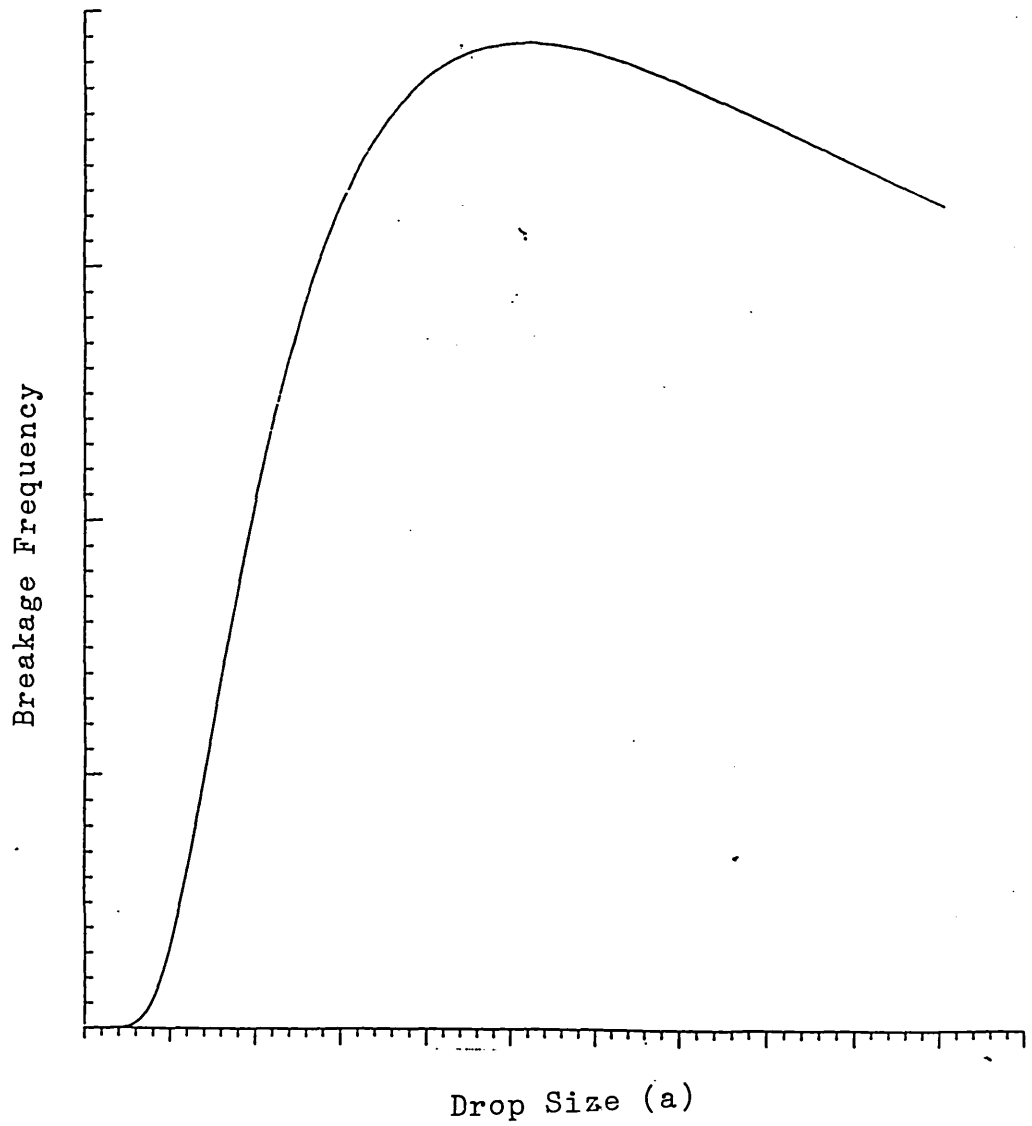


**Figure 5.4 :** *Generalized plot of equation 5.13 : Breakage frequency vs drop size*

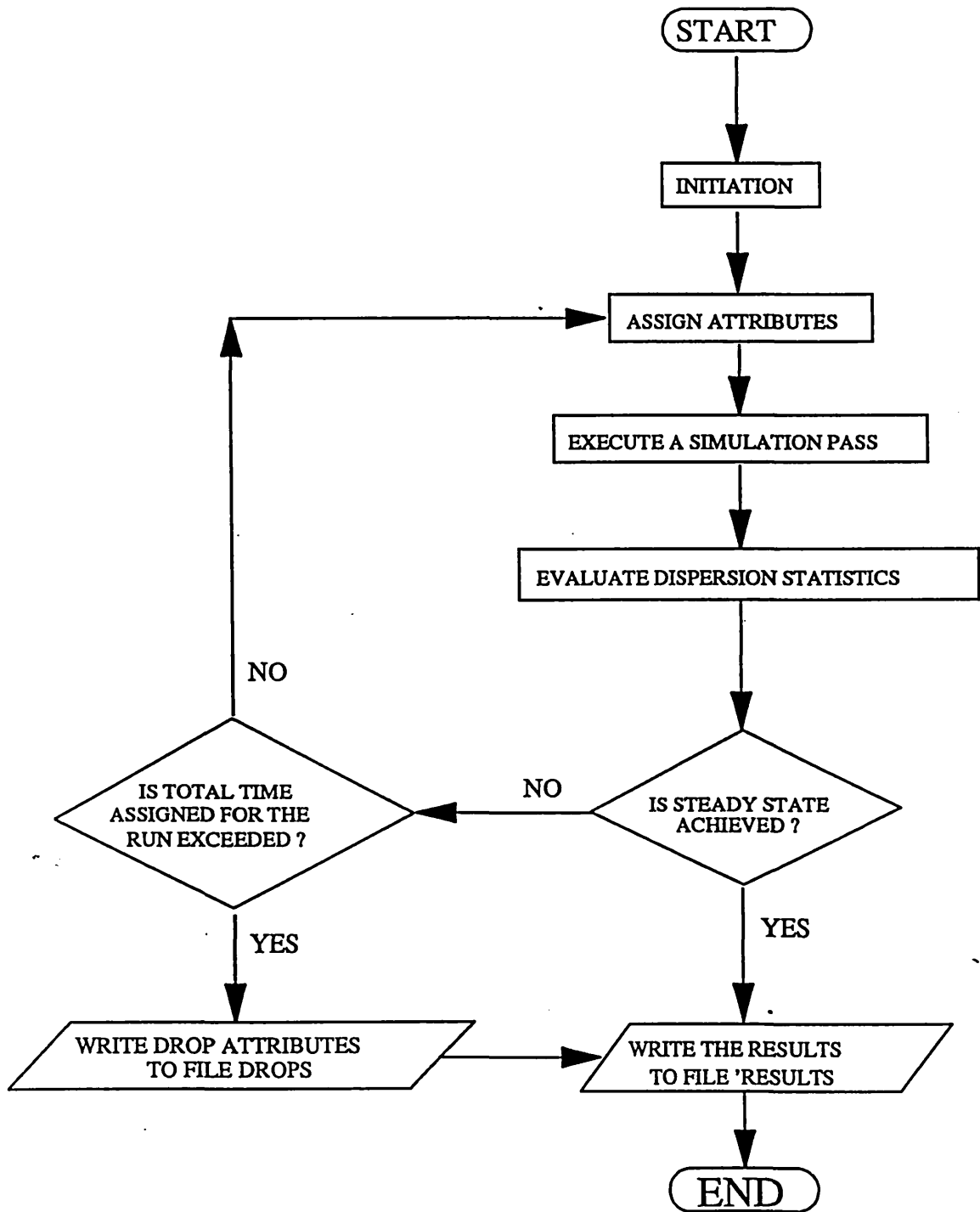


**Figure 5.5 :** *Simulation algorithm : General block diagram*

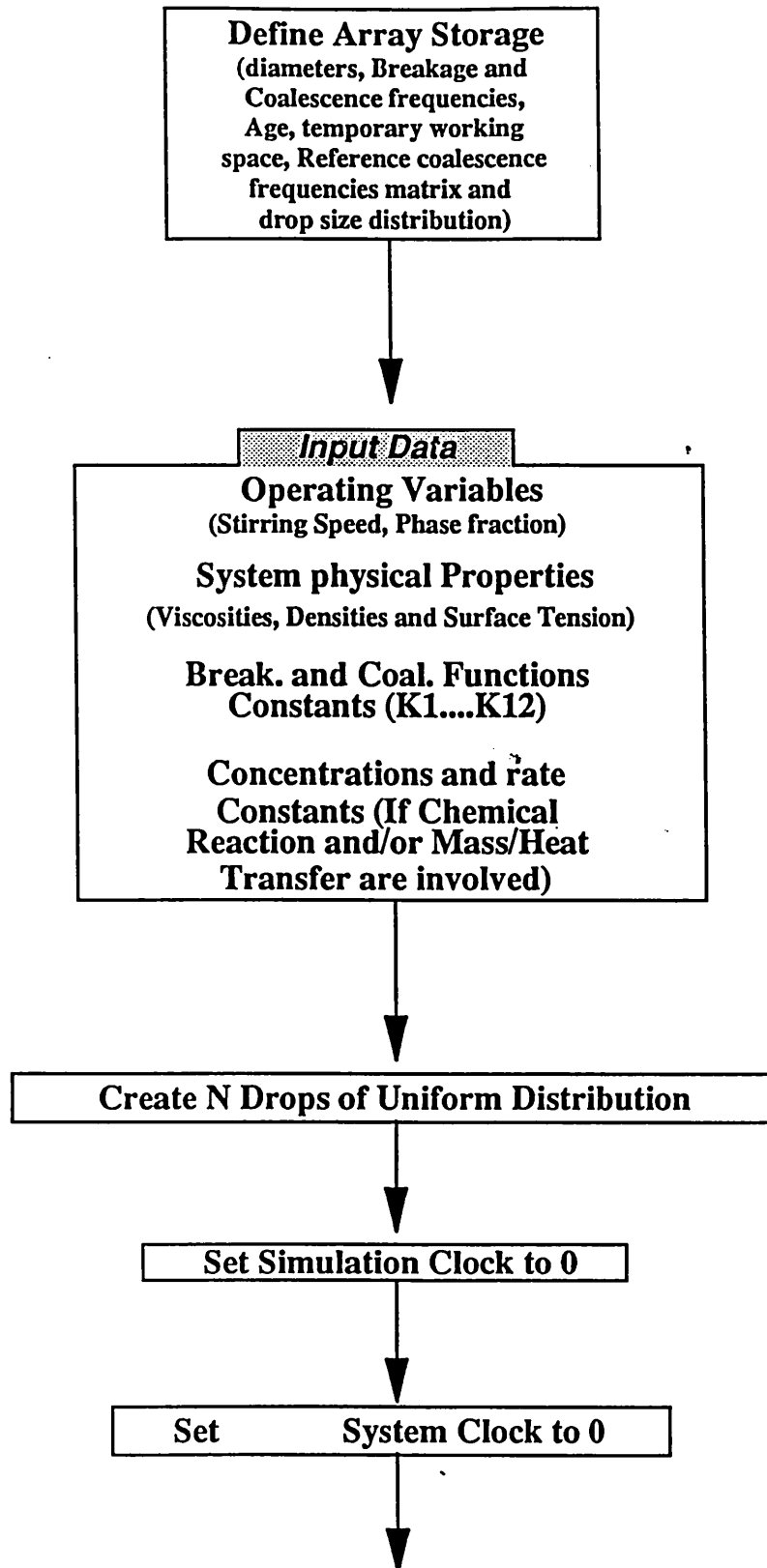


**Figure 5.6 : Simulation algorithm : Initiation**

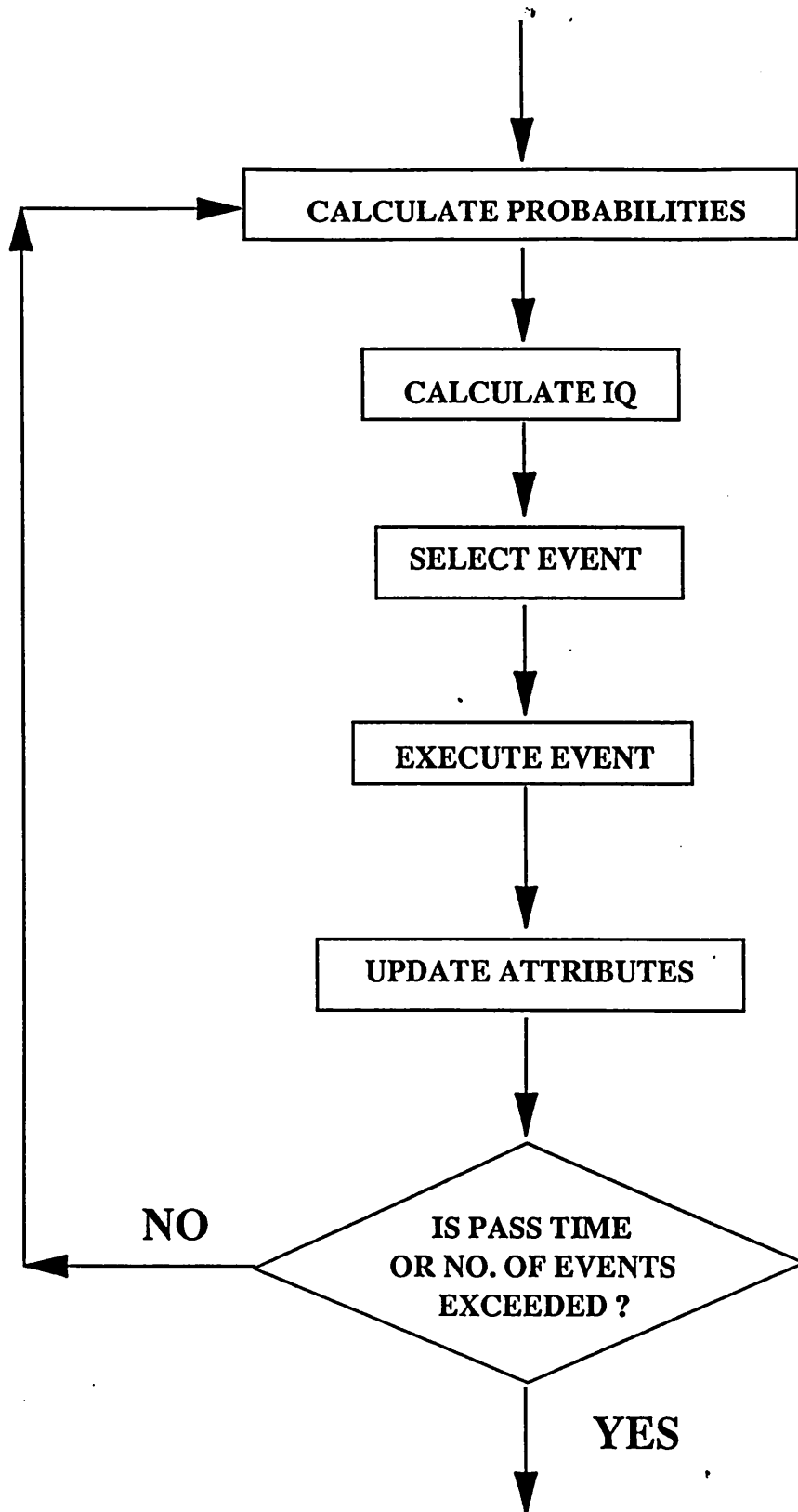


**Figure 5.7 :** *Simulation algorithm : Simulation pass*

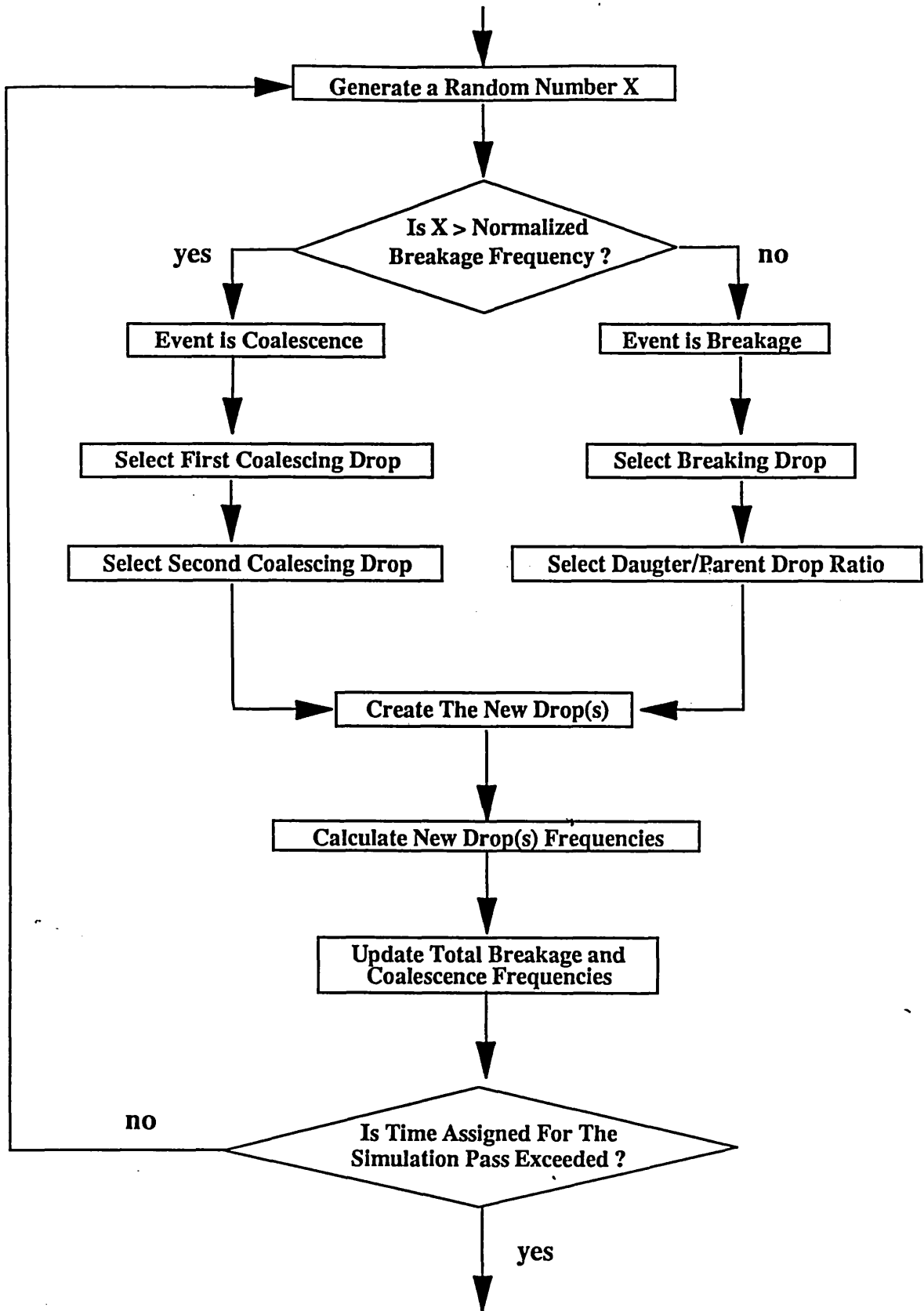


**Figure 5.8 :** *Simulation algorithm : Event selection and execution*

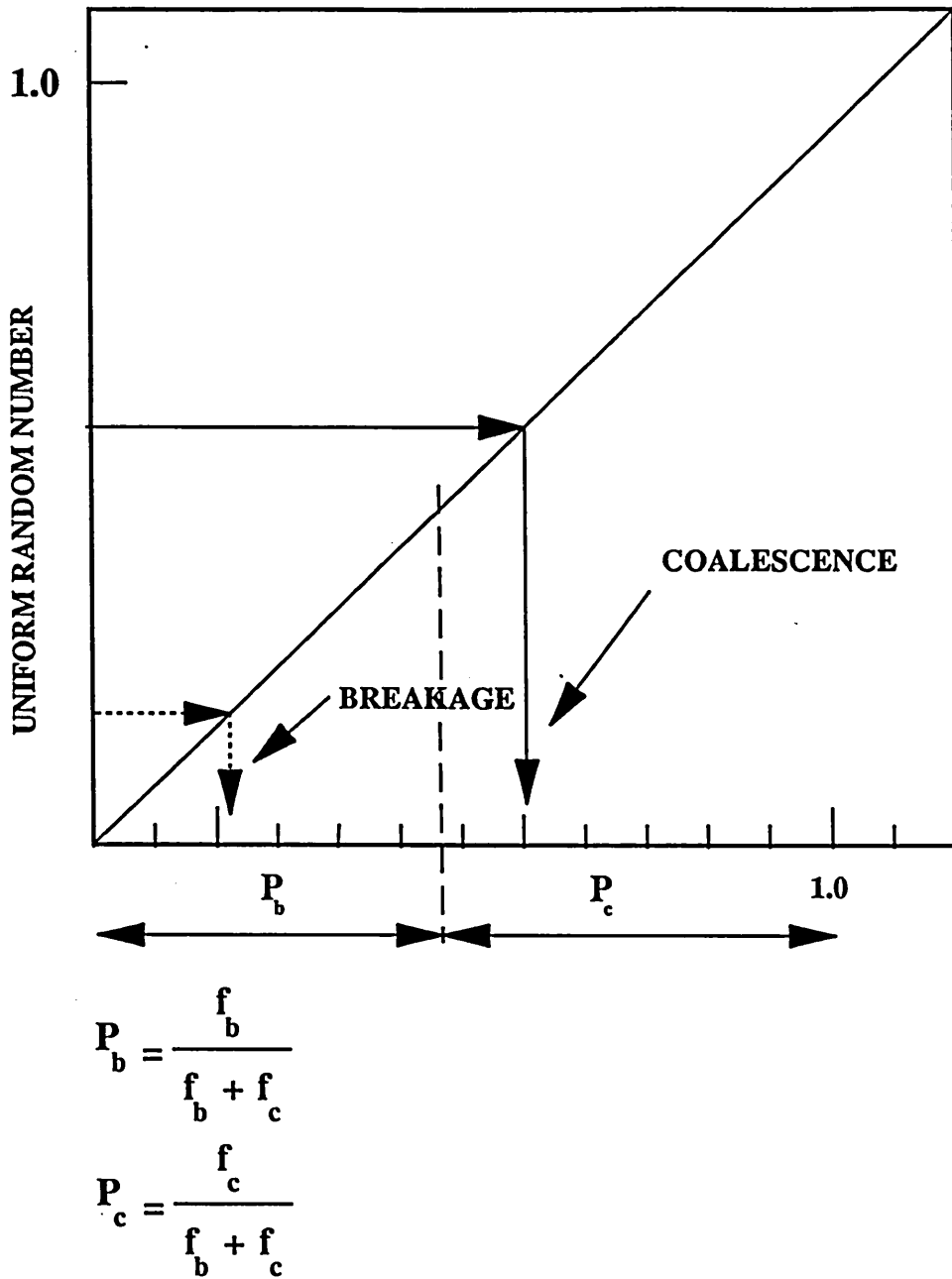
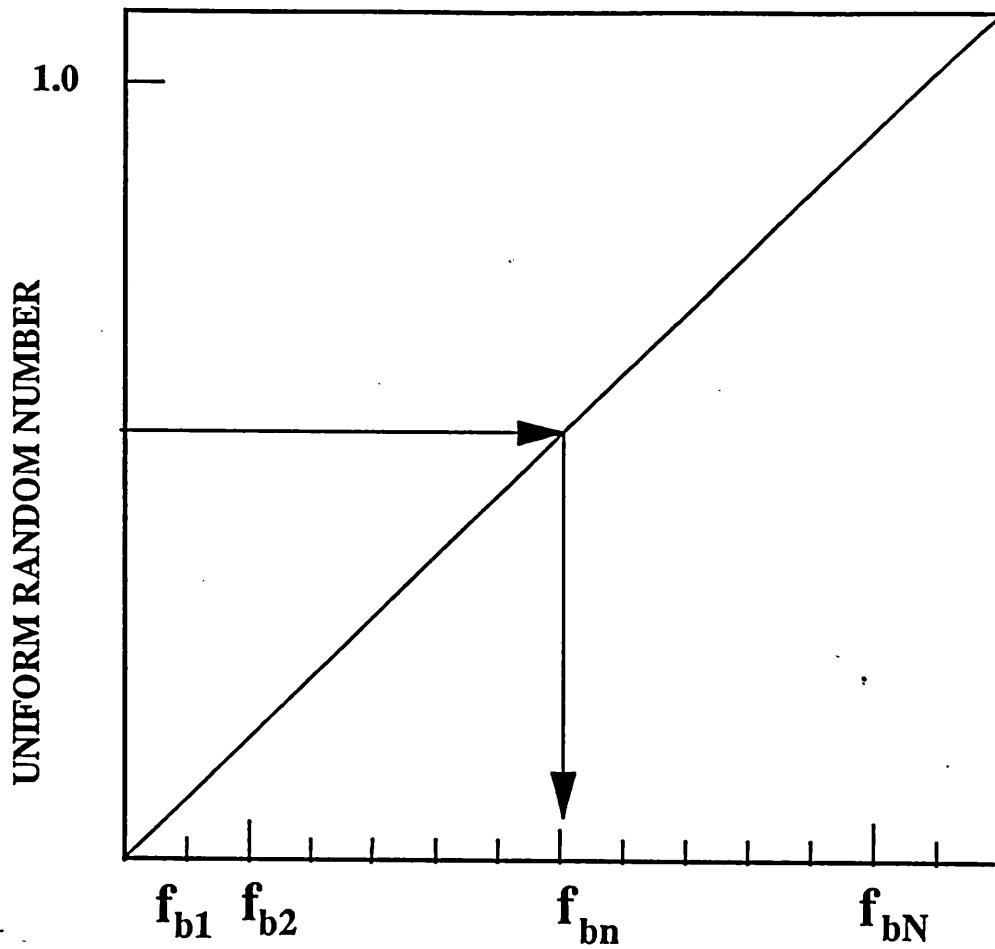
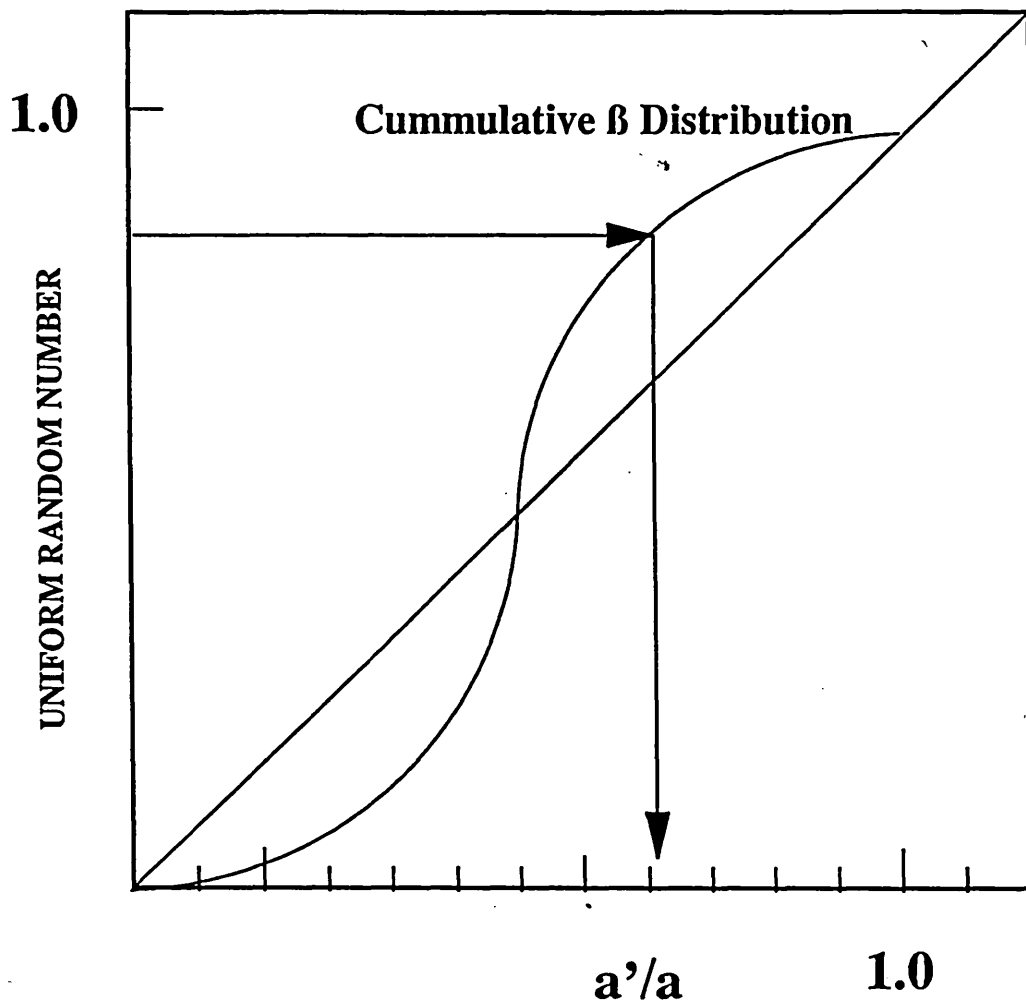


**Figure 5.9 :** *Simulation algorithm : Type of event selection*



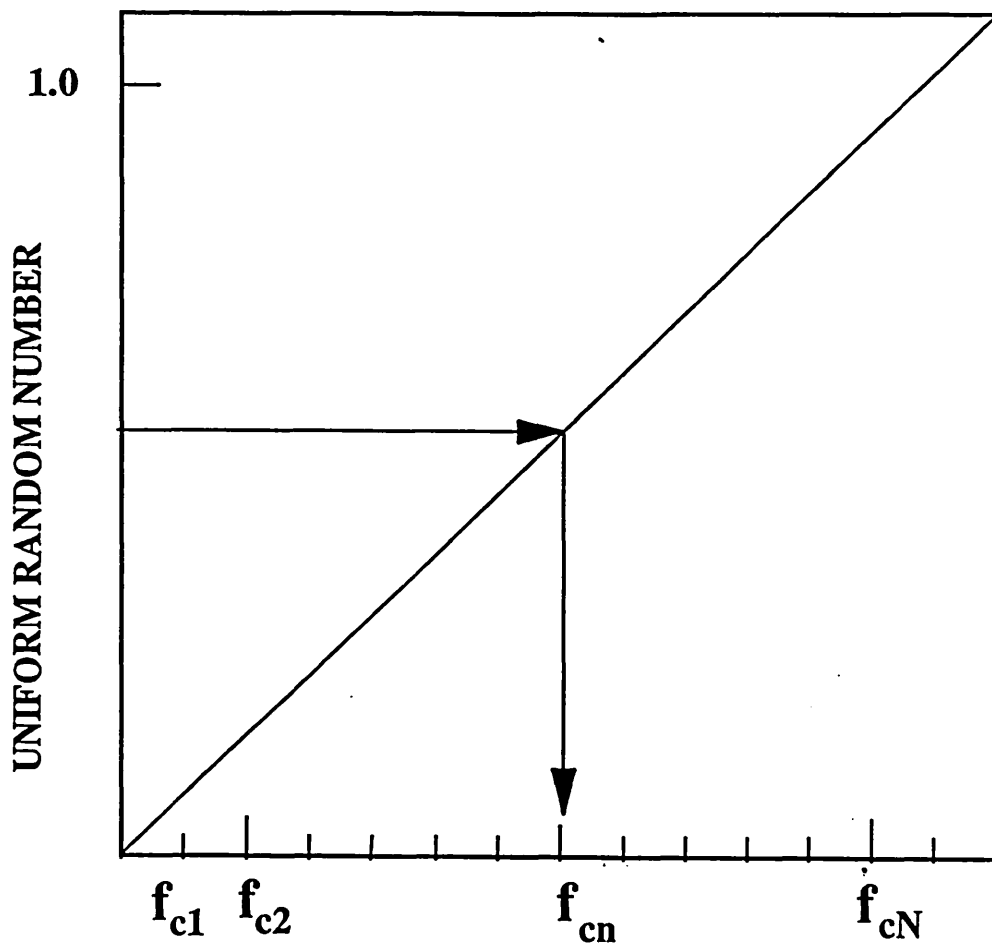
$$f_{bn} = \frac{\sum_{i=1}^{i=n} g(a_i)}{\sum_{i=1}^{i=N} g(a_i)} \quad ; \quad f_{bN} = \frac{\sum_{i=1}^{i=N} g(a_i)}{\sum_{i=1}^{i=N} g(a_i)} = \mathbf{1}$$

**Figure 5.10 : Simulation algorithm : Breaking drop selection**



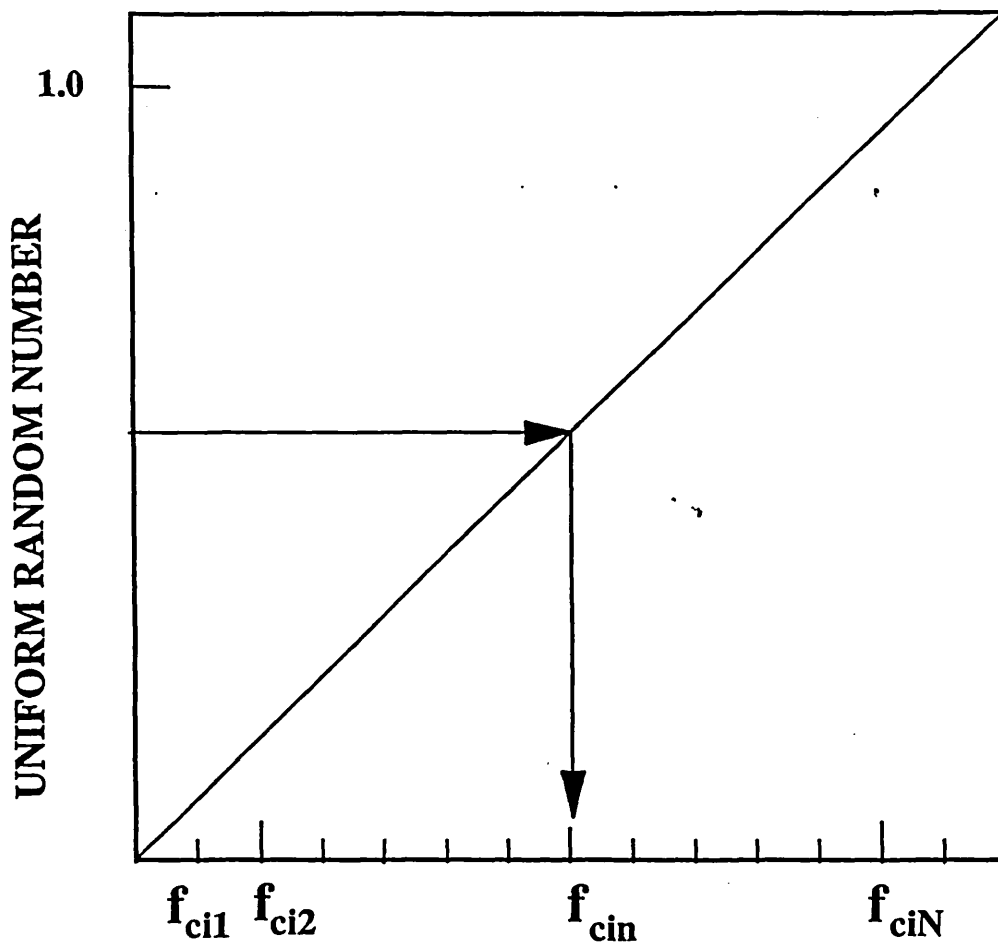
$a'/a$  = diameter of the first daughter drop/ diameter of parent drop

Figure 5.11 : Simulation algorithm : Daughter droplets size selection



$$f_{cn} = \frac{\sum_{i=1}^{i=n} f_c(a_i)}{\sum_{i=1}^{i=N} f_c(a_i)} \quad ; \quad f_{cN} = \frac{\sum_{i=1}^{i=N} f_c(a_i)}{\sum_{i=1}^{i=N} f_c(a_i)} = 1$$

Figure 5.12 : Simulation algorithm : First coalescing drop selection



$$f_{cin} = \frac{\sum_{\substack{j=1 \\ j \neq i}}^n f_c(a_i, a_j)}{\sum_{\substack{i=1 \\ i \neq j}}^N f_c(a_i, a_j)} ; \quad f_{ciN} = \frac{\sum_{\substack{i=1 \\ i \neq j}}^N f_c(a_i, a_j)}{\sum_{\substack{i=1 \\ i \neq j}}^N f_c(a_i, a_j)} = 1$$

Figure 5.13 : Simulation algorithm : Second coalescing drop selection

## **CHAPTER VI**

# **SIMULATION MODEL BEHAVIOUR AND RESULTS**

A Monte Carlo algorithm that utilizes the event scan technique of simulation time management was used to simulate liquid-liquid dispersions.

The time taken by the computer to evaluate the coalescence interactions is more than 90% of the total simulation time in all Monte Carlo algorithms reported in the literature review, a fact that prompted the development of a new algorithm using the time saving approach discussed in chapter V.

The algorithm was designed in a modular form so that it allows for the incorporation of different dispersion mechanisms, mass transfer, mass transfer with chemical reaction and heat transfer. However in this work the simulation did not include interfacial transfer.

The discussion is divided into two sections :

- (i) General description of the simulation model behaviour
- (ii) Comparison between simulated and experimental results obtained by Okufi(1984) using the system DEHPA-n-Heptane-Water

The data obtained by Okufi(1984) was used because the experiments reported in chapter IV were concerned with the spacial homogeneity of the dispersion in which few stirring speeds were studied. On the other hand, Okufi's data obtained at a single position but over a wide range of stirring speeds and dispersed phase fractions. This make them more suitable to be used in the simulation.

The model, as described earlier, combines different modes of drop breakage and coalescence corresponding to different turbulence modes.

The modes considered were :

- 1- Isotropic turbulence with breakage as the controlling process of dispersion formation.

2- Non-isotropic turbulence in which :

- (i) Small scale velocity fluctuations are functions of the main stream flow or proportional to the tip speed.
- (ii) Velocity fluctuations are random functions of spatial velocity distribution as modelled by Konno et al(1981)

In future these modes will be referred to as turbulence modes 1, 2(i) and 2(ii). The corresponding expressions for the velocity fluctuations were given in section 5.1.2.

In the following discussion all computer times reported are for the CDC CYBER-960 Mainframe.

## **6.1 General description of the simulation model behaviour**

In this part, the new algorithm was compared with the old one in order to study the effect of the differences in the system attributes especially at the start-up and to monitor the propagation of small errors or fluctuations produced by the coalescence frequency estimation.

### **6.1.1 Evaluation of constants in the breakage and coalescence functions**

As it is evident from the formulation of the equations used, for each turbulence mode functional constants are involved. Although the same phenomenological equations (5.12 and 5.23) have been used by different authors, no universal set has emerged yet. This may be attributed to the fact that a comprehensive understanding of the principles and factors governing dispersion is yet to be developed. The non-linearity the basic drop motion equations as well as the chaotic nature of turbulence poses serious difficulties in the theoretical treatment of such phenomena. Thus, in this work the constants were determined by parametric fitting.

The procedure followed in this work may be outlined as follows :

- (i) An experimental point was selected that was considered to represent the tank average for the Sauter mean diameter,  $\phi$  and drop size distribution.

- (ii) After deciding which turbulence modes were to be considered, the relevant expressions for breakage and coalescence were selected from equation 5.12, 5.23 and those of section 5.1.2 for the turbulent velocity fluctuations.
- (iii) For each individual turbulence modes and using the drop size distribution chosen, a first estimation of the constants was made by equating the breakage and coalescence probabilities of the drops using equations 5.25 to 5.30 and solving the resultant equations as a set of simultaneous algebraic equations. Four constants were evaluated for each mode.
- (iv) Using the previous estimate as the starting values, the simulation algorithm was used to find the value of the Sauter mean diameter. If it was found to be different from the experimental one, an iterative process was followed changing the values of the constants (i.e. the ratio  $k_{b1m}/k_{c1m}$  in equations 5.12 and 5.23) until the simulated Sauter mean diameter agreed with the experimental one. The process was repeated for all the modes under consideration. It is important to note that this approach assumed that the lines of Figure 5.2 intersect at the selected stirring speed. Since the intersection may take place at a different speed, these may not be the final values of the constants.
- (v) The modes were then combined using equations 5.13 and 5.24 then the dispersion was simulated at different stirring speeds. If the exponent of  $N$  in the expression  $a32 \propto N^x$  agreed with the experimental one then step 6 is carried out. Otherwise, the relative contributions of the different modes were changed and step 5 was repeated. The contributions of the different modes were changed by changing the values of the  $k_{b1m}$ 's and  $k_{c1m}$ 's in equations 5.12 and 5.23. The ratio  $k_{b1m}/k_{c1m}$  for each individual mode was kept constant. Figure 5.2 or a similar one, depending on the modes being investigated, may be used as a rough guide for the determination of the direction of the constants values movement by superimposing the experimental and simulated lines on the ones produced by the different modes considered.

- (vi) Using these constants drop size distributions were simulated. If these were reasonably close to the experimental ones, the values of the constants were confirmed. Otherwise, the constants in the exponential terms in equations 5.12 and 5.23 (i. e.  $k_{b2m}$ 's and  $k_{c2m}$ 's) were altered and steps 4, 5 and 6 repeated until agreement was reached.

Despite the iterative nature of this algorithm the reduction in simulation time that resulted from the procedure outlined in the previous chapter made it possible to experiment with different breakage and coalescence modes. Table 6.1 shows the results obtained for the system under consideration.

### 6.1.2 Computational load in the evaluation of population coalescence frequencies

As pointed out earlier, the number of interactions between coalescing drops increases the computational load exponentially as the population size grows. The use of the approximate interaction grid described in chapter V resulted in significant reduction in the computer time used in a simulation run. This was achieved through the reduction of coalescence frequencies calculation load which is the most time consuming process in the simulation.

If an appropriate number of categories is chosen, an optimum balance may be struck between the frequency deviations from the actual values and the computational time, provided no significant effect on the end results is experienced.

Table 6.2 shows the effect of the number of intervals on the computational load in comparison to the original model which calculates the actual frequency values using the whole drop population span. The savings in computer time proved to be more than 98% for up to 200 intervals which make the algorithm reasonably inexpensive compared with the previously reported ones.

### 6.1.3 Effect of the interval size on the coalescence frequencies

From the analysis of the differences in the coalescence frequencies given by the two algorithms, it may be concluded that the error in the sample overall coalescence frequency  $F_c$  and the difference in the individual drops coalescence

frequencies gradually decrease until a point is reached where no further reduction is experienced. The errors kept fluctuating within  $\pm .02\%$ . **Table 6.3** gives a listing of the errors produced for different numbers of intervals up to 200.

#### **6.1.4 Comparison between the two algorithms**

In this section a comparison is carried out between the two algorithms to study the effects of the coalescence frequency approximation on the simulation results. The operating conditions chosen and the starting drop size distributions are the same for the two models. The two models were run until at least 15000 events were executed, a number large enough to attain the steady state drop size distribution under the initial conditions chosen.

The original sample size was 400 drops uniformly distributed between 0. and .5 mm. The selected stirrer speed was 504 rpm and the dispersed phase fraction .4.

##### **6.1.4.1 Sauter and average mean diameters**

Depending on the rate at which the whole drop spectrum frequencies were updated, differences of up 5% in the Sauter mean diameters were observed during the first simulation pass. As soon as the frequencies were updated after the initial disintegration process the values given by the two algorithms were close. The only drawback that the initial differences may have is associated with the simulation of mass transfer with chemical reaction at start-up for highly reactive species. This situation may be corrected by adjusting the frequency update interval at the expense of computer time. This time becomes insignificant if only initial stages were involved. The load may increase if the treatment of mass transfer and/or chemical reaction required accurate drop size distribution data at the initial stages, but it is in no way comparable to the time required by the original algorithm. A balance is to be struck between the accuracy required and the computation resources available.

For the particular system studied, it appeared that 50 intervals were sufficient to obtain results comparable with the ones obtained from the original algorithm. This number of intervals may suffice for hydrodynamic studies, but since no interface transfer processes were studied in this work, it is not safe to generalize this conclusion especially if high accuracy is required at initial times. **Figure 6.1**

shows the Sauter mean diameters obtained from the two algorithms using different number of intervals while **Figure 6.2** gives a similar comparison for the arithmetic mean diameter. The overlapping of the curves is a clear indication of the goodness of fit.

#### **6.1.4.2 Breakage and Coalescence frequencies**

The same observations made in the previous section apply to breakage and coalescence frequencies with the exception that the difference between coalescence frequencies produced by the two algorithms does not vanish but stabilise at a value less than 3%. This difference as explained earlier, was due to the fact that drop sizes were distributed around the interval pivoting points and not exactly the same as the value assigned for the interval from equation 5.34. As a consequence, the position of the drops taking part in the coalescence process may be affected.

For the breakage frequencies the fit is very good despite the fact that the exponential term in the breakage expressions (Equation 5.12) is very sensitive to size changes as shown in **Figure 5.4**

**Figures 6.3** and **6.4** are graphical representations of the transient frequencies for different number of intervals.

#### **6.1.4.3 Computational Load**

**Figure 6.5** gives a comparison between the computer time used by the different models. The reduction obtained in the evaluation of coalescence frequencies time is translated into a more than 95% reduction in the overall simulation time, a result that renders the cost associated with simulation insignificant. Also the way the algorithm is written makes the cost of evaluating the interactions independent of the mechanism assumed because pre-defined grid elements were called whenever the frequencies were to be calculated.

#### **6.1.4.4 Drop Size distribution**

Drop size distributions are similar for both models despite some discrepancies at the initial stage of simulation. The same remedy mentioned in section 6.5.1 can be used to eliminate the disagreement. **Figures 6.6, 6.7** and **6.8** compare the

distributions at different stages in the simulation with the base being the original Monte Carlo algorithm. The starting distribution, which is uniform with sizes between 0. and .5 mm, is not shown in the figures.

### **6.1.5 General observations on Simulation model behaviour**

In the following sections, the transient behaviour of the algorithm is studied. The objectives of this part are to analyse the effect of the coalescence frequency approximation on the stability of the algorithm at intermediate stages.

#### **6.1.5.1 Transient Sauter and average mean diameters**

The algorithm proved to be highly stable in so far as the results produced were always consistent within the average drop sizes investigated. The general trend was a decrease in the diameter values until a point is reached where they fluctuate around a specific point with less than 1% change in the numerical value. The rate at which they approach steady state is a function of the operating parameters. The higher the speed the greater the number of events needed to approach steady state although the rate of evolution in real time terms is faster than for low stirring speeds. The combination of the two diameters is a good indication of the shape of the distribution as a large difference indicates a tendency for the distribution to be skewed while close values are consistent with normal distributions. **Figure 6.9** is a plot of Sauter mean diameter and arithmetic mean followed over a 50,000 events span.

#### **6.1.5.2 Transient drop size distributions**

In contrast to Sauter mean diameters, the distribution tend to fluctuate within a narrow band. This is not a surprise since the stochastic nature of drop dispersion leads to the assumption of a random distribution with well defined statistical features that varies within an acceptable range as the re-dispersion and coalescence processes continue. The distribution for the initial simulation stages takes a shape close to the original one, then tends to move towards the shape of the equilibrium distribution. The latter depends on physical properties, oper-

ating parameters and the relative effect of the different turbulence modes used in the algorithms.

Figure 6.10 is a follow up of distribution evolution over 50000 events.

### 6.1.5.3 Transient breakage and coalescence frequencies

Initially, as the drop sizes are greater than the equilibrium ones, the breakage frequency is higher than the coalescence one. They gradually approach each other, then level as the system equilibrates or reaches steady state. The initial size distribution has a profound effect on the rate at which the system reaches steady state because of the resulting frequencies. Figure 6.11 is drawn for the frequencies over a range of 50,000 events.

### 6.1.5.4 Effect of variation of stirring speed

#### 6.1.5.4.1 Sauter mean diameter

As a rule, the Sauter mean diameter is inversely proportional to the speed with an exponent determined by the mechanism that controls the dispersion process. At high stirring speeds, the exponent change slightly with stirrer speed reflecting the relative change in the role played by the different dispersions modes as significant change in drop spectrum or turbulence intensity is encountered. The behaviour is inherent in the nature of the expressions used for dispersion mechanisms (Equation 5.12) due to the presence of the exponential terms and their non-linearity. The same behaviour was observed experimentally by Shin-nar(1961) and Sprow(1967) who attributed it to coalescence being the dominant process. This conclusion could be the sole explanation if no values outside the range  $-0.75$  to  $-1.2$  were observed, which is not the case in this work. Figure 6.12 is a plot of the steady state Sauter mean diameter at different stirring speeds for the 22cm tank at .4 dispersed phase fraction.

The change in the exponent value is a direct consequence of the dynamic nature of the dispersion process where the relative effect of the importance of the forces acting on the drops changes as the size decreases. As the intensity of turbulence increases, the relative distribution of the flow structures within the tanks changes owing to the increase of the volume of the vessel affected by the highly non-isotropic impeller streams.

#### **6.1.5.4.2 Drop Size Distribution**

Increases in the stirring speed produce narrower drop size distributions resulting in a reduced standard deviation and skewness factor. The height of the peak increases and shifts towards the smaller sizes. The approach to steady state is faster (in real time terms) as the speed increases.

#### **6.1.5.4.3 Effect of the variation of hold-up**

##### **6.1.5.4.3.1 Sauter mean diameter**

Hold-up increases result in bigger Sauter mean diameters. Regardless of the stirring speed, the effect of hold-up on Sauter mean diameter values was the same and the increase in the Sauter mean diameter was a linear function of the hold-up as evident from **Figure 6.12** where the lines produced were parallel indicating linear dependency on hold-up.

Despite this, the results obtained were in good agreement with the experimental ones bearing in mind the experimental error as shown later in **Figure 6.15**.

##### **6.1.5.4.3.2 Drop size distributions**

The size distributions tended to widen and flatten as the hold-up increased with the peak shifting towards the larger sizes. The distribution standard deviation and curtosis increased while the skewness factor decreased. **Figure 6.13** is a graphical comparison for two different hold-up values at the same stirring conditions and constant system parameters.

#### **6.1.6 Comparison between isotropic and non-isotropic model behaviour**

The turbulence mode chosen for the simulation model has a profound effect on drop size distribution. Although no definite estimate could be made about the proportion of drops breaking under any mode, it may be safely concluded that the combination rather than the individual modes is responsible for the system behaviour.

#### 6.1.6.1 Sauter and arithmetic mean diameters

Using the simulation model for a given set of operating conditions, it was possible to obtain the same value of Sauter mean diameter using a combination of different turbulence modes in different combinations or with a single one provided that the functional constants were adjusted. Changing the stirring speeds causes the results of the different modes to depart producing different Sauter mean diameters as the speed increases or decreases with the slope for each combination being dictated by the expressions used for velocity fluctuations. Reference to **Figure 5.2** shows all possible values that the Sauter mean diameter may assume for the modes under consideration depending on the relative effect of the single modes if the speed is changed from  $N_0$  which is the pivoting point for constants evaluation.

The value of the arithmetic mean diameter is determined by the shape of the distribution produced but no clear relation between the arithmetic mean diameter and the stirring speed may be deduced.

#### 6.1.6.2 Drop size distribution

Depending on the turbulence mode used, different drop size distributions may be obtained for a single value of Sauter mean diameter, a result that limits the usefulness of the average interfacial area models used for the evaluation of extraction efficiency. This is due to the fact that rates of transfer and accumulation for different drop sizes are different.

It was observed that the assumption of local isotropy results in a normally distributed drop spectrum while a skewed distribution results from non-isotropic turbulence. It may be recalled that the oscillograms of non-isotropic turbulent velocity fluctuations, in contrast to isotropic ones, show a skewed distribution [Hinze(1975)]. Drawing a parallel with drop sizes, it can be concluded that the original small scale velocity fluctuations govern the resulting Sauter mean diameter and drop size distributions. **Figure 6.14** shows a comparison between two distributions having the same Sauter mean diameters but different arithmetic mean diameter and drop size distribution obtained by simulating the dispersion with an isotropic and a non-isotropic modes of turbulence.

## 6.2 Comparison between the simulated and experimental results

The simulation of the system DEHPA-n-Heptane - Water resulted in a good agreement between the model and the experimental values. The correspondence in the Sauter mean diameter was within  $\pm 5\%$  except for few values which were below 10% as seen in **Figure 6.15** which is a plot of the Simulated Sauter Mean plotted against the Experimental values. **Figure 6.16** is a graphical representation of the drop size distributions produced by the model and experiments. Bearing in mind the fact that the experiments were conducted for different hold-up values, stirring speeds and tank sizes, the results gave credence to the assumption of having more than one mode of turbulence affecting the dispersion process. Selecting one mode and simulating the system with it resulted in discrepancies in both Sauter and arithmetic mean diameters and consequently disagreement in drop size distributions. Combining the three modes, good agreement with experimental results was obtained.

Case 1 : Isotropic Turbulenc

$$k_{b1m} = .162 \times 10^{+2}$$

$$k_{b2m} = .8 \times 10^{-2}$$

$$k_{c1m} = .432 \times 10^{+3}$$

$$k_{c2m} = 1.89 \times 10^{+7}$$

Case 2(i) : Non-Isotropic Turbulenc

$$k_{b1m} = .1891 \times 10^{+2}$$

$$k_{b2m} = .100677 \times 10^{+6}$$

$$k_{c1m} = .173845 \times 10^{-1}$$

$$k_{c2m} = 3.45 \times 10^{+10}$$

Case 2(ii) : Non-Isotropic Turbulenc

$$k_{b1m} = .480974 \times 10^{-7}$$

$$k_{b2m} = .5625 \times 10^{-2}$$

$$k_{c1m} = .531968 \times 10^{+1}$$

$$k_{c2m} = 3.848 \times 10^{+10}$$

For the drop sizes investigated, the simulation results proved to be unaffected by the values chosen for  $k_{c2m}$  in all modes studied

**Table 6.1:** *Breakage and coalescence functions constants*

Number of Intervals	Time (CYBER CDC-960) seconds	% Saving
20	.091	99.87
50	.202	99.72
70	.275	99.62
100	.386	99.47
120	.461	99.37
150	.572	99.21
180	.686	99.05
200	.759	98.95

**Table 6.2:** *Computer time for the evaluation of the coalescence frequencies.*

*Original algorithm time : 72.73 sec*

*Sample size : 2000 drops*

Number of Intervals	Population Coalescence Frequency $f_c$	% Difference
20	7.689	.134
50	7.6810	.036
70	7.6784	.0036
100	7.6818	.0409
120	7.6782	.0059
150	7.6798	.0151
180	7.6788	.0018
200	7.6800	.00213

**Table 6.3:** *Comparison between the population coalescence frequencies  $f_c$  produced by the two algorithms*

*Original algorithm time : 7.6803*

*Sample size : 2000 drops*

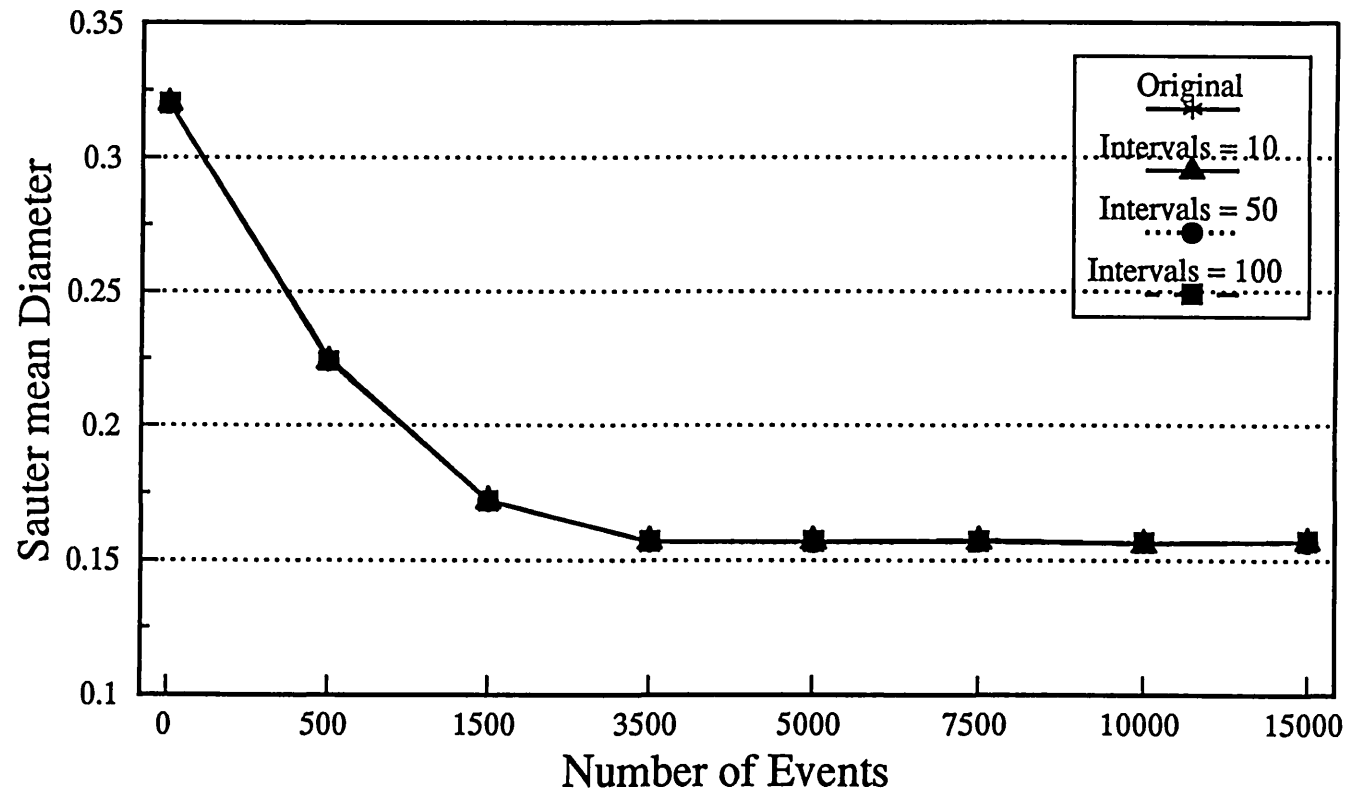


Figure 6.1 : Comparison between the two algorithms : Sauter Mean Diameter(mm)

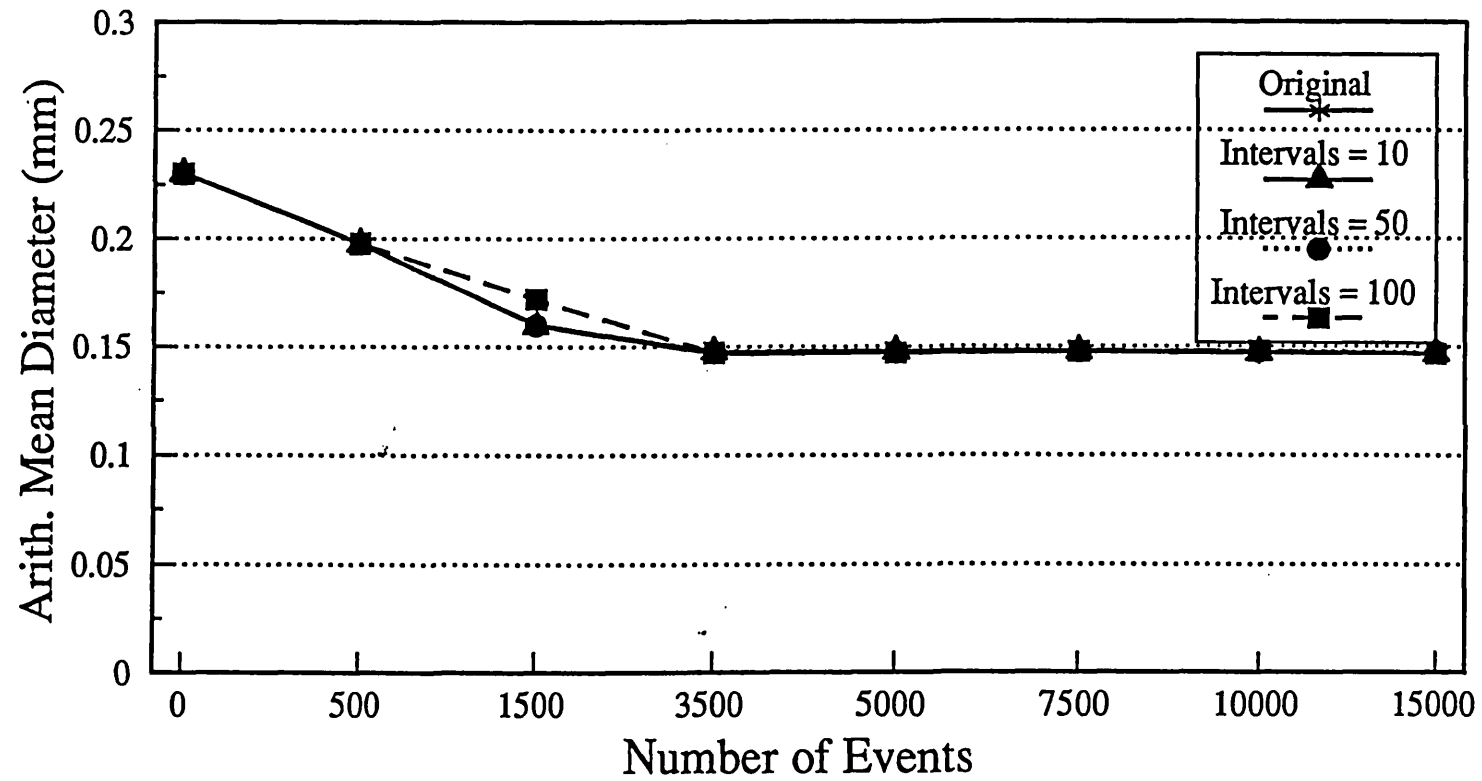


Figure 6.2 : Comparison between the two algorithms : Arith. Mean Diameter(mm)

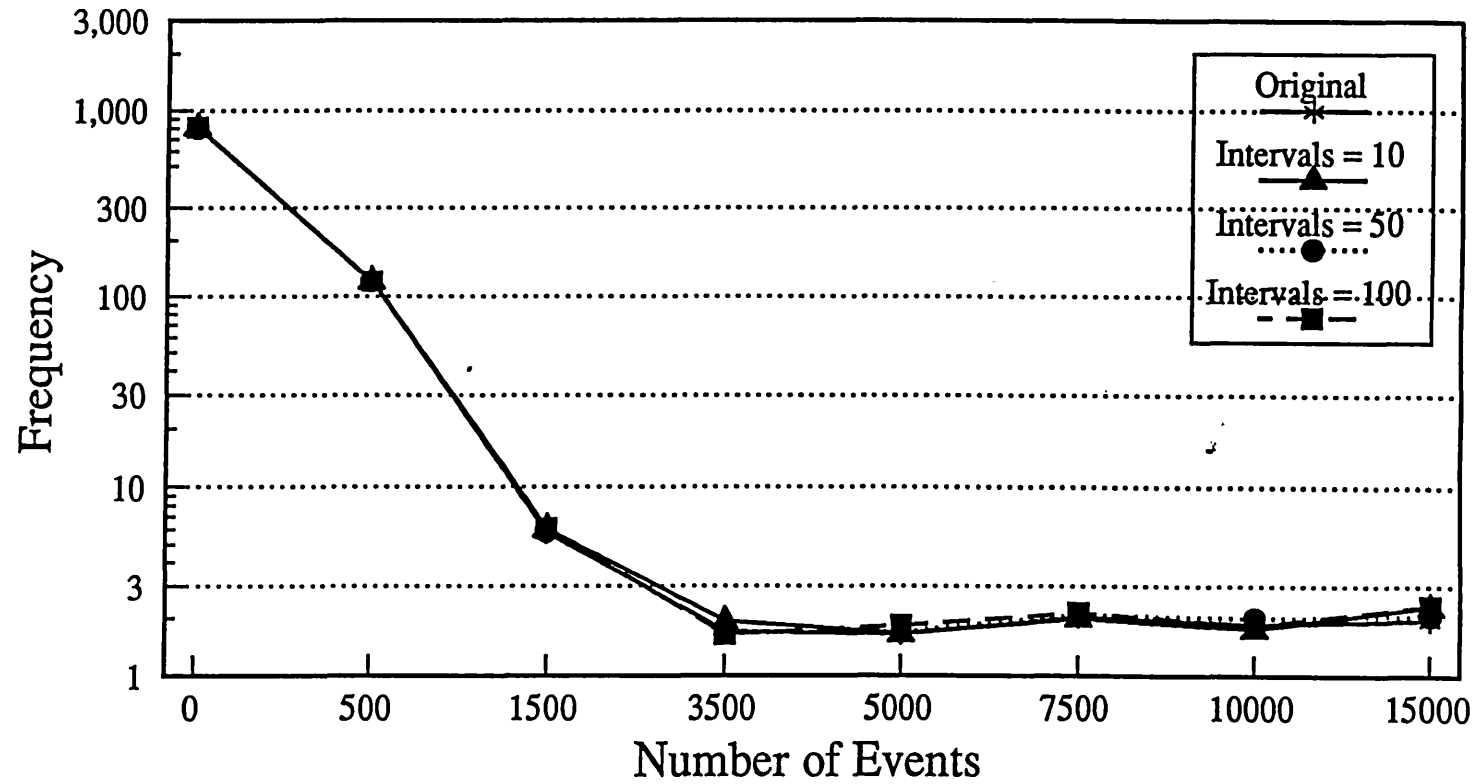


Figure 6.3 : Comparison between the two algorithms : Transient breakage frequency

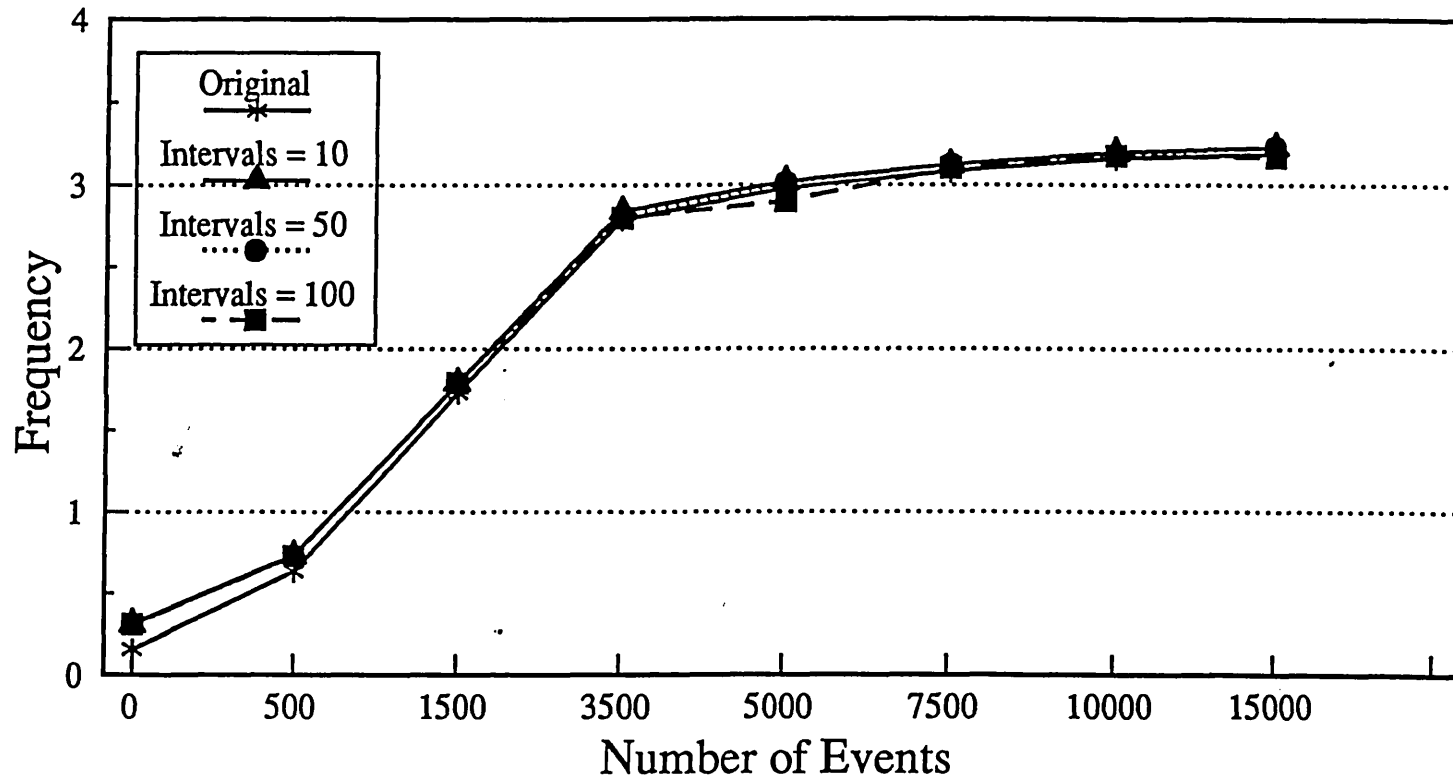


Figure 6.4 : Comparison between the two algorithms : Transient coalescence frequency

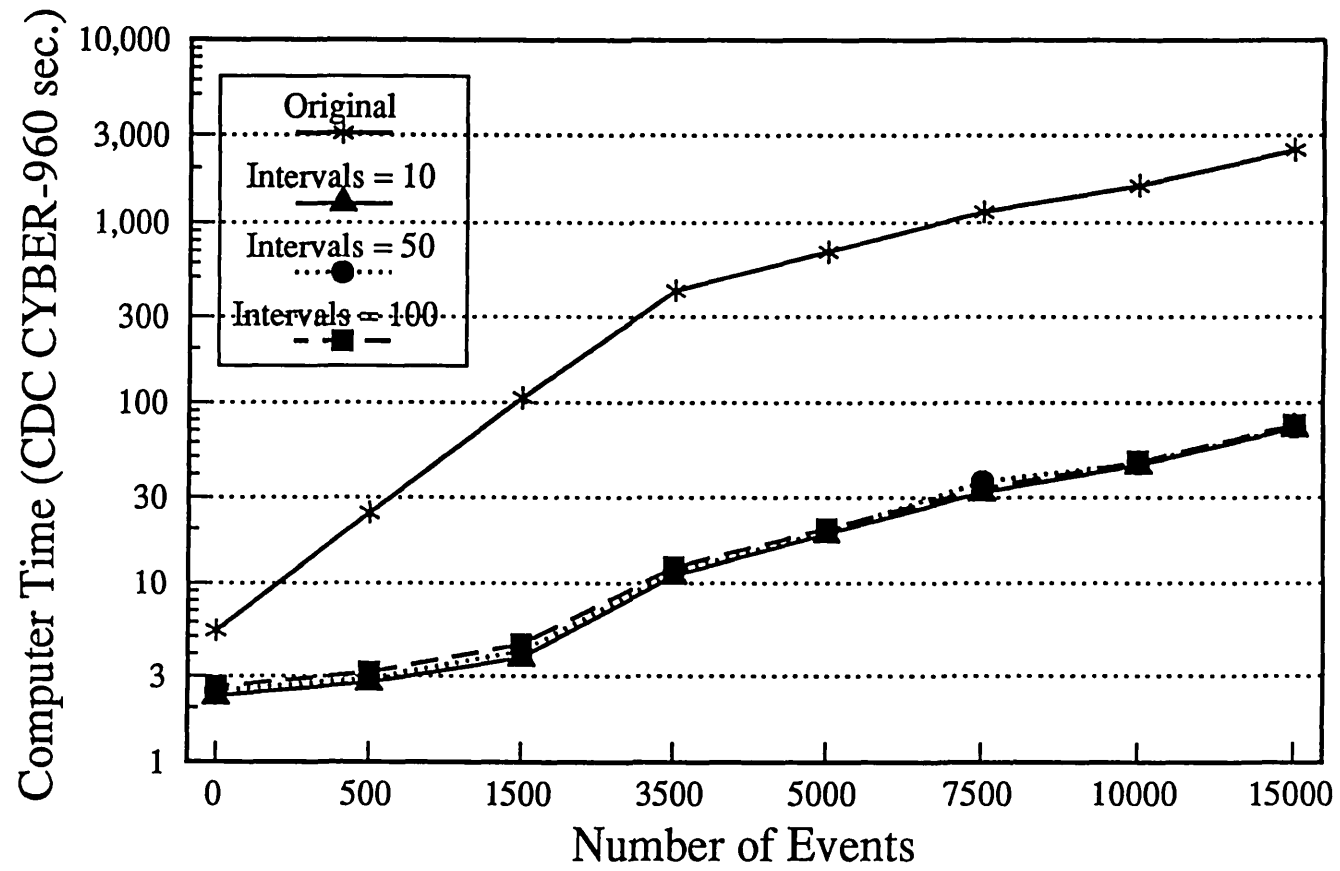
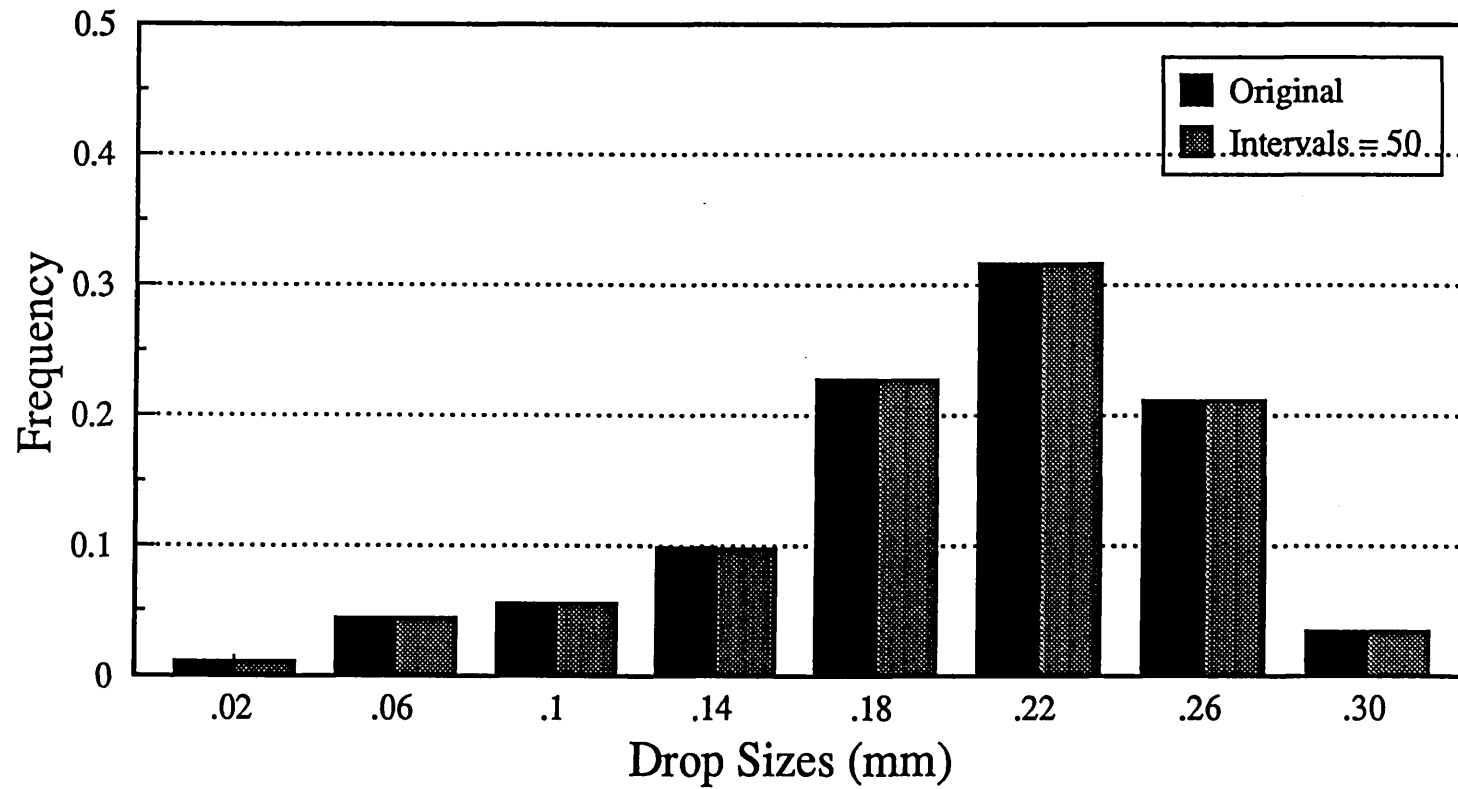
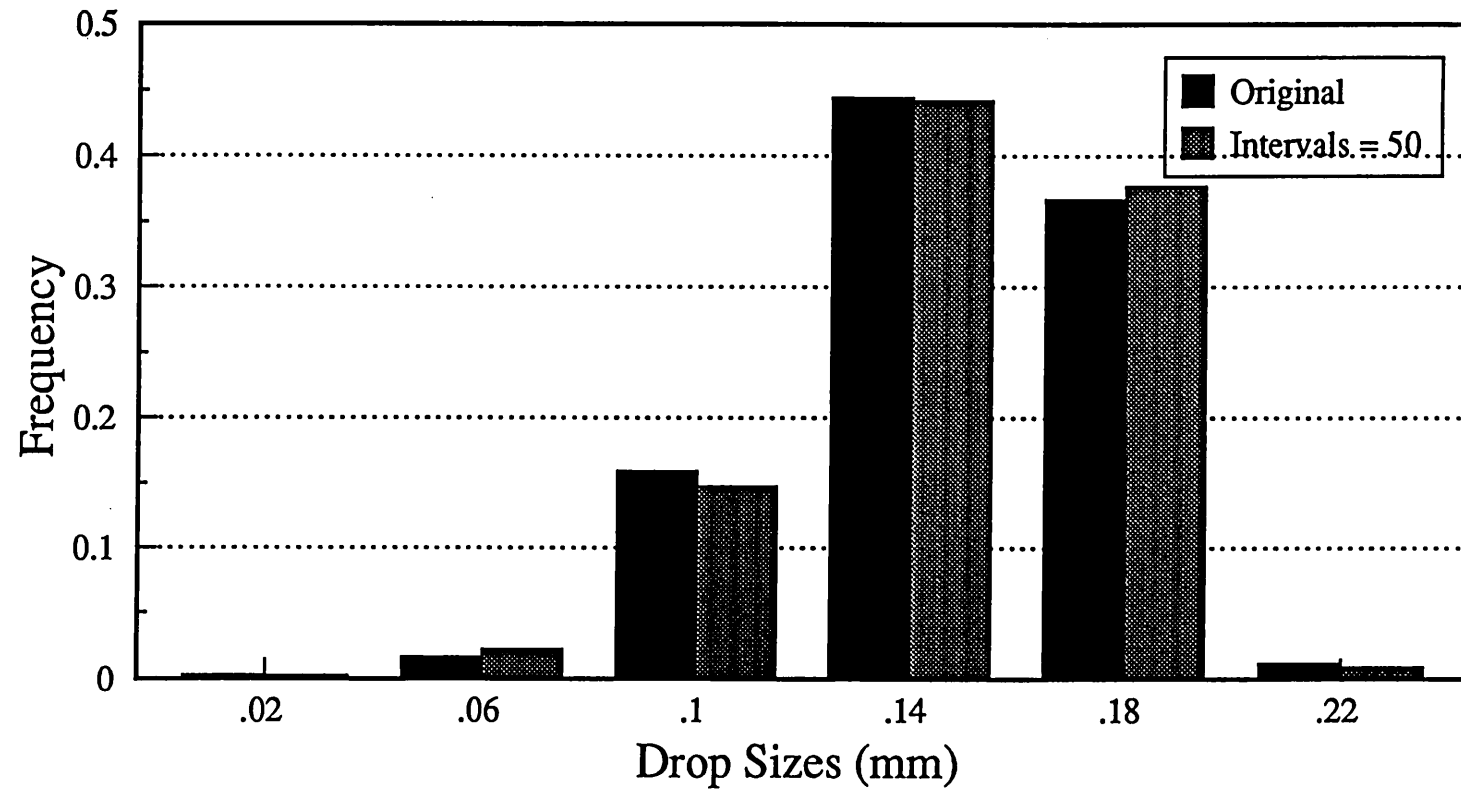


Figure 6.5 : Comparison between the two algorithms : Computer time



**Figure 6.6 :** *Comparison between the two algoritms : Drop size distribution  
Number of events = 500*



**Figure 6.7 :** *Comparison between the two algorithms : Drop size distribution  
Number of events = 5000*

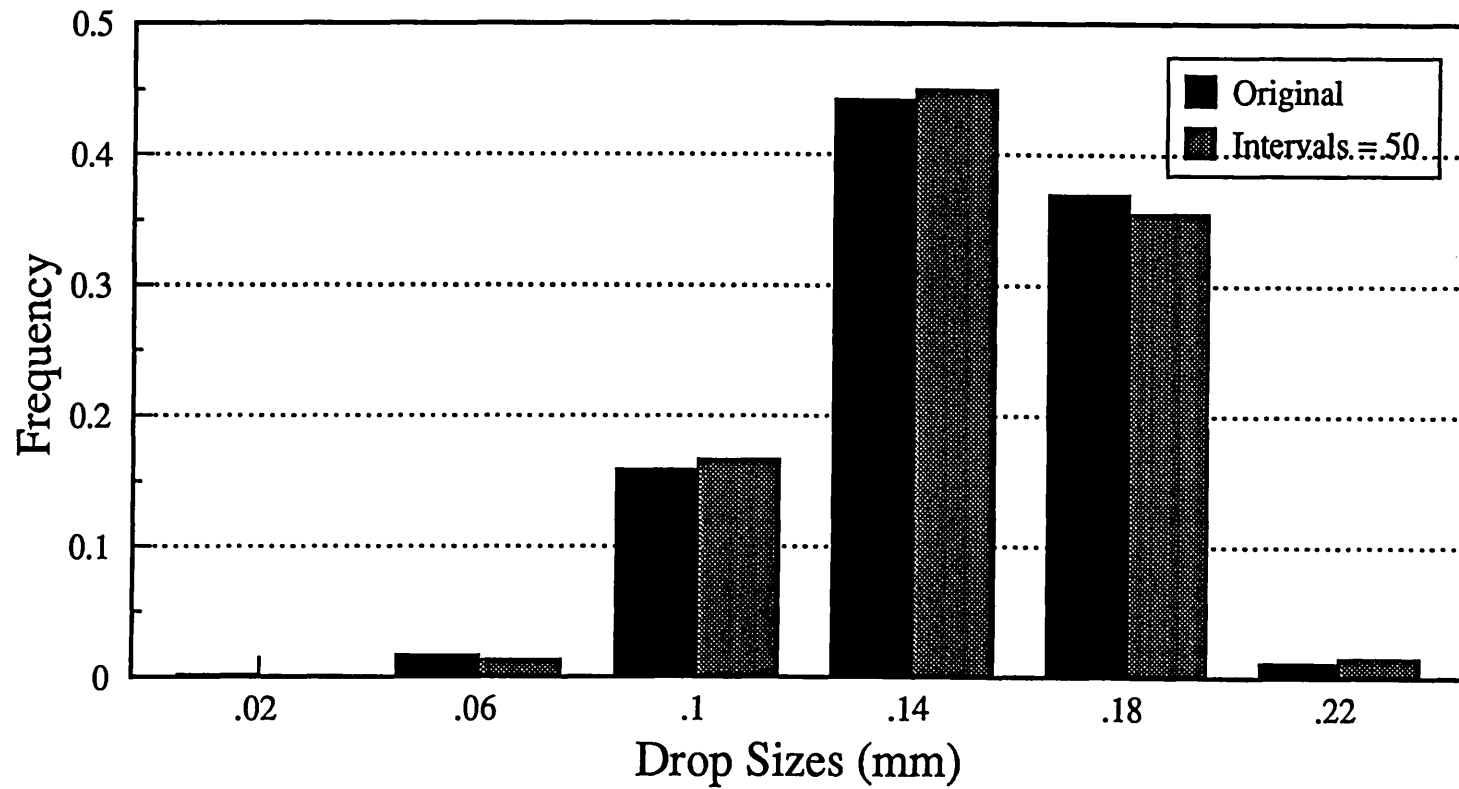


**Figure 6.8 :** *Comparison between the two algorithms : Drop size distribution*  
*Number of events = 15000*

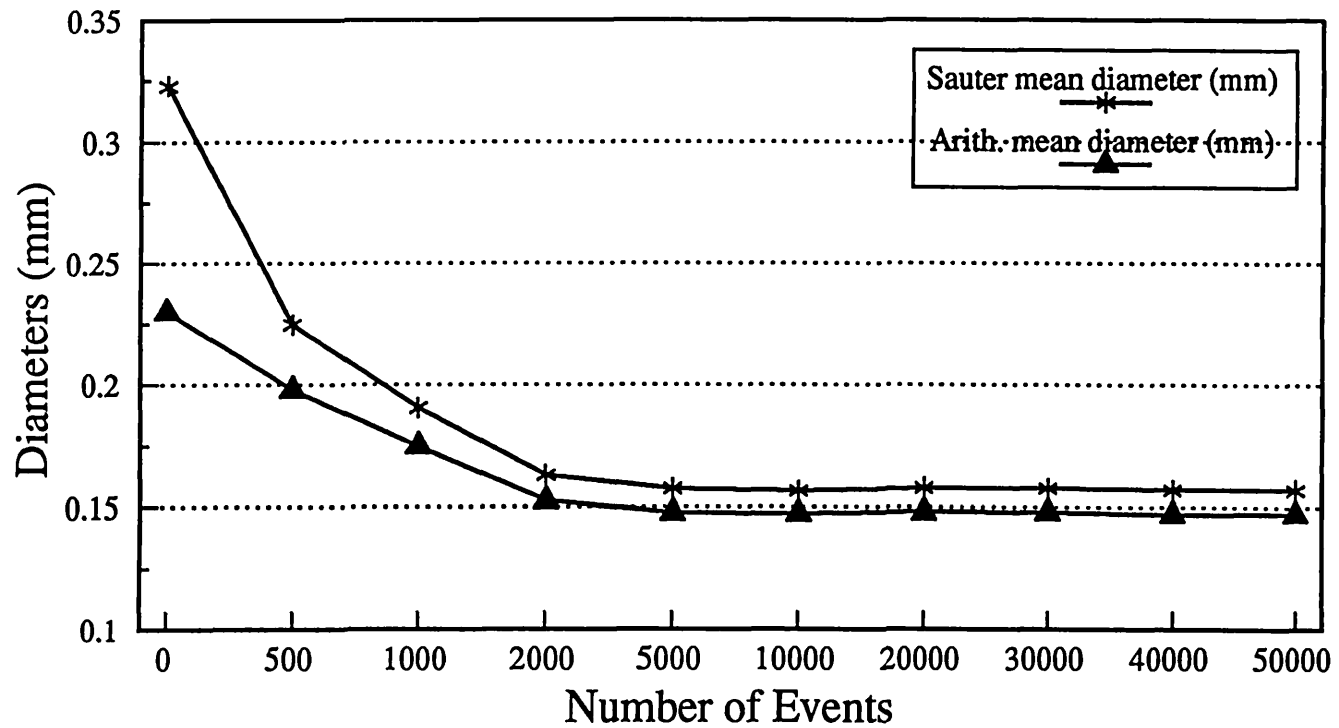


**Figure 6.9 :** *Transient algorithm behaviour : Sauter & Arith. mean diameters*  
*Number of intervals = 100*

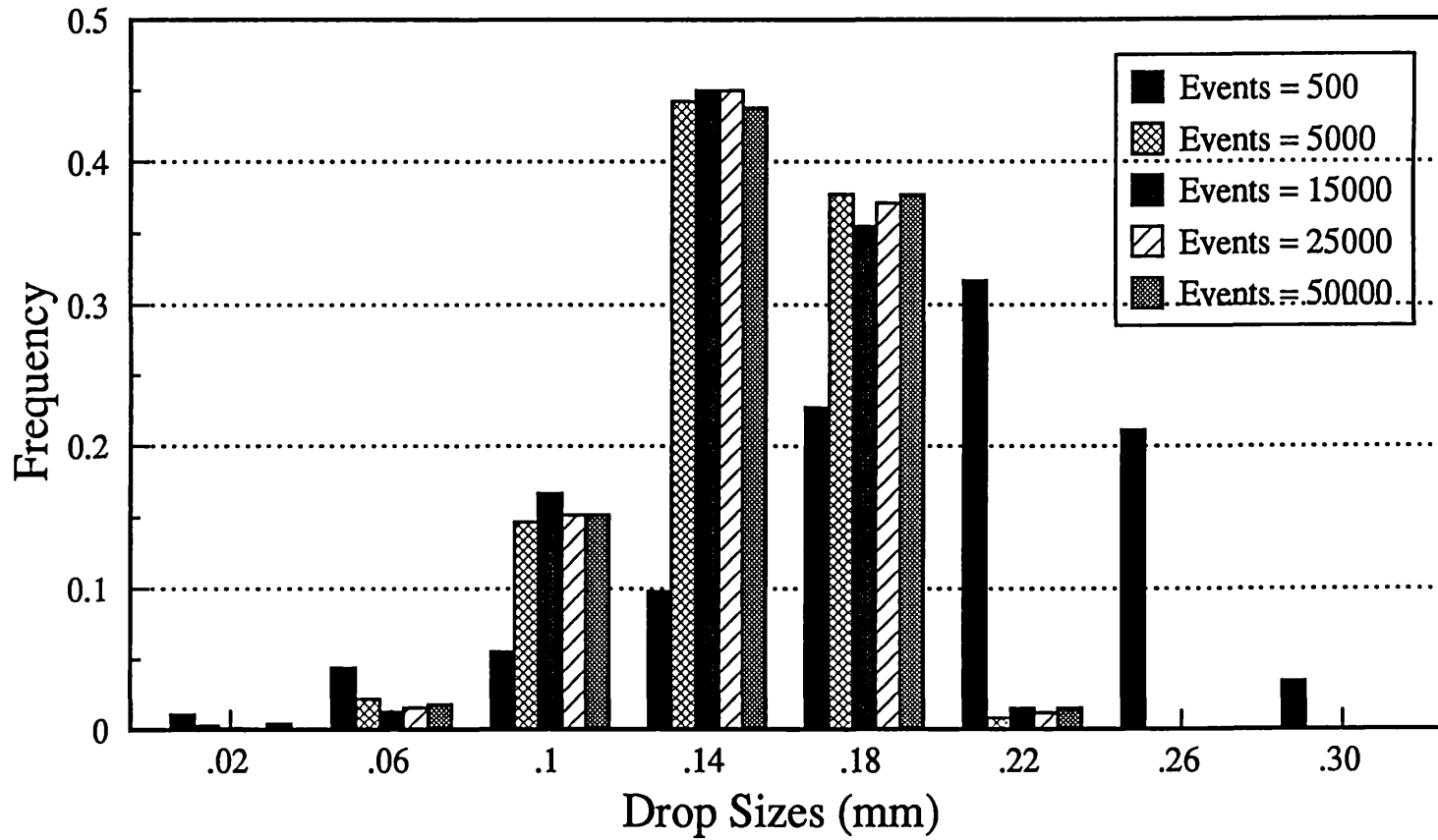


**Figure 6.10 :** *Transient algorithm behaviour : Drop size distribution evolvment*

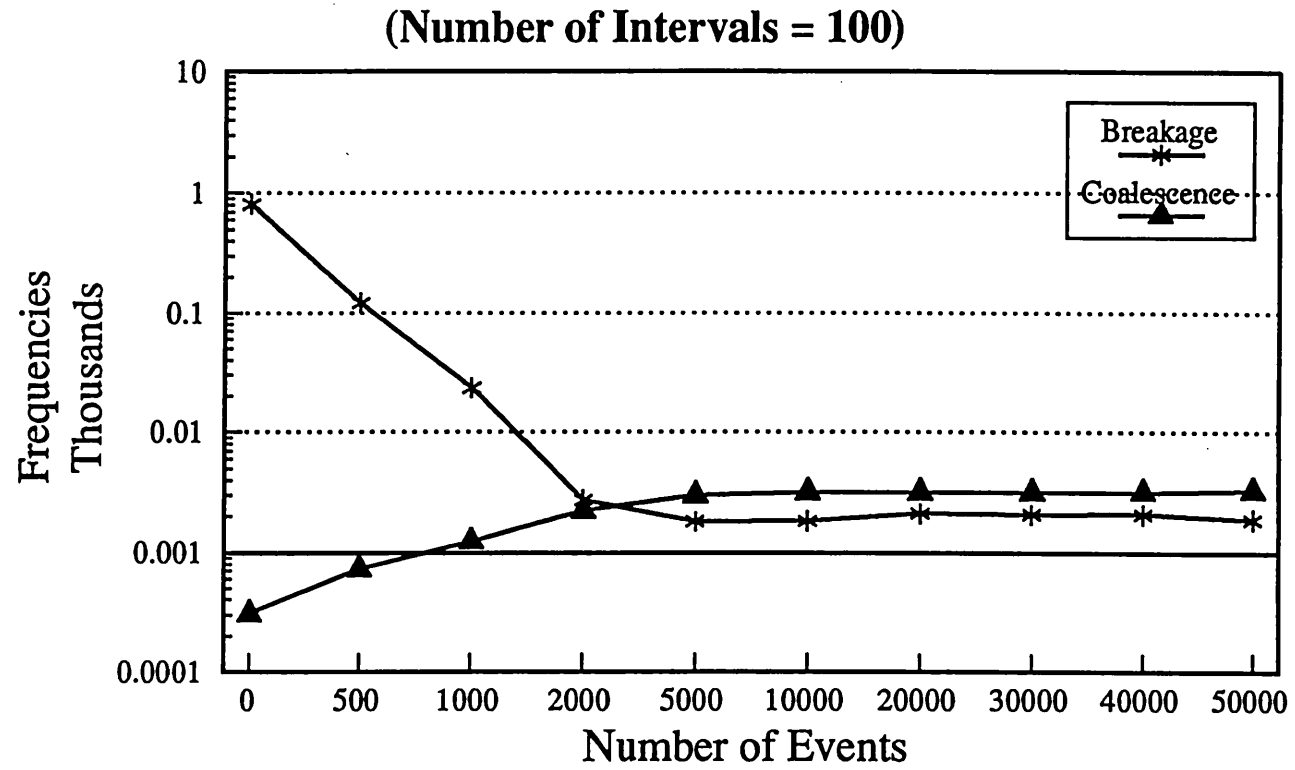
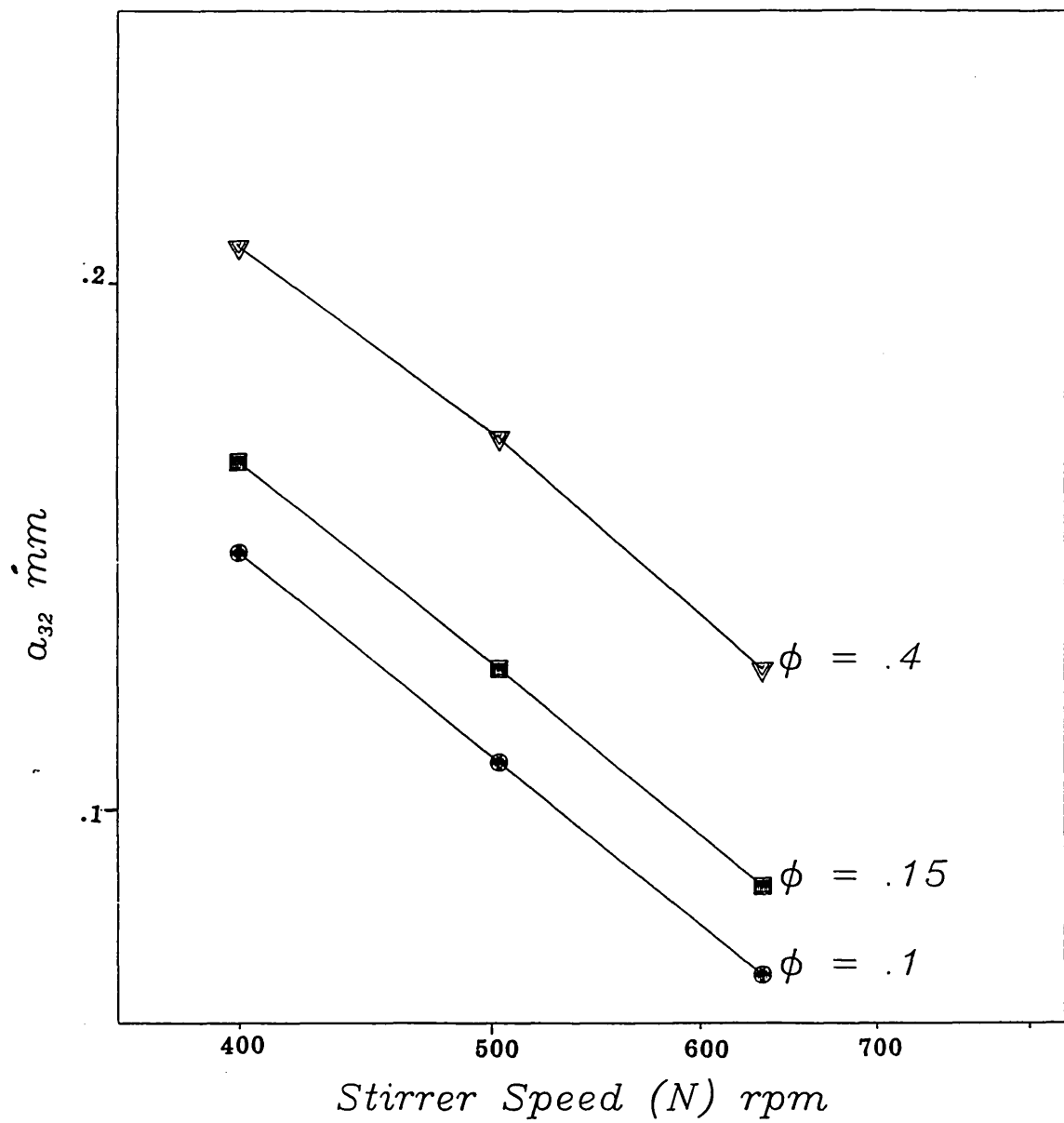
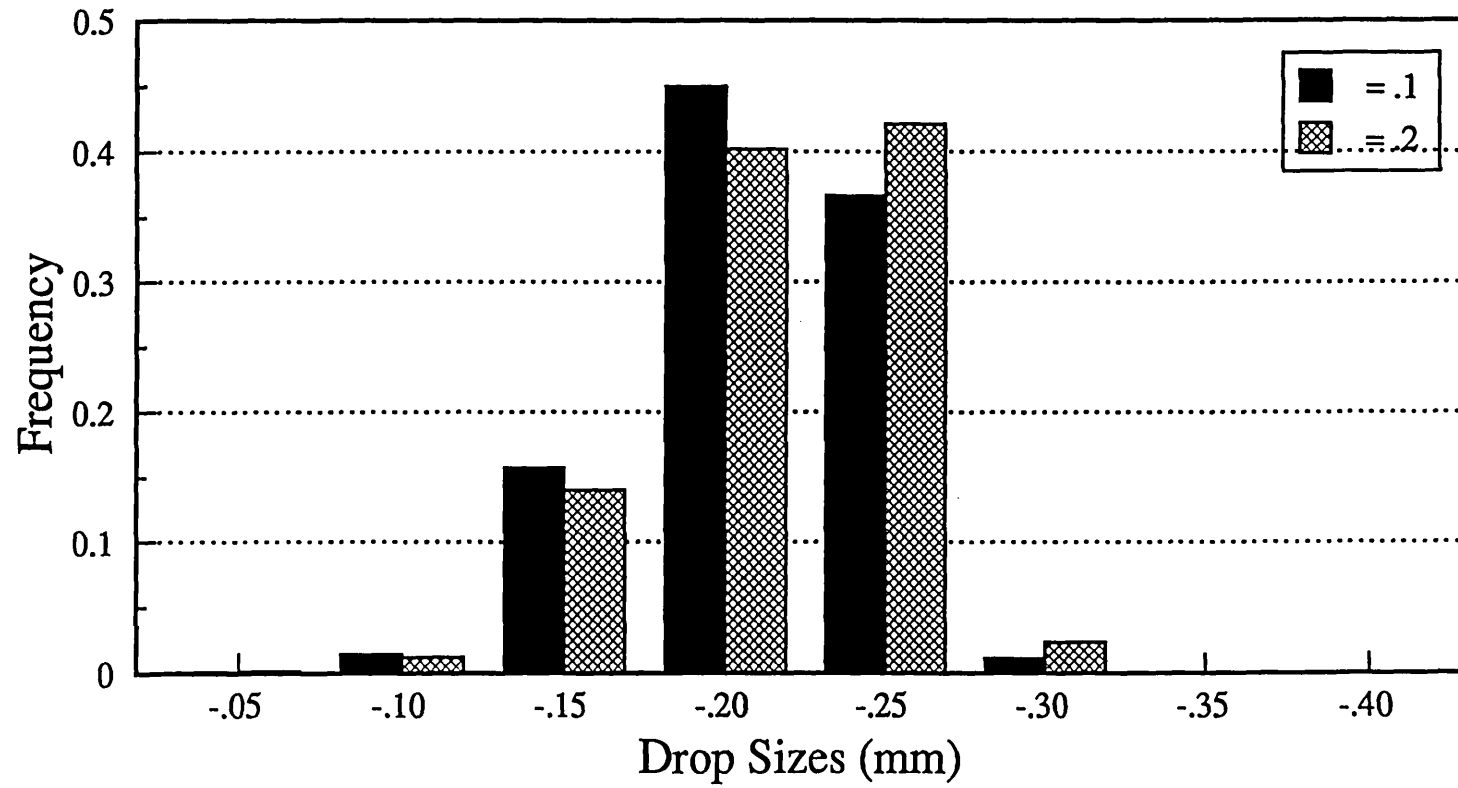


Figure 6.11 : *Transient algorithm behaviour : Breakage and coalescence frequencies*



**Figure 6.12 :** *Effect of stirring speed on Sauter mean diameter at different hold-up values*



**Figure 6.13 :** *Effect of tank hold-up on drop size distribution*  
*N = 504 ; Tank diameter = 22 cm*

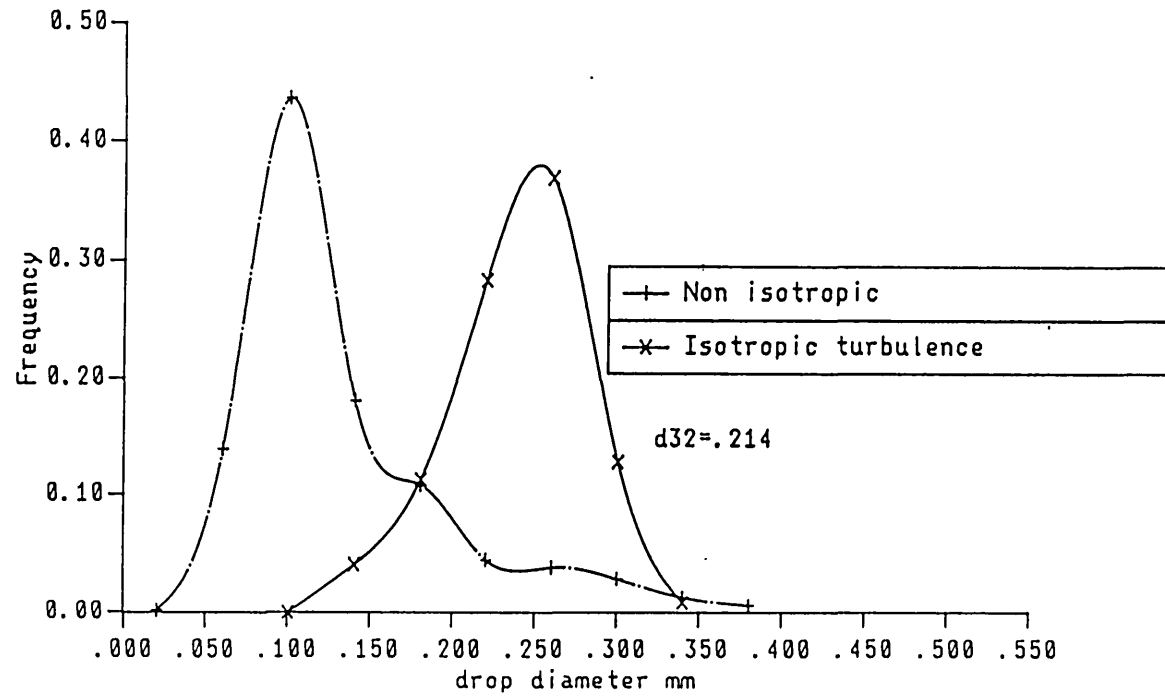


**Figure 6.14 :** Comparison between the isotropic and non-isotropic drop size distributions

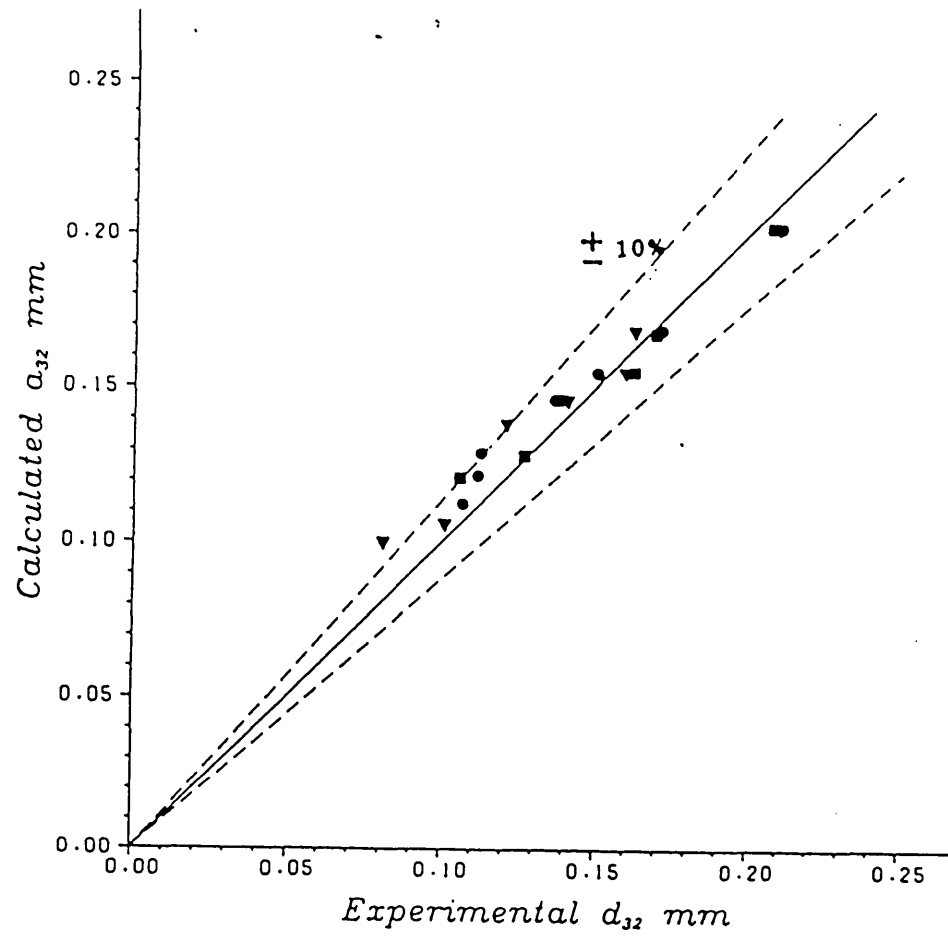
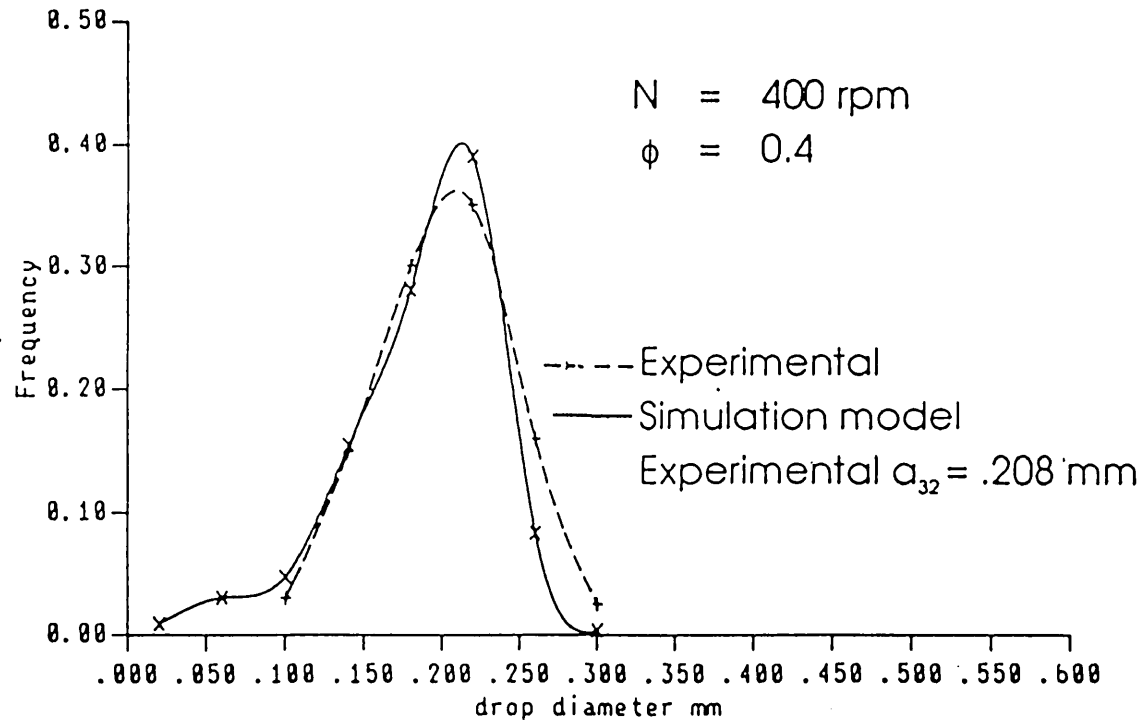


Figure 6.15 : Comparison between the simulated and experimental Sauter mean diameters



**Figure 6.16 :** Comparison between the simulated and experimental drop size distributions

## CHAPTER VII

### CONCLUSIONS AND RECOMMENDATIONS

The local drop size distributions as well as hold-up values for the system n-heptane-Water were measured at different locations in two geometrically similar batch stirred tanks of 22 and 44 cm diameter. The effects of stirring speed and hold-up were investigated.

The results obtained by Okufi(1984) were used to test the proposed Monte Carlo simulation algorithm with the procedure outlined for the coalescence frequency approximation. The following conclusions may be drawn :

- Drop sizes show large differences within the tank depending on position but with similar patterns for different operating conditions. No spatial homogeneity exists and the average characteristics of the dispersion depended on the whole vessel volume and not a specific region.
- The exponent in the relationship  $\alpha_{32} \propto N^{-x}$  at a point is not necessarily the result of the turbulence mode at that point but an equilibrium state resulting from the area characteristics as well as the surrounding regimes. Combination of different turbulence modes can result in a pseudo-isotropic flow field and a -1.2 slope is not a confirmation that the dispersion process is isotropic.
- Drop sizes show skewness the extent of which is a function of the position. The plane midway between the central axis and the wall shows minimum skewness
- The differences in local drop size distributions could not be attributed to the variations in local hold-up values since at high speeds the latter are minimal.
- For a standard tank configuration, as described by Rushton, the point that may be considered as an average representative is lying in the lower circulation region midway between the wall and the centre. A result that could be attributed to the shorter cycle that produced better mixing.
- The concept of equal tip speed scale-up criteria was found to be the best for the system under consideration despite the fact that the flow map is not exactly the same in both tanks but averages are equivalent.

- Local hold-up values were found to vary at moderate speeds from one location to the other. The extent of deviation decreased as the speed or original tank hold-up were increased.
- Simulation of the dispersion by using a coalescence frequency approximation mesh reduced the computer time significantly without impairing the accuracy.

It would be interesting to extend the present work to systems that involve interphase transfer processes to study the effect of the initial simulation stages as well as testing the algorithm with other systems.

A systematic study is needed to relate the breakage and coalescence functions' constants to the systems properties since a large volume of data is available from other researchers work. This may be done by developing a better understanding of the dispersion processes.

It would be interesting to extend the experimentation in this project to other hold-up and stirring speed values in order to test the validity of the simulation algorithm with this system.

## **APPENDICES**

# APPENDIX I

## PHYSICAL PROPERTIES

In this appendix, the physical properties of the systems investigated are listed. Measurements were made for the interfacial tension of n-heptane-water system.

System : n-heptane dispersed in water (20°C)

$\rho_c$	$\rho_d$	$\mu_c$	$\mu_d$	$\sigma$
Kg/m <sup>3</sup>	Kg/m <sup>3</sup>	Kg/ms	Kg /ms	
998.2	683.6	1.009 X 10 <sup>-3</sup>	4.114 X 10 <sup>-4</sup>	.0480

System : .2M HDEHP in n-heptane dispersed in aqueous solution of Na<sub>2</sub> SO<sub>4</sub> and H<sub>2</sub> SO<sub>4</sub> (Okufi(1984))<sup>1</sup>

$\rho_c$	$\rho_d$	$\mu_c$	$\mu_d$	$\sigma$
Kg/m <sup>3</sup>	Kg/m <sup>3</sup>	Kg/ms	Kg /ms	
1048	705.2	1.154 X 10 <sup>-3</sup>	5.011 X 10 <sup>-4</sup>	.0301

---

<sup>1</sup> Data reported by Okufi(1984)

## APPENDIX II

### Kolmogoroff's Microscale of Turbulence

According to Kolmogoroff(1941a,b), in any turbulent field at sufficiently high Reynolds numbers, the small scale components of the turbulent velocity fluctuations are statistically independent of the main flow and of the turbulence generating mechanism.

Kolmogoroff defined a length scale  $\eta$  as the microscale of turbulence. It is given by:

$$\eta = \left( \frac{v^3}{\epsilon} \right)^{1/4} \quad (A-II.1)$$

where  $v$  is the kinematic viscosity and  $\epsilon$  is the power dissipation per unit mass.

Under fully turbulent conditions, i.e.

$$\text{Reynolds number} \Leftrightarrow \frac{ND^2\rho_m}{\mu_m} > 10000 \quad (A-II.2)$$

Reynolds number greater than 10000,  $\epsilon$  is given by:

$$\epsilon = kN^3D^2 \quad (A-II.3)$$

where  $k$  is a constant.

From Equations 2.21 & 2.22, the mean physical properties of the dispersion could be obtained. They are

System	$\phi$	$\rho_m$	$\mu_m$
n-heptane - water	.1	966.74	$1.1698 \times 10^{-3}$
	.4	872.36	$1.9739 \times 10^{-3}$
HDEHP in n-heptane - Water +(Na <sub>2</sub> SO <sub>4</sub> and H <sub>2</sub> SO <sub>4</sub> )	.1	1013.72	$1.340 \times 10^{-3}$
	.4	910.88	$2.2727 \times 10^{-3}$

At the lowest stirring speed used (minimum  $\epsilon$ ) for the two systems in the 22cm tank,  $\eta$  may be estimated using equations A-II.1 through A-II.3 and substituting for  $k = .0012463$

System	$\phi$	Lowest stirring speed	$\eta$ (mm)
n-heptane - water	.1	450	.00734
	.4	450	.0117
HDEHP in n-heptane - Water +(Na <sub>2</sub> SO <sub>4</sub> and H <sub>2</sub> SO <sub>4</sub> )	.1	400	.00891
	.4	400	.01378

The values obtained for  $\eta$  are well below the drop sizes measured in this work which confirm the validity of the assumption made earlier of breakage being controlled by the inertia forces and not viscous forces

## **APPENDIX III**

### **Hold-up Measurements**

**Appendix III-1** : Tank Diameter = .22 m ;  $\phi_o = .1$

**Appendix III-2** : Tank Diameter = .22 m ;  $\phi_o = .2$

**Appendix III-3** : Tank Diameter = .22 m ;  $\phi_o = .3$

**Appendix III-4** : Tank Diameter = .22 m ;  $\phi_o = .4$

**Appendix III-1** : Tank Diameter = .44 m ;  $\phi_o = .2$

#### **Positions:**

The figure to the left of the digit indicates height while the one to the right corresponds to radial distance from centre (Please refer to **Figure 4.1**)

**APPENDIX III-1**  
**Tank diameter = .22 m ;  $\phi_o = .1$**

Tank Diameter m	Position	N	$\phi_o$	$\phi^*$
.22	1.1	450.0	.10	.531
.22	1.2	450.0	.10	.559
.22	1.3	450.0	.10	.605
.22	1.4	450.0	.10	.830
.22	1.5	450.0	.10	.823
.22	1.6	450.0	.10	.803

Tank Diameter m	Position	N	$\phi_o$	$\phi^*$
.22	1.1	500.0	.10	.472
.22	1.2	500.0	.10	.779
.22	1.3	500.0	.10	.799
.22	1.4	500.0	.10	.661
.22	1.5	500.0	.10	.776
.22	1.6	500.0	.10	.786

Tank Diameter m	Position	N	$\phi_o$	$\phi^*$
.22	1.1	550.0	.10	.654
.22	1.2	550.0	.10	.638
.22	1.3	550.0	.10	.735
.22	1.4	550.0	.10	.857
.22	1.5	550.0	.10	.847
.22	1.6	550.0	.10	.776

Tank Diameter m	Position	N	$\phi_o$	$\phi^*$
.22	1.1	600.0	.10	.664
.22	1.2	600.0	.10	.736
.22	1.3	600.0	.10	.667
.22	1.4	600.0	.10	.863
.22	1.5	600.0	.10	.837
.22	1.6	600.0	.10	.833

Tank Diameter m	Position	N	$\phi_o$	$\phi^*$
.22	1.1	700.0	.10	.832
.22	1.2	700.0	.10	.821
.22	1.3	700.0	.10	.895
.22	1.4	700.0	.10	.921
.22	1.5	700.0	.10	.926
.22	1.6	700.0	.10	.898

Tank Diameter m	Position	N	$\phi_o$	$\phi^*$
.22	2.1	450.0	.10	.760
.22	2.2	450.0	.10	.811
.22	2.3	450.0	.10	1.006
.22	2.4	450.0	.10	.927
.22	2.5	450.0	.10	1.005
.22	2.6	450.0	.10	.966

Tank Diameter m	Position	N	$\phi_o$	$\phi^*$
.22	2.1	500.0	.10	.885
.22	2.2	500.0	.10	1.005
.22	2.3	500.0	.10	.966
.22	2.4	500.0	.10	.968
.22	2.5	500.0	.10	.980
.22	2.6	500.0	.10	1.063

Tank Diameter m	Position	N	$\phi_o$	$\phi^*$
.22	2.1	550.0	.10	.800
.22	2.2	550.0	.10	.857
.22	2.3	550.0	.10	.988
.22	2.4	550.0	.10	1.056
.22	2.5	550.0	.10	.899
.22	2.6	550.0	.10	.879

Tank Diameter m	Position	N	$\phi_o$	$\phi^*$
.22	2.1	600.0	.10	.961
.22	2.2	600.0	.10	.924
.22	2.3	600.0	.10	1.018
.22	2.4	600.0	.10	.979
.22	2.5	600.0	.10	.966
.22	2.6	600.0	.10	.951

Tank Diameter m	Position	N	$\phi_o$	$\phi^*$
.22	2.1	700.0	.10	.974
.22	2.2	700.0	.10	1.011
.22	2.3	700.0	.10	.921
.22	2.4	700.0	.10	.958
.22	2.5	700.0	.10	.993
.22	2.6	700.0	.10	.981

Tank Diameter m	Position	N	$\phi_o$	$\phi^*$
.22	3.1	450.0	.10	.900
.22	3.2	450.0	.10	.930
.22	3.3	450.0	.10	.893
.22	3.4	450.0	.10	.894
.22	3.5	450.0	.10	.872
.22	3.6	450.0	.10	.847

Tank Diameter m	Position	N	$\phi_o$	$\phi^*$
.22	3.1	500.0	.10	.925
.22	3.2	500.0	.10	.899
.22	3.3	500.0	.10	.859
.22	3.4	500.0	.10	.790
.22	3.5	500.0	.10	.861
.22	3.6	500.0	.10	.757

Tank Diameter m	Position	N	$\phi_o$	$\phi^*$
.22	3.1	550.0	.10	.988
.22	3.2	550.0	.10	.995
.22	3.3	550.0	.10	.894
.22	3.4	550.0	.10	.930
.22	3.5	550.0	.10	.939
.22	3.6	550.0	.10	.952

Tank Diameter m	Position	N	$\phi_o$	$\phi^*$
.22	3.1	600.0	.10	1.048
.22	3.2	600.0	.10	.975
.22	3.3	600.0	.10	.994
.22	3.4	600.0	.10	.900
.22	3.5	600.0	.10	.943
.22	3.6	600.0	.10	.983

Tank Diameter m	Position	N	$\phi_o$	$\phi^*$
.22	3.1	700.0	.10	1.000
.22	3.2	700.0	.10	1.000
.22	3.3	700.0	.10	1.000
.22	3.4	700.0	.10	.961
.22	3.5	700.0	.10	.941
.22	3.6	700.0	.10	.946

Tank Diameter m	Position	N	$\phi_0$	$\phi^*$
.22	4.1	450.0	.10	.933
.22	4.2	450.0	.10	1.026
.22	4.3	450.0	.10	.918
.22	4.4	450.0	.10	1.009
.22	4.5	450.0	.10	.974
.22	4.6	450.0	.10	1.005

Tank Diameter m	Position	N	$\phi_0$	$\phi^*$
.22	4.1	500.0	.10	.933
.22	4.2	500.0	.10	.963
.22	4.3	500.0	.10	.928
.22	4.4	500.0	.10	.914
.22	4.5	500.0	.10	.852
.22	4.6	500.0	.10	.844

Tank Diameter m	Position	N	$\phi_0$	$\phi^*$
.22	4.1	550.0	.10	.829
.22	4.2	550.0	.10	.939
.22	4.3	550.0	.10	.968
.22	4.4	550.0	.10	.879
.22	4.5	550.0	.10	.865
.22	4.6	550.0	.10	.909

Tank Diameter m	Position	N	$\phi_0$	$\phi^*$
.22	4.1	600.0	.10	.977
.22	4.2	600.0	.10	.970
.22	4.3	600.0	.10	.953
.22	4.4	600.0	.10	.936
.22	4.5	600.0	.10	.962
.22	4.6	600.0	.10	.930

Tank Diameter m	Position	N	$\phi_0$	$\phi^*$
.22	4.1	700.0	.10	.992
.22	4.2	700.0	.10	.981
.22	4.3	700.0	.10	.996
.22	4.4	700.0	.10	.923
.22	4.5	700.0	.10	.960
.22	4.6	700.0	.10	.921

Tank Diameter m	Position	N	$\phi_o$	$\phi^*$
.22	5.1	450.0	.10	1.023
.22	5.2	450.0	.10	.987
.22	5.3	450.0	.10	1.036
.22	5.4	450.0	.10	.944
.22	5.5	450.0	.10	.977
.22	5.6	450.0	.10	.808

Tank Diameter m	Position	N	$\phi_o$	$\phi^*$
.22	5.1	500.0	.10	1.023
.22	5.2	500.0	.10	.979
.22	5.3	500.0	.10	.918
.22	5.4	500.0	.10	.927
.22	5.5	500.0	.10	.926
.22	5.6	500.0	.10	.853

Tank Diameter m	Position	N	$\phi_o$	$\phi^*$
.22	5.1	550.0	.10	.995
.22	5.2	550.0	.10	1.000
.22	5.3	550.0	.10	.943
.22	5.4	550.0	.10	.877
.22	5.5	550.0	.10	.886
.22	5.6	550.0	.10	.822

Tank Diameter m	Position	N	$\phi_o$	$\phi^*$
.22	5.1	600.0	.10	.993
.22	5.2	600.0	.10	.998
.22	5.3	600.0	.10	.904
.22	5.4	600.0	.10	.879
.22	5.5	600.0	.10	.985
.22	5.6	600.0	.10	.881

Tank Diameter m	Position	N	$\phi_o$	$\phi^*$
.22	5.1	700.0	.10	1.000
.22	5.2	700.0	.10	1.010
.22	5.3	700.0	.10	.947
.22	5.4	700.0	.10	.963
.22	5.5	700.0	.10	1.038
.22	5.6	700.0	.10	.972

Tank Diameter m	Position	N	$\phi_o$	$\phi^*$
.22	6.1	450.0	.10	1.230
.22	6.2	450.0	.10	1.162
.22	6.3	450.0	.10	1.139
.22	6.4	450.0	.10	1.207
.22	6.5	450.0	.10	1.092
.22	6.6	450.0	.10	1.003

Tank Diameter m	Position	N	$\phi_o$	$\phi^*$
.22	6.1	500.0	.10	1.184
.22	6.2	500.0	.10	1.133
.22	6.3	500.0	.10	1.132
.22	6.4	500.0	.10	1.061
.22	6.5	500.0	.10	1.039
.22	6.6	500.0	.10	1.026

Tank Diameter m	Position	N	$\phi_o$	$\phi^*$
.22	6.1	550.0	.10	1.165
.22	6.2	550.0	.10	1.142
.22	6.3	550.0	.10	1.112
.22	6.4	550.0	.10	1.080
.22	6.5	550.0	.10	1.057
.22	6.6	550.0	.10	1.000

Tank Diameter m	Position	N	$\phi_o$	$\phi^*$
.22	6.1	600.0	.10	1.070
.22	6.2	600.0	.10	1.121
.22	6.3	600.0	.10	1.046
.22	6.4	600.0	.10	1.092
.22	6.5	600.0	.10	1.021
.22	6.6	600.0	.10	1.004

Tank Diameter m	Position	N	$\phi_o$	$\phi^*$
.22	6.1	700.0	.10	1.120
.22	6.2	700.0	.10	1.082
.22	6.3	700.0	.10	1.059
.22	6.4	700.0	.10	1.007
.22	6.5	700.0	.10	1.120
.22	6.6	700.0	.10	.960

**APPENDIX III-2**  
**Tank diameter = .22 m ;  $\phi_o = .2$**

Tank Diameter m	Position	N	$\phi_o$	$\phi^*$
.22	1.1	450.0	.20	.783
.22	1.2	450.0	.20	.833
.22	1.3	450.0	.20	.820
.22	1.4	450.0	.20	.697
.22	1.5	450.0	.20	.904
.22	1.6	450.0	.20	.722

Tank Diameter m	Position	N	$\phi_o$	$\phi^*$
.22	1.1	500.0	.20	.810
.22	1.2	500.0	.20	.881
.22	1.3	500.0	.20	.867
.22	1.4	500.0	.20	.846
.22	1.5	500.0	.20	.896
.22	1.6	500.0	.20	.739

Tank Diameter m	Position	N	$\phi_o$	$\phi^*$
.22	1.1	550.0	.20	.726
.22	1.2	550.0	.20	.903
.22	1.3	550.0	.20	.860
.22	1.4	550.0	.20	.849
.22	1.5	550.0	.20	.907
.22	1.6	550.0	.20	.864

Tank Diameter m	Position	N	$\phi_o$	$\phi^*$
.22	1.1	600.0	.20	.721
.22	1.2	600.0	.20	.886
.22	1.3	600.0	.20	.909
.22	1.4	600.0	.20	.872
.22	1.5	600.0	.20	.897
.22	1.6	600.0	.20	.829

Tank Diameter m	Position	N	$\phi_o$	$\phi^*$
.22	1.1	700.0	.20	.886
.22	1.2	700.0	.20	.942
.22	1.3	700.0	.20	.969
.22	1.4	700.0	.20	.960
.22	1.5	700.0	.20	.981
.22	1.6	700.0	.20	.952

Tank Diameter m	Position	N	$\phi_o$	$\phi^*$
.22	2.1	450.0	.20	.833
.22	2.2	450.0	.20	.838
.22	2.3	450.0	.20	.928
.22	2.4	450.0	.20	.952
.22	2.5	450.0	.20	.964
.22	2.6	450.0	.20	.974

Tank Diameter m	Position	N	$\phi_o$	$\phi^*$
.22	2.1	500.0	.20	.933
.22	2.2	500.0	.20	.822
.22	2.3	500.0	.20	.920
.22	2.4	500.0	.20	.978
.22	2.5	500.0	.20	.938
.22	2.6	500.0	.20	.870

Tank Diameter m	Position	N	$\phi_o$	$\phi^*$
.22	2.1	550.0	.20	.926
.22	2.2	550.0	.20	.802
.22	2.3	550.0	.20	.850
.22	2.4	550.0	.20	.875
.22	2.5	550.0	.20	.915
.22	2.6	550.0	.20	.782

Tank Diameter m	Position	N	$\phi_o$	$\phi^*$
.22	2.1	600.0	.20	.926
.22	2.2	600.0	.20	.855
.22	2.3	600.0	.20	.870
.22	2.4	600.0	.20	.956
.22	2.5	600.0	.20	.928
.22	2.6	600.0	.20	.849

Tank Diameter m	Position	N	$\phi_o$	$\phi^*$
.22	2.1	700.0	.20	1.012
.22	2.2	700.0	.20	.978
.22	2.3	700.0	.20	.963
.22	2.4	700.0	.20	1.037
.22	2.5	700.0	.20	1.020
.22	2.6	700.0	.20	.890

Tank Diameter m	Position	N	$\phi_o$	$\phi^*$
.22	3.1	450.0	.20	1.076
.22	3.2	450.0	.20	1.034
.22	3.3	450.0	.20	1.012
.22	3.4	450.0	.20	1.000
.22	3.5	450.0	.20	.976
.22	3.6	450.0	.20	1.000

Tank Diameter m	Position	N	$\phi_o$	$\phi^*$
.22	3.1	500.0	.20	1.038
.22	3.2	500.0	.20	1.013
.22	3.3	500.0	.20	1.024
.22	3.4	500.0	.20	1.000
.22	3.5	500.0	.20	1.000
.22	3.6	500.0	.20	.955

Tank Diameter m	Position	N	$\phi_o$	$\phi^*$
.22	3.1	550.0	.20	1.054
.22	3.2	550.0	.20	1.000
.22	3.3	550.0	.20	.957
.22	3.4	550.0	.20	.976
.22	3.5	550.0	.20	.959
.22	3.6	550.0	.20	.944

Tank Diameter m	Position	N	$\phi_o$	$\phi^*$
.22	3.1	600.0	.20	.933
.22	3.2	600.0	.20	.966
.22	3.3	600.0	.20	.966
.22	3.4	600.0	.20	.941
.22	3.5	600.0	.20	.954
.22	3.6	600.0	.20	.895

Tank Diameter m	Position	N	$\phi_o$	$\phi^*$
.22	3.1	700.0	.20	1.000
.22	3.2	700.0	.20	1.000
.22	3.3	700.0	.20	.997
.22	3.4	700.0	.20	.993
.22	3.5	700.0	.20	.978
.22	3.6	700.0	.20	.962

Tank Diameter m	Position	N	$\phi_o$	$\phi^*$
.22	4.1	450.0	.20	.993
.22	4.2	450.0	.20	.953
.22	4.3	450.0	.20	.963
.22	4.4	450.0	.20	.915
.22	4.5	450.0	.20	.962
.22	4.6	450.0	.20	.849

Tank Diameter m	Position	N	$\phi_o$	$\phi^*$
.22	4.1	500.0	.20	1.011
.22	4.2	500.0	.20	.968
.22	4.3	500.0	.20	.990
.22	4.4	500.0	.20	.928
.22	4.5	500.0	.20	.892
.22	4.6	500.0	.20	.833

Tank Diameter m	Position	N	$\phi_o$	$\phi^*$
.22	4.1	550.0	.20	.959
.22	4.2	550.0	.20	.941
.22	4.3	550.0	.20	.952
.22	4.4	550.0	.20	.941
.22	4.5	550.0	.20	.941
.22	4.6	550.0	.20	.909

Tank Diameter m	Position	N	$\phi_o$	$\phi^*$
.22	4.1	600.0	.20	.941
.22	4.2	600.0	.20	.988
.22	4.3	600.0	.20	.978
.22	4.4	600.0	.20	.941
.22	4.5	600.0	.20	.909
.22	4.6	600.0	.20	.909

Tank Diameter m	Position	N	$\phi_o$	$\phi^*$
.22	4.1	700.0	.20	.990
.22	4.2	700.0	.20	.981
.22	4.3	700.0	.20	1.000
.22	4.4	700.0	.20	.978
.22	4.5	700.0	.20	.993
.22	4.6	700.0	.20	.953

Tank Diameter m	Position	N	$\phi_o$	$\phi^*$
.22	5.1	450.0	.20	1.264
.22	5.2	450.0	.20	1.124
.22	5.3	450.0	.20	1.098
.22	5.4	450.0	.20	1.011
.22	5.5	450.0	.20	.978
.22	5.6	450.0	.20	.872

Tank Diameter m	Position	N	$\phi_o$	$\phi^*$
.22	5.1	500.0	.20	1.061
.22	5.2	500.0	.20	1.065
.22	5.3	500.0	.20	1.028
.22	5.4	500.0	.20	1.029
.22	5.5	500.0	.20	.964
.22	5.6	500.0	.20	.862

Tank Diameter m	Position	N	$\phi_o$	$\phi^*$
.22	5.1	550.0	.20	1.090
.22	5.2	550.0	.20	1.000
.22	5.3	550.0	.20	.979
.22	5.4	550.0	.20	1.000
.22	5.5	550.0	.20	.988
.22	5.6	550.0	.20	.872

Tank Diameter m	Position	N	$\phi_o$	$\phi^*$
.22	5.1	600.0	.20	.974
.22	5.2	600.0	.20	.982
.22	5.3	600.0	.20	.973
.22	5.4	600.0	.20	1.000
.22	5.5	600.0	.20	.930
.22	5.6	600.0	.20	.914

Tank Diameter m	Position	N	$\phi_o$	$\phi^*$
.22	5.1	700.0	.20	.992
.22	5.2	700.0	.20	.997
.22	5.3	700.0	.20	1.003
.22	5.4	700.0	.20	1.000
.22	5.5	700.0	.20	1.010
.22	5.6	700.0	.20	.966

Tank Diameter m	Position	N	$\phi_o$	$\phi^*$
.22	6.1	450.0	.20	1.096
.22	6.2	450.0	.20	1.100
.22	6.3	450.0	.20	1.647
.22	6.4	450.0	.20	1.110
.22	6.5	450.0	.20	1.083
.22	6.6	450.0	.20	1.044

Tank Diameter m	Position	N	$\phi_o$	$\phi^*$
.22	6.1	500.0	.20	1.073
.22	6.2	500.0	.20	1.092
.22	6.3	500.0	.20	1.073
.22	6.4	500.0	.20	1.151
.22	6.5	500.0	.20	1.061
.22	6.6	500.0	.20	1.021

Tank Diameter m	Position	N	$\phi_o$	$\phi^*$
.22	6.1	550.0	.20	1.039
.22	6.2	550.0	.20	1.063
.22	6.3	550.0	.20	1.091
.22	6.4	550.0	.20	1.108
.22	6.5	550.0	.20	1.027
.22	6.6	550.0	.20	1.038

Tank Diameter m	Position	N	$\phi_o$	$\phi^*$
.22	6.1	600.0	.20	1.002
.22	6.2	600.0	.20	1.017
.22	6.3	600.0	.20	1.075
.22	6.4	600.0	.20	1.093
.22	6.5	600.0	.20	1.012
.22	6.6	600.0	.20	1.011

Tank Diameter m	Position	N	$\phi_o$	$\phi^*$
.22	6.1	700.0	.20	1.030
.22	6.2	700.0	.20	1.000
.22	6.3	700.0	.20	1.073
.22	6.4	700.0	.20	1.108
.22	6.5	700.0	.20	1.024
.22	6.6	700.0	.20	.983

**APPENDIX III-3**  
**Tank diameter = .22 m ;  $\phi_o = .3$**

Tank Diameter m	Position	N	$\phi_o$	$\phi^*$
.22	1.1	450.0	.30	.655
.22	1.2	450.0	.30	.675
.22	1.3	450.0	.30	.699
.22	1.4	450.0	.30	.857
.22	1.5	450.0	.30	.916
.22	1.6	450.0	.30	.745

Tank Diameter m	Position	N	$\phi_o$	$\phi^*$
.22	1.1	500.0	.30	.586
.22	1.2	500.0	.30	.687
.22	1.3	500.0	.30	.637
.22	1.4	500.0	.30	.868
.22	1.5	500.0	.30	.925
.22	1.6	500.0	.30	.889

Tank Diameter m	Position	N	$\phi_o$	$\phi^*$
.22	1.1	550.0	.30	.641
.22	1.2	550.0	.30	.739
.22	1.3	550.0	.30	.829
.22	1.4	550.0	.30	.903
.22	1.5	550.0	.30	.993
.22	1.6	550.0	.30	.837

Tank Diameter m	Position	N	$\phi_o$	$\phi^*$
.22	1.1	600.0	.30	.705
.22	1.2	600.0	.30	.750
.22	1.3	600.0	.30	.731
.22	1.4	600.0	.30	.912
.22	1.5	600.0	.30	.952
.22	1.6	600.0	.30	.825

Tank Diameter m	Position	N	$\phi_o$	$\phi^*$
.22	1.1	700.0	.30	.910
.22	1.2	700.0	.30	.929
.22	1.3	700.0	.30	.970
.22	1.4	700.0	.30	.981
.22	1.5	700.0	.30	.987
.22	1.6	700.0	.30	.952

Tank Diameter m	Position	N	$\phi_o$	$\phi^*$
.22	2.1	450.0	.30	.971
.22	2.2	450.0	.30	.947
.22	2.3	450.0	.30	.948
.22	2.4	450.0	.30	.938
.22	2.5	450.0	.30	.988
.22	2.6	450.0	.30	.982

Tank Diameter m	Position	N	$\phi_o$	$\phi^*$
.22	2.1	500.0	.30	.940
.22	2.2	500.0	.30	.952
.22	2.3	500.0	.30	.952
.22	2.4	500.0	.30	.971
.22	2.5	500.0	.30	.947
.22	2.6	500.0	.30	1.011

Tank Diameter m	Position	N	$\phi_o$	$\phi^*$
.22	2.1	550.0	.30	.973
.22	2.2	550.0	.30	.983
.22	2.3	550.0	.30	.972
.22	2.4	550.0	.30	.989
.22	2.5	550.0	.30	.995
.22	2.6	550.0	.30	.943

Tank Diameter m	Position	N	$\phi_o$	$\phi^*$
.22	2.1	600.0	.30	.967
.22	2.2	600.0	.30	.964
.22	2.3	600.0	.30	.952
.22	2.4	600.0	.30	.995
.22	2.5	600.0	.30	.997
.22	2.6	600.0	.30	.961

Tank Diameter m	Position	N	$\phi_o$	$\phi^*$
.22	2.1	700.0	.30	.983
.22	2.2	700.0	.30	.983
.22	2.3	700.0	.30	.970
.22	2.4	700.0	.30	1.000
.22	2.5	700.0	.30	.999
.22	2.6	700.0	.30	.982

Tank Diameter m	Position	N	$\phi_o$	$\phi^*$
.22	3.1	450.0	.30	1.054
.22	3.2	450.0	.30	1.039
.22	3.3	450.0	.30	1.011
.22	3.4	450.0	.30	.989
.22	3.5	450.0	.30	.964
.22	3.6	450.0	.30	.919

Tank Diameter m	Position	N	$\phi_o$	$\phi^*$
.22	3.1	500.0	.30	.972
.22	3.2	500.0	.30	1.011
.22	3.3	500.0	.30	1.020
.22	3.4	500.0	.30	1.004
.22	3.5	500.0	.30	.986
.22	3.6	500.0	.30	.970

Tank Diameter m	Position	N	$\phi_o$	$\phi^*$
.22	3.1	550.0	.30	.967
.22	3.2	550.0	.30	1.011
.22	3.3	550.0	.30	.994
.22	3.4	550.0	.30	.958
.22	3.5	550.0	.30	.930
.22	3.6	550.0	.30	.958

Tank Diameter m	Position	N	$\phi_o$	$\phi^*$
.22	3.1	600.0	.30	.980
.22	3.2	600.0	.30	1.004
.22	3.3	600.0	.30	.986
.22	3.4	600.0	.30	.969
.22	3.5	600.0	.30	.952
.22	3.6	600.0	.30	.915

Tank Diameter m	Position	N	$\phi_o$	$\phi^*$
.22	3.1	700.0	.30	1.009
.22	3.2	700.0	.30	1.000
.22	3.3	700.0	.30	1.003
.22	3.4	700.0	.30	.992
.22	3.5	700.0	.30	.997
.22	3.6	700.0	.30	.979

Tank Diameter m	Position	N	$\phi_o$	$\phi^*$
.22	4.1	450.0	.30	1.057
.22	4.2	450.0	.30	1.059
.22	4.3	450.0	.30	1.027
.22	4.4	450.0	.30	1.036
.22	4.5	450.0	.30	.983
.22	4.6	450.0	.30	.947

Tank Diameter m	Position	N	$\phi_o$	$\phi^*$
.22	4.1	500.0	.30	1.058
.22	4.2	500.0	.30	1.010
.22	4.3	500.0	.30	1.008
.22	4.4	500.0	.30	.990
.22	4.5	500.0	.30	1.018
.22	4.6	500.0	.30	.980

Tank Diameter m	Position	N	$\phi_o$	$\phi^*$
.22	4.1	550.0	.30	.988
.22	4.2	550.0	.30	.985
.22	4.3	550.0	.30	.985
.22	4.4	550.0	.30	1.008
.22	4.5	550.0	.30	.986
.22	4.6	550.0	.30	.922

Tank Diameter m	Position	N	$\phi_o$	$\phi^*$
.22	4.1	600.0	.30	1.034
.22	4.2	600.0	.30	1.005
.22	4.3	600.0	.30	.998
.22	4.4	600.0	.30	.998
.22	4.5	600.0	.30	1.004
.22	4.6	600.0	.30	.980

Tank Diameter m	Position	N	$\phi_o$	$\phi^*$
.22	4.1	700.0	.30	1.017
.22	4.2	700.0	.30	1.000
.22	4.3	700.0	.30	1.000
.22	4.4	700.0	.30	1.022
.22	4.5	700.0	.30	1.000
.22	4.6	700.0	.30	.970

Tank Diameter m	Position	N	$\phi_o$	$\phi^*$
.22	5.1	450.0	.30	1.061
.22	5.2	450.0	.30	1.034
.22	5.3	450.0	.30	.988
.22	5.4	450.0	.30	.980
.22	5.5	450.0	.30	.958
.22	5.6	450.0	.30	.958

Tank Diameter m	Position	N	$\phi_o$	$\phi^*$
.22	5.1	500.0	.30	1.061
.22	5.2	500.0	.30	1.000
.22	5.3	500.0	.30	.930
.22	5.4	500.0	.30	.940
.22	5.5	500.0	.30	.946
.22	5.6	500.0	.30	.909

Tank Diameter m	Position	N	$\phi_o$	$\phi^*$
.22	5.1	550.0	.30	.988
.22	5.2	550.0	.30	.959
.22	5.3	550.0	.30	.952
.22	5.4	550.0	.30	.936
.22	5.5	550.0	.30	.945
.22	5.6	550.0	.30	.906

Tank Diameter m	Position	N	$\phi_o$	$\phi^*$
.22	5.1	600.0	.30	.988
.22	5.2	600.0	.30	.981
.22	5.3	600.0	.30	.973
.22	5.4	600.0	.30	.959
.22	5.5	600.0	.30	.966
.22	5.6	600.0	.30	.891

Tank Diameter m	Position	N	$\phi_o$	$\phi^*$
.22	5.1	700.0	.30	.991
.22	5.2	700.0	.30	1.031
.22	5.3	700.0	.30	1.031
.22	5.4	700.0	.30	1.001
.22	5.5	700.0	.30	.981
.22	5.6	700.0	.30	.949

Tank Diameter m	Position	N	$\phi_o$	$\phi^*$
.22	6.1	450.0	.30	1.100
.22	6.2	450.0	.30	1.013
.22	6.3	450.0	.30	1.162
.22	6.4	450.0	.30	1.110
.22	6.5	450.0	.30	1.051
.22	6.6	450.0	.30	1.149

Tank Diameter m	Position	N	$\phi_o$	$\phi^*$
.22	6.1	500.0	.30	1.091
.22	6.2	500.0	.30	1.004
.22	6.3	500.0	.30	1.139
.22	6.4	500.0	.30	1.110
.22	6.5	500.0	.30	1.032
.22	6.6	500.0	.30	1.025

Tank Diameter m	Position	N	$\phi_o$	$\phi^*$
.22	6.1	550.0	.30	1.055
.22	6.2	550.0	.30	1.038
.22	6.3	550.0	.30	1.101
.22	6.4	550.0	.30	1.067
.22	6.5	550.0	.30	1.041
.22	6.6	550.0	.30	1.002

Tank Diameter m	Position	N	$\phi_o$	$\phi^*$
.22	6.1	600.0	.30	1.000
.22	6.2	600.0	.30	1.023
.22	6.3	600.0	.30	1.109
.22	6.4	600.0	.30	1.000
.22	6.5	600.0	.30	1.000
.22	6.6	600.0	.30	.999

Tank Diameter m	Position	N	$\phi_o$	$\phi^*$
.22	6.1	700.0	.30	1.000
.22	6.2	700.0	.30	1.039
.22	6.3	700.0	.30	1.061
.22	6.4	700.0	.30	.998
.22	6.5	700.0	.30	1.000
.22	6.6	700.0	.30	1.081

**APPENDIX III-4**  
**Tank diameter = .22 m ;  $\phi_o = .4$**

Tank Diameter m	Position	N	$\phi_o$	$\phi^*$
.22	1.1	450.0	.40	.758
.22	1.2	450.0	.40	.917
.22	1.3	450.0	.40	.894
.22	1.4	450.0	.40	.861
.22	1.5	450.0	.40	.903
.22	1.6	450.0	.40	.786

Tank Diameter m	Position	N	$\phi_o$	$\phi^*$
.22	1.1	500.0	.40	.732
.22	1.2	500.0	.40	.939
.22	1.3	500.0	.40	.908
.22	1.4	500.0	.40	.885
.22	1.5	500.0	.40	.928
.22	1.6	500.0	.40	.812

Tank Diameter m	Position	N	$\phi_o$	$\phi^*$
.22	1.1	550.0	.40	.778
.22	1.2	550.0	.40	.856
.22	1.3	550.0	.40	.821
.22	1.4	550.0	.40	.887
.22	1.5	550.0	.40	.906
.22	1.6	550.0	.40	.793

Tank Diameter m	Position	N	$\phi_o$	$\phi^*$
.22	1.1	600.0	.40	.821
.22	1.2	600.0	.40	.812
.22	1.3	600.0	.40	.887
.22	1.4	600.0	.40	.894
.22	1.5	600.0	.40	.918
.22	1.6	600.0	.40	.842

Tank Diameter m	Position	N	$\phi_o$	$\phi^*$
.22	1.1	700.0	.40	.951
.22	1.2	700.0	.40	.942
.22	1.3	700.0	.40	.970
.22	1.4	700.0	.40	.972
.22	1.5	700.0	.40	.979
.22	1.6	700.0	.40	.942

Tank Diameter m	Position	N	$\phi_o$	$\phi^*$
.22	2.1	450.0	.40	.935
.22	2.2	450.0	.40	.950
.22	2.3	450.0	.40	.924
.22	2.4	450.0	.40	.944
.22	2.5	450.0	.40	.938
.22	2.6	450.0	.40	.934

Tank Diameter m	Position	N	$\phi_o$	$\phi^*$
.22	2.1	500.0	.40	.993
.22	2.2	500.0	.40	.933
.22	2.3	500.0	.40	.959
.22	2.4	500.0	.40	.942
.22	2.5	500.0	.40	.975
.22	2.6	500.0	.40	.839

Tank Diameter m	Position	N	$\phi_o$	$\phi^*$
.22	2.1	550.0	.40	1.042
.22	2.2	550.0	.40	.904
.22	2.3	550.0	.40	.984
.22	2.4	550.0	.40	.990
.22	2.5	550.0	.40	.967
.22	2.6	550.0	.40	.984

Tank Diameter m	Position	N	$\phi_o$	$\phi^*$
.22	2.1	600.0	.40	1.051
.22	2.2	600.0	.40	.915
.22	2.3	600.0	.40	.938
.22	2.4	600.0	.40	.989
.22	2.5	600.0	.40	.976
.22	2.6	600.0	.40	.888

Tank Diameter m	Position	N	$\phi_o$	$\phi^*$
.22	2.1	700.0	.40	1.010
.22	2.2	700.0	.40	1.000
.22	2.3	700.0	.40	.982
.22	2.4	700.0	.40	1.000
.22	2.5	700.0	.40	1.000
.22	2.6	700.0	.40	.967

Tank Diameter m	Position	N	$\phi_o$	$\phi^*$
.22	3.1	450.0	.40	1.049
.22	3.2	450.0	.40	1.022
.22	3.3	450.0	.40	1.003
.22	3.4	450.0	.40	.987
.22	3.5	450.0	.40	.988
.22	3.6	450.0	.40	.879

Tank Diameter m	Position	N	$\phi_o$	$\phi^*$
.22	3.1	500.0	.40	1.006
.22	3.2	500.0	.40	.994
.22	3.3	500.0	.40	1.019
.22	3.4	500.0	.40	.952
.22	3.5	500.0	.40	.985
.22	3.6	500.0	.40	.948

Tank Diameter m	Position	N	$\phi_o$	$\phi^*$
.22	3.1	550.0	.40	.994
.22	3.2	550.0	.40	.988
.22	3.3	550.0	.40	.981
.22	3.4	550.0	.40	.975
.22	3.5	550.0	.40	.994
.22	3.6	550.0	.40	.932

Tank Diameter m	Position	N	$\phi_o$	$\phi^*$
.22	3.1	600.0	.40	1.000
.22	3.2	600.0	.40	.983
.22	3.3	600.0	.40	.989
.22	3.4	600.0	.40	.980
.22	3.5	600.0	.40	.945
.22	3.6	600.0	.40	.969

Tank Diameter m	Position	N	$\phi_o$	$\phi^*$
.22	3.1	700.0	.40	1.000
.22	3.2	700.0	.40	1.000
.22	3.3	700.0	.40	1.007
.22	3.4	700.0	.40	.990
.22	3.5	700.0	.40	.996
.22	3.6	700.0	.40	.982

Tank Diameter m	Position	N	$\phi_o$	$\phi^*$
.22	4.1	450.0	.40	1.083
.22	4.2	450.0	.40	1.036
.22	4.3	450.0	.40	1.000
.22	4.4	450.0	.40	.987
.22	4.5	450.0	.40	.988
.22	4.6	450.0	.40	.884

Tank Diameter m	Position	N	$\phi_o$	$\phi^*$
.22	4.1	500.0	.40	1.023
.22	4.2	500.0	.40	1.029
.22	4.3	500.0	.40	.992
.22	4.4	500.0	.40	.983
.22	4.5	500.0	.40	1.000
.22	4.6	500.0	.40	.973

Tank Diameter m	Position	N	$\phi_o$	$\phi^*$
.22	4.1	550.0	.40	1.000
.22	4.2	550.0	.40	.993
.22	4.3	550.0	.40	.988
.22	4.4	550.0	.40	.964
.22	4.5	550.0	.40	.972
.22	4.6	550.0	.40	.941

Tank Diameter m	Position	N	$\phi_o$	$\phi^*$
.22	4.1	600.0	.40	.986
.22	4.2	600.0	.40	.952
.22	4.3	600.0	.40	.989
.22	4.4	600.0	.40	.995
.22	4.5	600.0	.40	.985
.22	4.6	600.0	.40	.969

Tank Diameter m	Position	N	$\phi_o$	$\phi^*$
.22	4.1	700.0	.40	1.020
.22	4.2	700.0	.40	.989
.22	4.3	700.0	.40	1.010
.22	4.4	700.0	.40	1.010
.22	4.5	700.0	.40	.998
.22	4.6	700.0	.40	.972

Tank Diameter m	Position	N	$\phi_o$	$\phi^*$
.22	5.1	450.0	.40	1.006
.22	5.2	450.0	.40	1.047
.22	5.3	450.0	.40	.988
.22	5.4	450.0	.40	.992
.22	5.5	450.0	.40	.978
.22	5.6	450.0	.40	.888

Tank Diameter m	Position	N	$\phi_o$	$\phi^*$
.22	5.1	500.0	.40	.986
.22	5.2	500.0	.40	1.000
.22	5.3	500.0	.40	.963
.22	5.4	500.0	.40	.959
.22	5.5	500.0	.40	.962
.22	5.6	500.0	.40	.949

Tank Diameter m	Position	N	$\phi_o$	$\phi^*$
.22	5.1	550.0	.40	.977
.22	5.2	550.0	.40	.975
.22	5.3	550.0	.40	.964
.22	5.4	550.0	.40	.942
.22	5.5	550.0	.40	.929
.22	5.6	550.0	.40	.972

Tank Diameter m	Position	N	$\phi_o$	$\phi^*$
.22	5.1	600.0	.40	.987
.22	5.2	600.0	.40	.947
.22	5.3	600.0	.40	.988
.22	5.4	600.0	.40	.933
.22	5.5	600.0	.40	.951
.22	5.6	600.0	.40	.943

Tank Diameter m	Position	N	$\phi_o$	$\phi^*$
.22	5.1	700.0	.40	.991
.22	5.2	700.0	.40	.987
.22	5.3	700.0	.40	1.002
.22	5.4	700.0	.40	.989
.22	5.5	700.0	.40	.999
.22	5.6	700.0	.40	.976

Tank Diameter m	Position	N	$\phi_o$	$\phi^*$
.22	6.1	450.0	.40	1.127
.22	6.2	450.0	.40	1.061
.22	6.3	450.0	.40	1.034
.22	6.4	450.0	.40	1.082
.22	6.5	450.0	.40	1.103
.22	6.6	450.0	.40	1.052

Tank Diameter m	Position	N	$\phi_o$	$\phi^*$
.22	6.1	500.0	.40	1.090
.22	6.2	500.0	.40	1.082
.22	6.3	500.0	.40	1.016
.22	6.4	500.0	.40	1.122
.22	6.5	500.0	.40	1.098
.22	6.6	500.0	.40	1.074

Tank Diameter m	Position	N	$\phi_o$	$\phi^*$
.22	6.1	550.0	.40	1.001
.22	6.2	550.0	.40	1.039
.22	6.3	550.0	.40	.978
.22	6.4	550.0	.40	1.032
.22	6.5	550.0	.40	1.011
.22	6.6	550.0	.40	.997

Tank Diameter m	Position	N	$\phi_o$	$\phi^*$
.22	6.1	600.0	.40	1.031
.22	6.2	600.0	.40	1.032
.22	6.3	600.0	.40	1.109
.22	6.4	600.0	.40	1.001
.22	6.5	600.0	.40	1.007
.22	6.6	600.0	.40	.995

Tank Diameter m	Position	N	$\phi_o$	$\phi^*$
.22	6.1	700.0	.40	1.000
.22	6.2	700.0	.40	1.021
.22	6.3	700.0	.40	1.009
.22	6.4	700.0	.40	1.026
.22	6.5	700.0	.40	1.031
.22	6.6	700.0	.40	1.081

**APPENDIX III-5**  
**Tank diameter = .44 m ;  $\phi_o = .2$**

Tank Diameter m	Position	N	$\phi_o$	$\phi^*$
.22	1.1	225.0	.20	.821
.22	1.2	225.0	.20	.807
.22	1.3	225.0	.20	.883
.22	1.4	225.0	.20	.941
.22	1.5	225.0	.20	.895
.22	1.6	225.0	.20	.862

Tank Diameter m	Position	N	$\phi_o$	$\phi^*$
.22	1.1	250.0	.20	.890
.22	1.2	250.0	.20	.942
.22	1.3	250.0	.20	.918
.22	1.4	250.0	.20	.937
.22	1.5	250.0	.20	.981
.22	1.6	250.0	.20	.874

Tank Diameter m	Position	N	$\phi_o$	$\phi^*$
.22	1.1	283.0	.20	.821
.22	1.2	283.0	.20	.892
.22	1.3	283.0	.20	.910
.22	1.4	283.0	.20	.984
.22	1.5	283.0	.20	.923
.22	1.6	283.0	.20	.801

Tank Diameter m	Position	N	$\phi_o$	$\phi^*$
.22	1.1	314.0	.20	.976
.22	1.2	314.0	.20	.983
.22	1.3	314.0	.20	.950
.22	1.4	314.0	.20	.992
.22	1.5	314.0	.20	.921
.22	1.6	314.0	.20	.910

Tank Diameter m	Position	N	$\phi_o$	$\phi^*$
.22	2.1	225.0	.20	.892
.22	2.2	225.0	.20	.927
.22	2.3	225.0	.20	.919
.22	2.4	225.0	.20	.962
.22	2.5	225.0	.20	.941
.22	2.6	225.0	.20	.882

Tank Diameter m	Position	N	$\phi_o$	$\phi^*$
.22	2.1	250.0	.20	.913
.22	2.2	250.0	.20	.907
.22	2.3	250.0	.20	.966
.22	2.4	250.0	.20	.958
.22	2.5	250.0	.20	1.037
.22	2.6	250.0	.20	.916

Tank Diameter m	Position	N	$\phi_o$	$\phi^*$
.22	2.1	283.0	.20	.951
.22	2.2	283.0	.20	.911
.22	2.3	283.0	.20	.971
.22	2.4	283.0	.20	.996
.22	2.5	283.0	.20	.989
.22	2.6	283.0	.20	.873

Tank Diameter m	Position	N	$\phi_o$	$\phi^*$
.22	2.1	314.0	.20	.987
.22	2.2	314.0	.20	1.000
.22	2.3	314.0	.20	1.000
.22	2.4	314.0	.20	.993
.22	2.5	314.0	.20	.974
.22	2.6	314.0	.20	.921

Tank Diameter m	Position	N	$\phi_o$	$\phi^*$
.22	3.1	225.0	.20	.994
.22	3.2	225.0	.20	.997
.22	3.3	225.0	.20	1.037
.22	3.4	225.0	.20	.964
.22	3.5	225.0	.20	.947
.22	3.6	225.0	.20	.920

Tank Diameter m	Position	N	$\phi_o$	$\phi^*$
.22	3.1	250.0	.20	.991
.22	3.2	250.0	.20	1.007
.22	3.3	250.0	.20	.982
.22	3.4	250.0	.20	1.000
.22	3.5	250.0	.20	.961
.22	3.6	250.0	.20	.972

Tank Diameter m	Position	N	$\phi_o$	$\phi^*$
.22	3.1	283.0	.20	.973
.22	3.2	283.0	.20	1.042
.22	3.3	283.0	.20	1.000
.22	3.4	283.0	.20	.980
.22	3.5	283.0	.20	1.000
.22	3.6	283.0	.20	.958

Tank Diameter m	Position	N	$\phi_o$	$\phi^*$
.22	3.1	314.0	.20	1.000
.22	3.2	314.0	.20	1.020
.22	3.3	314.0	.20	1.000
.22	3.4	314.0	.20	.974
.22	3.5	314.0	.20	1.000
.22	3.6	314.0	.20	.961

Tank Diameter m	Position	N	$\phi_o$	$\phi^*$
.22	4.1	225.0	.20	.950
.22	4.2	225.0	.20	.913
.22	4.3	225.0	.20	.997
.22	4.4	225.0	.20	1.000
.22	4.5	225.0	.20	.932
.22	4.6	225.0	.20	.841

Tank Diameter m	Position	N	$\phi_o$	$\phi^*$
.22	4.1	250.0	.20	.947
.22	4.2	250.0	.20	.964
.22	4.3	250.0	.20	.995
.22	4.4	250.0	.20	.986
.22	4.5	250.0	.20	1.031
.22	4.6	250.0	.20	.922

Tank Diameter m	Position	N	$\phi_o$	$\phi^*$
.22	4.1	283.0	.20	.962
.22	4.2	283.0	.20	.995
.22	4.3	283.0	.20	1.000
.22	4.4	283.0	.20	1.000
.22	4.5	283.0	.20	.996
.22	4.6	283.0	.20	.942

Tank Diameter m	Position	N	$\phi_o$	$\phi^*$
.22	4.1	314.0	.20	1.091
.22	4.2	314.0	.20	1.030
.22	4.3	314.0	.20	1.000
.22	4.4	314.0	.20	1.042
.22	4.5	314.0	.20	.973
.22	4.6	314.0	.20	.951

Tank Diameter m	Position	N	$\phi_o$	$\phi^*$
.22	5.1	225.0	.20	1.073
.22	5.2	225.0	.20	.985
.22	5.3	225.0	.20	1.022
.22	5.4	225.0	.20	1.000
.22	5.5	225.0	.20	.995
.22	5.6	225.0	.20	.911

Tank Diameter m	Position	N	$\phi_o$	$\phi^*$
.22	5.1	250.0	.20	1.033
.22	5.2	250.0	.20	.998
.22	5.3	250.0	.20	1.000
.22	5.4	250.0	.20	1.017
.22	5.5	250.0	.20	1.000
.22	5.6	250.0	.20	.944

Tank Diameter m	Position	N	$\phi_o$	$\phi^*$
.22	5.1	283.0	.20	.988
.22	5.2	283.0	.20	1.000
.22	5.3	283.0	.20	1.010
.22	5.4	283.0	.20	1.000
.22	5.5	283.0	.20	1.047
.22	5.6	283.0	.20	.970

Tank Diameter m	Position	N	$\phi_o$	$\phi^*$
.22	5.1	314.0	.20	.983
.22	5.2	314.0	.20	1.020
.22	5.3	314.0	.20	.979
.22	5.4	314.0	.20	1.000
.22	5.5	314.0	.20	1.000
.22	5.6	314.0	.20	1.120(?)

## APPENDIX IV

### Drop Sizing Results

**Appendix IV-1a** : Tank Diameter = .22 m ;  $\phi_o = .1$  ;  
Stirring Speed = 450 rpm

**Appendix IV-1b** : Tank Diameter = .22 m ;  $\phi_o = .1$  ;  
Stirring Speed = 450 rpm

**Appendix IV-2** : Tank Diameter = .22 m ;  $\phi_o = .3$

**Appendix IV-3a** : Tank Diameter = .44 m ;  $\phi_o = .1$  ;  
Stirring Speed = 225 rpm

**Appendix IV-3b** : Tank Diameter = .44 m ;  $\phi_o = .1$  ;  
Stirring Speed = 300 rpm

Please Note

1st Moment  $\Leftrightarrow$  Arithmetic mean diameter

2nd Moment  $\Leftrightarrow$  Standard deviation

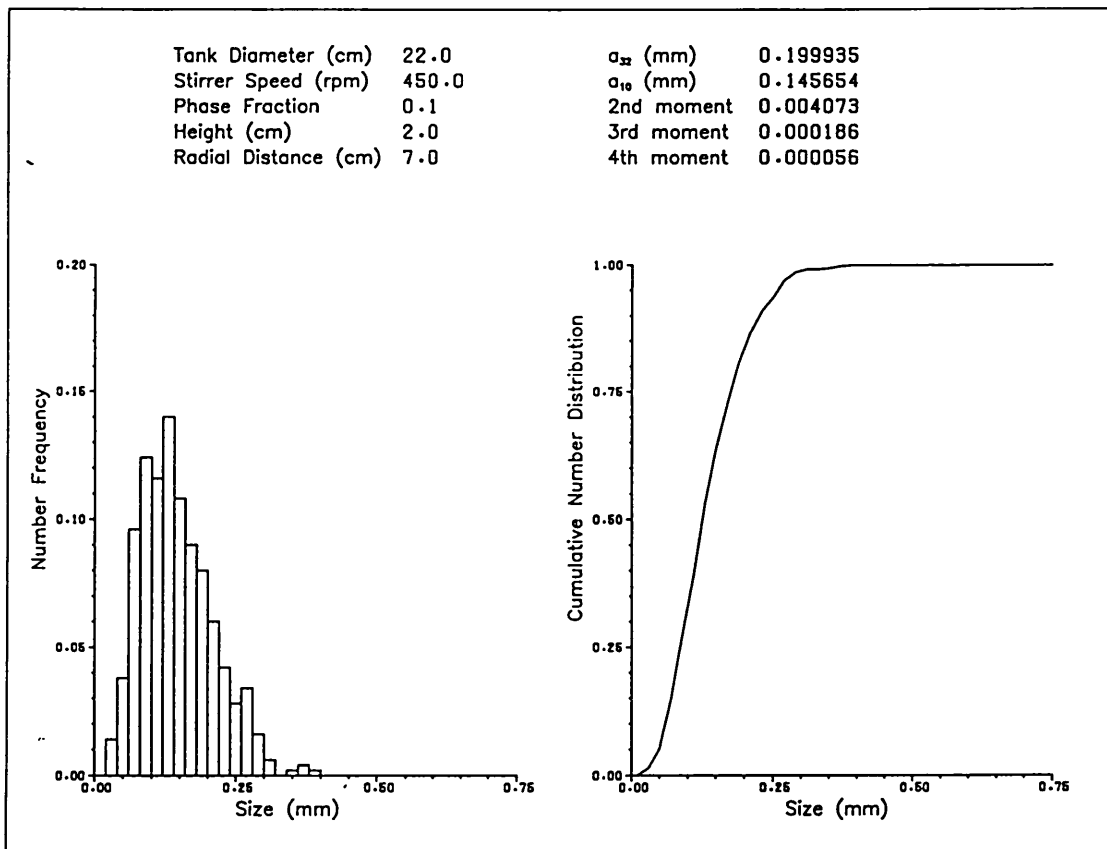
3rd Moment  $\Leftrightarrow$  Skewness factor

4th Moment  $\Leftrightarrow$  Curtosis factor

# APPENDIX IV-1a

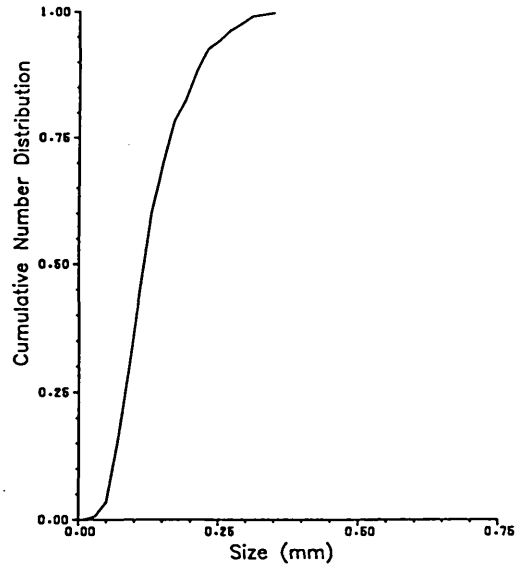
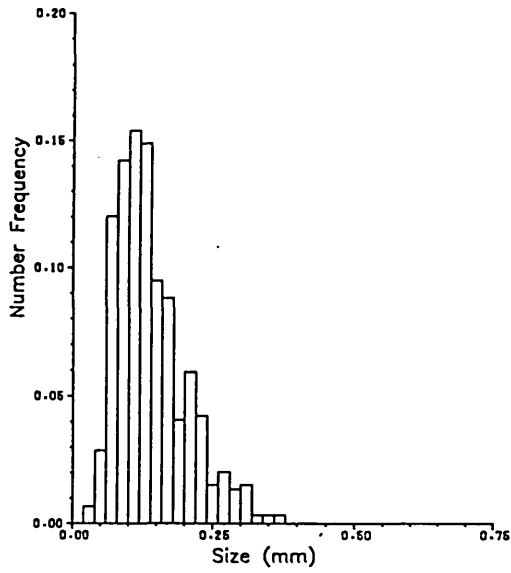
## Drop Sizing Results

Tank Diameter = .22 m ;  $\phi_o = .1$  ; Stirring Speed = 450 rpm



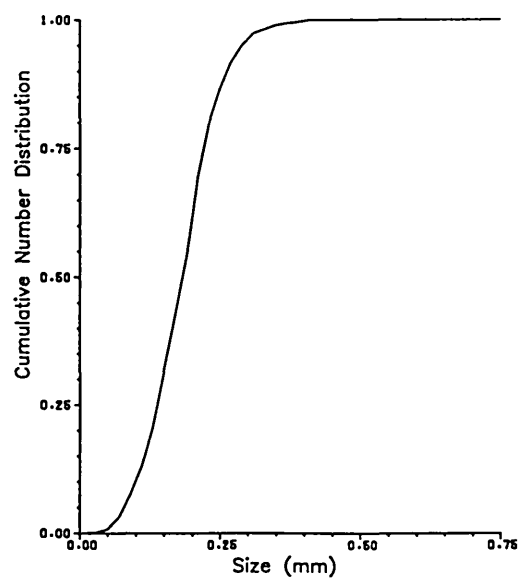
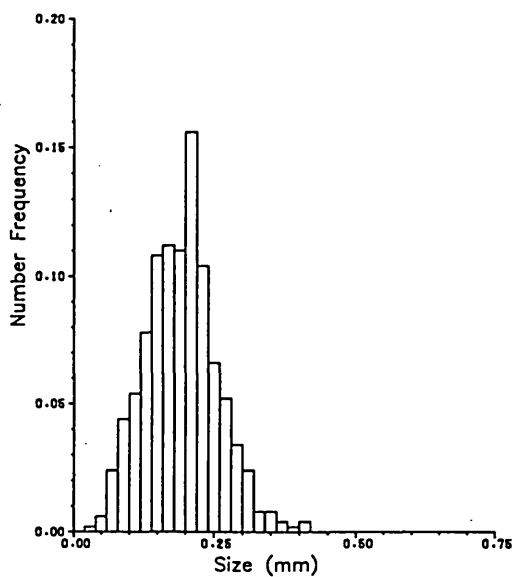
Tank Diameter (cm) 22.0  
 Stirrer Speed (rpm) 450.0  
 Phase Fraction 0.1  
 Height (cm) 2.0  
 Radial Distance (cm) 9.0

$a_{32}$  (mm) 0.196864  
 $a_{10}$  (mm) 0.139212  
 2nd moment 0.003934  
 3rd moment 0.000249  
 4th moment 0.000059



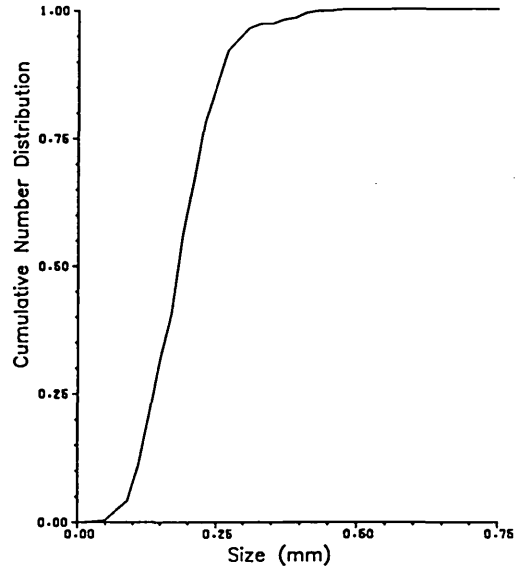
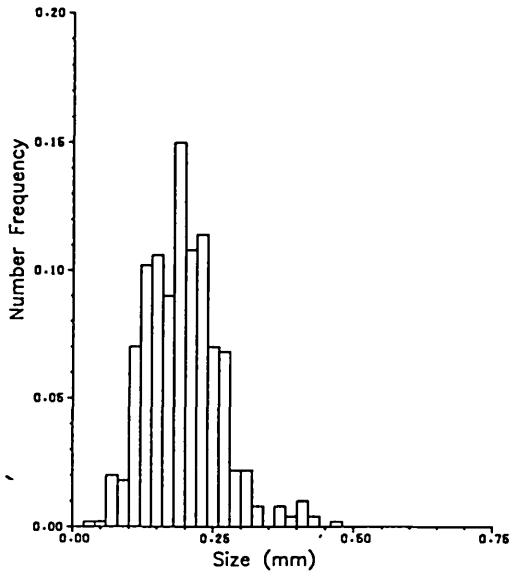
Tank Diameter (cm) 22.0  
 Stirrer Speed (rpm) 450.0  
 Phase Fraction 0.1  
 Height (cm) 6.0  
 Radial Distance (cm) 5.0

$a_{32}$  (mm) 0.231447  
 $a_{10}$  (mm) 0.191974  
 2nd moment 0.004006  
 3rd moment 0.000075  
 4th moment 0.000052



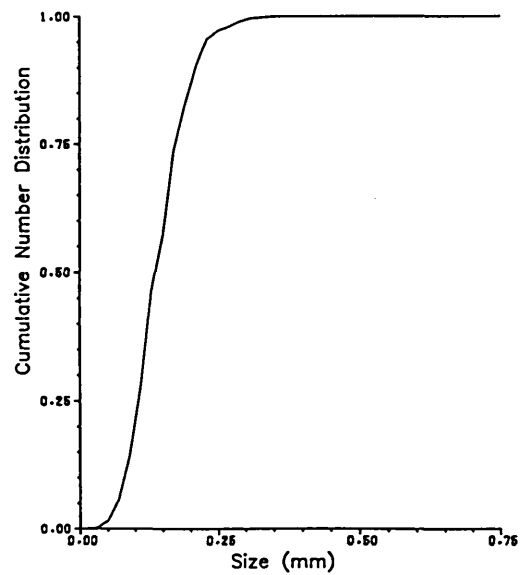
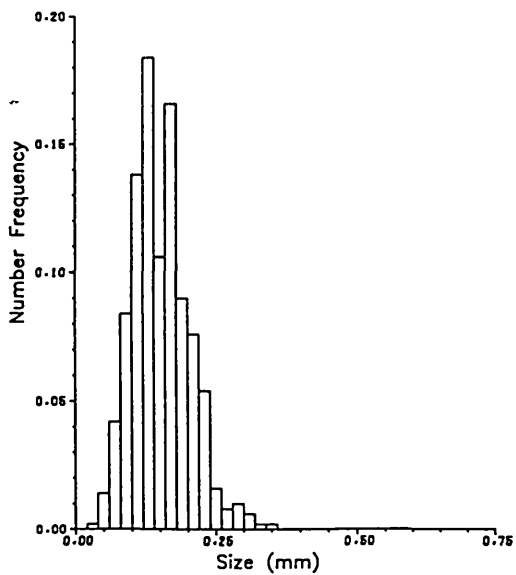
Tank Diameter (cm) 22.0  
 Stirrer Speed (rpm) 450.0  
 Phase Fraction 0.1  
 Height (cm) 6.0  
 Radial Distance (cm) 7.0

$\alpha_{33}$  (mm) 0.241409  
 $\alpha_{10}$  (mm) 0.195494  
 2nd moment 0.004426  
 3rd moment 0.000227  
 4th moment 0.000086



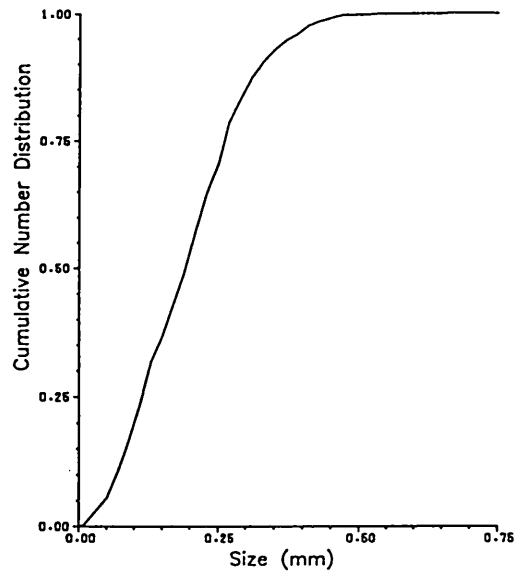
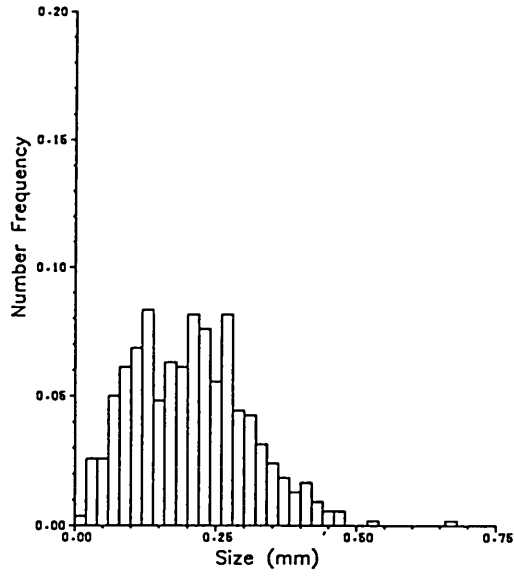
Tank Diameter (cm) 22.0  
 Stirrer Speed (rpm) 450.0  
 Phase Fraction 0.1  
 Height (cm) 6.0  
 Radial Distance (cm) 9.0

$\alpha_{33}$  (mm) 0.186113  
 $\alpha_{10}$  (mm) 0.152314  
 2nd moment 0.002630  
 3rd moment 0.000072  
 4th moment 0.000023



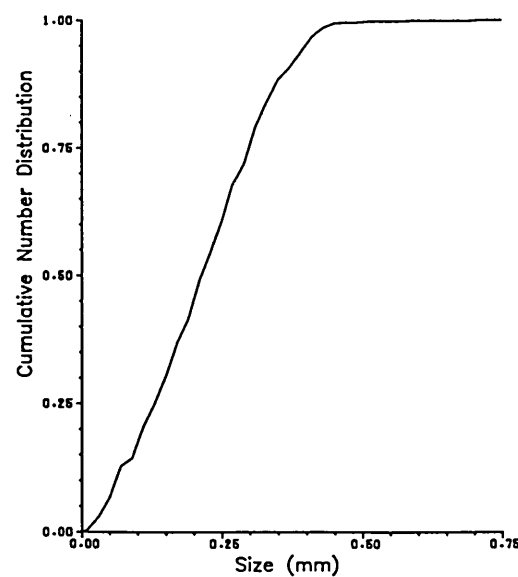
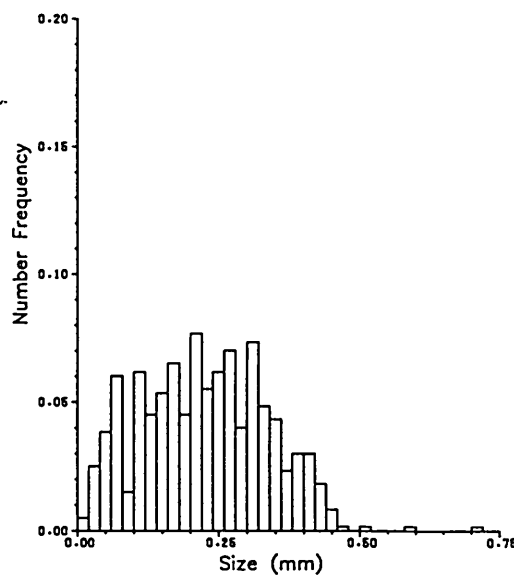
Tank Diameter (cm) 22.0  
 Stirrer Speed (rpm) 450.0  
 Phase Fraction 0.1  
 Height (cm) 10.0  
 Radial Distance (cm) 5.0

$a_{32}$  (mm) 0.295331  
 $a_{10}$  (mm) 0.204346  
 2nd moment 0.010277  
 3rd moment 0.000534  
 4th moment 0.000349



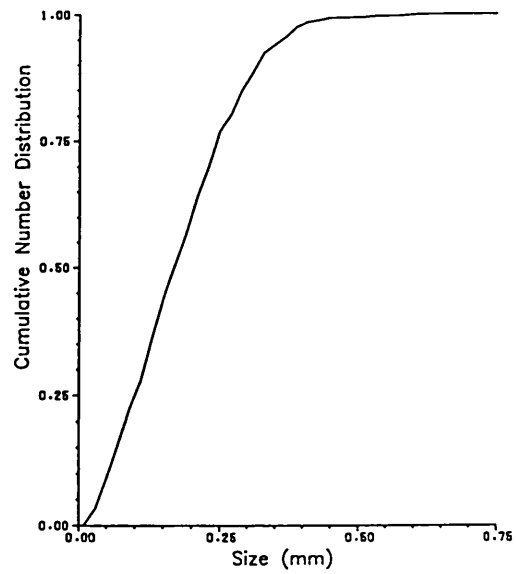
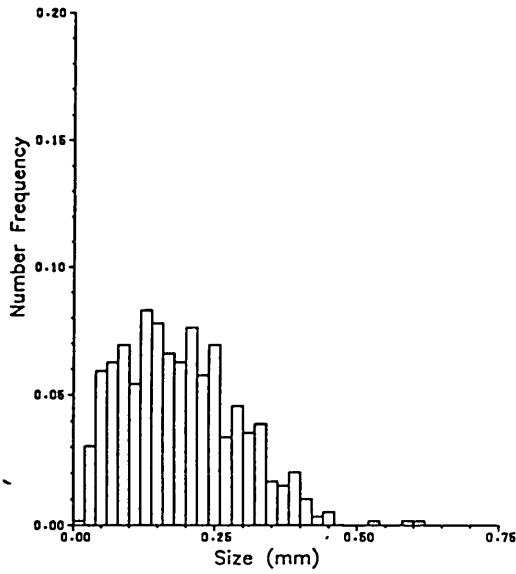
Tank Diameter (cm) 22.0  
 Stirrer Speed (rpm) 450.0  
 Phase Fraction 0.1  
 Height (cm) 10.0  
 Radial Distance (cm) 7.0

$a_{32}$  (mm) 0.318458  
 $a_{10}$  (mm) 0.225423  
 2nd moment 0.012355  
 3rd moment 0.000307  
 4th moment 0.000427



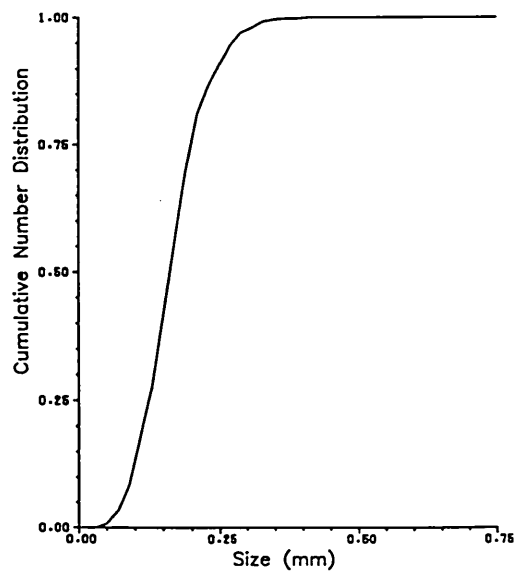
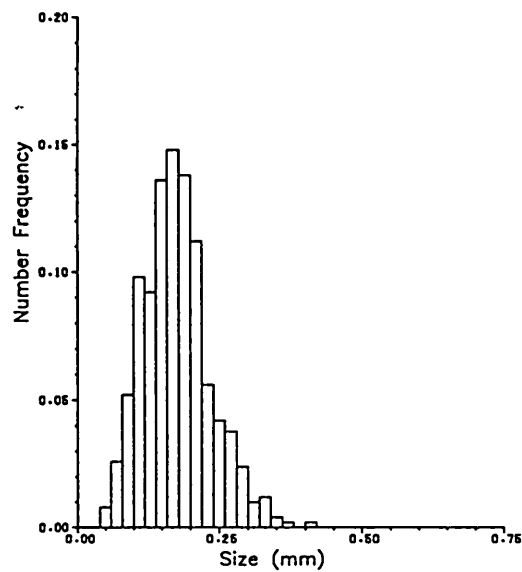
Tank Diameter (cm) 22.0  
 Stirrer Speed (rpm) 450.0  
 Phase Fraction 0.1  
 Height (cm) 10.0  
 Radial Distance (cm) 9.0

$a_{32}$  (mm) 0.287141  
 $a_{10}$  (mm) 0.188632  
 2nd moment 0.010281  
 3rd moment 0.000639  
 4th moment 0.000346



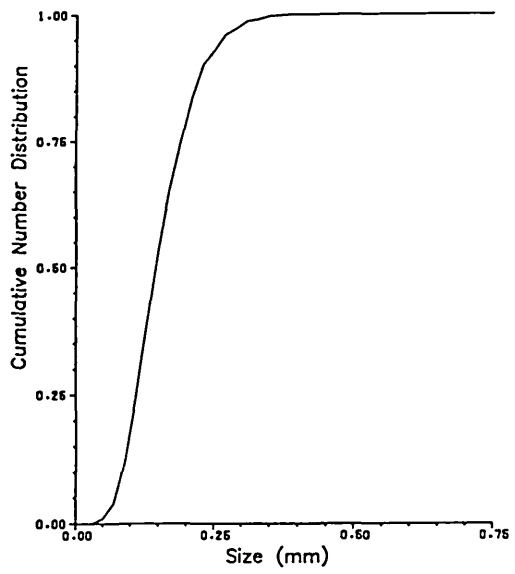
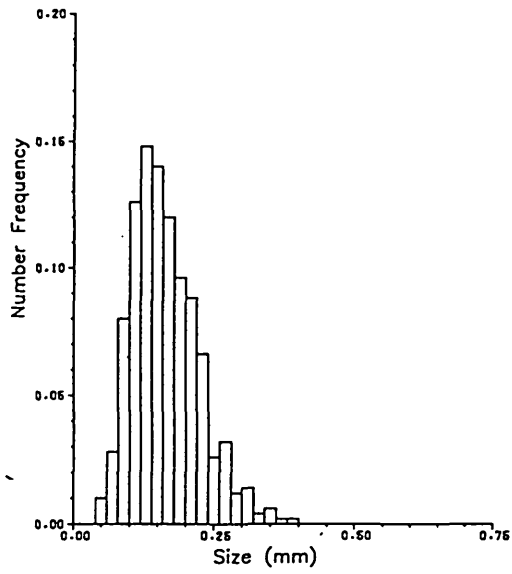
Tank Diameter (cm) 22.0  
 Stirrer Speed (rpm) 450.0  
 Phase Fraction 0.1  
 Height (cm) 14.0  
 Radial Distance (cm) 5.0

$a_{32}$  (mm) 0.213947  
 $a_{10}$  (mm) 0.175022  
 2nd moment 0.003454  
 3rd moment 0.000118  
 4th moment 0.000043



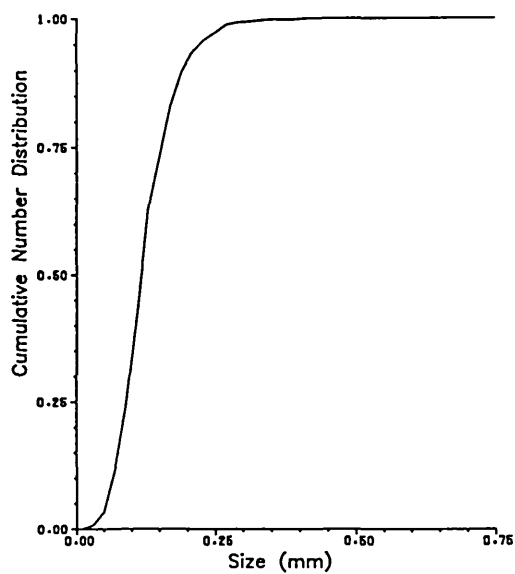
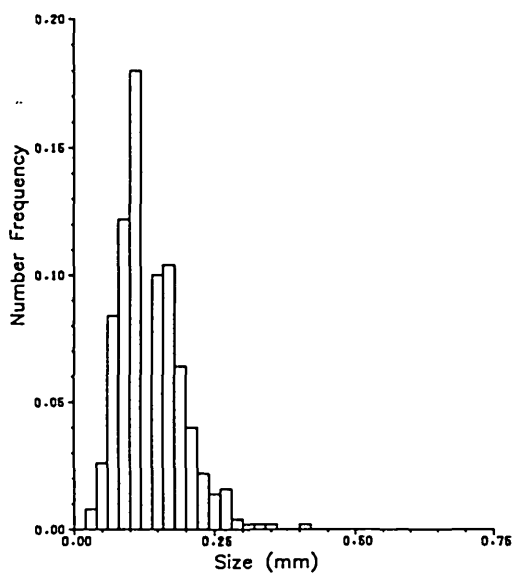
Tank Diameter (cm) 22.0  
 Stirrer Speed (rpm) 450.0  
 Phase Fraction 0.1  
 Height (cm) 14.0  
 Radial Distance (cm) 7.0

$\sigma_{32}$  (mm) 0.206184  
 $\sigma_{10}$  (mm) 0.164010  
 2nd moment 0.003454  
 3rd moment 0.000147  
 4th moment 0.000043



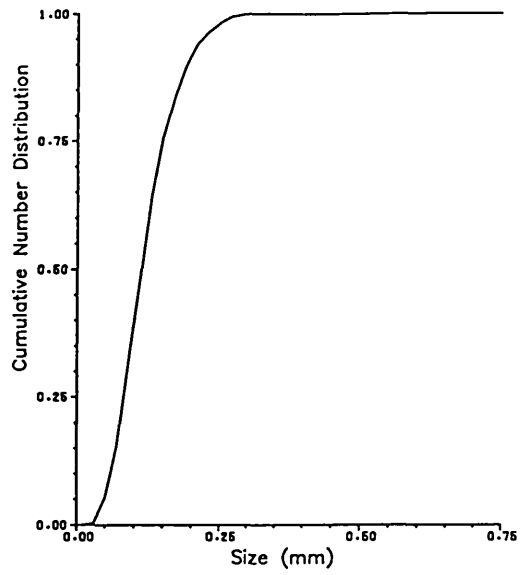
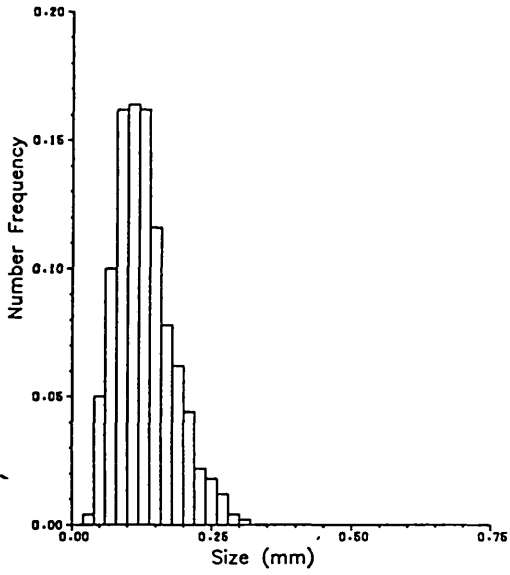
Tank Diameter (cm) 22.0  
 Stirrer Speed (rpm) 450.0  
 Phase Fraction 0.1  
 Height (cm) 14.0  
 Radial Distance (cm) 9.0

$\sigma_{32}$  (mm) 0.176163  
 $\sigma_{10}$  (mm) 0.135415  
 2nd moment 0.002636  
 3rd moment 0.000141  
 4th moment 0.000036



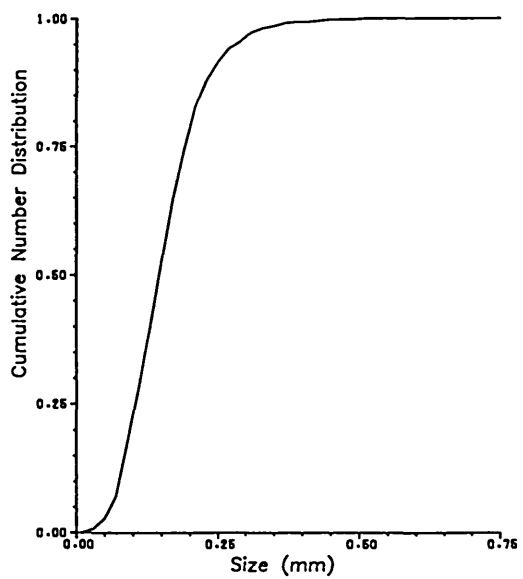
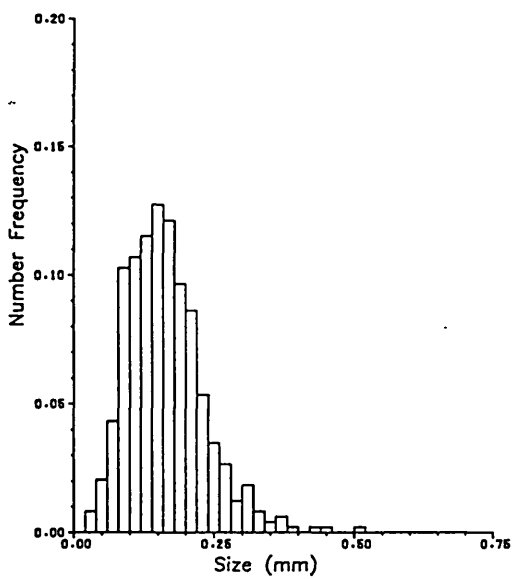
Tank Diameter (cm) 22.0  
 Stirrer Speed (rpm) 450.0  
 Phase Fraction 0.1  
 Height (cm) 18.0  
 Radial Distance (cm) 7.0

$\sigma_{32}$  (mm) 0.168996  
 $\sigma_{10}$  (mm) 0.130131  
 2nd moment 0.002552  
 3rd moment 0.000093  
 4th moment 0.000021



Tank Diameter (cm) 22.0  
 Stirrer Speed (rpm) 450.0  
 Phase Fraction 0.1  
 Height (cm) 18.0  
 Radial Distance (cm) 9.0

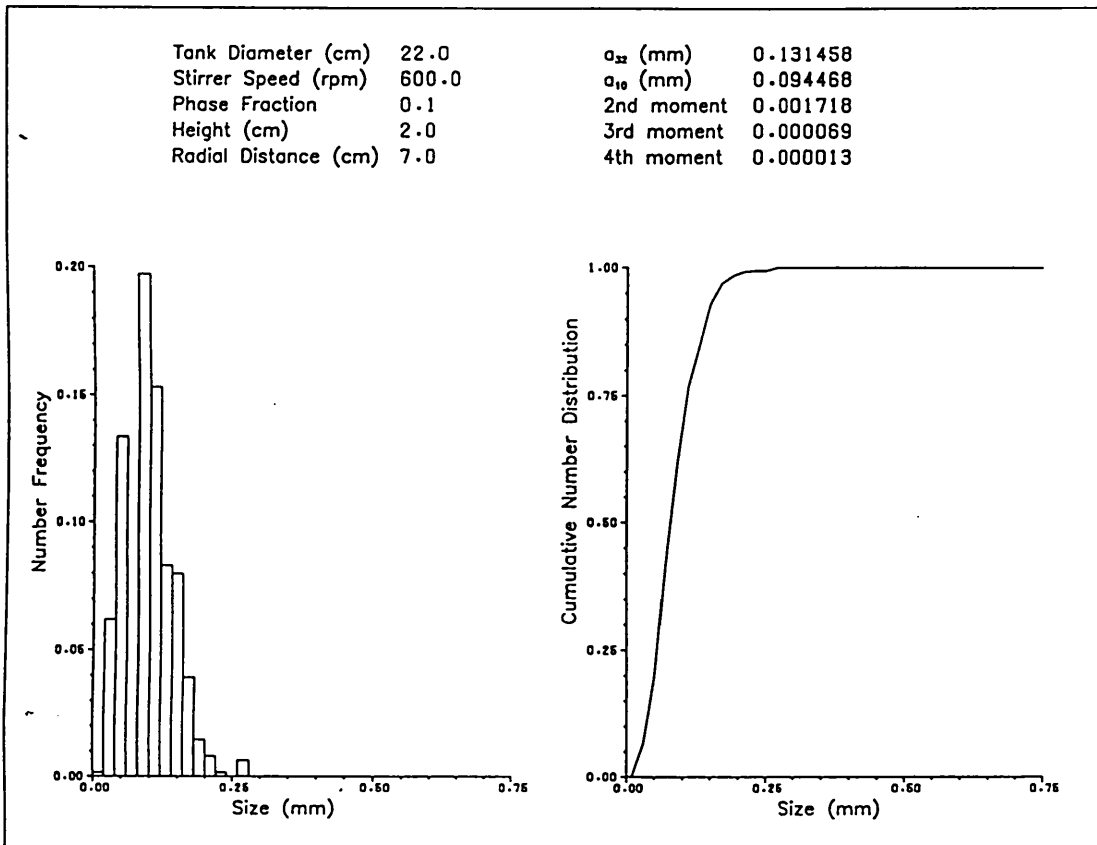
$\sigma_{32}$  (mm) 0.222795  
 $\sigma_{10}$  (mm) 0.164181  
 2nd moment 0.004673  
 3rd moment 0.000319  
 4th moment 0.000108



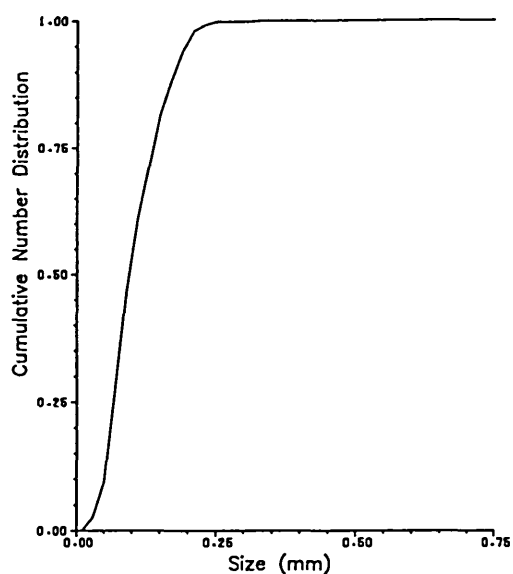
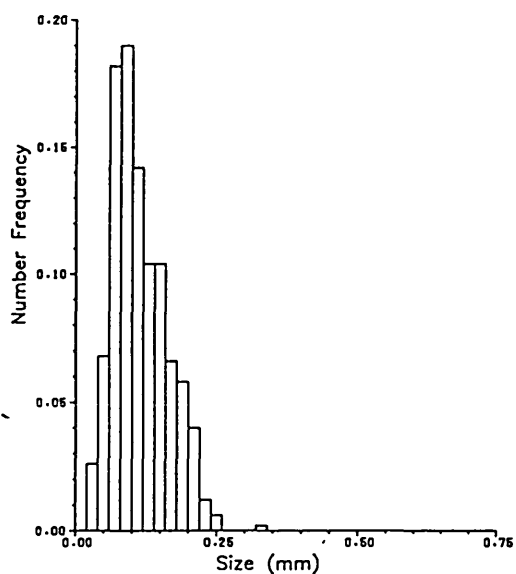
# APPENDIX IV-1b

## Drop Sizing Results

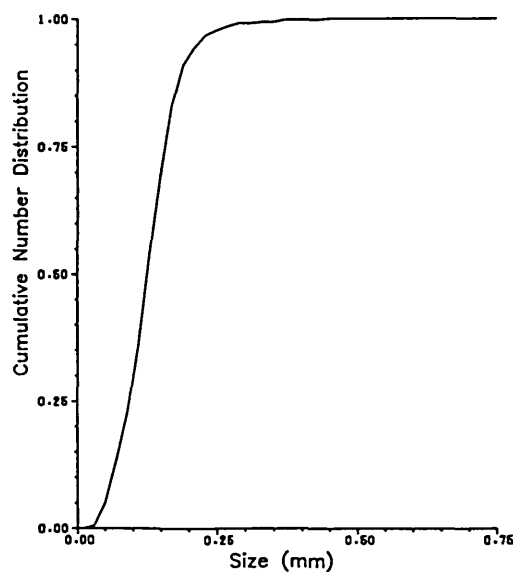
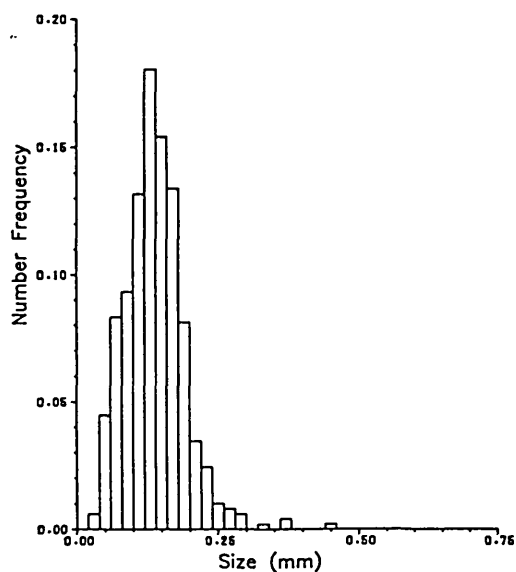
Tank Diameter = .22 m ;  $\phi_o = .1$  ; Stirring Speed = 600 rpm



Tank Diameter (cm)	22.0	$\sigma_{32}$ (mm)	0.153518
Stirrer Speed (rpm)	600.0	$\sigma_{10}$ (mm)	0.114305
Phase Fraction	0.1	2nd moment	0.002293
Height (cm)	2.0	3rd moment	0.000078
Radial Distance (cm)	9.0	4th moment	0.000018

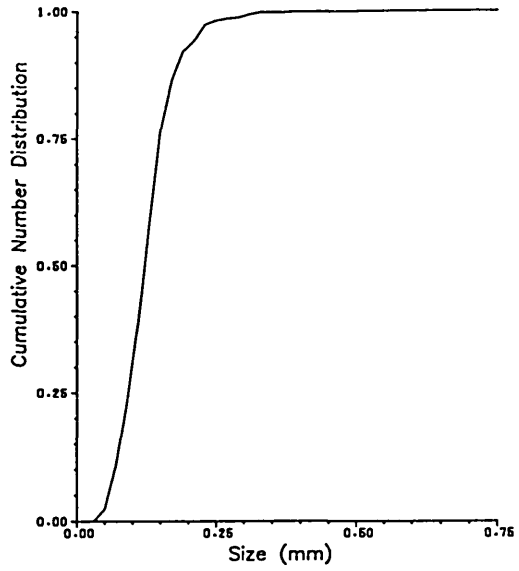
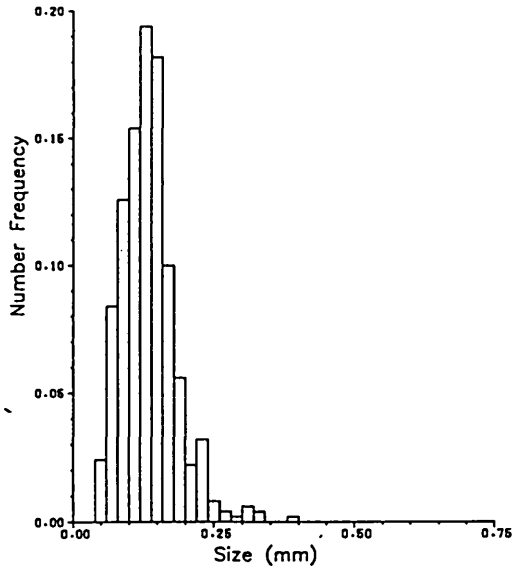


Tank Diameter (cm)	22.0	$\sigma_{32}$ (mm)	0.180114
Stirrer Speed (rpm)	600.0	$\sigma_{10}$ (mm)	0.138785
Phase Fraction	0.1	2nd moment	0.002751
Height (cm)	6.0	3rd moment	0.000146
Radial Distance (cm)	5.0	4th moment	0.000047



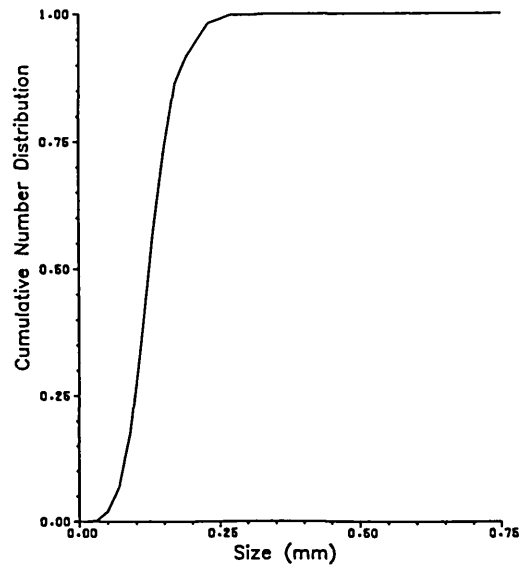
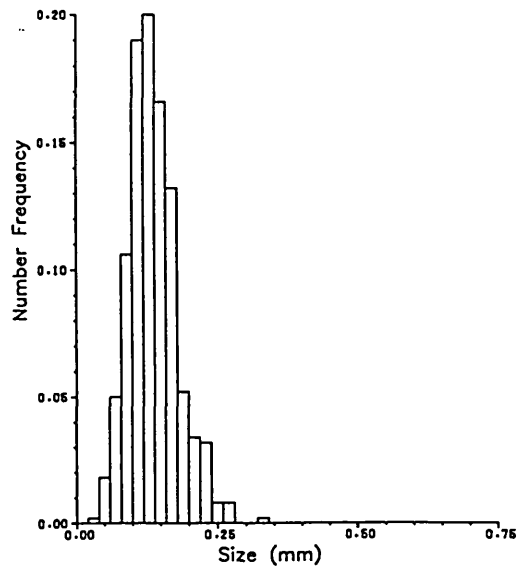
Tank Diameter (cm) 22.0  
 Stirrer Speed (rpm) 600.0  
 Phase Fraction 0.1  
 Height (cm) 6.0  
 Radial Distance (cm) 7.0

$\sigma_{32}$  (mm) 0.172023  
 $\sigma_{10}$  (mm) 0.135180  
 2nd moment 0.002351  
 3rd moment 0.000124  
 4th moment 0.000032



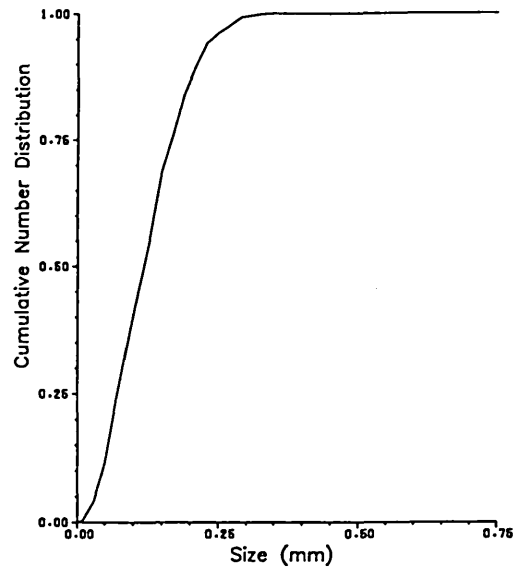
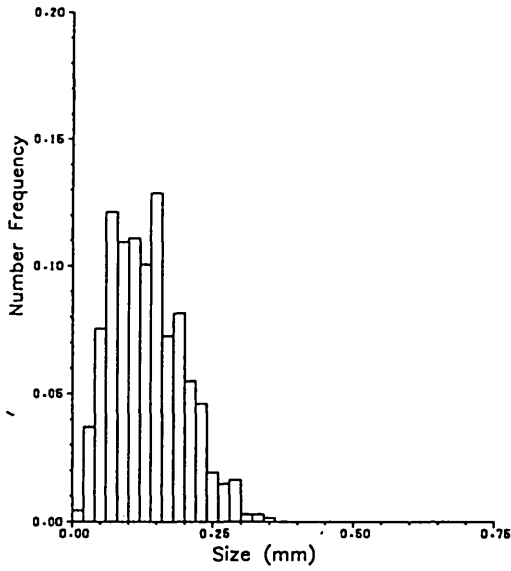
Tank Diameter (cm) 22.0  
 Stirrer Speed (rpm) 600.0  
 Phase Fraction 0.1  
 Height (cm) 6.0  
 Radial Distance (cm) 9.0

$\sigma_{32}$  (mm) 0.164302  
 $\sigma_{10}$  (mm) 0.137766  
 2nd moment 0.001831  
 3rd moment 0.000048  
 4th moment 0.000012



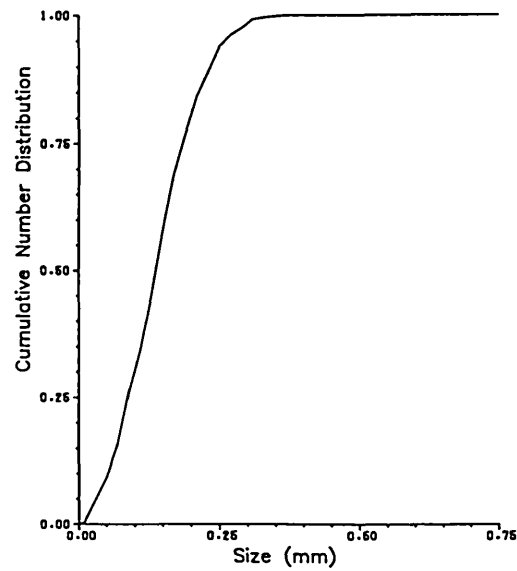
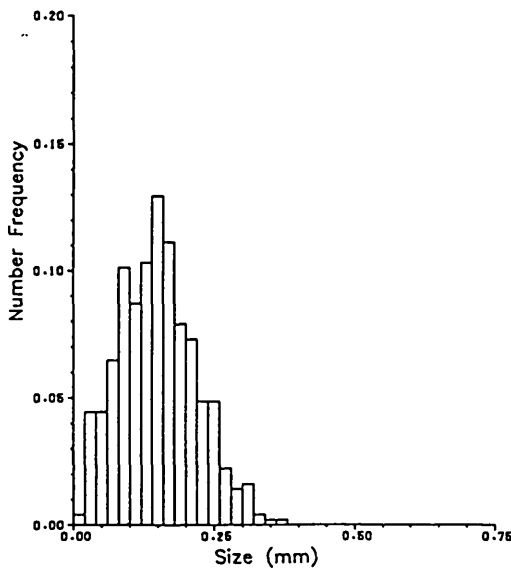
Tank Diameter (cm) 22.0  
 Stirrer Speed (rpm) 600.0  
 Phase Fraction 0.1  
 Height (cm) 10.0  
 Radial Distance (cm) 5.0

$\sigma_{32}$  (mm) 0.189490  
 $\sigma_{10}$  (mm) 0.133609  
 2nd moment 0.004065  
 3rd moment 0.000139  
 4th moment 0.000047



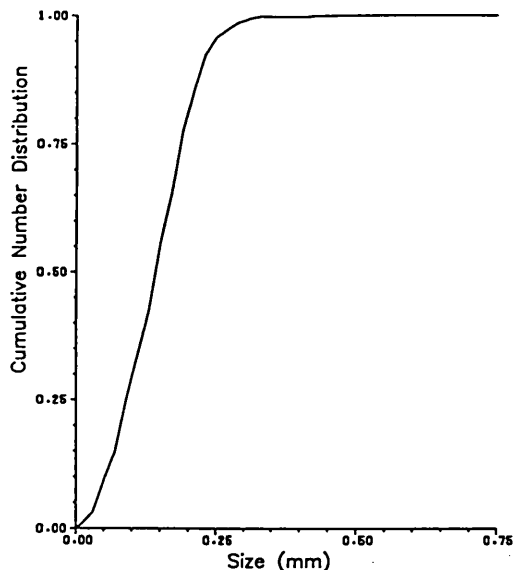
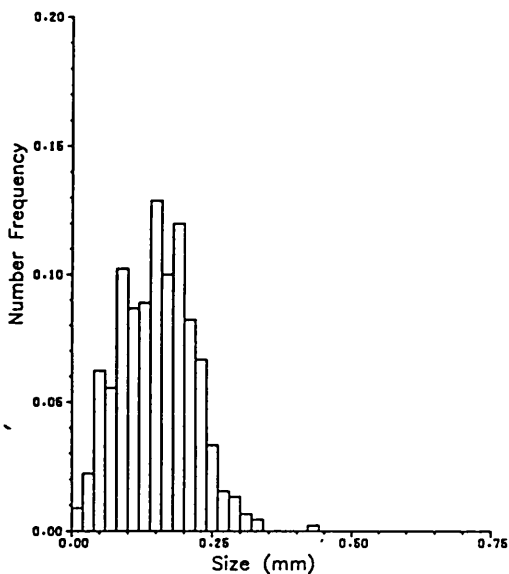
Tank Diameter (cm) 22.0  
 Stirrer Speed (rpm) 600.0  
 Phase Fraction 0.1  
 Height (cm) 10.0  
 Radial Distance (cm) 7.0

$\sigma_{32}$  (mm) 0.204584  
 $\sigma_{10}$  (mm) 0.150059  
 2nd moment 0.004613  
 3rd moment 0.000095  
 4th moment 0.000058



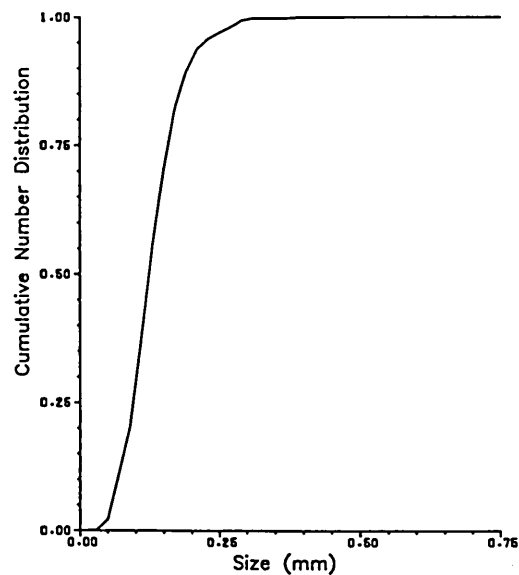
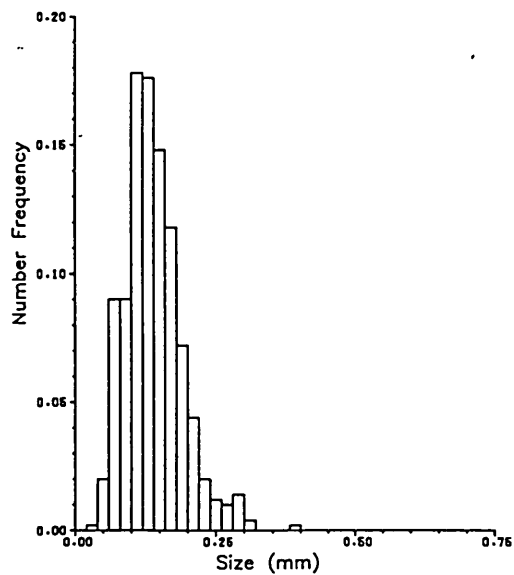
Tank Diameter (cm) 22.0  
 Stirrer Speed (rpm) 600.0  
 Phase Fraction 0.1  
 Height (cm) 10.0  
 Radial Distance (cm) 9.0

$\alpha_{32}$  (mm) 0.200609  
 $\alpha_{10}$  (mm) 0.150266  
 2nd moment 0.004236  
 3rd moment 0.000077  
 4th moment 0.000056



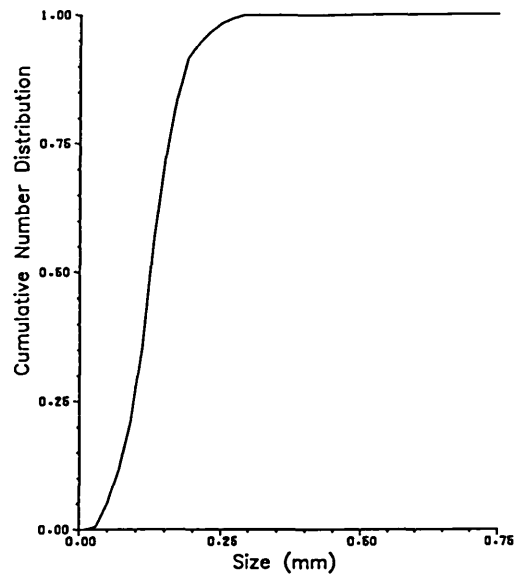
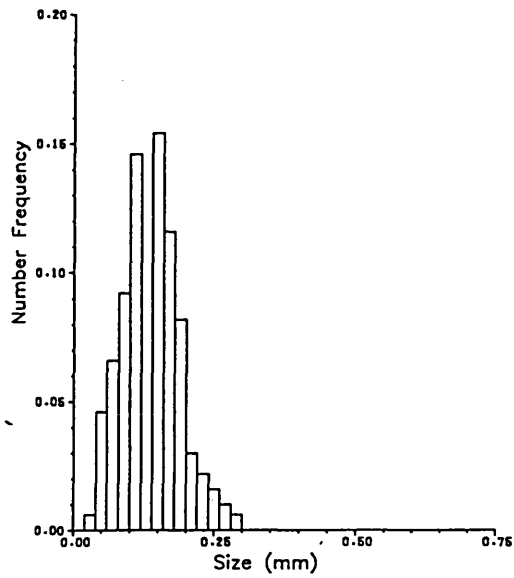
Tank Diameter (cm) 22.0  
 Stirrer Speed (rpm) 600.0  
 Phase Fraction 0.1  
 Height (cm) 14.0  
 Radial Distance (cm) 5.0

$\alpha_{32}$  (mm) 0.177384  
 $\alpha_{10}$  (mm) 0.139528  
 2nd moment 0.002565  
 3rd moment 0.000118  
 4th moment 0.000029



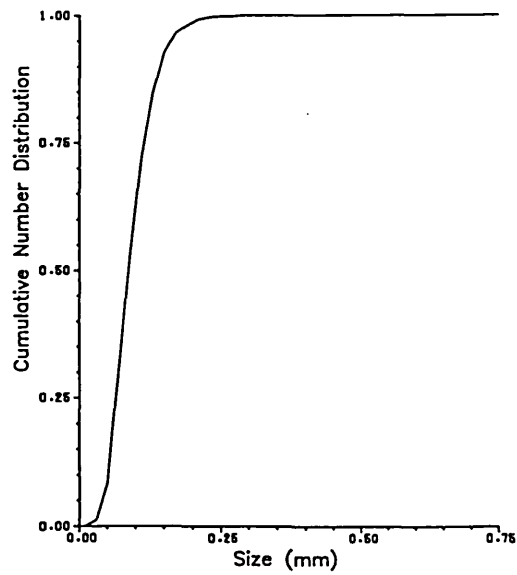
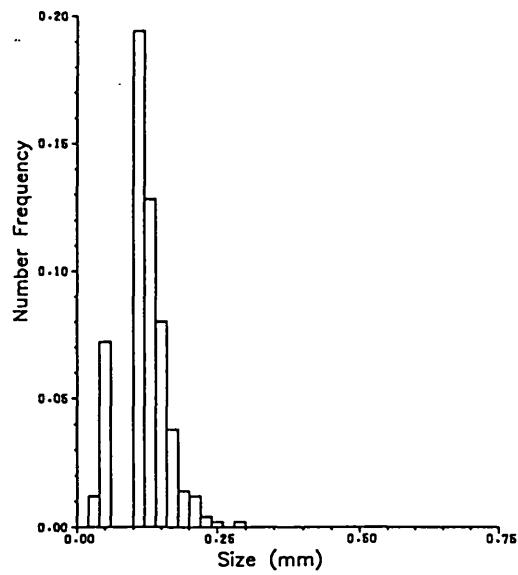
Tank Diameter (cm) 22.0  
 Stirrer Speed (rpm) 600.0  
 Phase Fraction 0.1  
 Height (cm) 14.0  
 Radial Distance (cm) 7.0

$\alpha_{32}$  (mm) 0.167900  
 $\alpha_{10}$  (mm) 0.136315  
 2nd moment 0.002237  
 3rd moment 0.000048  
 4th moment 0.000017



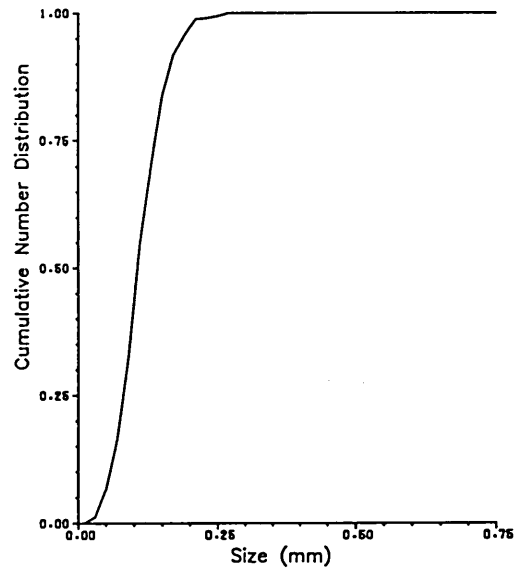
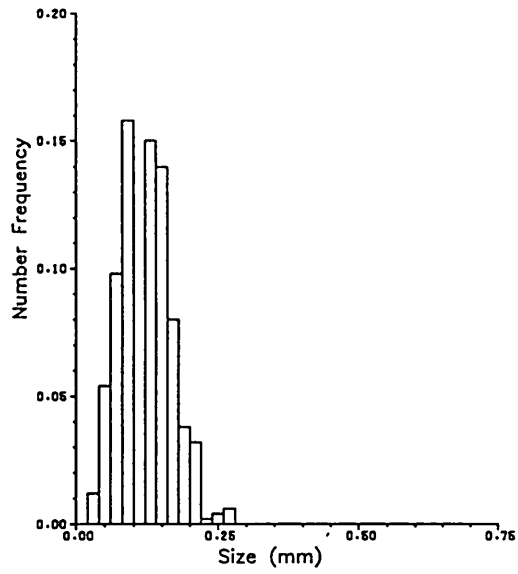
Tank Diameter (cm) 22.0  
 Stirrer Speed (rpm) 600.0  
 Phase Fraction 600.0  
 Height (cm) 18.0  
 Radial Distance (cm) 7.0

$\alpha_{32}$  (mm) 0.130622  
 $\alpha_{10}$  (mm) 0.103185  
 2nd moment 0.001363  
 3rd moment 0.000048  
 4th moment 0.000009



Tank Diameter (cm) 22.0  
Stirrer Speed (rpm) 600.0  
Phase Fraction 0.1  
Height (cm) 18.0  
Radial Distance (cm) 9.0

$a_{32}$  (mm) 0.148752  
 $a_{10}$  (mm) 0.119830  
2nd moment 0.001774  
3rd moment 0.000042  
4th moment 0.000011



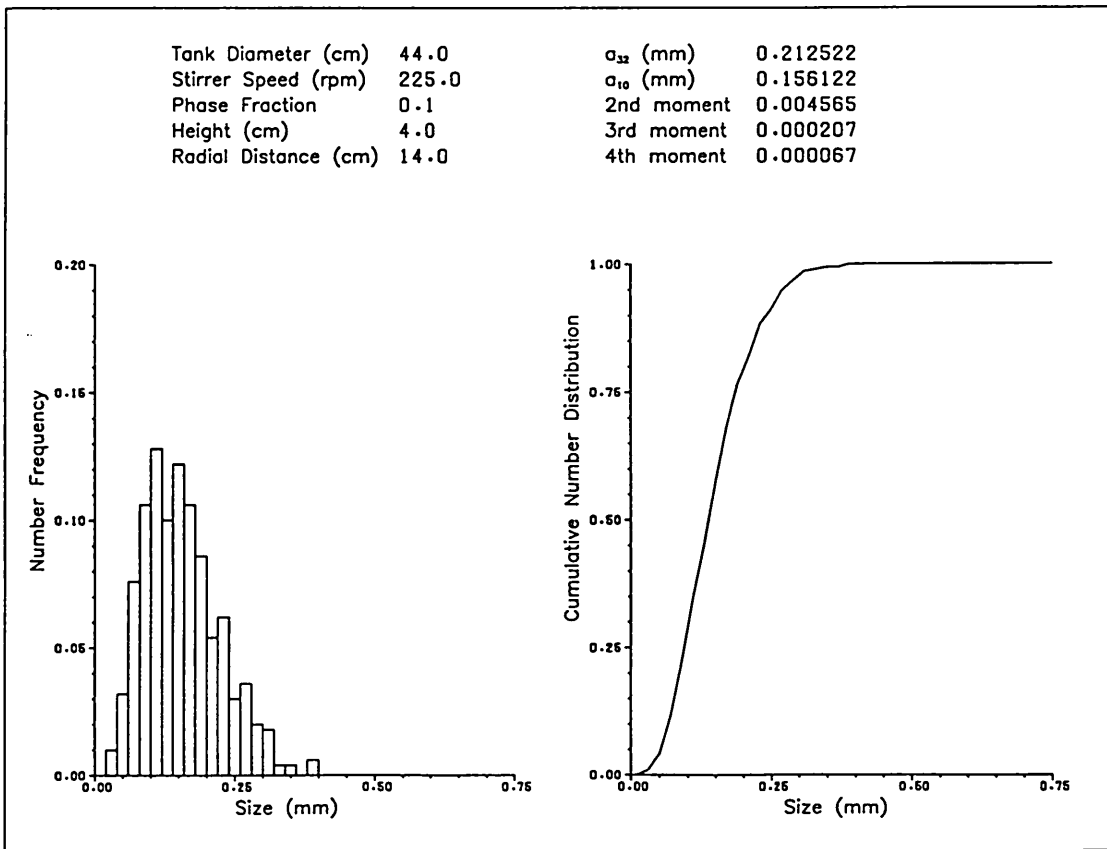
**APPENDIX IV-2**  
**Drop Sizing Results**  
 Tank Diameter = .22 m ;  $\phi_o = .3$

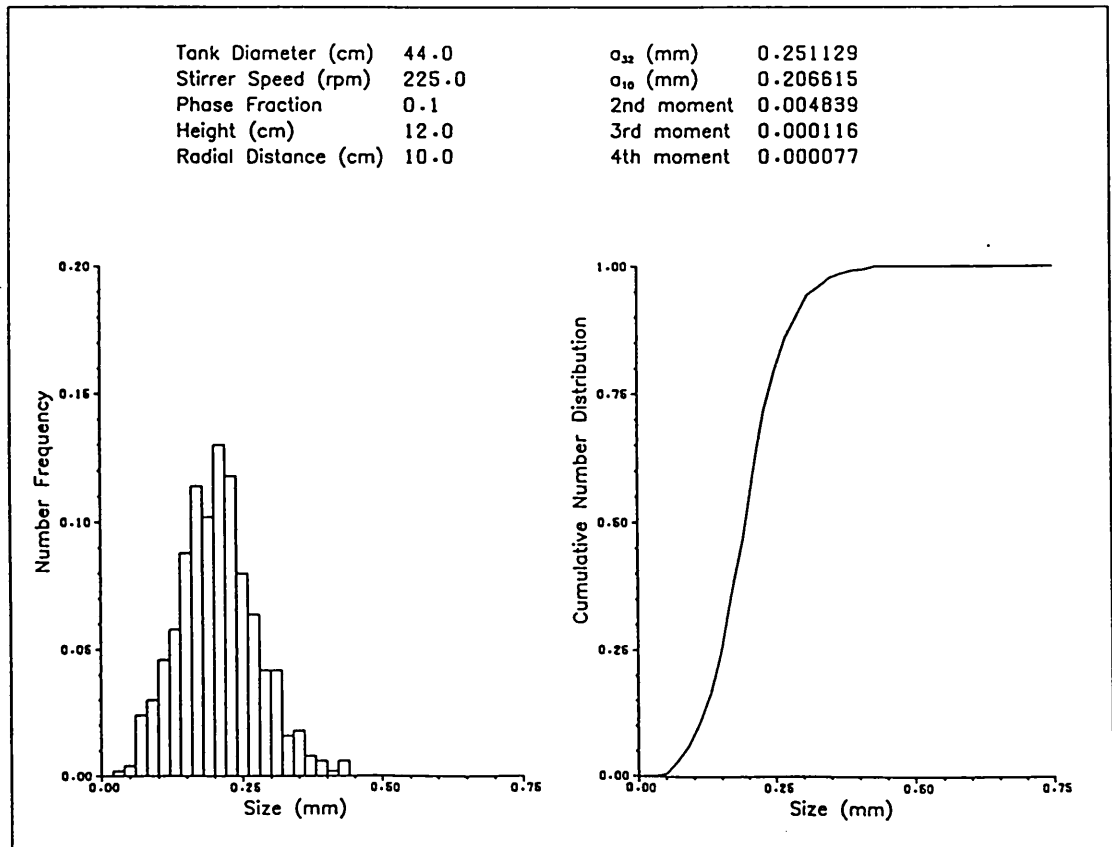
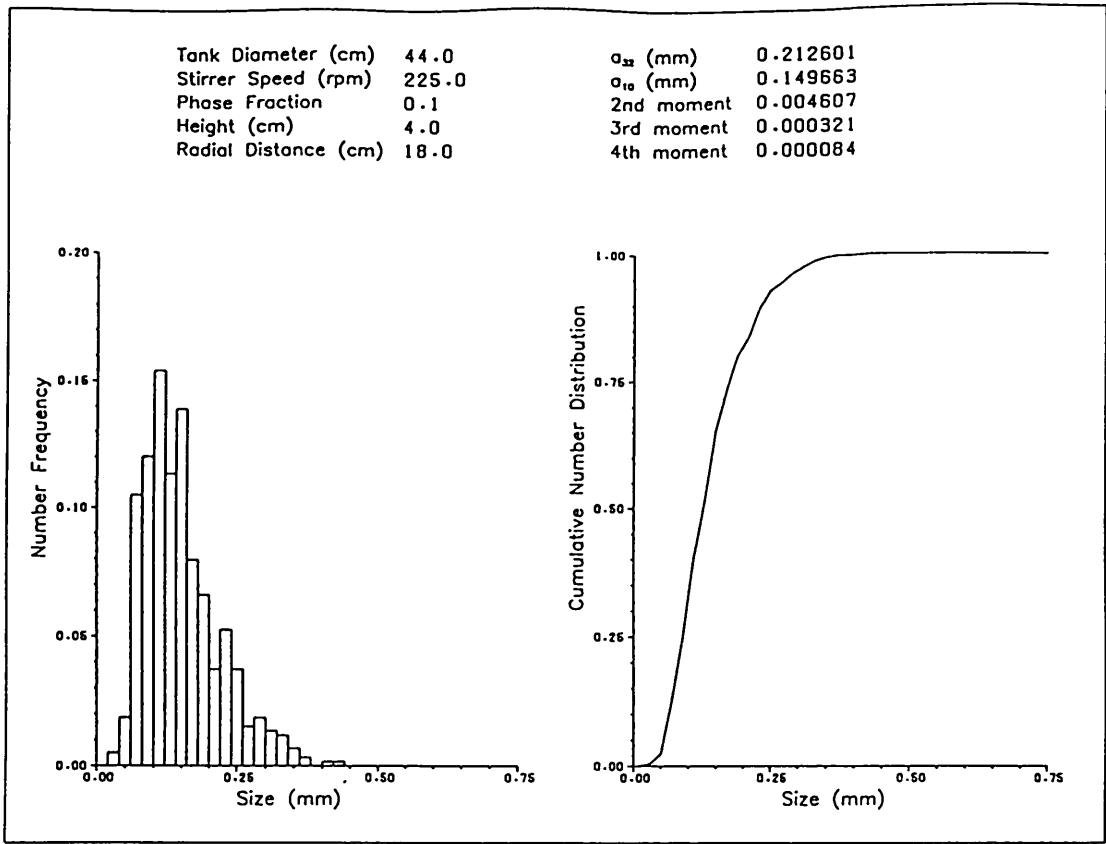
Height (cm)	Radial Distance (cm)	Stirring Speed	Sauter Mean Diameter (mm)
2	7	450	.352
2	9	450	.337
6	5	450	.4165
6	7	450	.4093
6	9	450	.3277
10	5	450	.486
10	7	450	.556
10	9	450	.573
14	5	450	.3829
14	7	450	.3582
14	9	450	.340
18	7	450	.2837
18	9	450	.312
2	7	600	.2397
2	9	600	.2932
6	5	600	.366
6	7	600	.3422
6	9	600	.343
10	5	600	.35
10	7	600	.3825
10	9	600	.4217
14	5	600	.349
14	7	600	.329
14	9	600	.3822
18	7	600	.249
18	9	600	.3048

# APPENDIX IV-3a

## Drop Sizing Results

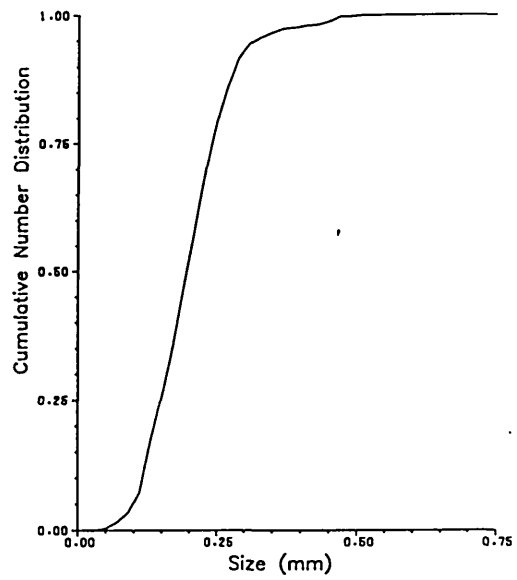
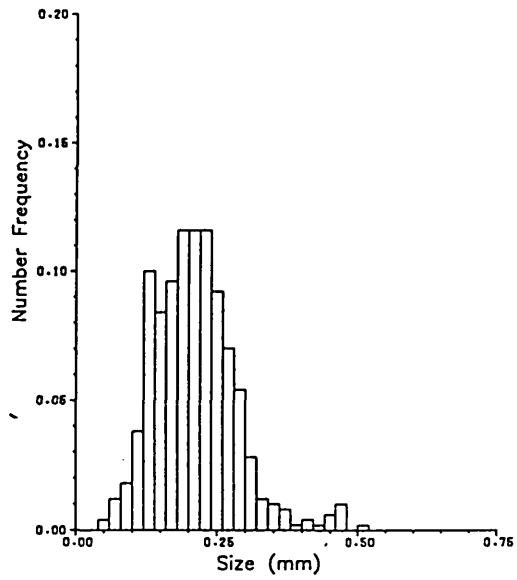
Tank Diameter = .44 m ;  $\phi_o = .1$  ; Stirring Speed = 225 rpm





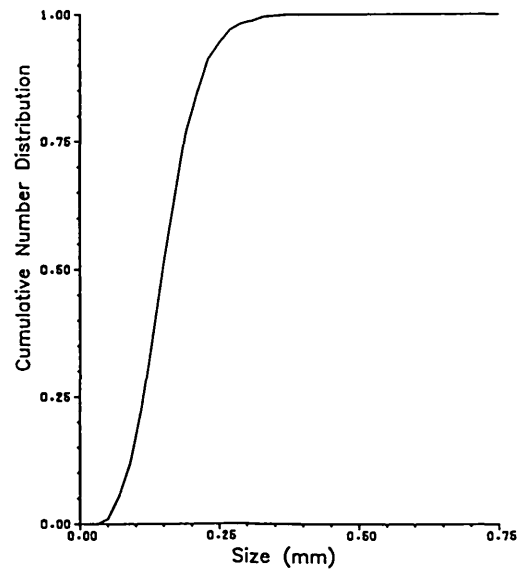
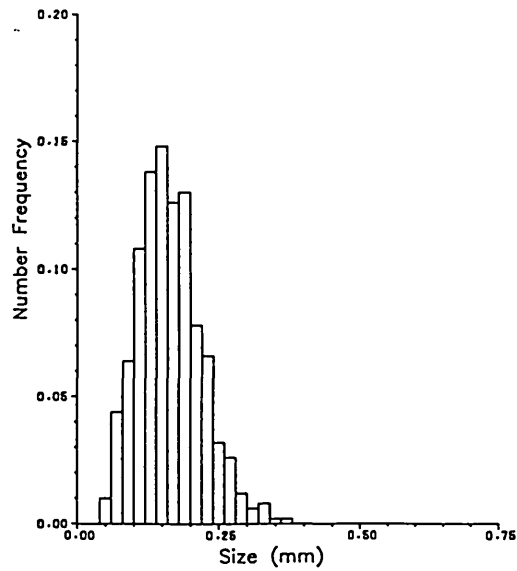
Tank Diameter (cm) 44.0  
 Stirrer Speed (rpm) 225.0  
 Phase Fraction 0.1  
 Height (cm) 12.0  
 Radial Distance (cm) 14.0

$\alpha_{32}$  (mm) 0.261904  
 $\alpha_{10}$  (mm) 0.210110  
 2nd moment 0.005282  
 3rd moment 0.000340  
 4th moment 0.000133



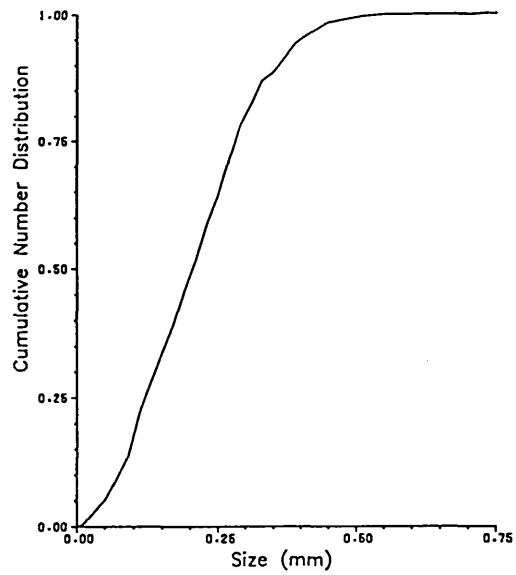
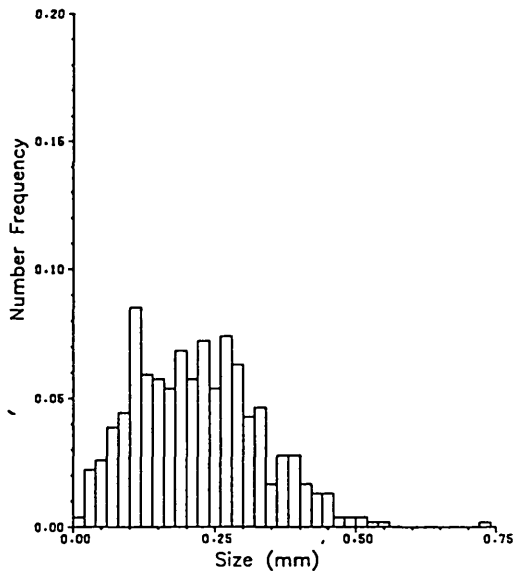
Tank Diameter (cm) 44.0  
 Stirrer Speed (rpm) 225.0  
 Phase Fraction 0.1  
 Height (cm) 12.0  
 Radial Distance (cm) 18.0

$\alpha_{32}$  (mm) 0.200856  
 $\alpha_{10}$  (mm) 0.163743  
 2nd moment 0.003104  
 3rd moment 0.000094  
 4th moment 0.000032



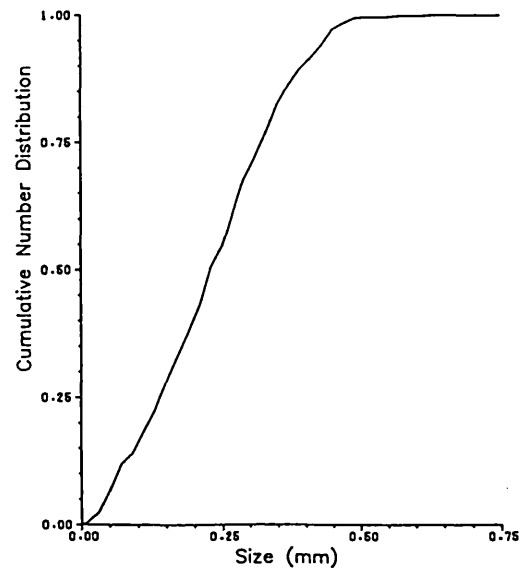
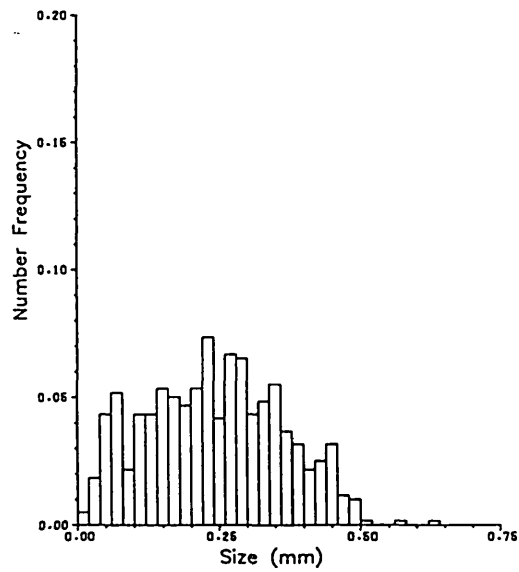
Tank Diameter (cm) 44.0  
 Stirrer Speed (rpm) 225.0  
 Phase Fraction 0.1  
 Height (cm) 20.0  
 Radial Distance (cm) 10.0

$\sigma_{32}$  (mm) 0.317900  
 $\sigma_{10}$  (mm) 0.219641  
 2nd moment 0.011963  
 3rd moment 0.000661  
 4th moment 0.000460



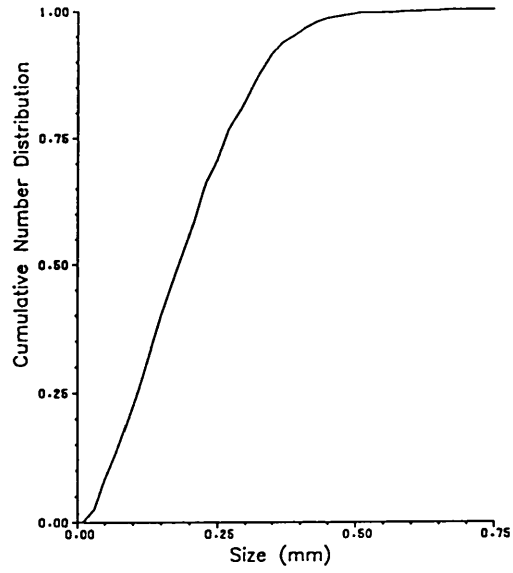
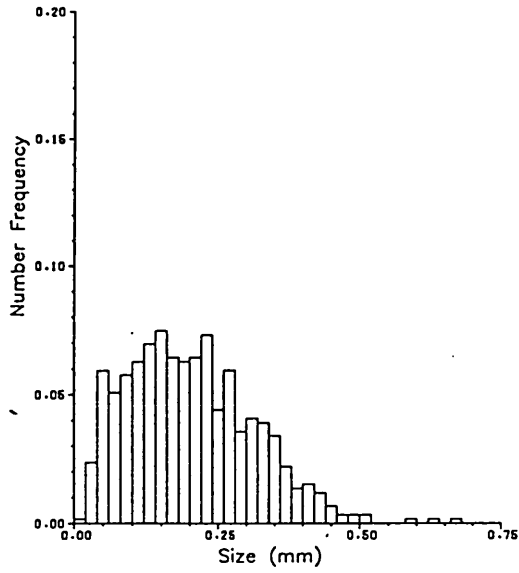
Tank Diameter (cm) 44.0  
 Stirrer Speed (rpm) 225.0  
 Phase Fraction 0.1  
 Height (cm) 20.0  
 Radial Distance (cm) 14.0

$\sigma_{32}$  (mm) 0.346717  
 $\sigma_{10}$  (mm) 0.242969  
 2nd moment 0.014778  
 3rd moment 0.000476  
 4th moment 0.000623



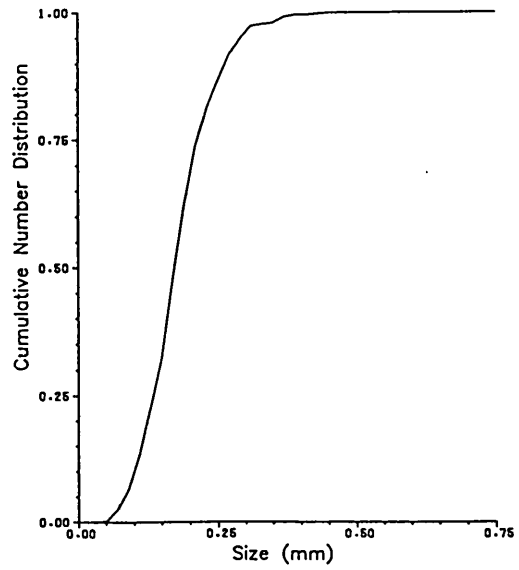
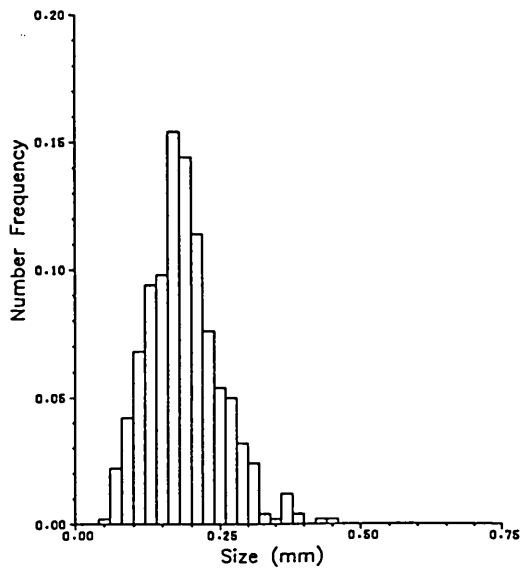
Tank Diameter (cm) 44.0  
 Stirrer Speed (rpm) 225.0  
 Phase Fraction 0.1  
 Height (cm) 20.0  
 Radial Distance (cm) 18.0

$a_{32}$  (mm) 0.310773  
 $a_{10}$  (mm) 0.202913  
 2nd moment 0.012059  
 3rd moment 0.000848  
 4th moment 0.000485



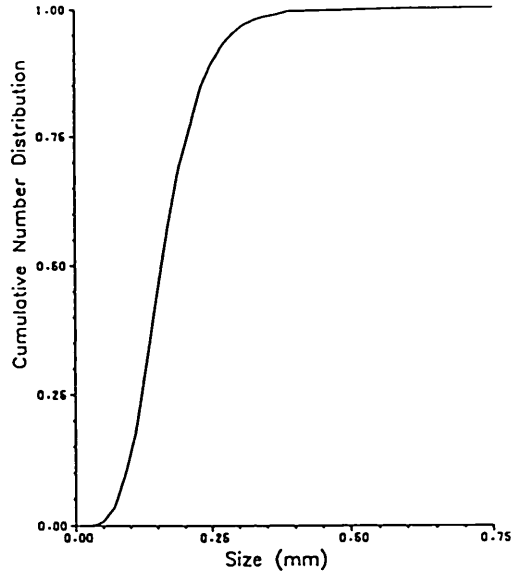
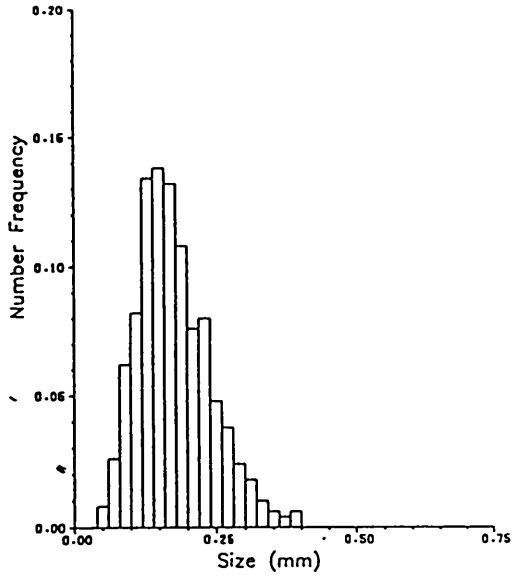
Tank Diameter (cm) 44.0  
 Stirrer Speed (rpm) 225.0  
 Phase Fraction 0.1  
 Height (cm) 28.0  
 Radial Distance (cm) 10.0

$a_{32}$  (mm) 0.230769  
 $a_{10}$  (mm) 0.187943  
 2nd moment 0.004039  
 3rd moment 0.000168  
 4th moment 0.000062



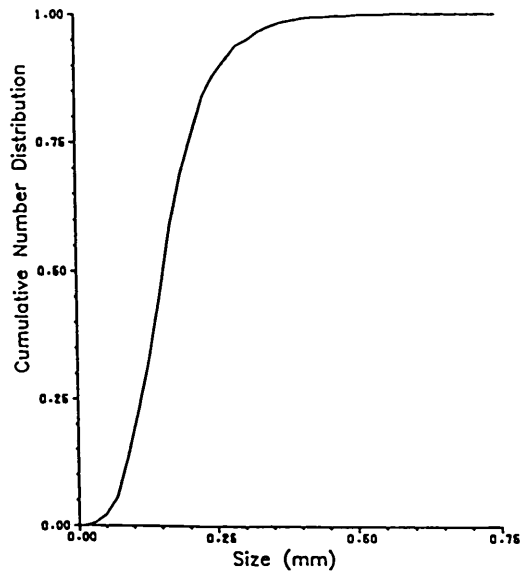
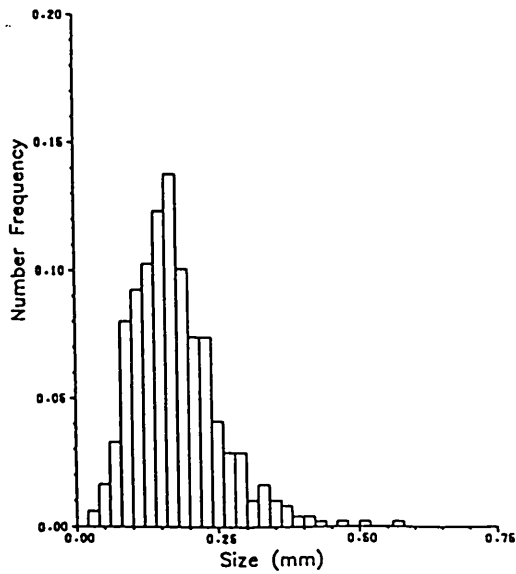
Tank Diameter (cm) 44.0  
 Stirrer Speed (rpm) 225.0  
 Phase Fraction 0.1  
 Height (cm) 28.0  
 Radial Distance (cm) 14.0

$\sigma_{32}$  (mm) 0.221865  
 $\sigma_{10}$  (mm) 0.176229  
 2nd moment 0.004033  
 3rd moment 0.000180  
 4th moment 0.000056



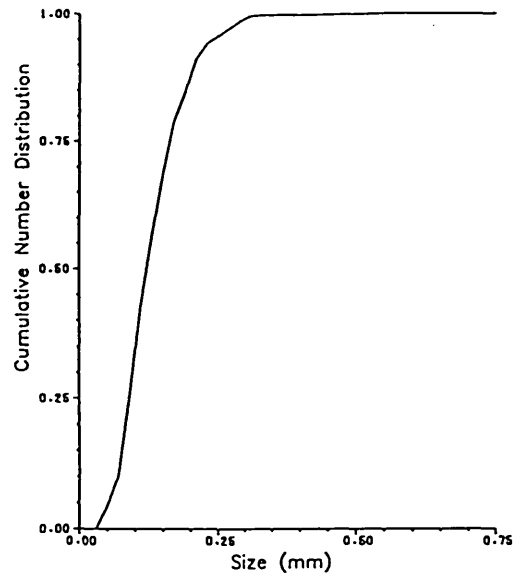
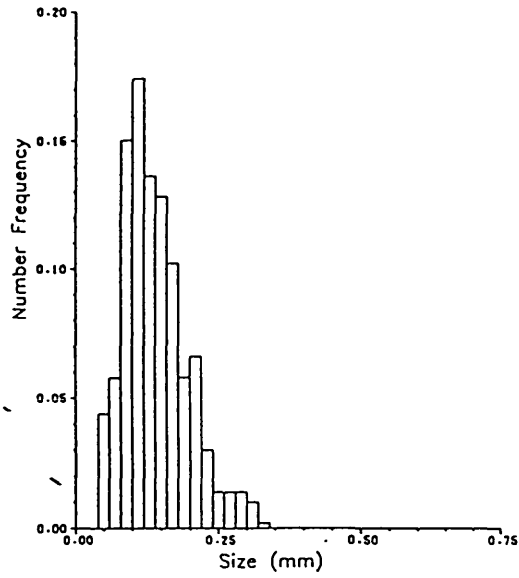
Tank Diameter (cm) 44.0  
 Stirrer Speed (rpm) 225.0  
 Phase Fraction 0.1  
 Height (cm) 28.0  
 Radial Distance (cm) 18.0

$\sigma_{32}$  (mm) 0.190917  
 $\sigma_{10}$  (mm) 0.145736  
 2nd moment 0.003154  
 3rd moment 0.000183  
 4th moment 0.000050



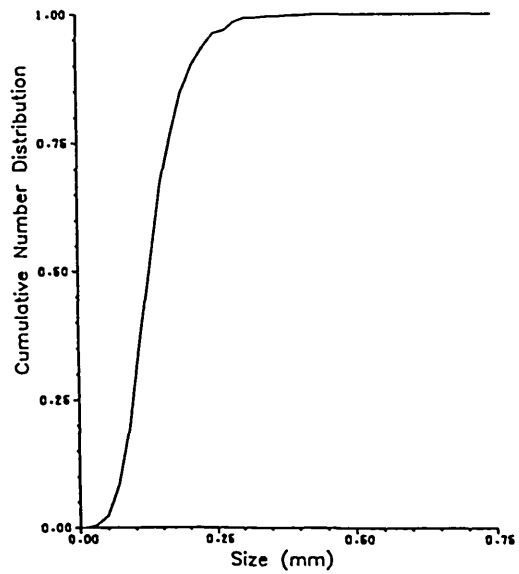
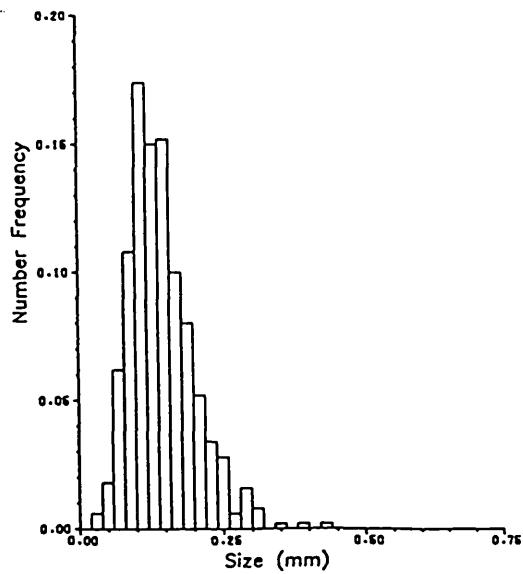
Tank Diameter (cm) 44.0  
 Stirrer Speed (rpm) 225.0  
 Phase Fraction 0.1  
 Height (cm) 36.0  
 Radial Distance (cm) 14.0

$\sigma_{32}$  (mm) 0.184000  
 $\sigma_{10}$  (mm) 0.140037  
 2nd moment 0.003076  
 3rd moment 0.000136  
 4th moment 0.000033



Tank Diameter (cm) 44.0  
 Stirrer Speed (rpm) 225.0  
 Phase Fraction 0.1  
 Height (cm) 36.0  
 Radial Distance (cm) 18.0

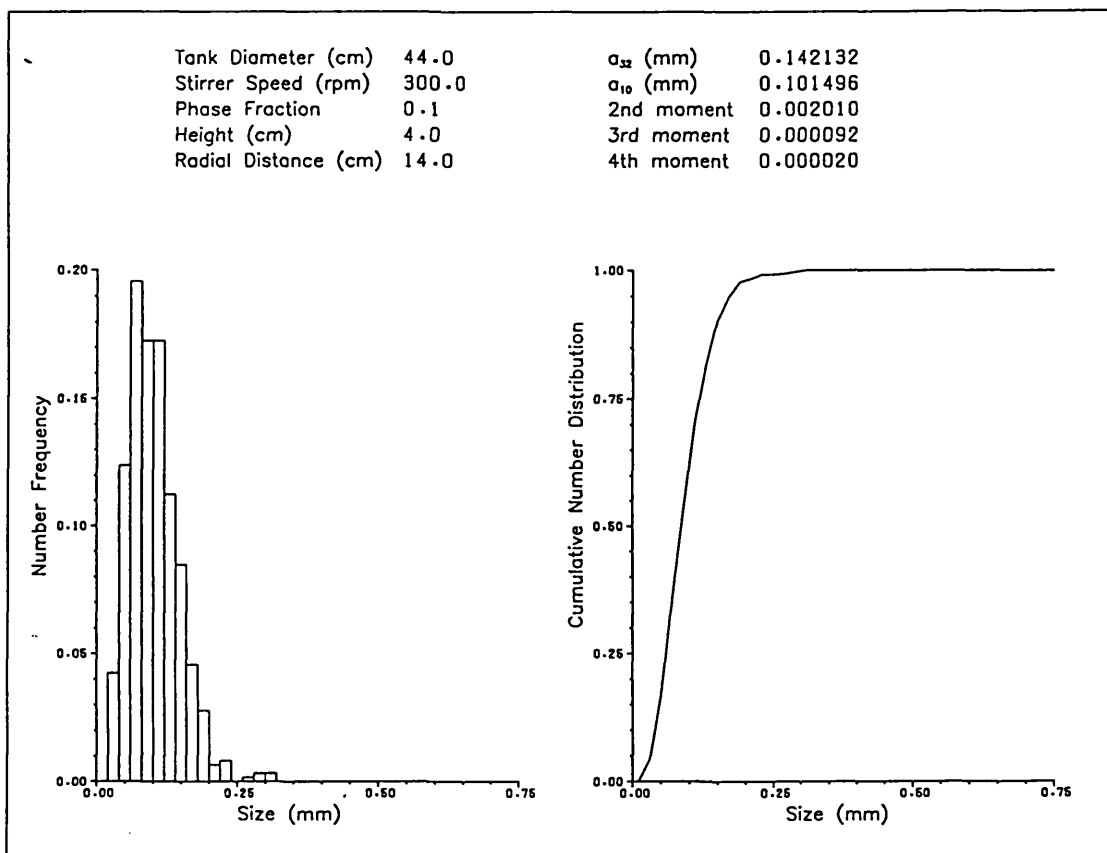
$\sigma_{32}$  (mm) 0.244322  
 $\sigma_{10}$  (mm) 0.176847  
 2nd moment 0.005707  
 3rd moment 0.000477  
 4th moment 0.000175



# APPENDIX IV-3b

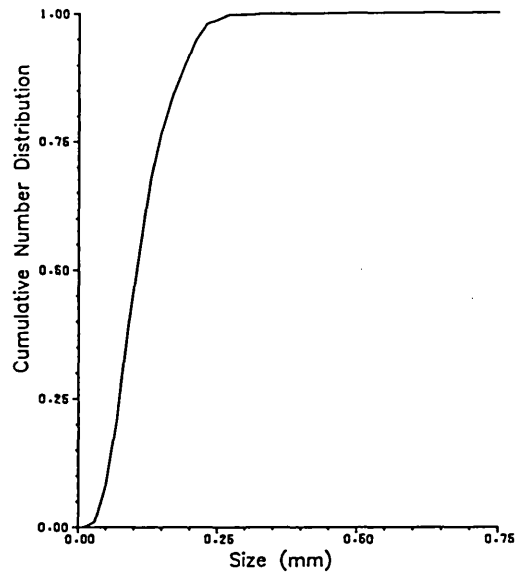
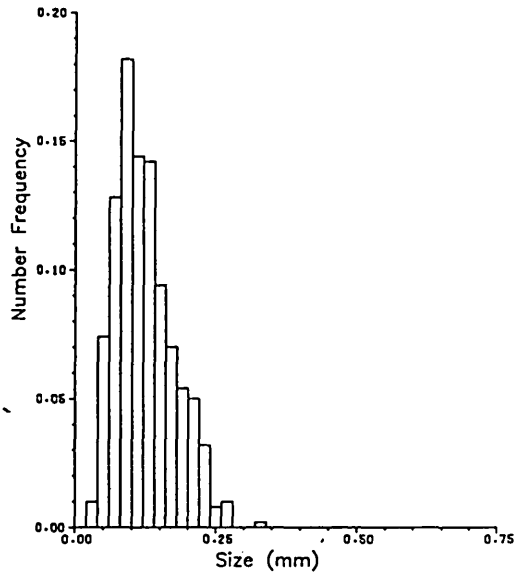
## Drop Sizing Results

Tank Diameter = .44 m ;  $\phi_o = .1$  ; Stirring Speed = 300 rpm



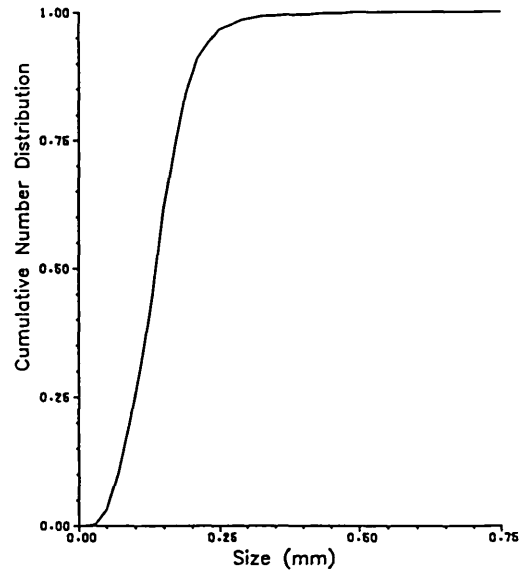
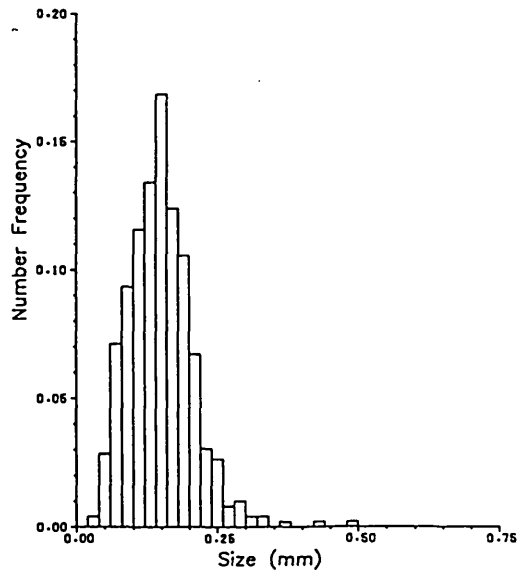
Tank Diameter (cm) 44.0  
 Stirrer Speed (rpm) 300.0  
 Phase Fraction 0.1  
 Height (cm) 4.0  
 Radial Distance (cm) 18.0

$\alpha_{32}$  (mm) 0.164850  
 $\alpha_{10}$  (mm) 0.122747  
 2nd moment 0.002649  
 3rd moment 0.000096  
 4th moment 0.000022



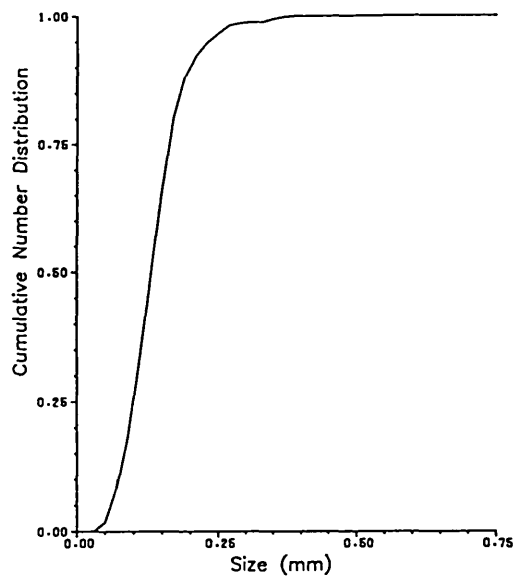
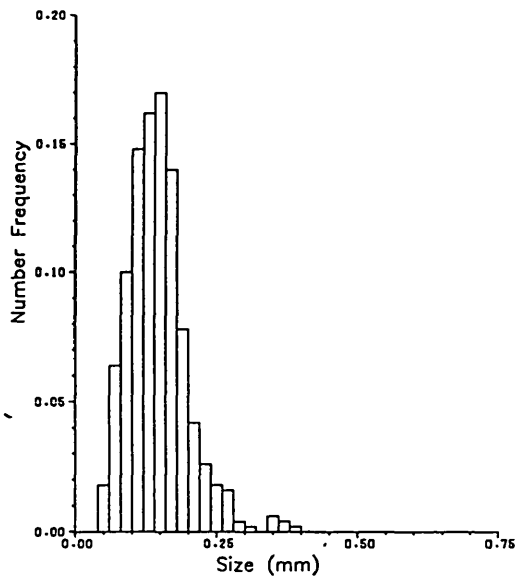
Tank Diameter (cm) 44.0  
 Stirrer Speed (rpm) 300.0  
 Phase Fraction 0.1  
 Height (cm) 12.0  
 Radial Distance (cm) 10.0

$\alpha_{32}$  (mm) 0.195255  
 $\alpha_{10}$  (mm) 0.149411  
 2nd moment 0.003300  
 3rd moment 0.000189  
 4th moment 0.000066



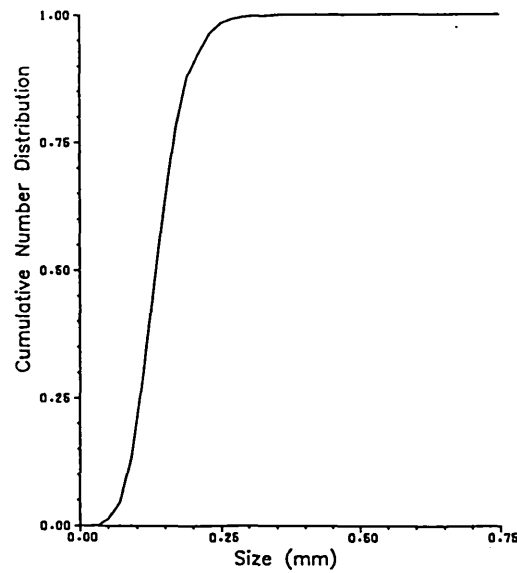
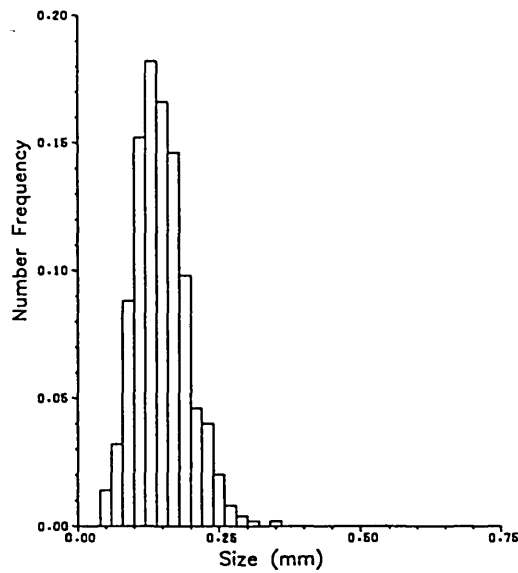
Tank Diameter (cm) 44.0  
 Stirrer Speed (rpm) 300.0  
 Phase Fraction 0.1  
 Height (cm) 12.0  
 Radial Distance (cm) 14.0

$\alpha_{32}$  (mm) 0.186363  
 $\alpha_{10}$  (mm) 0.145337  
 2nd moment 0.002797  
 3rd moment 0.000168  
 4th moment 0.000045



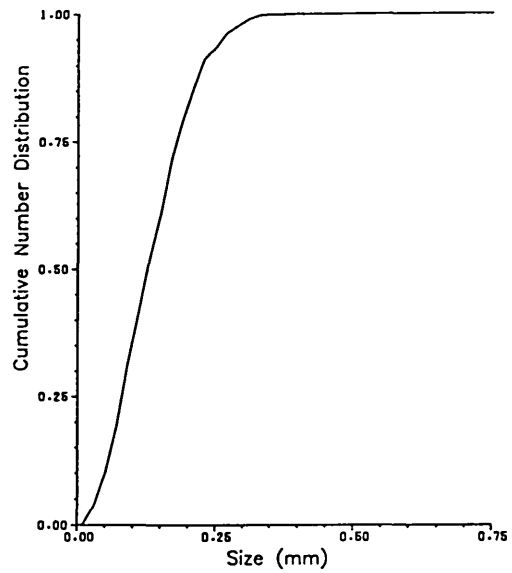
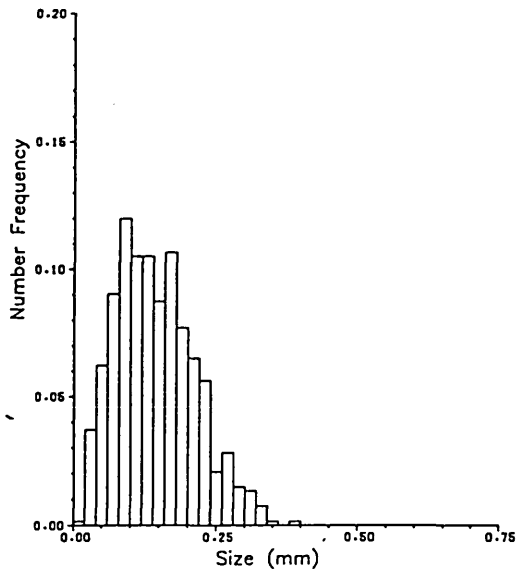
Tank Diameter (cm) 44.0  
 Stirrer Speed (rpm) 300.0  
 Phase Fraction 0.1  
 Height (cm) 12.0  
 Radial Distance (cm) 18.0

$\alpha_{32}$  (mm) 0.176187  
 $\alpha_{10}$  (mm) 0.147927  
 2nd moment 0.002101  
 3rd moment 0.000056  
 4th moment 0.000016



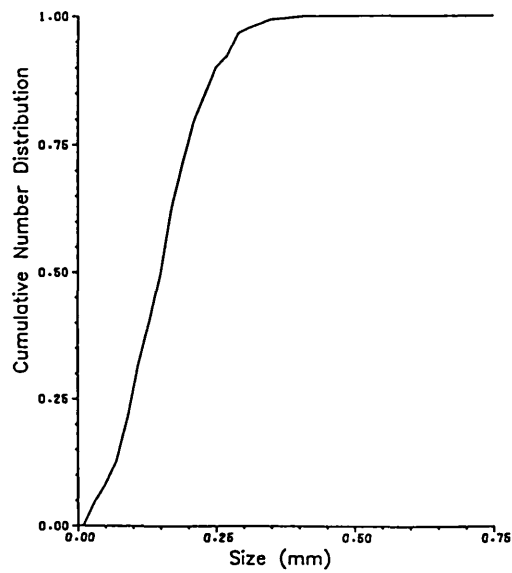
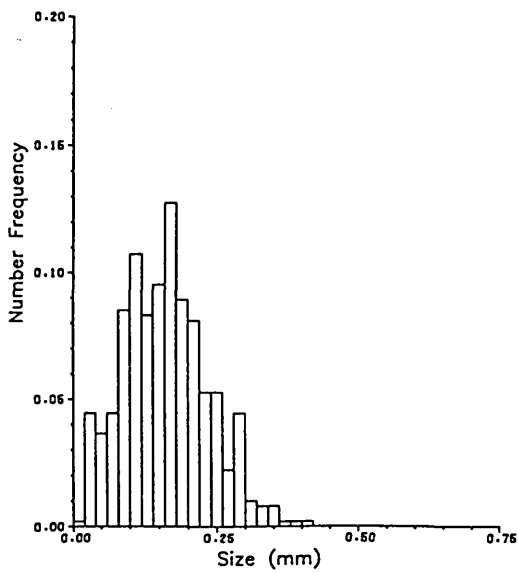
Tank Diameter (cm) 44.0  
 Stirrer Speed (rpm) 300.0  
 Phase Fraction 0.1  
 Height (cm) 20.0  
 Radial Distance (cm) 10.0

$\sigma_{32}$  (mm) 0.203131  
 $\sigma_{10}$  (mm) 0.143345  
 2nd moment 0.004665  
 3rd moment 0.000170  
 4th moment 0.000061



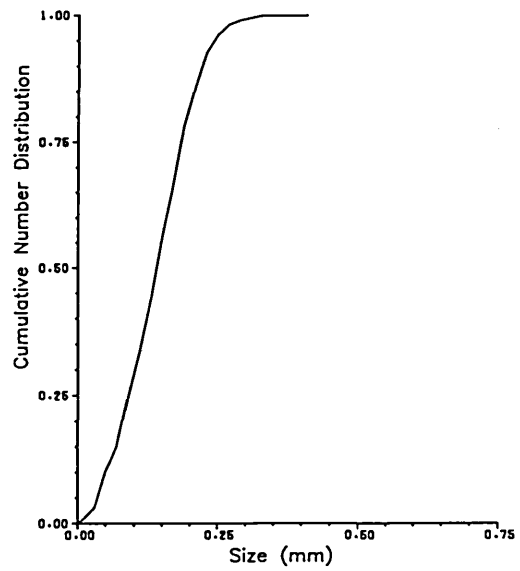
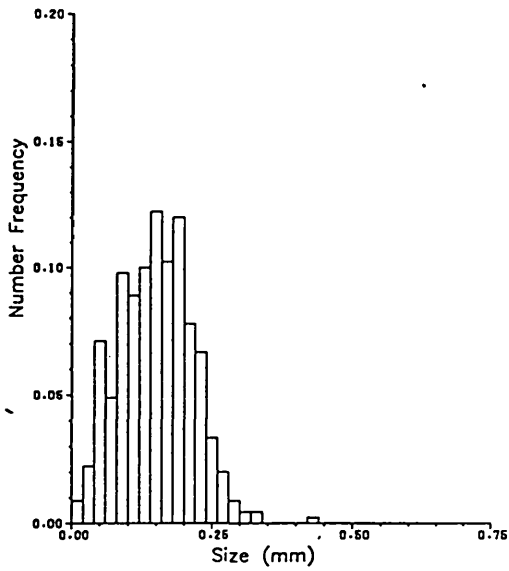
Tank Diameter (cm) 44.0  
 Stirrer Speed (rpm) 300.0  
 Phase Fraction 0.1  
 Height (cm) 20.0  
 Radial Distance (cm) 14.0

$\sigma_{32}$  (mm) 0.221371  
 $\sigma_{10}$  (mm) 0.161286  
 2nd moment 0.005420  
 3rd moment 0.000140  
 4th moment 0.000084



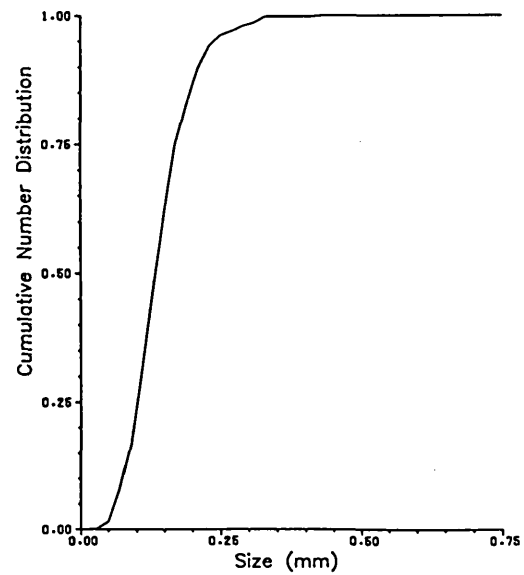
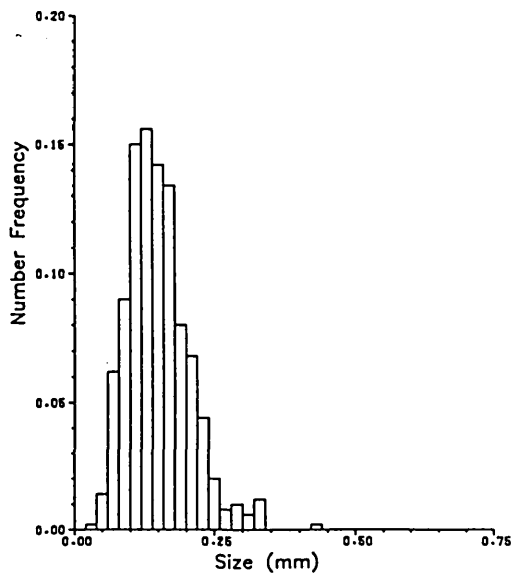
Tank Diameter (cm) 44.0  
 Stirrer Speed (rpm) 300.0  
 Phase Fraction 0.3  
 Height (cm) 20.0  
 Radial Distance (cm) 18.0

$d_{32}$  (mm) 0.199678  
 $d_{10}$  (mm) 0.149619  
 2nd moment 0.004201  
 3rd moment 0.000074  
 4th moment 0.000055



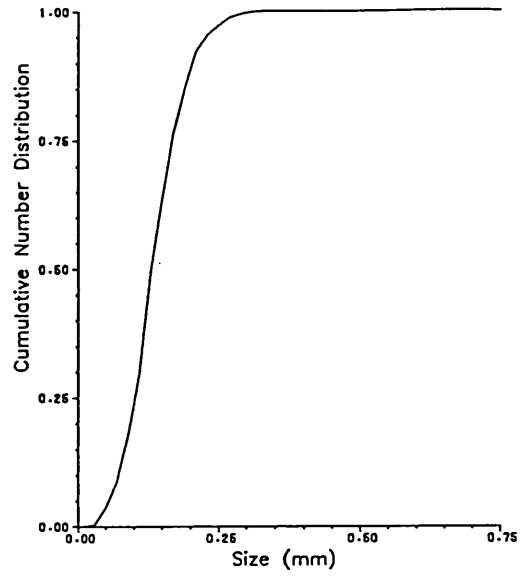
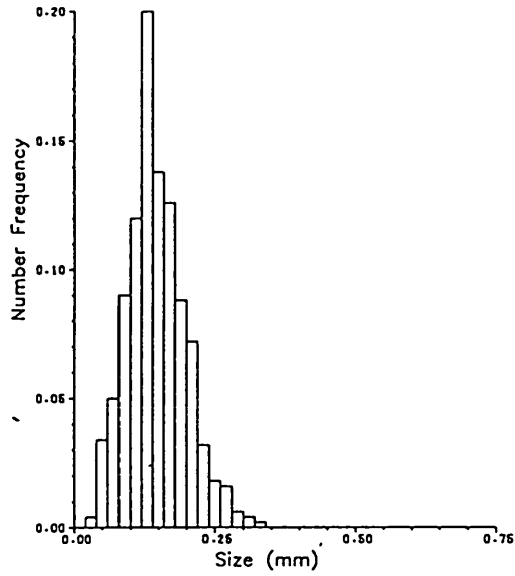
Tank Diameter (cm) 44.0  
 Stirrer Speed (rpm) 300.0  
 Phase Fraction 0.1  
 Height (cm) 28.0  
 Radial Distance (cm) 10.0

$d_{32}$  (mm) 0.192901  
 $d_{10}$  (mm) 0.150151  
 2nd moment 0.003089  
 3rd moment 0.000168  
 4th moment 0.000046



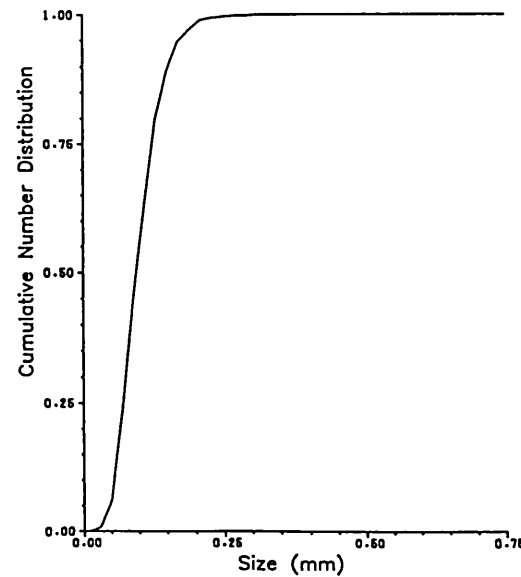
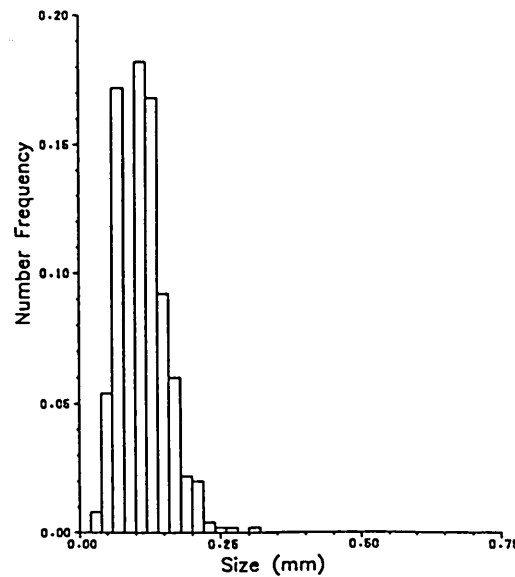
Tank Diameter (cm) 44.0  
 Stirrer Speed (rpm) 300.0  
 Phase Fraction 0.1  
 Height (cm) 28.0  
 Radial Distance (cm) 14.0

$a_{32}$  (mm) 0.180786  
 $a_{10}$  (mm) 0.146511  
 2nd moment 0.002617  
 3rd moment 0.000058  
 4th moment 0.000023



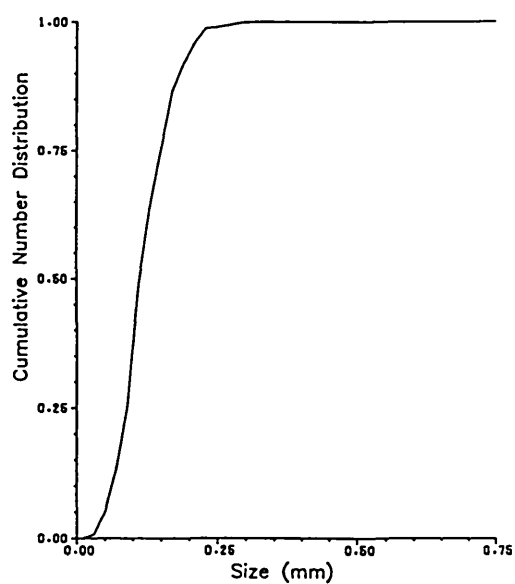
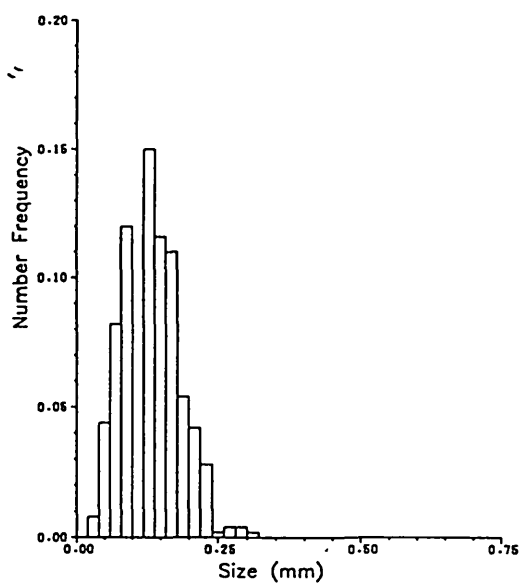
Tank Diameter (cm) 44.0  
 Stirrer Speed (rpm) 300.0  
 Phase Fraction 0.1  
 Height (cm) 36.0  
 Radial Distance (cm) 14.0

$a_{32}$  (mm) 0.139774  
 $a_{10}$  (mm) 0.110867  
 2nd moment 0.001565  
 3rd moment 0.000054  
 4th moment 0.000011



Tank Diameter (cm) 44.0  
Stirrer Speed (rpm) 300.0  
Phase Fraction 0.1  
Height (cm) 36.0  
Radial Distance (cm) 18.0

$\sigma_{32}$  (mm) 0.161027  
 $\sigma_{10}$  (mm) 0.128935  
2nd moment 0.002117  
3rd moment 0.000056  
4th moment 0.000015



# **APPENDIX V**

## **MONTE CARLO SIMULATION ALGORITHM**

**APPENDIX V-1 : Simulation algorithm nomenclature**

**APPENDIX V-2 : Simulation algorithm**

**APPENDIX V-1 : Simulation algorithm sample results**

**APPENDIX V-1**  
**SIMULATION PROGRAMME ALGORITHM**  
**NOMENCLATURE<sup>1</sup>**

AMD	Arithmetic mean diameter
D32	Sauter mean diameter
D32DIF	Difference in Sauter mean diameter for two consecutive cycles
DI	Impeller diameter
E	Power dissipation per unit mass
FB	Sample overall breakage frequency
FCC	Sample overall coalescence frequency
K1..K12	Breakage and coalescence functions constants
M	Number of drops
MUCON	Continuous phase viscosity
MUD	Dispersed phase viscosity
NC	Number of categories for coalescence frequency approximation
NOB	Number of breakage events
NOC	Number of cycles
NOCO	Number of coalescence events
NOE	Total number of events
PB	Probability of breakage
PC	Probability of coalescence
PCDIF	Percentage difference in Sauter mean diameter between two consecutive cycles

---

<sup>1</sup> All other variables not listed here are temporary ones defined by their relevant statements

PHI	Dispersed phase fraction
QI	Interval of Quiescence
RPM	Stirring speed
RUCON	Continuous phase density
RUD	Dispersed phase density
RUMEAN	Dispersion mean density
SC	Tolerance
SIGMA	Interfacial tension
T	Time
TD	Tank diameter
TREM	Computer time remaining
TREQU	Time required for the next cycle(estimate)
TSC	Time for a simulation cycle
TSTND	Computer time assigned for the run
X	Random number
XV	Interval length

#### Arrays

S	Drop diameters
G	Breakage frequencies
FCI	Coalescence frequencies
BETA	Beta distribution
RATIO	Ratio $a'/a$
CF	Coalescence frequency reference matrix
JK	Number of drops in an interval

## APPENDIX V-2

### MONTE CARLO SIMULATION PROGRAM

PROGRAM MOSIM

C ..... Monte Carlo simulation program for Liquid-Liquid dispersions

C ..... A computer program written as a part of Ph.D. research programme

C ..... of Zaki M. O. El-Hassan. Supervisor: Dr. E. S. Perez de Ortiz,

C ..... Dept. of Chem. Eng. & Chem. Tech., Imperial College of Science,

C ..... Technology & Medicine, London SW7.

C ..... Assigning array storage space for drops properties as well as

C ..... temporary working space

DIMENSION S(3005),G(3005),FCI(3005),BETA(501),RATIO(501)

DIMENSION XQ(50),RQ(50),YQ(50),UQ(50),W(3005)

DIMENSION IST(3005),IP(3005),CF(200,200),JK(200)

REAL K1,K2,K3,K4,K5,K6,MUCON,MUD

C ..... Positioning data and results files at their beginning

REWIND 6

REWIND 5

C ..... Establishing the datum for computer CPU time (CDC-secs)

TAU1=SECOND()

C ..... Reading data (see simulation algorithm nomenclature for details)

READ(5,\*) TD,MUCON,MUD,RUD,RUCON,SIGMA,TT,XIMOU,FB,FCC,

+ TSC,SC,FACTOR,PHI,QU,T,TP,TSTND,M,RPM,K1,K2,K3,K4,K5,K6,

+ K7,K8,K9,K10,K11,K12,NC,NOE,NOERR,NOB,NOCO,NOC,XD32,TREQU

WRITE(6,\*) 'NUMBER OF INTERVALS = ',NC

TREM= TSTND

DI=TD/3.

C ..... Random number generator initiation (Numerical Algorithms Group NAG)

C ..... The subroutine G05CAF (Uniform random numbers) is used

CALL G05CBF(0)

C ..... Arrays initiation: All elements assigned zeros

DO 1 I= 1,3005

S(I)=0.

G(I)=0.

FCI(I)=0.

IP(I)=0

IST(I)=0

1 CONTINUE

DO 2 I= 1,50

XQ(I)=0.

YQ(I)=0.

RQ(I)=0.

UQ(I)=0.

2 CONTINUE

C ..... Preparing the Beta distribution for daughter droplets sizes

B1=0.

DO 3 I= 1,501

RATIO(I)=FLOAT(I)/501.

B1=B1+30.\*(RATIO(I)\*\*6)\*((1.-(RATIO(I)\*\*3))\*\*2)

BETA(I)=B1/297.2967031536

3 CONTINUE

RUMEAN=PHI\*RUD+(1.-PHI)\*RUCON

E=.0012463\*(RPM\*\*3)\*(DI\*\*2)/RUMEAN

WRITE(6,93) TD,PHI,RPM

#

```
C ..... Grouping and calculations of the breakage and coalescence functions
C ..... Parameters to avoid unnecessary repetition of calculations
PR1=K1*RPM*DI/(1.+PHI)
PR2=-K2*SIGMA*((1.+PHI)**2)/(RUD*RPM*RPM*DI*DI)
PR3=K3*RPM/(1.+PHI)
PR4=-K4*SIGMA*((1.+PHI)**2)/(RUD*RPM*RPM)
PR5=K5*RPM*DI/(1.+PHI)
PR6=K6*RPM
FT=MUC*RUD/SIGMA**2
PR7=-K7*FT*N**3*DI**3
PR8=-K8*FT*N**3
F1=K9*(E**(1./3.))/(1.+PHI)
F2=-k10*(.0301*((1.4)**2)/(705.2*(E**(2./3.))))
F3=K11*(E**(1./3.))/(1.+PHI)
F4=-K12*FT*RPM**(-3)*DI**(-2)
XV=.0005/FLOAT(NC)
C ..... Calculating the reference sizes for coalescence frequency
C ..... approximation (Equation 5.33)
DO 4 I=1,NC
S(I)=XV*FLOAT(I-1)+XV/2.
JK(I)=0
4 CONTINUE
C ..... Assigning the coalescence frequency reference matrix elements
DO 5 I=1,NC
D=S(I)
D2=D**QU
D3=D*D
DO 5 J=I,NC
D1=S(J)
DT1=D+D1
DT2=(D*D1/DT1)**4
CF(I,J)=(D3+D1*D1)*(PR6*(SQRT(D3+D1*D1))*EXP(PR8*DT2*DT1**2)+
+ PR5*EXP(PR7*DT2/DT1)+F3*(SQRT(D2+D1**QU))*EXP(F4*DT1))
CF(J,I)=CF(I,J)
5 CONTINUE
4 CONTINUE
C ..... Creation of the initial sample (Typically 400 drops)
DO 6 I=1,M
MY=M-I+1
S(MY)=.00003+FLOAT(I)*.001/(FLOAT(M)*2.5)
IM=S(MY)/XV+1
JK(IM)=JK(IM)+1
6 CONTINUE
C ..... Initial sample breakage frequency calculations
FB=0.
DO 7 I=1,M
G(I)=PR1/S(I)*EXP(PR2/S(I))+PR3*EXP(PR4/(S(I)**3))
G(I)=G(I)+F1/((S(I)**(2./3.))*EXP(F2/(S(I)**(5./3.)))
FB=FB+G(I)
7 CONTINUE
C ..... Initial sample coalescence frequency calculations
```

```

FCC=0.
DO 8 I=1,M
FCI(I)=0.
DO 9 J=1,NC
FLJ=CF((INT(S(I)/XV)+1),J)
FCI(I)=FCI(I)+FLJ*FLOAT(JK(J))
9 CONTINUE
IND=S(I)/XV+1
FCI(I)=FCI(I)-CF(IND,IND)
FCC=FCC+.5*FCI(I)
8 CONTINUE
TAU1=SECOND()
GOTO 85
C ..... Start of a simulation pass
81 T=0.
DO 9 I=1,10
RQ(I)=XQ(I)
UQ(I)=YQ(I)
9 CONTINUE
NOERR=NOE-NOERR
IF(NOERR.LT.100) TSC=TSC+10.
NOERR=NOE
TAU=SECOND()
TREM=TSTND-TAU/FACTOR
XMO=FLOAT(M)
TREQU=100.+NOERR*XMO*.00015
C ..... IF(TREM.LT.TREQU) GOTO 86
82 CONTINUE
IF(M.GT.3001) GOTO 86
C ..... Calculation of breakage and coalescence probabilities
PS=FB+FCC
PB=FB/PS
PC=FCC/PS
83 CONTINUE
IF(T.GT.TSC) GOTO 85
C ..... The previous step check the time assigned for a simulation cycle
C ..... Calculation of the Interval of Quiescence
X=G05CAF(X)
QI= - ALOG(X)/PS
T=T+QI
C ..... Determination of event type
X=G05CAF(X)
IF(X.GT.PB)GOTO 84
C ..... Event is breakage. Determine the drop breaking
X=G05CAF(X)
XE=X*FB
SE=0.
DO 10 I=1,M
SE=SE+G(I)
IF(SE.LT.XE) GOTO 90
IM=S(I)/XV+1
JK(IM)=JK(IM)-1
J1=I
DU1=S(J1)

```

```

DU2=G(J1)
DU3=FCI(J1)
S(J1)=S(M)
G(J1)=G(M)
FCI(J1)=FCI(M)
GOTO 11
10 CONTINUE
C ..... Determination of daughter droplets sizes
11 X=G05CAF(X)
IQI=1
IF(BETA(1).GT.X) GOTO 19
DO 12 I=101,501,100
IF(BETA(I).LT.X) GOTO 12
IQI=I
GOTO 13
12 CONTINUE
13 DO 14 I=IQI-100,IQI,25
IF(BETA(I).LT.X) GOTO 14
IQI=I
GOTO 15
14 CONTINUE
15 DO 16 I=IQI-25,IQI,5
IF(BETA(I).LT.X) GOTO 16
IQI=I
GOTO 17
16 CONTINUE
17 DO 18 I=IQI-5,IQI,1
IF(BETA(I).LT.X) GOTO 18
IQI=I
GOTO 19
18 CONTINUE
19 XR=RATIO(IQI)
C ..... Calculation of new drops attributes and updating of the sample ones
S(M)=XR*DU1
IM=S(M)/XV+1
JK(IM)=JK(IM)+1
G(M)=PR1/S(M)*EXP(PR2/S(M))+PR3*EXP(PR4/(S(M)**3))
G(M)=G(M)+F1/((S(M)**(2./3.))*EXP(F2/(S(M)**(5./3.)))
M=M+1
NOB=NOB+1
NOE=NOE+1
S(M)=((DU1**3)-((XR*DU1)**3))**(1./3.)
G(M)=PR1/S(M)*EXP(PR2/S(M))+PR3*EXP(PR4/(S(M)**3))
G(M)=G(M)+F1/((S(M)**(2./3.))*EXP(F2/(S(M)**(5./3.)))
IM=S(M)/XV+1
JK(IM)=JK(IM)+1
NOECD=INT(FLOAT(INT(NOE/500))*500.-FLOAT(NOE))
IF(NOECD.EQ. 0) GOTO 85
FCI(M)=0.
FCI(M-1)=0.
IF(M.GT.3001) GOTO 85
IND1=S(M)/XV+1
IND2=S(M-1)/XV+1
DO 20 I=1,NC

```

```

      FIJ1=CF(I,IND1)
      FIJ2=CF(I,IND2)
      FCI(M)=FCI(M)+FIJ1*FLOAT(JK(I))
      FCI(M-1)=FCI(M-1)+FIJ2*FLOAT(JK(I))
20    CONTINUE
      FCI(M)=FCI(M)-CF(IND1,IND1)-CF(IND1,IND2)
      FCI(M-1)=FCI(M-1)-CF(IND2,IND2)-CF(IND1,IND2)
      FB=FB-DU2+G(M)+G(M-1)
      FCC=FCC-.5*DU3+.5*(FCI(M-1)+FCI(M))
      GOTO 82
84    CONTINUE
C ..... Event is coalescence. Determine the drops taking part
      X=G05CAF(X)
      IF(X.GT.PC) GOTO 83
      UK1=2.*FCC*X
      SE=0.
      DO 21 IWW=1,M
      I=M-IWW+1
      SE=SE+FCI(I)
      IF (SE.LT.UK1) GOTO 115
      IM=S(I)/XV+1
      JK(IM)=JK(IM)-1
      LL1=I
      FB1=G(I)
      FC1=FCI(I)
      D11=S(I)
      S(I)=S(M)
      G(I)=G(M)
      FCI(I)=FCI(M)
      GOTO 22
21    CONTINUE
22    X=G05CAF(X)
      XE=X*FC1
      SE=0.
      KJL=M-1
      DO 23 IWW=1,KJL
      I=KJL-IWW+1
      FIJ4=CF((INT(S(I)/XV)+1),IM)
      SE=SE+FIJ4
      IF(XE.GT.SE) GOTO 23
      IM=S(I)/XV+1
      JK(IM)=JK(IM)-1
      LL2=I
      D12=S(I)
      FB2=G(I)
      FC2=FCI(I)
      S(I)=S(M-1)
      G(I)=G(M-1)
      FCI(I)=FCI(M-1)
      GOTO 24
23    CONTINUE

```

```

JK(IM)=JK(IM)+1
S(M)=D11
G(M)=FB1
FCI(M)=FC1
LL1=0
KJL=0
GOTO 83
C ..... Calculate new drops attributes and update the system ones
24 S(M)=0.
G(M)=0.
FCI(M)=0.
M=M-1
NOCO=NOCO+1
NOE=NOE+1
S(M)=(D11**3+D12**3)**(1./3.)
IM=S(M)/XV+1
JK(IM)=JK(IM)+1
G(M)=PR1/S(M)*EXP(PR2/S(M))+PR3*EXP(PR4/(S(M)**3))
G(M)=G(M)+F1/((S(M)**(2./3.))*EXP(F2/(S(M)**(5./3.)))
NOECD=INT(FLOAT(INT(NOE/500))*500.-FLOAT(NOE))
IF(NOECD.EQ. 0) GOTO 85
FCI(M)=0.
DO 25 I=1,NC
FIJ4=CF(IM,I)
FCI(M)=FCI(M)+FIJ4*FLOAT(JK(I))
25 CONTINUE
FCI(M)=FCI(M)-CF(IM,IM)
FB=FB-FB1-FB2+G(M)
FCC=FCC+.5*(FCI(M)-FC1-FC2)
GOTO 82
85 CONTINUE
C ..... Update sample statistics and write results to tape6
TP=TP+T
NOC=NOC+1
A1=0.
A2=0.
A3=0.
DO 26 I=1,M
A1=A1+S(I)**3
A2=A2+S(I)**2
A3=A3+S(I)
26 CONTINUE
D32=A1/A2
AMD=A3/FLOAT(M)
D32DIF=(D32-XD32)/D32
PCDIF=ABS(D32DIF)*100.
XD32=D32
FD32=D32*1000.
FAMD=AMD*1000.
Z=SECOND()-TAU1
WRITE(*,*) NOC,Z
WRITE(6,91) NOC,TP,NOB+NOCO,NOB,NOCO,M,FD32,FAMD,FB,FCC,Z
WRITE(7,92) NOC,TP,NOE,NOB,NOCO,M,FD32,FAMD,FB,FCC,SECOND()
C ..... Subroutine to calculate drop size distribution

```

```

CALL RESORT(S,M,XQ,YQ,12,.04)
C ..... IF(M.GT.3001 .OR. TREQU.GT.TREM) GOTO 86
C ..... A module to arrange the drop sizes in ascending order to
C ..... accelerate calculations
IFAIL=0
CALL M01ABF(S,1,M,IP,IST,IFAIL)
DO 51 I=1,M
W(IP(I))=FCI(I)
51 CONTINUE
DO 52 I=1,M
FCI(I)=W(I)
52 CONTINUE
DO 53 I=1,M
W(IP(I))=G(I)
53 CONTINUE
DO 54 I=1,M
G(I)=W(I)
54 CONTINUE
C ..... Test for steady state and time or number of events assigned to the run
IF(NOC.LT.3) GOTO 81
Y1=0.
Y2=0.
PO=0.
DO 711 I=1,12
IF(RQ(I).EQ.(0.0)) GOTO 61
Y1=ABS((XQ(I)-RQ(I))/RQ(I))*100.
61 IF(UQ(I).EQ.(0.0)) GOTO 62
Y2=ABS((YQ(I)-UQ(I))/UQ(I))*100.
62 IF(Y2.LE.Y1) GOTO 63
Y1=Y2
63 IF(Y1.LE.PO) GOTO 64
PO=Y1
64 CONTINUE
TAR=450-SECOND()
IF(TAR.LT.50) GOTO 86
IF(NOE.GT.49999) GOTO 86
GOTO 81
C ..... Calculation of the drop size distribution in .01mm intervals
86 CALL RESORT(S,M,XQ,YQ,50,.01)
WRITE(7,*)*****
WRITE(7,*)*****
WRITE(7,*)
WRITE(7,*)(S(I),I=1,M)
WRITE(7,*)*****
WRITE(7,*)*****
91 FORMAT(1X,"CYC",15X,I4,/,
+ 1X,"T S",10X,E17.7,/,1X,"NUMBER OF EVENTS",20X,I6,/,
+ "NUMBER OF BREAK.",10X,I6,20X,
+ "NUMBER OF COAL.",10X,I6,/,1X,"M",
+ 9X,I5,/,1X,"SAUTER & ARITH. MEAN DIA.",2(10X,E15.5,"MM"),/,
+ 1X,"FB =",E12.5,10X,"FCC =",E12.5,/,1X,"CO. T.E.",E12.5,/)
93 FORMAT(1X,////,1X,39X,"SIMULATION OF LIQUID-LIQUID DISPERSIONS",
+ ///,1X,"TD=",F5.3, "M",10X,"PHI=", F5.3,9X,"RPM=",F6.1,/)
92 FORMAT(1X,I3,2X,E12.5,2X,4(I5,2X),5(E12.5,2X),/)

```

```

      STOP
      END
      SUBROUTINE RESORT(P,J,O,QW,NEM,FRAC)
C ..... Subroutine to calculate drop size distribution
      DIMENSION P(J),O(50),PL(50),QW(50)
      DO 8 I=1,50
      PL(I)=0.
      O(I)=0.
      QW(I)=0.
8      CONTINUE
      AA=FRAC*1.0E-03
      SGA=FRAC*FLOAT(NEM)*.001
      DO 16 I=1,J
      IF(P(I).GT.SGA) GOTO 16
      N=IFIX(P(I)/AA)
      AD=P(I)/AA-FLOAT(N)
      IF(AD.EQ. 0.) GOTO 10
      K=N+1
      GOTO 11
10     K=N
11     PL(K)=PL(K)+1
16     CONTINUE
      AS=0.
      DO 24 I=1,50
      O(I)=PL(I)/FLOAT(J)
      AS=AS+O(I)
      QW(I)=AS
24     CONTINUE
      WRITE(6,26) FRAC
      WRITE(6,27)(O(I),I=1,NEM)
      WRITE(6,28) FRAC
      WRITE(6,27) (QW(I),I=1,NEM)
26     FORMAT(1X,"SIZE DISTRIBUTION IN ",F5.3," MM INTERVALS",/)
27     FORMAT(1X,10E12.5,/)
28     FORMAT(1X,///,1X,"COMMULATIVE SIZE DISTRIBUTION IN ",F5.3,
+ "MM INTERVALS",//)
      RETURN
      END

```

# APPENDIX V-3 MONTE CARLO SIMULATION SAMPLE OUTPUT

## SIMULATION OF LIQUID-LIQUID DISPERSIONS

TD = .220M    PHI = .400    RPM = 504.0

CYC            0

NUMBER OF EVENTS            0

NUMBER OF BREAK.            0            NUMBER OF COAL.            0

M            400

SAUTER & ARITH. MEAN DIA.            .32298E+00MM            .23050E+00MM

FB = .80864E+03    FCC = .30389E+00

CO. T.E. .10000E-02

SIZE DISTRIBUTION IN .040 MM INTERVALS

.25000E-01 .10000E+00 .10000E+00 .10000E+00 .10000E+00 .10000E+00 .10000E+00 .10000E+00 .10000E+00 .10000E+00  
.75000E-01 .00000E+00

COMMULATIVE SIZE DISTRIBUTION IN .040MM INTERVALS

.25000E-01 .12500E+00 .22500E+00 .32500E+00 .42500E+00 .52500E+00 .62500E+00 .72500E+00 .82500E+00 .92500E+00  
.10000E+01 .10000E+01

CYC            1

NUMBER OF EVENTS            200

NUMBER OF BREAK.            200            NUMBER OF COAL.            0

M            600

SAUTER & ARITH. MEAN DIA.            .26615E+00MM            .21711E+00MM

FB = .37438E+03    FCC = .44693E+00

CO. T.E. .24900E+00

SIZE DISTRIBUTION IN .040 MM INTERVALS

.16667E-01 .66667E-01 .71667E-01 .86667E-01 .12167E+00 .17500E+00 .22833E+00 .16833E+00 .50000E-01 .11667E-01  
.33333E-02 .00000E+00

CUMMULATIVE SIZE DISTRIBUTION IN .040MM INTERVALS

.16667E-01 .83333E-01 .15500E+00 .24167E+00 .36333E+00 .53833E+00 .76667E+00 .93500E+00 .98500E+00 .99667E+00  
.10000E+01 .10000E+01

CYC 2

NUMBER OF EVENTS 400

NUMBER OF BREAK. 400 NUMBER OF COAL. 0

M 800

SAUTER & ARITH. MEAN DIA. .23511E+00MM .20424E+00MM

FB = .16758E+03 FCC = .62459E+00

CO. T.E. .51800E+00

SIZE DISTRIBUTION IN .040 MM INTERVALS

.12500E-01 .50000E-01 .56250E-01 .87500E-01 .18125E+00 .28875E+00 .26250E+00 .57500E-01 .37500E-02 .00000E+00  
.00000E+00 .00000E+00

CUMMULATIVE SIZE DISTRIBUTION IN .040MM INTERVALS

.12500E-01 .62500E-01 .11875E+00 .20625E+00 .38750E+00 .67625E+00 .93875E+00 .99625E+00 .10000E+01 .10000E+01  
.10000E+01 .10000E+01

.  
.  
.  
.

CYC 4

NUMBER OF EVENTS 800

NUMBER OF BREAK. 800 NUMBER OF COAL. 0

M 1200

SAUTER & ARITH. MEAN DIA. .20176E+00MM .18299E+00MM

FB = .44349E+02 FCC = .10208E+01

CO. T.E. .10990E+01

SIZE DISTRIBUTION IN .040 MM INTERVALS

.83333E-02 .36667E-01 .50000E-01 .15417E+00 .33750E+00 .34917E+00 .64167E-01 .00000E+00 .00000E+00 .00000E+00  
.00000E+00 .00000E+00

CUMMULATIVE SIZE DISTRIBUTION IN .040MM INTERVALS

.83333E-02 .45000E-01 .95000E-01 .24917E+00 .58667E+00 .93583E+00 .10000E+01 .10000E+01 .10000E+01 .10000E+01  
.10000E+01 .10000E+01

.  
.  
.  
.

CYC 12

NUMBER OF EVENTS 2400  
NUMBER OF BREAK. 2157 NUMBER OF COAL. 243  
M 2314

SAUTER & ARITH. MEAN DIA. .15975E+00MM .14988E+00MM  
FB = .20038E+01 FCC = .24516E+01  
CO. T.E. .54270E+01

SIZE DISTRIBUTION IN .040 MM INTERVALS

.38894E-02 .21608E-01 .11798E+00 .42394E+00 .42524E+00 .73466E-02 .00000E+00 .00000E+00 .00000E+00 .00000E+00  
.00000E+00 .00000E+00

CUMMULATIVE SIZE DISTRIBUTION IN .040MM INTERVALS

.38894E-02 .25497E-01 .14347E+00 .56742E+00 .99265E+00 .10000E+01 .10000E+01 .10000E+01 .10000E+01 .10000E+01  
.10000E+01 .10000E+01

CYC 13

NUMBER OF EVENTS 2600  
NUMBER OF BREAK. 2262 NUMBER OF COAL. 338  
M 2324

SAUTER & ARITH. MEAN DIA. .15946E+00MM .14975E+00MM  
FB = .18957E+01 FCC = .25109E+01  
CO. T.E. .64690E+01

SIZE DISTRIBUTION IN .040 MM INTERVALS

.34423E-02 .20224E-01 .12177E+00 .42298E+00 .42513E+00 .64544E-02 .00000E+00 .00000E+00 .00000E+00 .00000E+00  
.00000E+00 .00000E+00

CUMMULATIVE SIZE DISTRIBUTION IN .040MM INTERVALS

.34423E-02 .23666E-01 .14544E+00 .56842E+00 .99355E+00 .10000E+01 .10000E+01 .10000E+01 .10000E+01 .10000E+01  
.10000E+01 .10000E+01

.  
.  
.

CYC 32

NUMBER OF EVENTS 6400

NUMBER OF BREAK. 4229 NUMBER OF COAL. 2171

M 2458

SAUTER & ARITH. MEAN DIA. .15690E+00MM .14687E+00MM

FB = .20448E+01 FCC = .30285E+01

CO. T.E. .28027E+02

SIZE DISTRIBUTION IN .040 MM INTERVALS

.24410E-02 .18714E-01 .16233E+00 .43653E+00 .36819E+00 .11798E-01 .00000E+00 .00000E+00 .00000E+00 .00000E+00  
.00000E+00 .00000E+00

CUMMULATIVE SIZE DISTRIBUTION IN .040MM INTERVALS

.24410E-02 .21155E-01 .18348E+00 .62002E+00 .98820E+00 .10000E+01 .10000E+01 .10000E+01 .10000E+01 .10000E+01  
.10000E+01 .10000E+01

CYC 33

NUMBER OF EVENTS 6600

NUMBER OF BREAK. 4321 NUMBER OF COAL. 2279

M 2442

SAUTER & ARITH. MEAN DIA. .15734E+00MM .14708E+00MM

FB = .21253E+01 FCC = .30225E+01

CO. T.E. .29287E+02

SIZE DISTRIBUTION IN .040 MM INTERVALS

.24570E-02 .19247E-01 .16544E+00 .42424E+00 .37674E+00 .11876E-01 .00000E+00 .00000E+00 .00000E+00 .00000E+00  
.00000E+00 .00000E+00

CUMMULATIVE SIZE DISTRIBUTION IN .040MM INTERVALS

.24570E-02 .21704E-01 .18714E+00 .61138E+00 .98812E+00 .10000E+01 .10000E+01 .10000E+01 .10000E+01 .10000E+01  
 .10000E+01 .10000E+01

.  
 .  
 .

CYC 49

NUMBER OF EVENTS 9800  
 NUMBER OF BREAK. 5908 NUMBER OF COAL. 3892  
 M. 2416

SAUTER & ARITH. MEAN DIA. .15738E+00MM .14816E+00MM

FB = .18607E+01 FCC = .30725E+01  
 CO. T.E. .48291E+02

SIZE DISTRIBUTION IN .040 MM INTERVALS

.16556E-02 .16142E-01 .13369E+00 .47061E+00 .36962E+00 .82781E-02 .00000E+00 .00000E+00 .00000E+00 .00000E+00  
 .00000E+00 .00000E+00

CUMMULATIVE SIZE DISTRIBUTION IN .040MM INTERVALS

.16556E-02 .17798E-01 .15149E+00 .62210E+00 .99172E+00 .10000E+01 .10000E+01 .10000E+01 .10000E+01 .10000E+01  
 .10000E+01 .10000E+01

CYC 50

NUMBER OF EVENTS 10000  
 NUMBER OF BREAK. 6013 NUMBER OF COAL. 3987  
 M 2426

SAUTER & ARITH. MEAN DIA. .15707E+00MM .14806E+00MM

FB = .18769E+01 FCC = .30802E+01  
 CO. T.E. .49469E+02

SIZE DISTRIBUTION IN .040 MM INTERVALS

.16488E-02 .15251E-01 .13149E+00 .47980E+00 .36603E+00 .57708E-02 .00000E+00 .00000E+00 .00000E+00 .00000E+00  
 .00000E+00 .00000E+00

CUMMULATIVE SIZE DISTRIBUTION IN .040MM INTERVALS

.16488E-02 .16900E-01 .14839E+00 .62819E+00 .99423E+00 .10000E+01 .10000E+01 .10000E+01 .10000E+01 .10000E+01  
 .10000E+01 .10000E+01

SIZE DISTRIBUTION IN .010 MM INTERVALS

.00000E+00 .00000E+00 .00000E+00 .16488E-02 .20610E-02 .16488E-02 .61830E-02 .53586E-02 .10305E-01 .19373E-01  
.42045E-01 .59769E-01 .89860E-01 .11088E+00 .14633E+00 .13273E+00 .14509E+00 .13397E+00 .61418E-01 .25556E-01  
.28854E-02 .20610E-02 .41220E-03 .41220E-03 .00000E+00 .00000E+00 .00000E+00 .00000E+00 .00000E+00 .00000E+00  
.00000E+00 .00000E+00 .00000E+00 .00000E+00 .00000E+00 .00000E+00 .00000E+00 .00000E+00 .00000E+00 .00000E+00  
.00000E+00 .00000E+00 .00000E+00 .00000E+00 .00000E+00 .00000E+00 .00000E+00 .00000E+00 .00000E+00 .00000E+00

CUMMULATIVE SIZE DISTRIBUTION IN .010MM INTERVALS

.00000E+00 .00000E+00 .00000E+00 .16488E-02 .37098E-02 .53586E-02 .11542E-01 .16900E-01 .27205E-01 .46579E-01  
.88623E-01 .14839E+00 .23825E+00 .34913E+00 .49547E+00 .62819E+00 .77329E+00 .90725E+00 .96867E+00 .99423E+00  
.99711E+00 .99918E+00 .99959E+00 .10000E+01 .10000E+01 .10000E+01 .10000E+01 .10000E+01 .10000E+01 .10000E+01  
.10000E+01 .10000E+01 .10000E+01 .10000E+01 .10000E+01 .10000E+01 .10000E+01 .10000E+01 .10000E+01 .10000E+01  
.10000E+01 .10000E+01 .10000E+01 .10000E+01 .10000E+01 .10000E+01 .10000E+01 .10000E+01 .10000E+01 .10000E+01

**APPENDIX VI**  
**DROP SIZE MEASUREMENTS (OKUFI (1984))**

Tank Diameter (cm)	Stirring Speed (rpm)	Dispersed phase fraction	Sauter mean Diameter mm
11	800	.10	.137
11	1000	.10	.112
11	1000	.15	.113
11	800	.40	.211
11	1000	.40	.172
11	1000	.10	.107
11	800	.05	.088
11	800	.15	.164
22	400	.10	.139
22	400	.15	.163
22	400	.40	.208
22	504	.10	.106
22	504	.15	.127
22	504	.40	.170
44	200	.10	.141
44	200	.15	.160
44	317	.10	.081
44	317	.15	.101
44	200	.40	.210
44	317	.40	.121
44	250	.40	.163

## NOMENCLATURE

$a, a'$	drop diameter
$A(a')da'$	Fraction of drops with diameters $a' \rightarrow a' + da'$
$a^*$	Transient Sauter mean diameter
$a_{10}$	Arithmetic mean diameter
$a_{32}$	Sauter mean diameter
$a_i, a_j$	Sample $i$ th and $j$ th drop respectively
$C$	Impeller clearance from the bottom of the tank
$D_i, D$	Impeller diameter
$D_T$	Tank diameter
$E_a$	Adhesion energy between two drops
$E_k$	Kinetic energy of two drops
$E_s$	Shear energy
$F$	Adhesion force between two drops
$F(a, a')dada'$	Rate of coalescence per unit volume
$f_b$	Population breakage frequency
$f_c$	Population coalescence frequency
$f_{c,ai}$	Coalescence frequency of the $i$ th drop with the rest of the sample
$g$	Acceleration due to gravity
$G$	Shear stress
$g(a)$	Breakage frequency of a drop of diameter $a$
$h$	Separation distance between two coalescing drops
$h(a, a')$	Collision frequency between drops of size $a$ and $a'$
$\tilde{h}_o$	Minimum separation distance between two coalescing drops
$H$	Liquid height in the vessel
$i, j, k$	Unit vectors in the $x, y$ and $z$ -directions respectively
$IQ$	Interval of Quiescence
$J_k$	Number of drops per $k$ th interval
$k's$	Constants
$k_{b1m}, k_{b2m}$	Breakage functions constants ( $m$ refers to turbulence mode)
$k_{c1m}, k_{c2m}$	Coalescence functions constants ( $m$ refers to turbulence mode)
$L_e$	Linear scale of energy containing eddies
$M$	Number of drops per unit volume; population size(in simulation)

$M(a,a')da da'$	Number of daughter droplets of diameter $a' \rightarrow a' + da'$ produced by the breakage of drops of size $a \rightarrow a + da$
$N$	Stirrer speed
$NC$	Number of intervals
$P$	Power
$P_b$	Population normalized breakage probability
$P_c$	Population normalized coalescence probability
$r$	Eddy size
$r(a)da$	Number of drops with diameter $a \rightarrow a + da$ breaking per unit time per unit volume
$T_o$	Reference tank diameter (1 m)
$u$	Instantaneous velocity
$\bar{u}$	Average velocity
$u'$	Velocity fluctuations around the mean
$(\overline{u^2(a)})^{1/2}$	Root mean square of velocity fluctuation across a distance $a$
$u_\phi$	the instantaneous velocity corrected for the presence of the dispersed phase
$u_1^2, u_2^2$	Root mean square values of the velocity in the longitudinal and lateral directions
$\frac{t}{u}$	Time average velocity for a stationary turbulence
$\frac{s}{u}$	Space average velocity for a homogeneous turbulence
$\frac{e}{u}$	Ensemble average velocity of N identical experiments
$\nu$	Kolmogoroff's velocity scale
$V$	Volume of the vessel occupied by the liquids
$x_l$	Impeller disc thickness
<b>Greek symbols</b>	
$\beta(a, a')$	Probability density function for the appearance of a drop of size $a$ when a drop of size $a'$ breaks
$\Delta s$	Interval size
$\varepsilon$	Average power dissipation per unit mass

$\varepsilon_c$	Average power dissipated in the circulation region
$\varepsilon_i$	Average power dissipated in the impeller region
$\eta$	Kolmogoroff's length scale
$\lambda(a, a')$	Collision efficiency of drops of sizes $a$ and $a'$
$\lambda_g$	Lateral microscale of turbulence
$\lambda_f$	Longitudinal microscale of turbulence
$\mu$	Viscosity
$\nu$	Kinematic viscosity
$\nu(a')$	Number of daughter drops produced by the breakage of a drop of diameter $a' \rightarrow a' + da'$
$\rho$	Density
$\sigma$	Surface tension
$\phi$	Point hold-up
$\phi_o$	Vessel average hold-up (as charged)
$\phi^*$	Dimensionless hold-up
$\tau$	Coalescence time

### Subscripts

$c$	Continuous phase, critical
$d$	Dispersed phase
$min$	Minimum
$crit$	Critical
$I, imp, Imp$	Impeller
$T$	Tank
$max$	Maximum
$m$	Mean

### Dimensionless groups

$N_{Fr}$	Froude Number
$N_p$	Power Number
$N_{Re}$	Reynolds Number
$N_{\nu i}$	Viscosity group
$N_{We}$	Weber Number

## BIBLIOGRAPHY

- Abrahamson, J., *Chem. Eng. Sci.*, **30** (1975) 1371
- Aihara, T., Shimoyama, T., Hongoh, M. and Fujinawa, K., *ICLASS-85*, VC/5/1
- Al-Aswad, K.K., Mumford, G.J. and Jeffreys, G.V., *AIChE. J.*, **31**(9) (1985) 1488
- Ali, A.M., Yuan, H.H.S., Dickey, D.S. and Tatterson, G.B., *Chem. Eng. Commun.*, **10** (1981) 205
- Arai, K, Konno, M, Matunaga, Y. and Saito, S., *J Chem Eng Jap.*, **10**(4) (1977) 325
- Askew, W.S. and Beckmann, R.B., *Ind Eng Chem Process Des Dev*, **5**(3) (1966) 268
- Azzopardi, B.J., *Int. J. Heat Mass Transfer*, **22** (1979) 1245
- Bachalo, W. D. and M. J. Houser, *ICLASS 85* (1985)
- Bailes, P.J., Godfrey, J.C. and Slater, M.J., *The Chemical Engineer*, (1981) 331
- Bajpai, R.K., Ramkrishna, D and Prokop, A., *Biotech. & Bioengng.*, **19** (1977) 1761
- Baldyga, J. and Bourne, J.R., *Chem. Eng. Commun.*, **28** (1984) 231
- Baldyga, J. and Bourne, J.R., *Chem. Eng. Commun.*, **28** (1984) 243
- Baldyga, J. and Bourne, J.R., *Chem. Eng. Commun.*, **28** (1984) 259
- Baldyga, J. and Bourne, J.R., *Chem. Eng. Sci.*, **43**(1) (1988) 107
- Bapat, P.M., Tavlarides, L.L. and Smith, G.W., *Chem. Eng. Sci.*, **38** (1983) 2003
- Bapat, P.M. and Tavlarides, L.L., *AIChEJ*, **31**(4) (1985) 659
- Bapat, P.M. and Tavlarides, L.L., *Ind. Eng. Chem. Fundam.*, **23** (1984) 120
- Barnea, D., Hoffer, M.S. and Resnick, W., *Chem. Eng. Sci.*, **33** (1978) 205
- Barnea, D., Hoffer, M.S. and Resnick, W., *Chem. Eng. Sci.*, **33** (1978) 219
- Barnea, D., Hoffer, M.S. and Resnick, W., *Chem. Eng. Sci.*, **34** (1979) 901
- Barnea, D., Hoffer, M.S. and Resnick, W., *Chem. Eng. Sci.*, **38**(1) (1983) 182
- Barthès-Biesel and Rallison, J.M., *J. Fluid Mech.*, **113** (1986) 251
- Bertrand, J., Couderc, J.P. and Angelino, H., *Chem. Eng. Sci.*, **35** (1980) 2157
- Bhave, R.R. and Sharma, M.M., *Trans. IChemE*, **59** (1981) 161
- Bonnet, J.C. and Tavlarides, L.L., *Ind. Eng. Chem. Res.*, **26** (1987) 811
- Bouyatiotis, B.A. and Thornton, J.D., *IChemE Symposium Series*, **26** (1967) 43

- Brodkey, R.S., *Chem. Eng. Commun.*, **8** (1981) 1
- Brown, D.E. and Pitt, K., *Chem. Eng. Sci.*, **29** (1974) 345
- Bujalski, W., Nienow, A.W., Chatwin, S. and Cooke, M., *Chem. Eng. Sci.*, **42**(2) (1987) 317
- Buurman, C., Resoort, G. and Plaschkes, A., *Chem. Eng. Sci.*, **41**(11) (1986) 2865
- Calabrese, R.V., Chang, T.P.K. and Dang, P.L., *AIChEJ*, **32**(4) (1986) 657
- Calabrese, R.V., Wang, C.Y. and Bryner, N.P., *AIChEJ*, **32**(4) (1986) 677
- Calderbank, P.H., *Trans IChemE*, **36** (1858) 443
- Carpenter, K.J., *Chem. Eng. Res. Des.*, **64** (1986) 3
- Chang, T.P.K., Sheu, Y.H.E, Tatterson, G.B. and Dickey, D.S., *Chem. Eng. Commun.*, **10** (1981) 215
- Chappelear, D. C., *J. Colloid Sci.*, **16** (1963) 236
- Chen, H.T. and Middleman, S., *AIChEJ*, **13**(5) (1967) 989
- Cholette, A. and Leonce Cloutier, *Can. J. Chem. Eng.*, **37** (1959) 105
- Chudacek, M.W., *Ind. Eng. Chem. Fundam.*, **25** (1986) 391
- Church, J.M. and Shinnar, R., *Ind. Eng. Chem.*, **53**(6) (1961) 479
- Clark, Mark M., *Chem. Eng. Sci.*, **43**(3) (1988) 671
- Clark, Mark M., *Chem. Eng. Sci.*, **43**(3) 681
- Clarke, S.I. and Sawistowski, H., *Trans IChemE*, **56** (1978) 50
- Clift, R., Grace, J. R. & Weber, M. E., "Bubbles, Drops and Particles", Academic Press, 1978
- Collias, D.J. and PRUD'HOMME, *Chem. Eng. Sci.*, **40**(8) (1985) 1495
- Collins, S.B. and Knudsen, J.G., *AIChEJ*, **16**(6) (1970) 1072
- Coulaloglou, C.A. and Tavlarides, L.L., *AIChEJ*, **22**(2) (1976) 289
- Coulaloglou, C.A. and Tavlarides, L.L., *Chem. Eng. Sci.*, **32** (1977) 1289
- Cox, R.G., *J. Fluid Mech.*, **37**(3) (1969) 601
- Crochet, M.J., *Chem. Eng. sci.*, **42**(5) (1987) 979
- Cruz-Pinto, J.J.C. and Korchinsky, W.J., *Chem. Eng. Sci.*, **35** (1980) 2213
- Curl, R.L., *AIChEJ*, **9**(2) (1963) 175
- Cutter, L.A., *AIChEJ*, **12**(1) (1966) 35

- Das, P.K., Kumar, R. and Ramkrishna, D, *Chem. Eng. Sci.*, **42**(2) (1987) 213
- Das, P.K., Ramkrishna, D. and Narsimhan, G., *AIChEJ*, **33**(11) (1987) 1899
- Davies, J. T., "Turbulence Phenomena", Academic Press, 1972
- Davies, J.T., *Chem. Eng. Sci.*, **40**(5) (1985) 839
- Davies, J.T., *Chem. Eng. Sci.*, **42**(7) (1987) 1671
- Delichastios, M.A. and Probstein, R.F., *J. Colloid Interface Sci.*, **51** (1975) 394
- Delichastios, M.A., *Phys. Fluids*, **18**(6) (1975) 662
- Delichastios, M.A. and Probstein, *Ind. Eng. Chem. Fundam.*, **15**(2) (1976) 137
- Doherty, Micheal F. and Ottino, Julio M., *Chem. Eng. Sci.*, **43**(2) (1988) 139
- Doraiswamy, L.K., Dabke, S.S., Kulkarni, B.D. and Doraiswamy, L.K., *Chem. Eng. sci.*, **41**(7) (1986)1771
- Doulah, M.S., *Ind. Eng. Chem. Fundam.*, **14**(2) (1975) 137
- Durlofsky, L., Brady, J.F. and Bossis, G., *J. Fluid Mech.*, **180** (1987) 21
- Eckert, R.E., McLaughlin, C.M. and Rushton, J.H., *AIChEJ*, **31**(11) (1985) 1811
- Eleni Chatzi and Lee, James M., *Ind. Eng. Chem. Res.*, **26** (1987) 2263
- Fernandes, J.B. and Sharma, M.M., *Chem. Eng. Sci.*, **22** (1967) 1267
- Flumerfelt, R.W., *Ind. Eng. Chem. Fundam.*, **11**(3) (1972) 312
- Fox, R.O. and Fan, L.T., *Chem. Eng. Sci.*, **43**(3) (1988) 655
- Gal-Or, B. and H. E. Hoelscher, *AIChEJ*, **12**(3) (1966) 499
- Garbini, J. L., F. K. Forster and J. E. Jorgensen, *J. Fluid Mech.*, **118** (1982) 445
- Garbini, J. L., F. K. Forster and J. E. Jorgensen, *J. Fluid Mech.*, **118** (1982) 471
- Garbini, J.L., Forster, F.K. and Jorgensen, J.E., *J Fluid Mech*, **118** (1982) 445
- Garbini, J.L., Forster, F.K. and Jorgensen, J.E., *J Fluid Mech* **118** (1982) 471
- Geffreys, G. V. and G. A. Davies, in *Recent Advances in Liquid-Liquid Extraction*, Ed. C Hanson, 1971
- Giles, J. W., Hanson, C. and Marshland, J. G., *ISEC71* **1** (1971) 94
- Godfrey, J. C., and Hanson, C., in: *Handbook of Multiphase Systems (Chapter 10)*, Hetsroni, G. (Editor), Hemisphere Publishing Corporation, 1982
- Godfrey, J. C., F. I. N. Obi and R. N. Reeve, *ICHEME Symposium Series* **108** (1987) 123
- Godfrey, J.C, Reeve, R.N. and Grilc, V., *ICHEME Symposium Series* **89** (1984) 107

- Grace, H. P., *Chem Eng Comm*, **14** (1982) 225
- Gray, D. J., R. E. Treybal and S. M. Barnett, *AIChEJ*, **28**(2) (1982) 195
- Graybeal, W.J. & Pooch, U. W., "Simulation: Principles and Methods", Winthorp Publishers Inc., 1980
- Groothius, H. and F. J. Zuiderweg, *Chem Eng Sci*, **12** (1960) 288
- Groothius, H. and F. J. Zuiderweg, *Chem Eng Sci*, **19** (1964) 63
- Guimaraes, M. M. L. and J. J. C. Cruz-Pinto, *Computers ans Chemical Engineering*, **12**(11) (1988) 1075
- Günkel, A. A. and M. E. Weber, *AIChEJ*, **21**(5) (1975) 931
- Günkel, A. A. and M. E. Weber, *AIChEJ*, **21**(5) (1975) 939
- Haas, P. A., *AIChEJ*, **33**(6) (1987) 987
- Hamdullahpur, F., M. J. Pegg and G. D. Mackay, *Int. J. Multiphase Flow*, **13**(3) (1987) 379
- Hanzevack, E. L., C. B. Bowers Jr. and Ju Chi-Hang, *AIChEJ*, **33**(12) (1987) 2003
- Hazlett, R. D., R. S. Schechter and J. K. Aggawai, *Ind Eng Chem Fundam*, **24** (1985) 101
- Hetsroni, G (Editor), "Handbook of Multiphase Systems", Hemisphere Publishing Corporation, 1982
- HeuVan Heuven, J. W. and W. J. Beek, *Proc Isec71*, Hague, Society of Chemical Industry, **Paper 51**, (1971) 70
- Hewitt, G. F., in: *Handbook of Multiphase Systems (Chapter 10)*, Hetsroni, G. (Editor), Hemisphere Publishing Corporation, 1982
- Hewitt, G. F., in *Handbook of Multiphase Systems*, Ed. G. Hetsroni, (1986) 10-102
- Hinch, E. T., *J Fluid Mech*, **101** Part 3 (1980) 545
- Hinch, E. T. and A. Acrivos, *J Fluid Mech*, **98** Part 2 (1980) 305
- Hinze, J. O., "Turbulence", 2nd Edition, McGraw Hill, 1975
- Hinze, J. O., *AIChEJ*, **1**(3) (1955) 289
- Hoffer, M. S. and W. Resnick, *Chem Eng Sci*, **30** (1975) 473
- Hoffer, M. S. and W. Resnick, *Chem Eng Sci*, **30** (1975) 481
- Hoffer, M. S. and W. Resnick, *Chem Eng Sci*, **30** (1975) 493

- Hoffer, M. S. and W. Resnick, *Trans IChemE*, **57** (1979) 1
- Hoffer, M. S. and W. Resnick, *Trans IChemE*, **57** (1979) 8
- Holland, F. A. & Chapman, F. S., "Liquid Mixing and Processing in Stirred Tanks", Reinhold Publishing Corporation, 1966
- Holmes, D. B., R. M. Voncken and J. A. Dekker, *Chem Eng Sci*, **19** (1964) 201
- Hong, P. O. and J. M. Lee, *Ind Eng Chem: Process Des Dev*, **22** (1983) 130
- Hong, P. O. and J. M. Lee, *Ind Eng Chem: Process Des Dev*, **24**(3) (1985) 868
- Howarth, W. J., *AIChEJ*, **13**(5) (1967) 1007
- Howarth, W. J., *Chem Eng Sci*, **19** (1964) 33
- Hsia, M. A. and L. L. Tavlarides, *The Chem Eng J.*, **26**(1983) 189
- Hulburt, H. H. and S. L. Katz, *Chem Eng Sci*, **19** (1964) 555
- Janjua, Z., PhD Thesis, University of London, 1982
- Jeon, Y. M. and W. K. Lee, *Ind Eng Chem Fundam*, **25** (1986) 293
- Karam, H. J. and J. C. Bellinger, *Ind Eng Chem Fundam*, **7**(4) (1968) 576
- Kataoka, T. and T. Nishiki, *J Chem Eng Jap*, **19**(5) (1986) 408
- Katz, S., *Chem Eng Sci*, **9** (1958) 61
- Kawecki, W., Reith, T., Van Heuven, J. W. and Beek, W. J., *Chem Eng Sci*, **22** (1967) 1519
- Khakhar, D. V. and J. M. Ottino, *J Fluid Mech*, **166** (1986) 265
- Khang, J. Soon and O. Levenspiel, *Chem Eng Sci*, **31** (1976) 569
- Kim, T. O. and W. K. Kang, *Int Chem Eng*, **28**(4) (1988) 690
- King, R. L., R. A. Hiller and G. B. Tatterson, *AIChEJ*, **34**(3) (1988) 506
- Kirou, V. I., L. L. Tavlarides, J. C. Bonnet and C. Tsouris, *AIChEJ*, **34**(2) (1988) 283
- Kirou, V. I., L. L. Tavlarides and J. C. Bonnet, *Ind Eng Chem Res*, **27** (1988) 1084
- Kolarik, Z. and N. Pipkin, *Hydrometallurgy*, **9** (1983) 371
- Kolmogoroff, A. N., *Comptes Rendus (Doklady) de l' Académie des Sciences de l' URSS*, **XXXII**(1) (1941)16
- Kolmogoroff, A. N., *Comptes Rendus Acad Sci USSR*, **XXX**(4) (1941)301

- Kolmogoroff , A. N., *Dokl. Akad. Nauk. SSSR*, **LXVI**(5) (1949) 825
- Komasawa, I, R. Kuboi and T. Otake, *Chem Eng Sci*, **29** (1964) 641
- Komasawa, I, R. Kuboi and T. Otake, *Chem Eng Sci*, **29** (1964) 651
- Komasawa, I, R. Kuboi and T. Otake, *Chem Eng Sci*, **29** (1964) 659
- Komori, S. and Y. Murakami, *AIChEJ*, **34**(6) (1988) 932
- Konno, M., K. Arai and S. Saito, *J Chem Eng Jap.*, **10**(6) (1977) 474
- Konno, M., M. Aoki and S. Saito, *J Chem Eng Jap.*, **16** (1983) 312
- Konno, M., T. Muto and S. Saito, *J Chem Eng Jap.*, **21**(4) (1988) 335
- Konno, M., Y. Matsunaga and K. Arai, *J Chem Eng Jap.*, **13**(1) (1980)
- Konno, M. and S. Saito, *J Chem Eng Jap.* **20**(5) (1987) 533
- Koshy, A., T. R. Das and R. Kumar, *Chem Eng Sci*, **43**(3) (1988) 649
- Kuboi, R., I. Komasawa and T. Otake, *J Chem Eng Jap.*, **5**(4) (1972) 349
- Lagisetty, J. S., P. K. Das, R. Kumar and K. S. Gandhi, *Chem Eng Sci*, **41**(1) (1986) 65
- Laso, M., L. Steiner and S. Hartland, *Chem Eng Sci*, **42**(10) (1987) 2429
- Laso, M., L. Steiner and S. Hartland, *Chem Eng Sci*, **42**(10) (1987) 2437
- Laufhütte, H. D. and A. Mersmann, *Chem Eng Tech* **10** (1987) 56
- Laufhütte, H. D. and A. Mersmann, *Ger. Chem Eng*, **8** (1985) 371
- Lee, J. M. and Y Soong, *Ind Eng Chem Process Des Dev*, **24** (1985) 118
- Lee S. L. and J. Srinivasan, *Int J Multiphase Flow*, **4** (1978) 141
- Levich, V. G., "Physicochemical Hydrodynamic", Prentice Hall, New York, 1962
- Mahn, Won Kim, W. D. Dozier and R. Klein, *J Chem Phys*, **84**(10) (1986)
- Mann, R., P. Knysh, E. A. Rasekoala and M. Bidari, *ICHEME Symposium Series*, **108** (1987) 49
- Mann, R., *Process Engineering*, (1988) 40
- McAvoy, R. M., W. A. Weigomd, E. E. Tompkins and R. C. Kintner, *AIChE-ICHEME Symposium Series No. 1*, (London: Instn Chem Engrs), (1965) 1:18

- McManamey, W., *Chem Eng Sci*, **34** (1979) 434
- Mikami, T., R. G. Cox and S. G. Mason, *Int J Multiphase Flow*, **2** (1975) 113
- Miller, R. S., J. L. Ralph, R. L. Curl and G. R. Towell, *AIChEJ*, **9**(2) (1963) 196
- Mlyneck, Y. and W. Resnick, *AIChEJ*, **18**(1) (1972) 122
- Molag, M., G. E. H. Joosten and A. A. H. Drinkenburg, *Ind Eng Fundam*, **19**(3) (1980) 276
- Mok, Y. I. and Treybal, R. E., *AIChEJ*, **17** (1971) 916
- Mujumdar, A. S., B. Huang, D. Wolf, M. E. Weber and W. J. M. Douglas, *Can J Chem Eng*, **48** (1970) 475
- Muralldhar, R. and D. Ramkrishna, *Ind Eng Chem Fundam*, **25** (1986) 554
- Naagata, S., "Mixing Principles and Applications", Halsted Press, 1975
- Nakada and M. Tanaka, *Trans IChemE*, **55** (1977) 143
- Narsimhan, G., D. Ramkrishna and J. P. Gupta, *AIChEJ*, **26**(6) (1980) 991
- Narsimhan, G., G. Nejfelt and D. Ramkrishna, *AIChEJ*, **30**(3) (1984) 457
- Narsimhan, G., J. P. Gupta and D. Ramkrishna, *Chem Eng Sci*, **34** (1979) 257
- Nauman, E. B. & Buffman, B. A., "Mixing in Continuous Flow Systems", John Wiley & Sons, 1983
- Nienow, A. W. and D. Miles, *Ind Eng Chem Process Des Dev*, **10**(1) (1971) 41
- Nishikawa, M., F. Mori, S. Fujieda and T. Kayam, *J Chem Eng Jap.*, **20**(5) (1987) 545
- Nishikawa, M., F. Mori and S. Fujieda, *J Chem Eng Jap.*, **20**(1) (1987) 82
- Nishikawa, M., Y. Okamoto, K. Hashimoto and S. Nagata, *J Chem Eng Jap.*, **9**(6) (1976) 489
- Ogawa, K., C. Kuroda and S. Yoshikawa, *J Chem Eng Jap.*, **19**(4) (1986) 345
- Ohatake, T., T. Hono, K. Takagi and F. Nakashio, *J Chem Eng Jap.*, **20**(5) (1987) 443
- Okamoto, Y., M. Nishikawa and K. Hashimoto, *Int Chem Eng*, **21**(1) (1981) 88
- Okufi, S. Z., PhD Thesis, University of London, 1984
- Okufi, S., E. S. Perez de Ortiz and H. Sawistowski, *CHISA84* (1984)
- Oldshue, J. Y. (Editor), "Fluid Mixing Technology", McGraw Hill, 1983
- Park and Blair, *Chem Eng Sci*, **30** (1975) 1057

- Patterson, G. K., *Chem Eng Commun*, **8** (1981) 25
- Peleg, M. and M. D. Normand, *AIChEJ*, **32**(11) (1986) 1928
- Pilhofer, T., *Chem Eng Tech*, **11** (1988) 259
- Placek, J., Tavlarides, L. L., G. W. Smith and I Fort, *AIChEJ*, **31**(11) (1986) 1771
- Placek, J. and Tavlarides, L. L., *AIChEJ*, **31**(7) (1986) 1113
- Plawsky, J. L. and Hatton, T. A., *ISEC86 III* (1986) 89
- Rajamani, K., W. T. Pate and D. J. Kinnerberg, *Ind Eng Chem Fundam*, **25** (1986) 746
- Rallison, J. M., *Ann Rev Fluid Mech*, **16** (1984) 45
- Rallison, J. M., *J Fluid Mech*, **109** (1981) 465
- Rallison, J. M. and A. Acrivos, *J Fluid Mech*, **89** Part 1 (1978) 191
- Ramkrishna, D., *Chem Eng Sci*, **29** (1974) 987
- Ramkrishna, D., *Chem Eng Sci*, **36** (1981) 1203
- Ramkrishna, D. and J. D. Borwanker, *Chem Eng Sci*, **28** (1973) 1423
- Ramkrishna, D. and J. D. Borwanker, *Chem Eng Sci*, **29** (1974) 1711
- Ramkrishna, D. and J. D. Borwanker, *Chem Eng Sci*, **31** (1976) 435
- Rao, A. and R. S. Brodkey, *Chem Eng Sci*, **27** (1972) 137
- Rao, D. P. and I. R. Dunn, *Chem Eng Sci*, **25** (1970) 1275
- Ravikumar, V. and Doraiswamy, L.K., *Chem. Eng. sci.*, **40**(10) (1985)1951
- Rietema, K., *Advances in Chemical Engineering*, **5** (1964) 237
- Rietema, K., *Chem Eng Sci*, **37**(8) (1982) 1125
- Rod, V. and T. Misek, *Trans IChemE*, **60** (1982) 60
- Rodger, W. A., V. G. Trice Jr and J. H. Rushton, *Chem Eng Progress*, **52**(12) (1956) 515
- Ross, S. L., F. H. Verhoff and R. L. Curl, *Ind Eng Chem Fundam*, **17**(2) (1978) 101
- Rushton, J. H., *Chem Eng Progress*, **47**(9) (1951) 485
- Rushton, J. H., E. W. Gostich and H. J. Everett, *Chem Eng Progress*, **46**(8) (1950) 397
- Rushton, J. H., E. W. Gostich and H. J. Everett, *Chem Eng Progress*, **46**(9) (1950) 467

- Rushton, J. H., In: *Interfacial Synthesis, Vol 2*, Ed. C. E. and Millich, F., Marcell Dekker Inc NY, 1977
- Sachs, J. P., and J. H. Rushton, *Chem Eng Progress*, 50(12) (1954) 597
- Saffman, P. G. and J. S. Turner, *J Fluid Mech*, 1 (1956)16
- Sarjeant, M., BHRA MIXING III
- Sato, Y. and K. Yamamoto, *J Chem Eng Jap.*, 6(6) (1973) 495
- Schwartzberg, H. G. and R. E. Treybal, *Ind & Eng Chem Fundam*, 7(1) (1968) 6
- Schwartzberg, H. G. and R. E. Treybal, *Ind & Eng Chem Fundam*, 7(1) (1968) 1
- Semiati, R. and A. E. Dukler, *AIChEJ*, 27 (1981) 148
- Shiloh, K., S. Sideman and W. Resnick, *Canadian J Chem Eng*, 51 (1973) 542
- Shinnar, R., *J Fluid Mech*, 10 (1961) 259
- Shinnar, R. and J. M. Church, *Ind Eng Chem*, 52(3) (1960) 523
- Skelland, A. H. P. and G. G. Ramsay, *Ind Eng Chem Res*, 26 (1987) 77
- Skelland, A. H. P. and J. M. Lee, *AIChEJ*, 27(1) (1981) 99
- Skelland, A. H. P. and J. M. Lee, *Ind Eng Chem Process Des Dev*, 17(4) (1978) 473
- Skelland, A. H. P. and Moeto, L. T., *Ind Eng Chem Res*, 28 (1989) 122
- Skelland, A. H. P. and R. Seksaria, *Ind Eng Chem Process Des Dev*, 17(1) (1978) 56
- Sleicher, C. A. Jr., *AIChEJ*, 8(4) (1962) 471
- Sovová, H. and J. Procházka, *Chem Eng Sci*, 36 (1981) 1567
- Sovová, H. and J. Procházka, *Chem Eng Sci*, 36 (1981) 163
- Spielman, L. A. and Levenspiel, *Chem Eng Sci*, 20 (1965) 247
- Sprow, F. B., *AIChEJ*, 13(5) (1967) 995
- Sprow, F. B., *Chem Eng Sci*, 22 (1967) 435
- Stamatoudis, M. and L. L. Tavlarides, *Advances in Chemical Engineering*, 11 (1981) 199
- Stamatoudis, M. and L. L. Tavlarides, *Ind Eng Chem Process des Dev*, 24 (1985) 1175
- Stamatoudis, M. and L. L. Tavlarides, *The Chem Eng J*, 21 (1981) 77
- Stamatoudis, M. and L. L. Tavlarides, *The Chem Eng J*, 35 (1987) 137
- Steiner, L. M. Laso and S. Hartland, *Chem Eng Sci*, 42(10) (1987) 2429

- Steiner, L. M. Laso and S. Hartland, *Chem Eng Sci*, **42**(10) (1987) 2437
- Stone, H. A., B. J. Bentley and L. G. Leal, *J. Fluid Mech.*, **173** (1986) 131
- Swartz, J. E. and D. P. Kessler, *AIChEJ*, **16**(2) (1970) 254
- Tambe, S.S., Kulkarni, B.D. and Doraiswamy, L.K., *Chem. Eng. sci.*, **40**(10) (1985)1943
- Tanaka, M., *The Canadian J Chem Eng*, **63** (1985) 723
- Tavlarides, L. L., *Chem Eng Commun*, **8** (1981) 133
- Taylor, G. I., *Proc Royal Society*, **138-A** (1932) 41
- Taylor, G. I., *Proc Royal Society*, **146-A** (1934) 501
- Tomotika, S., *Proc Royal Society*, **150-A** (1935) 322
- Tomotika, S., *Proc Royal Society*, **153-A** (1935) 302
- Uhl, V. W. & Gray, J. B. (Editors), "Mixing Theory & Practice: Vol. 1", Academic Press, 1966
- Uhl, V. W. & Gray, J. B. (Editors), "Mixing Theory & Practice: Vol. 2", Academic Press, 1967
- Valentas, K. J., O. Bilous and N. R. Amundson, *Ind Eng Chem Fundam*, **5**(2) (1966) 271
- Valentas, K. J. and N. R. Amundson, *Ind Eng Chem Fundam*, **5**(4) (1966) 533
- Valentas, K. J. and N. R. Amundson, *Ind Eng Chem Fundam*, **7**(1) (1968) 66
- Van't Riet, K., W. Bruijn and J. M. Smith, *Chem Eng Sci*, **31** (1976) 407
- Van't Riet, K. and J. M. Smith, *Chem Eng Sci*, **30** (1975) 1093
- Van Der Molen and H. R. E. Van Maanen, *Chem Eng Sci*, **33** (1978) 1161
- Verhoff, F. H., S. L. Ross and R. L. Curl, *Ind Eng Chem Fundam*, **16**(3) (1977) 371
- Vermeulen, T., G. M. Williams and G. E. Longlois, *Chem Eng Progress*, **51**(2) (1955) 85F
- Voit, H. and A. Mersmann, *Ger Chem Eng*, **9** (1986) 101
- Vonker, R. M., D. B. Holmes and H. W. Den Hartog, *Chem Eng Sci*, **19** (1964) 209
- Wang, C. Y. and R. V. Calabrese, *AIChEJ*, **32**(4) (1986) 667
- Weinstein, B. and R. E. Treybal, *AIChEJ*, **19**(2) (1973) 305

- Yeoman, M. L., B. J. Azzopardi, H. J. White, C. J. Bates and P. J. Roberts, *AERE Report No. 10468* (1982)
- Zeitlin, M. A. and L. L. Tavlarides, *AIChEJ*, **18**(6) (1977) 1268
- Zeitlin, M. A. and L. L. Tavlarides, *Canadian J Chem Eng*, **50** (1972) 207
- Zher, Yang, MSc Dept Chem Eng Fac of Eng Univ of Birmingham 1986
- Zielinski, J. M. and E. E. Peterson, *AIChEJ*, **33**(12) (1987) 1993
- Zlokarnik, M., *Int Chem Eng*, **27**(1) (1987) 1